UNIWERSYTET
IM. ADAMA MICKIEWICZA
W POZNANIU

Doctoral thesis

Architecture-Engineered Semiconductor Nanocomposites for Photocatalytic and Photoelectrochemical Applications

Architektonicznie projektowane nanokompozyty półprzewodnikowe do zastosowań fotokatalitycznych i fotoelektrochemicznych

by

mgr. Andrii Lys

Doctoral dissertation conducted at the NanoBioMedical Centre under the supervision of **Prof. dr. hab. Igor Iatsunskyi**

The dissertation is submitted for the degree of
Doctor of Philosophy in Chemistry

Faculty of Chemistry
Adam Mickiewicz University, Poznań
Poznań 2026

Contents

Acknowledgments

This work was financially supported by the National Science Centre, Poland, under project No. 2020/38/E/ST5/00176, “Nanocomposites based on 1D semiconductors modified by MXene and ALD for efficient photoelectrochemical water splitting”, funded within the SONATA BIS 10 call.

It has been a difficult path, and an even more challenging one may still lie ahead. Throughout my life, however, I have been fortunate to receive enormous support from the people around me. The least I can do is leave a few words of gratitude here.

I would like to thank my beloved family, my primary and secondary school teachers, my incredible high school physics and mathematics teachers, my research advisors from around the world, as well as my friends and colleagues. Each of them has written an important chapter in the book of my life. I sincerely hope that, in the future, I will be able to return at least a small part of this kindness to the world.

I would like to express special gratitude to my supervisor, Prof. dr. hab. Igor Iatsunskyi, who helped me greatly not only in my scientific work, but also in my life. His support, trust, and guidance were very important during my doctoral studies.

The cornerstone of my path and of the meaning I seek in life is my mother. She is a woman who sacrificed so much for me, our family, and society by teaching and sharing her extraordinary experience with younger generations. Her strength, kindness, and belief in me have always been among the most important sources of support in my life.

To everyone who has supported me, taught me, helped me, or simply stayed by my side during this journey, I offer my sincere gratitude.

Abstract

Photocatalytic water purification and photoelectrochemical hydrogen production address two closely related needs: removal of pollutants from water and production of renewable chemical fuels. In both cases, the useful response of a semiconductor material depends not only on photon absorption, but also on the separation, transport, and interfacial use of photogenerated charge carriers. However, many semiconductor systems are still limited by weak light utilisation, fast electron-hole recombination, poor interfacial charge transfer, and insufficient stability under working conditions. Therefore, the development of efficient photocatalysts and photoelectrodes requires a design strategy in which the chemical composition is considered together with the architecture, surface geometry, and interface quality.

Titanium dioxide was treated in this thesis as the main reference semiconductor because of its chemical stability, low toxicity, availability, and well-established photocatalytic and photoelectrochemical behaviour. At the same time, the wide band gap of TiO_2, together with recombination and transport losses, limits its direct performance. For this reason, the work focused on TiO_2-based and related metal-oxide nanocomposites in which the material function was improved through structural and interfacial design. In such systems, TiO_2 was used not only as a photoactive oxide, but also as a chemically stable surface layer, a conformal coating, and an interface-forming component. Other oxide systems, including WO_3 and $ZnFe_2O_4$/ZnO, were also examined to place the TiO_2-based architectures within a broader metal-oxide framework. Their behaviour showed that heterostructure formation, visible-light response, and fibrous oxide design are important factors in controlling charge separation and photoinduced processes.

The research included several material platforms prepared by femtosecond laser structuring, atomic layer deposition, electrospinning, and heterostructure formation. Highly regular silicon nanoripples modified with MXene and ALD TiO_2 were developed as a structured photocatalytic surface for dye degradation. In this system, the laser-formed ripple morphology played an active role in light management by increasing scattering, internal reflection, and light trapping at the structured silicon surface. The ALD-grown TiO_2 coating added a second function: it stabilised the surface by covering the silicon/MXene structure with a continuous oxide layer and created a chemically more suitable interface for photocatalytic reactions. As a result, the SiNR/MXene/TiO_2 architecture exhibited considerably higher photocatalytic activity than SiNR/TiO_2. This improvement indicates that the photocatalytic response was governed by the joint effect of the structured silicon surface, the stabilising TiO_2 layer, and MXene-assisted interfacial charge transfer.

Electrospun polyimide nanofibres modified with TiO_2, WO_3, and $Ti_3C_2T_x$ MXene were investigated as immobilised photocatalytic membranes. Here, the fibrous format was important not only as a support for the active phases, but also as a practical form of the

photocatalyst. Unlike dispersed powders, the membrane could be recovered and reused more easily, and its open fibre network helped the dye solution reach the photoactive regions. In the TiO_2/WO_3/MXene system, the improvement was associated with broader light absorption, more effective interfacial charge transfer, and a reduced recombination rate. The PID/TiO_2/WO_3/MXene membrane exhibited the best photocatalytic response among the tested samples and retained its activity after repeated use.

Photoelectrochemical behaviour was studied using two oxide systems in which the architecture of the material played a central role. Coaxially electrospun $ZnFe_2O_4$/ZnO core-shell nanofibres were examined as a visible-light-responsive heterostructured platform. In this case, the final optical and PEC response was shaped by the core-shell arrangement and by Fe/Zn interdiffusion during annealing. The second PEC system was based on Ti-TiO_2 membranes. In this case, femtosecond laser ablation was used to form a hierarchical titanium scaffold, which was subsequently coated with TiO_2 layers of controlled thickness by ALD. This architecture improved light harvesting and increased the accessible surface area, while also favouring electrolyte contact and charge extraction through the conductive Ti support. The strongest PEC response was obtained for the membrane coated with 100 nm of TiO_2, showing that the final performance depended on the balance between oxide thickness, crystallinity, interface quality, and the geometry of the titanium scaffold.

The results presented in this thesis show that architecture is not only a morphological feature, but also a functional design parameter. Laser structuring provides optical benefits by increasing light trapping and reducing reflection losses. ALD provides chemical and interfacial benefits by forming continuous TiO_2 coatings on complex surfaces. Electrospinning enabled the preparation of recoverable membrane-type photocatalysts, in which improved handling was combined with a fibrous network favourable for liquid transport and access to active regions. Core-shell and hybrid oxide systems provided additional routes for controlling charge separation and extending the photoresponse into the visible-light range. Taken together, the results show that TiO_2-based and related semiconductor nanocomposites benefit most when optical enhancement, chemical protection, surface accessibility, and interfacial charge transfer are considered together during architectural design, rather than treated as separate and independent material features.

Streszczenie

Fotokatalityczne oczyszczanie wody oraz fotoelektrochemiczna produkcja wodoru należą do ważnych procesów indukowanych światłem, istotnych z punktu widzenia ograniczania zanieczyszczenia środowiska oraz rozwoju odnawialnych nośników energii. W obu przypadkach użyteczna odpowiedź materiału półprzewodnikowego zależy nie tylko od absorpcji fotonów, lecz także od separacji, transportu oraz międzyfazowego wykorzystania fotogenerowanych nośników ładunku. Wiele układów półprzewodnikowych nadal jest jednak ograniczonych przez słabe wykorzystanie światła, szybką rekombinację par elektron-dziura, niewystarczający międzyfazowy transfer ładunku oraz ograniczoną stabilność w warunkach pracy. Dlatego opracowanie wydajnych fotokatalizatorów i fotoelektrod wymaga strategii projektowania, w której skład chemiczny rozpatrywany jest łącznie z architekturą, geometrią powierzchni oraz jakością interfejsów.

Ditlenek tytanu został w niniejszej rozprawie potraktowany jako główny półprzewodnik odniesienia ze względu na jego stabilność chemiczną, niską toksyczność, dostępność oraz dobrze poznane właściwości fotokatalityczne i fotoelektrochemiczne. Jednocześnie szeroka przerwa energetyczna TiO_2, a także straty związane z rekombinacją i transportem nośników ładunku, ograniczają jego bezpośrednią wydajność. Z tego powodu praca koncentrowała się na nanokompozytach opartych na TiO_2 oraz pokrewnych tlenkach metali, w których funkcjonalność materiału była poprawiana poprzez inżynierię architektury. W takich układach TiO_2 pełnił rolę nie tylko fotoaktywnego tlenku, lecz także chemicznie stabilnej warstwy powierzchniowej, konforemnej powłoki oraz składnika odpowiedzialnego za tworzenie interfejsu. Badano również inne układy tlenkowe, w tym WO_3 oraz $ZnFe_2O_4$/ZnO, aby umiejscowić architektury oparte na TiO_2 w szerszym kontekście tlenków metali. Ich zachowanie pokazało, że tworzenie heterostruktur, odpowiedź w zakresie światła widzialnego oraz projektowanie włóknistych układów tlenkowych są ważnymi czynnikami kontrolującymi separację ładunku i procesy fotoindukowane.

Badania obejmowały kilka platform materiałowych otrzymywanych z wykorzystaniem femtosekundowego strukturyzowania laserowego, osadzania warstw atomowych, elektroprzędzenia oraz tworzenia heterostruktur. Wysoce regularne nanofałdy krzemowe modyfikowane MXenem i TiO_2 osadzanym metodą ALD opracowano jako strukturyzowaną powierzchnię fotokatalityczną do degradacji barwników. W tym układzie morfologia fałd wytworzonych laserowo odgrywała aktywną rolę w zarządzaniu światłem poprzez zwiększenie rozpraszania, wewnętrznego odbicia oraz pułapkowania światła na strukturyzowanej powierzchni krzemu. Powłoka TiO_2 otrzymana metodą ALD pełniła drugą funkcję: stabilizowała powierzchnię poprzez pokrycie układu krzem/MXene ciągłą warstwą tlenkową oraz tworzyła chemicznie bardziej odpowiedni interfejs dla reakcji fotokatalitycznych. W rezultacie architektura SiNR/MXene/TiO_2 wykazywała znacznie

wyższą aktywność fotokatalityczną niż SiNR/TiO_2. Poprawa ta wskazuje, że odpowiedź fotokatalityczna była kontrolowana przez łączny efekt strukturyzowanej powierzchni krzemowej, stabilizującej warstwy TiO_2 oraz wspomaganego przez MXene międzyfazowego transferu ładunku.

Elektroprzędzone nanowłókna poliimidowe modyfikowane TiO_2, WO_3 i $Ti_3C_2T_x$ MXenem badano jako immobilizowane membrany fotokatalityczne. W tym przypadku forma włóknista była istotna nie tylko jako nośnik faz aktywnych, lecz także jako praktyczna postać fotokatalizatora. W przeciwieństwie do proszków zdyspergowanych w roztworze, membrana mogła być łatwiej odzyskiwana i ponownie wykorzystywana, a jej otwarta sieć włókien ułatwiała dostęp roztworu barwnika do obszarów fotoaktywnych. W układzie TiO_2/WO_3/MXene poprawę właściwości powiązano z szerszą absorpcją światła, bardziej efektywnym międzyfazowym transferem ładunku oraz ograniczoną rekombinacją. Membrana PID/TiO_2/WO_3/MXene wykazała najlepszą odpowiedź fotokatalityczną spośród badanych próbek i zachowała aktywność po wielokrotnym użyciu.

Właściwości fotoelektrochemiczne badano z wykorzystaniem dwóch układów tlenkowych, w których architektura materiału odgrywała kluczową rolę. Współosiowo elektroprzędzone nanowłókna rdzeń-powłoka $ZnFe_2O_4$/ZnO analizowano jako heterostrukturalną platformę reagującą na światło widzialne. W tym przypadku końcowa odpowiedź optyczna i fotoelektrochemiczna była kształtowana przez układ rdzeń-powłoka oraz przez interdyfuzję Fe/Zn zachodzącą podczas wyżarzania. Drugi układ fotoelektrochemiczny opierał się na membranach Ti-TiO_2. W tym przypadku ablacja laserem femtosekundowym została zastosowana do wytworzenia hierarchicznego rusztowania tytanowego, które następnie pokryto warstwami TiO_2 o kontrolowanej grubości metodą ALD. Taka architektura poprawiała wykorzystanie światła i zwiększała dostępną powierzchnię, a jednocześnie sprzyjała kontaktowi z elektrolitem oraz ekstrakcji ładunku przez przewodzące podłoże tytanowe. Najsilniejszą odpowiedź fotoelektrochemiczną uzyskano dla membrany pokrytej warstwą TiO_2 o grubości 100 nm, co pokazuje, że końcowa wydajność zależała od równowagi między grubością tlenku, krystalicznością, jakością interfejsu oraz geometrią rusztowania tytanowego.

Wyniki przedstawione w niniejszej rozprawie pokazują, że architektura nie jest jedynie cechą morfologiczną, lecz funkcjonalnym parametrem projektowym. Strukturyzowanie laserowe zapewnia korzyści optyczne poprzez zwiększenie pułapkowania światła i ograniczenie prostych strat odbiciowych. ALD zapewnia korzyści chemiczne i międzyfazowe poprzez tworzenie ciągłych powłok TiO_2 na złożonych powierzchniach. Elektroprzędzenie umożliwiło otrzymanie odzyskiwalnych fotokatalizatorów membranowych, w których lepsza obsługa materiału została połączona z włóknistą siecią sprzyjającą transportowi cieczy i dostępowi do obszarów aktywnych. Układy rdzeń-powłoka oraz hybrydowe układy tlenkowe zapewniły dodatkowe możliwości kontrolowania separacji ładunku i rozszerzania fotoodpowiedzi w kierunku zakresu światła widzialnego. Łącznie

wyniki te pokazują, że nanokompozyty półprzewodnikowe oparte na TiO_2 oraz materiały pokrewne osiągają największe korzyści wtedy, gdy wzmocnienie optyczne, ochrona chemiczna, dostępność powierzchni oraz międzyfazowy transfer ładunku są rozpatrywane wspólnie podczas projektowania architektury, a nie traktowane jako oddzielne i niezależne cechy materiału.

Author publication included into thesis

1. *Highly regular laser-induced periodic silicon surface modified by MXene and ALD TiO_2 for organic pollutants degradation*
   Andrii Lys, Iaroslav Gnilitskyi, Emerson Coy, Mariusz Jancelewicz, Oleksiy Gogotsi, Igor Iatsunskyi
   Applied Surface Science, 640, 158336, 2023
   doi.org/10.1016/j.apsusc.2023.158336
2. *Electrospun Polyimide Nanofibers Modified with Metal Oxide Nanowires and MXene for Photocatalytic Water Purification*
   Andrii Lys, Valerii Myndrul, Mykola Pavlenko, Błażej Anastaziak, Pavel Holec, Kateřina Vodseďálková, Emerson Coy, Mikhael Bechelany, Igor Iatsunskyi
   Nanomaterials 2025, 15(17), 1371, 2025
   doi.org/10.3390/nano15171371
3. *Core-shell nanofibers of $ZnFe_2O_4$/ZnO for enhanced visible-light photoelectrochemical performance*
   Andrii Lys, Viktor Zabolotnii, Mária Čaplovičová, Iryna Tepliakova, Agris Berzin, Martin Sahul, Ľubomír Čaplovič, Alexander Pogrebnjak, Igor Iatsunskyi, Roman Viter
   Journal of Alloys and Compounds, 984, 173885, 2024
   doi.org/10.1016/j.jallcom.2024.173885
4. *Hierarchically Structured Ti-TiO_2 Membranes Fabricated by Femtosecond Laser Ablation and Atomic Layer Deposition for Enhanced Photoelectrochemical Water Splitting*
   Andrii Lys, Iaroslav Gnilitskyi, Emerson Coy, Mariusz Jancelewicz, Mikhael Bechelany, Igor Iatsunskyi
   ACS Applied Materials & Interfaces, 17(30), 43390-43402, 2025
   doi.org/10.1021/acsami.5c07488

List of abbreviations

ABPE – applied bias photon-to-current efficiency
AFM – atomic force microscopy
ALD – atomic layer deposition
Ar – argon
ATR – attenuated total reflectance
CA – chronoamperometry
CB – conduction band
CPE – constant phase element
CV – cyclic voltammetry
DI – deionised
DMA – N,N-dimethylacetamide
DMF – N,N-dimethylformamide
EDX – energy-dispersive X-ray spectroscopy
EIS – electrochemical impedance spectroscopy
FTO – fluorine-doped tin oxide
FTIR – Fourier-transform infrared spectroscopy
HER – hydrogen evolution reaction
HR-LIPSS – highly regular laser-induced periodic surface structures
HR-TEM – high-resolution transmission electron microscopy
IPCE – incident photon-to-current efficiency
IR – infrared
LiF – lithium fluoride
LIPSS – laser-induced periodic surface structures
LPFSS – laser-processed functional surface structures
LSV – linear sweep voltammetry
MAX phase – layered ternary carbide or nitride precursor phase delamination
MILD – minimally intensive layer
MXene – two-dimensional transition metal carbide, nitride, or carbonitride
NHE – normal hydrogen electrode
OER – oxygen evolution reaction
PEC – photoelectrochemical
PID – polyimide
PL – photoluminescence
PVP – polyvinylpyrrolidone
R6G – rhodamine 6G
Rct – charge-transfer resistance
RHE – reversible hydrogen electrode
RMS – root mean square
Rs – solution resistance
SEM – scanning electron microscopy
SiNR – silicon nanoripples
STH – solar-to-hydrogen efficiency
TEM – transmission electron microscopy
Ti_3AlC_2 – titanium aluminium carbide MAX phase
$Ti_3C_2T_x$ – titanium carbide MXene with surface terminations
UV – ultraviolet
UV-Vis – ultraviolet-visible spectroscopy
VB – valence band
VIS – visible
WE – working electrode
XPS – X-ray photoelectron spectroscopy
XRD – X-ray diffraction
Xe – xenon

Declaration

Declaration of the Author of this dissertation:

I hereby declare that this dissertation entitled **"Architecture-Engineered Semiconductor Nanocomposites for Photocatalytic and Photoelectrochemical Applications"**, submitted to the Faculty of Chemistry at Adam Mickiewicz University, Poznań, for obtaining the degree of Doctor of Philosophy in Chemistry, is my original work, except where specific reference is made to the work of other authors.

I declare that this dissertation has not been submitted, either in whole or in part, for any other degree, award, or qualification at any university or other institution. The dissertation is an authentic work of the Author, and all materials, data, publications, and reproduced content included in it have been used in accordance with applicable academic and legal requirements.

The peer-reviewed publications included in this dissertation were prepared in collaboration with the co-authors. The Author's contributions to these publications are described in the relevant sections of the dissertation and in the author contribution statements.

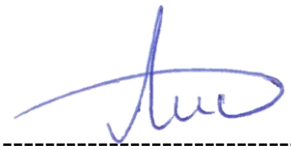

MSc Andrii Lys

Declaration of the thesis Supervisor:

I hereby certify that, to the best of my knowledge, the above statement is true and that this dissertation is ready to be submitted for review.

Supervisor

Prof. dr hab. Igor Iatsunskyi
NanoBioMedical Centre
Adam Mickiewicz University
Poznan, Poland

Aim and scope of the dissertation

This dissertation focuses on the design, preparation, and evaluation of advanced micro- and nanostructured materials for photocatalytic and photoelectrochemical applications. The work is based on the assumption that the behaviour of semiconductor systems is influenced not only by their chemical composition, but also by the architecture of the active material (morphological features), the geometry of the support, and the quality of the interfaces responsible for the transfer and use of photogenerated charge carriers. From this perspective, the dissertation examines how structural design at different length scales can be used to improve light absorption, charge separation, carrier transport, accessibility of the active surface, and the operational stability of the developed systems.

The scientific scope of the dissertation includes three closely connected research directions. The first concerns structured and laser-modified substrates used as platforms for photoactive oxide coatings and hybrid photocatalytic systems. The second research direction is related to immobilised photocatalytic membranes and fibrous systems, including electrospun hybrid materials intended to improve contact with pollutants during irradiation. The third one involves photoelectrochemical electrodes based on structured supports covered with conformal semiconductor coatings, in which interfacial charge transfer and effective extraction of photogenerated carriers are particularly important. Although these research directions involve different material systems and experimental approaches, they are linked by a shared strategy centred on architecture-driven optimisation of semiconductor-based materials.

The dissertation is situated within the field of chemical sciences, with particular attention to functional inorganic and hybrid nanomaterials intended for light-driven applications. It brings together materials synthesis, surface engineering, thin-film deposition, laser structuring, electrospinning, physicochemical characterisation, as well as photocatalytic and photoelectrochemical testing. In this way, the work aims to provide both fundamental and application-related insight into the relationship between structure, interface design, and photoinduced behaviour.

The main aim of the dissertation was to determine how rational structural and interfacial engineering of semiconductor-based materials can improve their photocatalytic and photoelectrochemical behaviour. Particular emphasis was placed on TiO_2-based and related hybrid architectures, especially immobilised and hierarchically organised systems in which morphology, support geometry, heterointerface formation, and deposition strategy may decisively affect the generation, separation, transport, and utilisation of photogenerated charge carriers.

Research questions

In order to achieve this aim, the dissertation addresses the following research questions:

1. To what extent can hierarchical structuring of substrates and supporting architectures improve light management, surface accessibility, and charge transport in semiconductor-based photocatalytic and photoelectrochemical systems?
2. How far can atomic layer deposition-based conformal oxide coatings improve the continuity of the deposited layer and the quality of the oxide-support interface, and how do these changes translate into the functional behaviour of structured metallic or semiconducting supports?
3. What role does the formation of heterostructures and hybrid materials play in limiting charge-carrier recombination and improving photocatalytic or photoelectrochemical performance?
4. How do immobilised fibrous and membrane-type photocatalysts compare with conventional particulate systems in terms of practical use, reusability, and transport-related limitations?
5. Which changes in performance can be associated with reasonable confidence with structural and interfacial factors, and which need to be interpreted more cautiously because they may also be influenced by adsorption, optical effects, differences in surface area, or wetting behaviour?
6. Can the joint consideration of photocatalytic and photoelectrochemical systems provide a broader mechanistic picture of how architecture-driven materials design influences photoinduced processes in semiconducting materials?

Originality and scientific contribution of the dissertation

The originality of the dissertation lies in its joint consideration of photocatalytic and photoelectrochemical material systems from a common architecture-oriented perspective. Rather than analysing each material platform as a separate case, the work treats morphology, hierarchical organisation, interface design, immobilisation strategy, and fabrication route as interconnected factors that collectively shape functional behaviour across different photoactive systems.

A major contribution of the work is the demonstration that structured supports and immobilised architectures may function not only as carriers of the active phase, but also as elements that influence optical behaviour, charge-transport pathways, interfacial kinetics,

and system stability. This aspect is particularly important in the case of membrane-type and fibrous materials, where geometric organisation and accessibility of the active surface strongly affect the observable photocatalytic response.

Another original aspect of the dissertation is the use of advanced fabrication and modification approaches, including femtosecond-laser structuring, atomic layer deposition, and electrospinning-based preparation of hybrid fibrous systems, to generate materials with controlled architecture across several length scales. The combination of these methods made it possible to investigate how micro- and nanoscale organisation influences the behaviour of semiconductor-based systems under irradiation.

The dissertation also contributes to the interpretation of photocatalytic and photoelectrochemical data by considering performance trends with particular care. Attention is paid to separating apparent improvement from mechanistically relevant enhancement, including the possible effects of adsorption, immobilisation, interface quality, charge recombination, and carrier extraction. In this way, the work not only presents activity trends but also attempts to explain them in a chemically and physically grounded way.

From an application point of view, the dissertation provides useful design principles for the development of structured photocatalysts and photoelectrodes that combine improved functionality with greater practical relevance. This is especially significant for immobilised systems, where ease of recovery, reusability, and integration into larger devices are important considerations alongside the activity itself.

Structure of the dissertation

The dissertation follows a publication-based structure, but the published papers are not treated as independent chapters inserted into the main text without interpretation. Instead, the main body of the dissertation is organised as an integrating scientific narrative. It first develops the theoretical and literature background needed to understand the research problem, and then explains how the individual publications contribute to one common architecture-driven framework. The full publications are reproduced at the end of the thesis file as a separate publication section, so that the main text can remain focused on synthesis, interpretation, and the relationship between the studies.

Chapter 1 presents the broader scientific background of photocatalysis and photoelectrochemistry, with particular emphasis on the connection between environmental and energy-related challenges and the behaviour of semiconductor materials under irradiation. It discusses the main physicochemical principles governing light absorption, charge generation, charge separation, recombination, carrier transport, and interfacial redox processes, thereby providing the theoretical foundation for the dissertation.

Chapter 2 presents the literature background needed to understand the material systems and design choices used in the dissertation. It focuses on TiO_2-based photoactive materials, heterostructure and interface engineering, hierarchical and laser-structured supports, ALD thin-film deposition, MXene-containing hybrids, and electrospun membrane photocatalysts. The chapter is not written only as a general review. It also points out the main limitations in the field, including unclear mechanism assignment, difficult comparison between studies, incomplete stability discussion, and the need for better control of architecture and interfaces. These points provide the basis for the studies presented later in the dissertation.

Chapter 3 provides an overview of the publication-based research and explains how the included papers are connected scientifically. Although the individual publications concern different material systems and experimental configurations, they are united by a common focus on architecture-controlled enhancement of photocatalytic and photoelectrochemical behaviour. This chapter also clarifies the doctoral candidate's contribution to the presented works and shows how each publication fits into the broader research objective.

The following part of the dissertation provides a general discussion and conclusions based on the combined interpretation of the publication set. In this part, the results reported across the individual studies are compared from a broader perspective, with attention to common mechanisms, limitations, and design principles. The discussion does not simply repeat the results of the papers, but uses them to explain how architecture, interface quality, immobilisation strategy, and support geometry influence the utilisation of photogenerated charge carriers.

The full published papers are included at the end of the thesis in their published form. This final publication section serves as documentation of the peer-reviewed research output on which the dissertation is based. Short contextual introductions are used to connect the papers with the main thesis framework, but the scientific synthesis and interpretation are developed in the main dissertation text.

Relationship between the included publications and the main thesis objective

The publications included in this dissertation form a connected group of studies rather than separate examples. They all address the same main question: how the form of a semiconductor system affects its photocatalytic or photoelectrochemical behaviour. The papers differ in composition, fabrication route, and testing method, but each of them treats the material as more than a chemical phase. Morphology, support geometry, interface

contact, immobilisation, and charge-transfer pathways are considered as parts of the working system. This is the common link between the publication set.

The first publication focuses on laser-structured silicon modified with MXene and ALD TiO_2. The silicon nanoripples provide the ordered surface texture, the TiO_2 layer gives the system a stable photocatalytic oxide surface, and MXene is introduced to improve the contact for charge transfer. The importance of this work lies in the combination of these elements. The improved photocatalytic response is not assigned to one component alone, but to the way surface structuring, conformal oxide coating, and the conductive interphase are brought together in one material system.

The second publication deals with the electrospun membrane system. In this case, TiO_2, WO_3, and $Ti_3C_2T_x$ MXene are introduced into polyimide nanofibres to obtain a photocatalyst that is fixed in a recoverable form. This changes the interpretation of the result. The material is no longer only a set of active phases, because the fibre mat also controls how the dye solution enters the structure, how much surface is wetted, how light reaches the active regions, and how the sample behaves during reuse. The oxides and MXene are important for charge separation and recombination, but the membrane format decides how effectively these components are exposed during the test. For this reason, the study supports the idea that photocatalytic activity in immobilised systems depends on both composition and fibrous architecture.

The third direction is covered by the $ZnFe_2O_4$/ZnO core-shell nanofibre study. This paper brings a related, but non-TiO_2, oxide system into the dissertation. The important point is the way the two oxides are organised inside the fibre. During annealing, Fe- and Zn-containing regions interdiffuse, so the final material is shaped by both the intended core-shell design and the interface that forms between $ZnFe_2O_4$ and ZnO. This affects light absorption and the PEC response under visible illumination. The study is included because it shows the same architectural problem in another oxide system: the performance of a photoelectrode depends not only on which phases are present, but on how they are arranged, connected, and able to support charge separation.

The fourth publication returns to TiO_2, but in the form of a structured Ti-TiO_2 photoelectrode. Here, femtosecond laser ablation is used to shape the titanium support, and ALD is used to deposit TiO_2 layers with controlled thickness. The importance of this study is that the support and oxide layer are designed to work together. The laser-made titanium scaffold improves light interaction and surface accessibility, while the ALD coating provides the photoactive oxide interface. By changing the TiO_2 thickness, the work examines how coating continuity, crystallinity, charge-transfer behaviour, and light use affect the PEC response in a binder-free electrode platform.

Taken together, the publications show how the same research idea was tested in several material formats. The systems are not identical: one uses a laser-structured Si surface,

another uses an electrospun membrane, another is based on core-shell oxide fibres, and the final one uses laser-structured Ti coated with ALD TiO_2. What connects them is the way the active phase is built into the material. In each case, the final performance depends not only on the chemical composition, but also on whether the active layer or component is properly exposed, connected, and supported by the surrounding structure. For this reason, the publications are discussed as one research line focused on architecture-controlled photoactivity, rather than as separate studies grouped only by application.

The publications also make clear that the results have to be interpreted within limits. Better dye removal or a higher photocurrent does not automatically indicate a single cause. In the photocatalytic studies, the measured response can include the effect of adsorption, wetting, scattering, and access of the dye to the active surface. In the PEC studies, the current is shaped by the full electrode structure, including contact with the electrolyte, geometry of the support, interfacial resistance, and stability during operation. Therefore, the dissertation does not treat performance as a simple consequence of composition. The improvement is discussed in relation to how each material is built and how it works under the given test conditions.

.

Chapter 1. Background and theoretical framework

1.1. Motivation: water quality and renewable fuels as a unified challenge for materials and interfaces

The scientific motivation of this dissertation arises from two closely linked challenges that increasingly shape research on functional semiconductor materials: the need for more effective treatment of contaminated water and the need for low-carbon routes of solar energy conversion. Although these problems are often discussed separately, both depend on the development of materials capable of absorbing light, generating charge carriers, and directing interfacial redox processes in a controlled and efficient way. Conventional water-treatment methods, including adsorption, coagulation, membrane separation, and biological processing, are still commonly applied. However, they are often insufficient for persistent organic contaminants. They may also produce secondary waste, so the pollutant is not removed directly and additional treatment is still needed. For this reason, advanced oxidation methods, including heterogeneous photocatalysis, remain attractive because they can degrade contaminants chemically at illuminated solid-liquid interfaces, instead of only separating them from water or retaining them temporarily. [1], [2]

In parallel, interest in renewable fuels is growing because solar and wind energy are inherently intermittent and therefore require effective ways of storing energy in chemical form. Hydrogen is considered one of the most promising options, since it can be produced from water and later used in energy-conversion systems or chemical processes. In this context, photoelectrochemical water splitting aims to use light directly to drive electrochemical reactions leading to hydrogen and oxygen evolution. Although this application differs from photocatalytic pollutant degradation, the fundamental limitations are very similar. The absorption of light first produces electron-hole pairs. However, their contribution to the reaction depends on whether they reach the active interface and participate in redox processes before being lost by recombination. [3], [4]

Although photocatalytic pollutant degradation and photoelectrochemical energy conversion are usually treated as separate application fields, they are governed by closely related physicochemical requirements. In both cases, useful performance is determined not only by light absorption itself, but by a sequence of linked processes. These include the generation of electron-hole pairs, limiting their recombination, transport of the carriers to reactive interfaces, and a proper relationship between the material structure and the interfacial reaction pathway. Seen in this way, the main limitation is not simply the band structure of the semiconductor. It is also shaped by the combined effect of architecture and interface quality. Both surface structure and bulk organisation influence how light is utilised and how reactive sites are arranged. Interfaces, in turn, have a strong effect on charge transfer, recombination behaviour, and the stability of the system during operation. For this

reason, further improvement in photocatalysis and photoelectrochemistry increasingly depends on structured and hybrid systems in which light harvesting, charge transport, and interfacial reactions are considered together, rather than adjusted separately. [5], [6]

1.1.1 Why architecture and interfaces are central variables

In many photoactive systems, composition alone is insufficient to explain their functional performances. The final response of a photocatalyst or photoelectrode depends on several connected processes, including photon absorption, generation of charge carriers, their separation, transport to the interface, interfacial charge transfer, and the rate of the corresponding redox reaction. All of these stages can be affected by architectural features such as film thickness, porosity, hierarchical roughness, surface periodicity, or the way heterointerfaces are distributed in hybrid materials. Even if the composition does not change, differences in architecture may still modify the optical path length, diffusion distance, wetting behaviour, adsorption conditions, and the likelihood of recombination. This perspective is particularly important in the present dissertation, where structured substrates, conformal oxide coatings, immobilised photocatalytic membranes, fibrous hybrid materials, and photoelectrochemical electrodes are considered as systems in which geometry and interface quality are part of the functional design, not just secondary structural details. [2], [5]

Within this architecture-focused approach, atomic layer deposition (ALD) is particularly important because it allows conformal coatings to be deposited with nanometre-level thickness control even on complex surfaces with high aspect ratios. This makes it possible to adjust thickness, coverage, and interface quality in a controlled way without losing the original geometry of the support. As a result, reproducibility can be improved and the interpretation of the observed mechanisms becomes less ambiguous. [7]

1.1.2 Practical relevance of immobilised platforms and hybrid interfaces

Architecture is important not only for understanding the mechanism, but also for practical use of the material. In many photocatalytic studies, dispersed powders are chosen mainly because they provide a high surface area. However, this format creates obvious difficulties at later stages, especially when separation, reuse, and stable control of optical or transport conditions are needed. For this reason, immobilised systems such as thin films, coated structured substrates, and membrane-type architectures are an important alternative. They are easier to handle, they make reuse more realistic, and they usually allow better control over mass transport in the working system. [1]

Conductive interlayers and two-dimensional phases such as $Ti_3C_2T_x$ MXene, are often added to semiconductor systems to help remove photogenerated charges from the oxide and reduce recombination. In practice, however, this benefit appears only if the added phase is well dispersed, remains in close contact with the semiconductor, and does not

degrade during irradiation in water. For this reason, the presence of MXene or another conductive phase is not treated here as proof of improved charge transfer by itself. Its role is considered only in relation to the real material architecture, interface quality, and stability of the system. [8]

1.1.3 Thesis positioning and continuity

This dissertation is based on an architecture-driven view of photocatalysis and photoelectrochemistry. A central part of the work is the use of fabrication methods that allow deliberate control over the shape of the material, the quality of the interfaces, and the way the active phase is immobilised. This creates a link between photocatalytic degradation studies, where chemical conversion is the main result being followed, and photoelectrochemical experiments, where charge utilisation can be assessed more directly from electrochemical data. As a result, the common framework of the dissertation is based not simply on the application itself, but on the broader question of how structure and interfaces influence photoinduced behaviour in different experimental systems. [4]

1.2. From photons to chemical change: photoexcitation, carrier fate, and architecture-controlled losses

1.2.1. Photon energy, absorption threshold, and the physical meaning of photoexcitation

Any discussion of photocatalysis and photoelectrochemistry in this work must start from the same elementary event, namely, the absorption of light by the semiconductor. Only after that step does it become possible to discuss the generation of non-equilibrium charge carriers and their later role in photocatalytic or photoelectrochemical response. The energy of a photon is given by:

$$E = h\nu = \frac{hc}{\lambda} \tag{1}$$

where h is Planck's constant, c is the speed of light, ν is photon frequency, and λ is the wavelength. For a semiconductor, photoexcitation occurs when the incoming photon has an energy equal to or greater than the band gap. This promotes an electron from the valence band to the conduction band and leaves behind a hole. This process is usually written in its simplest form as the generation of an electron-hole pair:

$$Semiconductor + h\nu \longrightarrow e^-_{CB} + h^+_{VB} \tag{2}$$

This equation should be understood only as a representation of charge-carrier generation and not as a direct indicator of photocatalytic or photoelectrochemical performance.

In real photocatalytic and photoelectrochemical systems, the measurable chemical or electrochemical response depends on how many of the generated charge carriers avoid recombination, reach the relevant interface, and then take part in interfacial redox reactions. Consequently, even materials with apparently favourable band gaps may exhibit limited functional performance when recombination dominates or when interfacial charge transfer is sluggish. This is one of the main reasons why interface quality and architecture control are treated in this dissertation as primary variables in the interpretation of photoactive behaviour, especially in complex and structured systems. [9], [10]

Charge carriers are not generated uniformly throughout the material. Their formation depends partly on wavelength-dependent absorption, but also on how light is distributed inside the structure. This becomes especially important in thicker or strongly scattering systems, such as porous films, rough coatings, and fibrous membranes. In these cases, multiple scattering can make the light travel a longer effective path, but the photon flux inside the material is no longer evenly distributed. Some regions may therefore receive more light than others. This matters in practice for two reasons. First, carrier generation is more useful when it occurs closer to the reactive interface, because otherwise recombination may take place before the carriers arrive there. Second, comparison between samples becomes more difficult, since a change in architecture alone may already alter light distribution and apparent light utilisation, even if the intrinsic properties of the material remain unchanged. [11]

In dye-based photocatalytic experiments, the observed activity does not necessarily originate from a single mechanism. Besides direct excitation of the semiconductor, the dye may also absorb visible light and behave as a sensitiser, transferring electrons to the semiconductor. In that case, the degradation pathway no longer reflects only the intrinsic band-gap excitation of the photocatalyst. Because of this, results from dye systems need to be interpreted carefully. An increase in activity should not be explained only by electronic modification of the semiconductor unless this is supported by proper control experiments and additional evidence. [12], [13]

1.2.2. Charge carrier transport and recombination: diffusion length as an architectural constraint

The generation of charge carriers does not guarantee useful functions. At that stage, the important question is whether they recombine or whether they are transported to the interface and used there. In many semiconductor systems, this can be treated, in a first approximation, in terms of diffusion-based concepts:

$$D = \mu \frac{k_B T}{q} \tag{3}$$

where D is the carrier diffusion coefficient, μ is the mobility, k_B is the Boltzmann constant, T is the absolute temperature, *and* q is the elementary charge. The characteristic travel distance before recombination is the diffusion length:

$$L = \sqrt{D\tau} \tag{4}$$

where L is the diffusion length in cm or nm, and τ is the effective carrier lifetime, which includes bulk and surface recombination. In practical terms, these parameters show how far a generated charge carrier can move before it is lost by recombination. If a carrier is formed too far from the reactive interface, it is unlikely to take part in the reaction. For this reason, the efficiency of a photoactive layer depends strongly on the relation between the place where carriers are generated and the distance they need to travel. This explains why nanostructured materials and thin conformal coatings may give better performance than thicker planar layers, even when the composition is the same. [9], [10]

The architecture does not improve the performance by default. A larger surface area and a higher number of interfaces can provide more active contact with the electrolyte, but they can also create additional surface states and trap sites. In that case, recombination may become faster and the effective carrier lifetime shorter. Porous or high-aspect-ratio structures can also become resistive if the electrical pathway through the material is not sufficiently continuous. For this reason, architecture has to be optimised as a balance: it should shorten transport distances and increase accessibility without adding too many recombination sites or weakening charge transport. [14]

ALD was used because it can deposit TiO_2 evenly on structured surfaces while keeping the layer thickness under control. This is important for Ti/TiO_2 photoelectrodes, where the surface shape and the oxide coating both affect the final response. By changing the TiO_2 thickness, it is possible to see how much of the behaviour comes from the structured Ti support and how much from the deposited oxide layer. The coating thickness also affects light absorption, carrier transport, and whether the photoactive layer fully covers the surface. [7]

In this dissertation, these relations are used mainly to guide the interpretation of the later experimental chapters. If a particular architecture improves dye-degradation kinetics or increases photocurrent, the change is not attributed to composition alone. It is considered in terms of carrier transport, recombination, distance to the active interface, and the possible role of surface or defect states. [6]

1.2.3. Optical response in heterogeneous architectures: Kubelka-Munk analysis, Tauc plots, and limitations of band-gap inference

Optical characterisation is used in both photocatalysis and photoelectrochemistry mainly to assess light harvesting, compare samples that differ in composition or structure,

and estimate the optical band gap. At the same time, in heterogeneous materials, it is not always easy to move from raw reflectance or absorbance data to conclusions that are physically well justified. This becomes especially important in architecture-driven systems, where surface structuring, porosity, and the presence of several components can substantially affect the optical field distribution as well as the apparent position of the absorption edge. [15]

For samples that scatter light strongly, such as powders, porous films, rough membranes, and fibre mats, diffuse reflectance data are often analysed with the Kubelka-Munk approach. The corresponding Kubelka-Munk function is written as:

$$F(R) = \frac{(1-R)^2}{2R} \tag{5}$$

where R is diffuse reflectance. In the simplest interpretation, $F(R)$ is used as a proxy for an absorption-related quantity under the assumptions of an optically thick, diffusely scattering medium. The Kubelka-Munk function is often used as an absorption-related parameter for samples that are optically thick and diffusely scattering. However, this assumption is not equally valid for all materials. In structured samples, the result may depend strongly on morphology, scattering, and measurement geometry. Therefore, in this thesis, Kubelka-Munk analysis is treated mainly as a comparative tool for samples measured under the same conditions, not as a direct measure of the intrinsic absorption coefficient. [15]

Optical band-gap values are often estimated with the help of a Tauc-type relationship:

$$[F(R)h\nu]^n = A\left(h\nu - E_g\right) \tag{6}$$

where A is a constant, E_g is the optical band gap, and n is chosen based on the assumed transition type (e.g., direct allowed, indirect allowed). In porous and fibrous materials, scattering is usually strong and changes with wavelength. This can shift the baseline and make the selected linear part of the Tauc plot depend strongly on how the data are treated. For this reason, the obtained values should be treated as apparent optical gap estimates rather than exact band-gap values. This is especially important for structured materials, where changes in reflectance may come from light trapping by the geometry rather than from a real change in electronic structure. [11], [15]

Real oxides often exhibit defect-related states that give rise to sub-band-gap absorption tails. Such tails are often more pronounced in nanostructured and defect-rich surfaces, where the density of surface states and oxygen vacancies may increase. An apparent red shift in optical response should therefore not automatically be interpreted as a true reduction of the band gap, because it may instead reflect defect states, disorder, or overlapping optical processes. [9]

In hybrid systems, the measured optical response usually comes from more than one component. This is particularly important when the material contains several semiconductors or conductive additives such as MXene. These components may increase background absorption or change the scattering behaviour of the sample. However, this does not necessarily mean that more useful charge carriers are produced in the main photoactive phase. For this reason, optical data should be interpreted together with functional measurements, such as degradation kinetics, photocurrent response, and other indicators of interfacial charge transfer. [10]

For architecture-controlled systems, an important interpretive point is that improved functional performance may arise from optical management alone, including light trapping and multiple scattering, without any intrinsic change in electronic structure. This distinction is essential in later discussion of structured and porous platforms, where reflectance changes may be dominated by geometry rather than by genuine band-structure modification. [11]

1.2.4. Hybrid interfaces and conductive phases: mechanistic roles, risks of over-interpretation, and evidence standards

In many hybrid photocatalysts and photoelectrodes, the semiconductor is combined with other functional components in order to improve the use of photogenerated charge carriers. The goal is not just to absorb more light but to ensure that more of the generated carriers participate in interfacial chemistry or contribute to the photocurrent instead of recombining. This is particularly relevant for wide-band-gap oxides, where recombination and interfacial resistance may control the final response even if light absorption itself is not the main limiting factor. [10]

Conductive additives are often added to help extract electrons from the semiconductor and reduce electron–hole recombination. This effect is possible only when the additive is well connected to the photoactive phase. Good interfacial contact and continuous transport pathways are therefore important. If these conditions are not met, the additive may instead reduce performance by blocking active areas, changing light absorption, or introducing additional recombination sites. [8]

Hybrid interfaces are also frequently discussed using band-alignment arguments, for example when electron transfer from a semiconductor conduction band to a conductive phase or second semiconductor is proposed. Such models are useful as design tools, but in highly nanostructured and porous systems interfacial energetics may also be influenced by surface states, adsorption, hydroxylation, and local potential gradients. Therefore, band alignment arguments should be used with caution unless they are supported by independent evidence consistent with the proposed charge-transfer pathway. [5], [6]

In dye-degradation experiments, better activity does not always mean better charge separation. Hybridisation can also change dye adsorption, wetting, scattering, and the local

light intensity near the sample. All of these factors may influence the apparent degradation rate. For this reason, the results should be interpreted carefully and compared with dark adsorption tests, repeated-cycle measurements, and structural and optical data. [1], [12]

For conductive two-dimensional phases such as MXenes, stability has to be considered together with the proposed mechanism. During irradiation in water, MXenes may oxidise or change their surface terminations, and these changes can affect how charges are transferred at the interface. Therefore, in MXene-containing hybrids, the conductive additive should not be treated as a fixed and unchanged component during operation. Its possible chemical evolution has to be considered when the charge-transfer mechanism is discussed. [8]

1.2.5. Thermodynamic feasibility, band-edge requirements, and electrochemical potential scales (RHE/NHE)

A photoelectrochemical process can only proceed if it is thermodynamically feasible, that is, if the photogenerated carriers are able to drive the required redox reaction. For photoelectrochemical water splitting, this point is usually considered with respect to the thermodynamic potentials of hydrogen and oxygen evolution and how these vary with pH. However, thermodynamic feasibility is not the same as practical efficiency. Even if the band edges are favourably positioned from a thermodynamic point of view, the actual performance can still be limited by reaction kinetics, recombination, and resistive losses at the semiconductor-electrolyte interface:

$$E(O_2/H_2O) = 1.229V \text{ vs RHE} \tag{7}$$

$$E(H^+/H_2) = 0V \text{ vs RHE} \tag{8}$$

These values should be understood as thermodynamic limits, not as direct indicators of how well a real device performs in practice. For meaningful comparison between systems, it is also necessary to report the potential scale, illumination conditions, and electrode area in a consistent way. In addition, the interpretation becomes stronger when efficiency metrics are used to connect the measured current to the corresponding useful chemical output. [4]

In aqueous systems, redox potentials do not remain constant, because they depend on conditions such as pH and species activity. This dependence is usually described by the Nernst equation:

$$E = E° - \frac{RT}{nF} \ln Q \tag{9}$$

where $E°$ is the standard potential, R is the gas constant, T is temperature, F is the Faraday's constant, n is the number of electrons, and Q is the reaction quotient. This is important in photoelectrochemical analysis because pH changes both the thermodynamic reference level and the conditions at the semiconductor-electrolyte interface. Therefore, potentials should

be reported together with the pH and the reference electrode. Without these details, comparison between studies becomes uncertain and the interpretation of onset potentials or band positions is much weaker.

Because photoelectrochemical measurements are carried out with different reference electrodes, the reported potentials are not always directly comparable. Converting them to a common scale, for example RHE or NHE, is therefore important for correct interpretation of onset potentials and band-edge positions:

$$E_{RHE}=E_{ref}+E^{\circ}_{ref}+0.0591\ pH \tag{10}$$

where E_{ref} denotes the measured potential versus the reference electrode, and E°_{ref} is the standard potential of that reference relative to SHE. Because of this, meaningful comparison is only possible when the reference electrode, pH, and conversion procedure are reported explicitly. This is particularly relevant in structured electrodes, since both current density and local potential distribution may change across the surface. [4], [5]

Thermodynamic feasibility should not be considered the same as practical efficiency. Even if the band-edge positions are favourable for a given reaction, the actual performance still depends on factors such as interfacial kinetics, charge-transfer resistance, recombination losses, and transport limitations. This is particularly clear for oxygen evolution at semiconductor interfaces, which is a demanding multistep process that is strongly affected by charge accumulation at the interface. For that reason, meaningful improvement in photoanode behaviour depends to a large extent on careful interface engineering. [6]

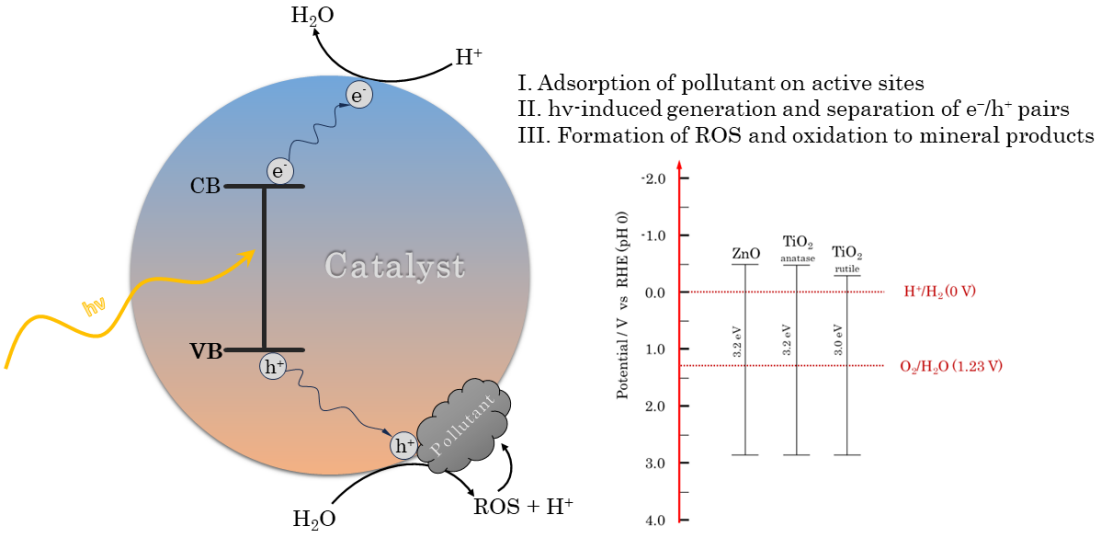

Figure 1.1. *General scheme of semiconductor photocatalysis in aqueous media, illustrating photon absorption, generation of electron-hole pairs, their separation and recombination pathways, interfacial charge transfer, and the formation of the main reactive oxygen species. Approximate band-edge positions and aqueous redox levels are also included to support the mechanistic discussion. Prepared by the author.*

1.2.6 Reactive oxygen species (ROS) pathways and their dependence on charge extraction, oxygen availability, and adsorption regime

In aqueous photocatalytic systems, degradation of organic pollutants is often discussed through the involvement of reactive oxygen species. When oxygen is present in solution, it can accept electrons from the irradiated semiconductor and participate in a series of reduction steps that form reactive intermediates. At the same time, photogenerated holes may contribute through separate oxidation pathways. The main reactions considered in this context are listed below.

$$O_2 + e^- \rightarrow O_2^{\bullet -} \quad (11)$$

Superoxide can then undergo protonation to form hydroperoxyl radicals:

$$O_2^{\bullet -} + H^+ \rightarrow HO_2^{\bullet} \quad (12)$$

Two hydroperoxyl radicals can disproportionate to yield hydrogen peroxide and oxygen:

$$2HO_2^{\bullet} \rightarrow H_2O_2 + O_2 \quad (13)$$

Hydrogen peroxide can subsequently accept an electron to form hydroxyl radicals:

$$H_2O_2 + e^- \rightarrow {\bullet}OH + OH^- \quad (14)$$

In parallel to oxygen-mediated routes, photogenerated holes can generate hydroxyl radicals via oxidation of water (or surface hydroxyls), represented as:

$$H_2O + h^+ \rightarrow {\bullet}OH + H^+ \quad (15)$$

These reactions provide a useful mechanistic framework, but the dominant pathway is not universal. The effective contribution of each route depends on the efficiency of electron delivery to the dissolved oxygen, the efficiency of hole delivery to surface-bound water or hydroxyl groups, and the strength of pollutant adsorption at or near the reactive interface. Architecture modifies all of these factors by changing transport distances, wetting behaviour, adsorption environment, and the density of recombination-active interfacial states. [2], [10]

The oxygen-reduction pathway may be restricted by limited oxygen availability close to the active interface and by the rate at which electrons are transferred to dissolved oxygen.

This issue becomes more important in porous films and membrane-type photocatalysts, where oxygen concentration may vary within the structure because diffusion is not uniform and liquid penetration may be incomplete. As a result, changes in the observed kinetics do not always reflect only intrinsic charge-carrier behaviour, but may also be influenced by transport conditions. For this reason, interpretation based on reactive oxygen species is more convincing when the proposed reaction pathways are considered together with practical operating conditions, including stirring, flow, irradiation geometry, solution composition, and whether the catalyst is used in dispersed or immobilised form. [1]

Oxidation driven by photogenerated holes may take place either through formation of hydroxyl radicals or through direct oxidation of adsorbed species. The importance of these routes depends on the adsorption conditions, surface chemistry, and efficiency of charge carrier extraction before recombination. For this reason, reactive-oxygen-species pathways should not be treated as a universal fixed sequence. In practice, they are better understood as the result of a coupled interplay between carrier behaviour and the interfacial environment. [10]

Dye-degradation experiments create additional interpretive difficulties. The dye does not always act only as a pollutant, because it may also function as a sensitiser. In that case, electron injection may proceed through pathways connected with dye adsorption and dye light absorption rather than with intrinsic excitation of the semiconductor. Rapid loss of colour should also be treated carefully, because decolourisation does not automatically mean full mineralisation. At early stages, the concentration decrease may be dominated by adsorption, especially in membrane and hybrid systems with large accessible surface area and many functional groups. For this reason, results obtained with dyes need to be discussed with clear attention to adsorption equilibration, sensitisation effects, and the limitations of UV-Vis monitoring as an indicator of deeper chemical conversion. [12], [13]

In photoelectrochemical platforms, charge utilisation is seen more directly through photocurrent recorded under controlled bias. Illumination-dependent impedance behaviour can also provide extra evidence for improved interfacial charge transfer. This is why the combined use of photocatalytic and photoelectrochemical readouts is an important strength of the research strategy adopted in this dissertation. This helps distinguish real charge-utilization effects from adsorption-related changes, which can strongly influence dye-based photocatalytic experiments. [4]

1.3. Photocatalysis in water purification: reaction pathways, kinetics, and practical limits of interpretation

This section focuses on the main reaction pathways involved in the photocatalytic removal of pollutants from water, together with the practical difficulties that arise when such results are interpreted. In aqueous media, these reactions may proceed by direct electron or

hole transfer to adsorbed species, but they may also involve reactive oxygen species that are formed first and then participate in further oxidation steps. In real systems, however, pollutant removal is not controlled by one process alone. It depends on the combined effect of light utilisation, charge-carrier separation and recombination, adsorption, accessibility of active sites, and transport conditions in the reactor. Therefore, photocatalytic results can only be compared meaningfully when key experimental factors, especially illumination geometry, catalyst architecture, and adsorption-equilibration conditions, are handled and described consistently. [1], [16]

1.3.1. Reactive oxygen species framework and its practical meaning in dye degradation experiments

In oxide-based photocatalysis, reactive oxygen species (ROS) are often used as the main framework for discussing dye degradation and, more generally, the oxidation of organic pollutants. Under oxygenated aqueous conditions, photogenerated electrons can reduce dissolved oxygen to superoxide-type species, whereas photogenerated holes may oxidise water or surface hydroxyl groups and thereby form hydroxyl radicals. These pathways provide a useful mechanistic basis for discussing photocatalytic oxidation, and they are summarised in this section by Eqs. (11)–(15).

These reactions are useful for describing possible degradation routes, but they should not be treated as one fixed sequence that applies to every photocatalyst. Oxygen-mediated oxidation and hole-driven oxidation can contribute to different extents, depending on the oxygen availability, pH, adsorption, intermediate protonation, and the ability of charge carriers to reach the surface before recombination. In immobilised films and membranes, the situation is even more dependent on the material format, because wetting and permeability can limit both oxygen supply and pollutant transport inside the structure. Under such conditions, the measured rate may be controlled partly by transport and accessibility, not only by the intrinsic photochemistry of the material. [2], [10]

An additional limitation concerns dye-based systems specifically. In addition to oxidation driven by reactive oxygen species, the dye itself may behave as a photosensitizer under visible light. In this case, electrons can be injected into the semiconductor and degradation pathways that do not arise directly from the intrinsic excitation of the photocatalyst are initiated. Because of this, dye degradation is useful mainly as a comparative screening tool. Stronger conclusions about visible-light photocatalysis should be based on suitable control experiments and, where possible, supported by consistent behaviour across different probes or pollutant types. [12]

1.3.2. Concentration tracking by UV-Vis and the role of adsorption equilibration

The most common method for monitoring dye removal is UV-Vis spectroscopy, in which absorbance at the characteristic wavelength is followed as a function of irradiation time. Concentration is then estimated from the Beer-Lambert relationship using the expressions given below:

$$A=\varepsilon l C \tag{16}$$

where A is absorbance, ε - molar extinction coefficient, l - optical path length, and C - concentration. Rearrangement gives:

$$C=\frac{A}{\varepsilon l} \tag{17}$$

Before illumination, the sample should first be allowed to reach adsorption equilibrium in the dark. This step is important because hybrid and membrane-type materials can remove part of the dye by adsorption alone. If this initial decrease is mixed with the illuminated stage, the photocatalytic rate may appear higher than it actually is. The problem is especially relevant for fibrous immobilised systems, where high accessible surface area, surface functional groups, and slow diffusion into the fibre network can all affect the measured concentration before photocatalysis actually starts. [12]

Optical artefacts also need to be taken into account. In scattering systems such as powders, fibre mats, and rough membranes, apparent absorbance changes do not always result only from concentration changes. They may also arise from baseline drift, light scattering, or inconsistencies during sampling. Because of this, UV-Vis data can be interpreted as real concentration changes only when sampling is carried out in a consistent way, the cuvette geometry is kept identical, and the timing of measurements remains stable. [15]

When photocatalysts are compared quantitatively, the test conditions must be described in sufficient detail for a meaningful comparison. Formal standards can help with this, but the same logic applies even when a custom reactor is used. The irradiation conditions, sampling procedure, adsorption-equilibration step, and measurement geometry should be stated clearly, otherwise differences in performance may reflect the experiment as much as the material itself. [17]

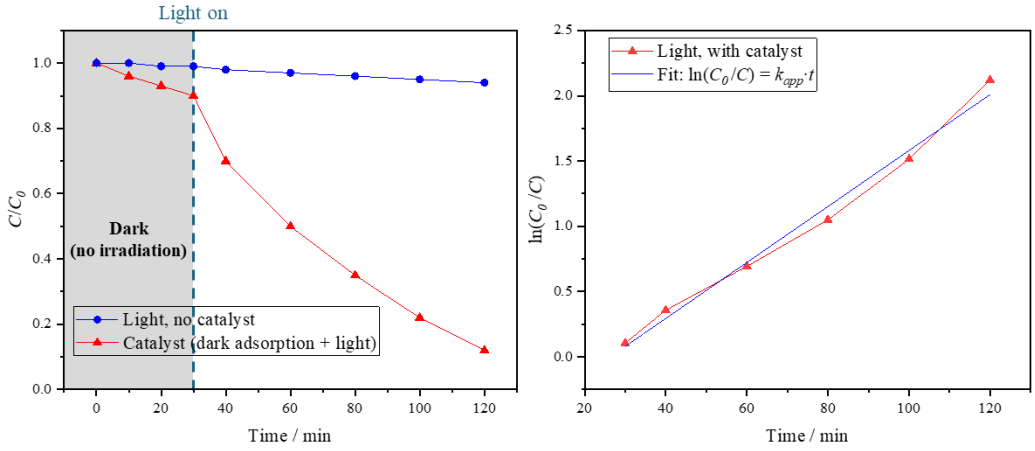

Figure 1.2. *Illustration of a typical photocatalytic dye-removal experiment, including dark adsorption equilibration followed by illumination, and the standard linearisation used for pseudo-first-order kinetics (e.g., ln(C₀/Cₜ) vs time) Prepared by the author.*

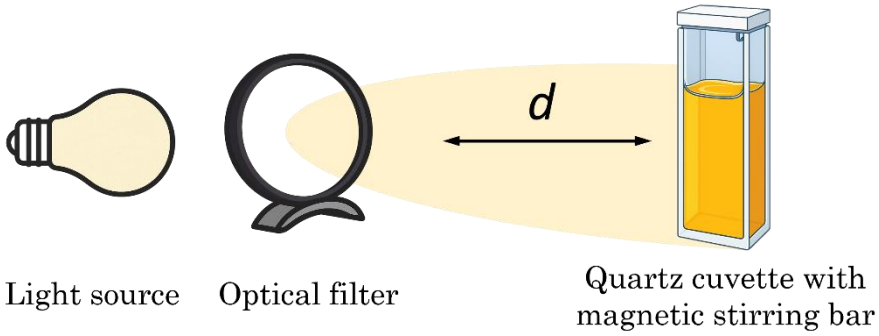

Figure 1.3 *Scheme of the UV-Vis absorption measurement arrangement, showing the optical path length (l) and emphasising that the measurement configuration should remain unchanged in order to obtain reproducible concentration values based on the Beer-Lambert relation. Prepared by the author.*

1.3.3. Pseudo-first-order kinetics: usefulness, limits, and what the rate constant represents

Photocatalytic dye degradation is often described with a pseudo-first-order kinetic model. This approach is usually applied when the dye concentration is low and the catalyst loading is sufficiently high to maintain approximately steady surface conditions. Under these assumptions, the degradation rate and its linearised form may be written as follows.

$$\eta_{deg}(\%) = \frac{C_0 - C_t}{C_0} \times 100 \qquad (18)$$

where C_0 denotes the starting concentration, often taken after the adsorption-equilibration stage, and C_t is the concentration measured at time t. Under conditions of low dye concentration and moderate catalyst loading, the experimental data are often approximated with an apparent pseudo-first-order expression:

$$ln\left(\frac{C_0}{C_t}\right) = k_{app}t \tag{19}$$

where k_{app} is the apparent rate constant. The apparent rate constant should be interpreted as an effective descriptor of the observed experiment rather than as a universal intrinsic constant of the material itself.

The plot of $\ln(C_0/C_t)$ versus time gives an apparent rate constant, which is useful for comparing samples tested in the same setup. This value should not be treated as a material constant, because it depends on the irradiation conditions, reactor geometry, catalyst loading, mixing, adsorption, and oxygen availability. For immobilised catalysts, wetting and internal transport may also affect the fitted value. Therefore, the rate constant is used here only as a comparative parameter under fixed experimental conditions. [18], [19]

One practical consequence is that the early part of the dataset may reflect adsorption-desorption behaviour more strongly than steady photocatalytic conversion. This is especially likely to occur in high-surface-area powders and fibrous membranes. Because of that, dark adsorption equilibration should be clearly separated from the illuminated degradation stage if the fitted kinetic parameters are to be interpreted in a meaningful way.

1.3.4 Langmuir–Hinshelwood framework: adsorption strength, surface saturation

If adsorption has a clear effect on the measured kinetics, the Langmuir-Hinshelwood model is often applied to describe the link between the reaction rate and surface coverage. Within this approach, the observed rate is influenced both by adsorption strength and by the reaction rate of the adsorbed species, as written below.

$$r = \frac{kKC}{1+KC} \tag{20}$$

where r is the reaction rate, C is the pollutant concentration in solution, K is an adsorption equilibrium constant (or an effective adsorption parameter), and k is a kinetic constant associated with the surface reaction of the adsorbed species.

The practical value of the Langmuir-Hinshelwood expression is that it links adsorption behaviour with the rate of the surface reaction. If $KC \ll 1$, the denominator does not differ much from 1, and the rate may then be treated as approximately first-order in concentration.

$$r \approx kKC \tag{21}$$

This is often consistent with the pseudo-first-order behaviour observed in dilute dye solutions. In the opposite limit, when $KC \gg 1$, the reactive surface approaches saturation and the rate moves towards a limiting value:

$$r \approx k \tag{22}$$

In this case, increasing the pollutant concentration does not increase the reaction rate in the same proportion, because the most active surface sites are already occupied. This is important for porous, fibrous, and other high-surface-area materials, where even small differences in adsorption can noticeably change the apparent kinetics. [18], [20]

In immobilised membranes and other structured catalysts, the interpretation requires additional caution because not all of the reactive surface is equally accessible. Wetting, diffusion inside the structure, and local differences in light intensity can produce non-uniform reaction conditions. As a result, the fitted Langmuir-Hinshelwood parameters may reflect transport limitations to some extent, not only adsorption and intrinsic surface kinetics. Even so, the model can still be useful for comparison under fixed experimental conditions, provided that the resulting parameters are interpreted with care.

1.3.5. Quantum yield and photon-normalised metrics: why they are stronger than "% degradation" under uncontrolled illumination

Reporting the percentage degradation after a fixed irradiation time is simple and intuitive, but the value is strongly affected by photon flux, illumination geometry, and pollutant loading. For that reason, photon-normalised metrics are more physically informative, because they relate the observed chemical conversion directly to the number of photons absorbed by the system or incident on it. The quantum yield is defined as follows:

$$\Phi = \frac{rate\ of\ chemical\ transformation\ (mol\ s^{-1})}{rate\ of\ photons\ absorbed\ (einstein\ s^{-1})} \tag{23}$$

Here, Φ represents the efficiency with which absorbed photons lead to chemical transformation. In principle, this makes the metric useful for comparing systems measured under different irradiation intensities or reactor geometries, as long as the absorbed photon rate is known with sufficient accuracy. The main advantage of quantum yield and related photon-normalised descriptors is that they connect the observed conversion directly with the light input, rather than only with irradiation time or final percentage removal.

A key advantage of the quantum yield and related photon-based metrics is that they explicitly link conversion to photon input, and therefore improve comparability when the illumination intensity and spectral distribution at the sample plane are known. However, the metric is meaningful only when photon flux is measured or estimated reliably and reported

clearly. Without this information, quantum-yield values become uncertain and are difficult to compare across studies, particularly when reactor geometry and optical conditions differ. [16], [21]

For water-purification studies, it is also important to distinguish decolourisation from deeper chemical conversion. Even when the quantum yield is not calculated for every dataset, the limitations of the dye-removal metrics should be stated explicitly, and the selected descriptors should be justified as appropriate for controlled comparative assessment rather than treated as universally sufficient measures of photocatalytic performance. [22]

1.3.6. Reporting discipline and comparability: why “same conditions” must be stated explicitly

Differences in reported photocatalytic performance do not always originate from the material itself. Even the same catalyst can yield noticeably different results when the experimental setup is changed. The apparent rate constant obtained from pseudo-first-order fitting and the apparent Langmuir-Hinshelwood parameters are both sensitive to photon flux at the sample plane, reactor geometry, mixing regime, catalyst amount, and the optical properties of the suspension or immobilised substrate. Therefore, photocatalytic kinetics are most safely interpreted within a clearly defined and reproducible experimental framework, and comparisons across different studies should be made with caution unless the irradiation and reactor conditions are sufficiently similar. [18], [23]

Several specific reporting elements have a disproportionate impact on comparability:

1. **Illumination definition.** Stating only the nominal lamp power is not enough for a meaningful description of the illumination conditions. More relevant are the photon flux that actually reaches the sample, its spectral distribution, and the intensity at the sample plane. This is particularly important in structured substrates and membrane-type systems, where scattering and reflection may modify both local light distribution and its effective use.
2. **Geometry and optical path.** In powder suspensions, factors such as suspension depth and stirring influence optical density and the amount of light that is effectively absorbed. For immobilised catalysts, the situation depends on other parameters, including the illumination angle, the wetted area, and membrane thickness, because these affect both the effective reaction volume and transport conditions within the active structure.
3. **Adsorption and sampling protocol.** Dark adsorption equilibration time, sampling frequency, and filtration or centrifugation procedures can all significantly influence the apparent kinetics and therefore need to be reported explicitly if meaningful comparison is intended.

A useful practical implication is that “better absorption” or “darker catalyst” should not be treated as direct evidence of enhanced photocatalysis unless photon flux and optical density are controlled and the functional output is evaluated under genuinely comparable conditions. [15], [23]

1.3.7. Decolourisation versus conversion: why “% removal” is not automatically “purification”

In dye-based systems, UV-Vis decolourisation is easy to follow and is therefore used very often, but it should not be treated as proof of mineralisation or complete purification by itself. A dye molecule may lose the part responsible for its colour and still form colourless organic intermediates that remain in solution. For that reason, “% degradation” should be read mainly as a decrease in the parent-dye concentration at the selected wavelength, not as direct proof of full conversion to CO_2 and H_2O. If the discussion is aimed at water purification rather than simple comparison between samples, it is better supported by additional evidence such as TOC reduction, identification of intermediates, or validation with a wider group of pollutants. [22], [23]

1.3.8. Transition: relevance of these constraints for immobilised membranes and structured platforms

The limitations outlined above become even more important in immobilised and structured systems. In such architectures, early-stage behaviour may be strongly influenced by adsorption, wetting, and transport, and these factors can vary markedly between samples even when their nominal chemistry is similar. For electrospun membranes, the fibrous architecture creates an internal surface area together with tortuous pathways and diffusion gradients. These features may strengthen adsorption and at the same time change how easily reactive sites can be reached. In laser-structured substrates, micro- and nanotopography can additionally influence the effective optical path length and the local photon-flux distribution. Because of this, performance in these systems should be interpreted within an architecture-aware framework that takes into account not only charge utilisation, but also the transport and accessibility limitations imposed by the physical form of the active material. [24], [25], [26]

1.4. Photoelectrochemistry: thermodynamics, kinetic descriptors, and device-relevant metrics

Photoelectrochemical (PEC) measurements provide a controlled framework for analysing charge utilisation in illuminated semiconductor electrodes. In comparison with photocatalytic batch tests, PEC measurements allow direct monitoring of photogenerated carrier extraction through photocurrent and also make it easier to control potential and electrolyte conditions. For that reason, PEC descriptors should be read not only as

performance numbers, but also as indicators of where the main losses come from, for example interfacial charge transfer, recombination, resistive drops, or transport limitations. [27], [28]

1.4.1. Thermodynamic reference points and overpotential as a practical descriptor

In PEC water splitting, it is first necessary to establish whether the reaction is thermodynamically feasible. This minimum energy requirement is determined by the corresponding redox potentials, and the overall reaction is written as:

$$2H_2O \rightarrow 2H_2 + O_2 \tag{24}$$

For interpretation of pH-dependent operation and electrode half-reactions, this expression is commonly resolved into hydrogen evolution and oxygen evolution half-reactions in acidic and alkaline media, as shown below.

In acidic media:

$$2H^+ + 2e^- \rightarrow H_2 \tag{24a}$$

$$2H_2O \rightarrow O_2 + 4H^+ + 4e^- \tag{24b}$$

In alkaline media:

$$2H_2O + 2e^- \rightarrow H_2 + 2OH^- \tag{24c}$$

$$4OH^- \rightarrow O_2 + 2H_2O + 4e^- \tag{24d}$$

These half-reaction forms are important because the relevant thermodynamic reference potentials and kinetic barriers depend on pH, electrolyte composition, and the reaction pathway operating at the semiconductor-electrolyte interface. [4]

Earlier in the chapter, thermodynamic potentials and their pH dependence were outlined using the Nernst-type relations given in Eqs. (7)–(10). These expressions are still used here as the reference framework for the PEC discussion.

In PEC measurements, it is not enough to know that a reaction is thermodynamically possible. A measurable current appears only when an additional driving force is applied. This extra potential is the overpotential, and it reflects kinetic barriers, interfacial losses, and resistive drops in the system. For this reason, overpotential connects the thermodynamic potential of the reaction with the real behaviour of the electrode under applied bias. [27], [29]

For structured and porous photoelectrodes, the overpotential should be considered in relation to the electrode architecture and not only as an intrinsic feature of the interface. In hierarchical structures, local potential and current density do not have to be uniform, and

electrolyte access together with bubble accumulation may further disturb transport conditions. As a result, onset potential and photocurrent may be influenced both by interfacial kinetics and by resistance or transport effects arising from the architecture. Because of this, current-potential curves are more informative when they are interpreted together with complementary methods such as impedance spectroscopy and wavelength-resolved response. [5], [28]

1.4.2. Kinetic descriptors: Butler–Volmer and Tafel analysis, and what can be concluded safely

How far the system is from equilibrium is measured by the overpotential:

$$\eta = E_{applied} - E_{eq} \tag{25}$$

where E_{eq} is the equilibrium potential of the relevant redox couple and $E_{applied}$ is the applied potential. Here, the overpotential is the difference between the applied potential and the equilibrium potential of the relevant redox couple, given on a consistent scale, usually RHE. It should not be viewed simply as a correction term, because in practice it reflects the kinetic barrier that must be overcome to obtain a certain reaction rate. Even when band-edge positions are thermodynamically favourable, weak interfacial kinetics may still require operation at higher applied bias and thus lower the practical efficiency. For PEC systems, overpotential depends not only on electrocatalytic considerations, but also on photovoltage, recombination, and charge-carrier availability at the interface. [4]

Interfacial charge-transfer kinetics are frequently described using the Butler-Volmer equation:

$$j = j_0 \left[exp\left(\frac{\alpha_a F \eta}{RT}\right) - exp\left(-\frac{\alpha_c F \eta}{RT}\right) \right] \tag{26}$$

where j is the current density, j_0 exchange current density, and α_a, α_c are anodic/cathodic charge-transfer coefficients, F is the Faraday constant, R is the gas constant, and T is temperature. Within PEC discussion, this expression is useful because it clarifies what is meant by improved interface kinetics: an increase in the exchange current density, or an effective change in the charge-transfer coefficients, is consistent with more facile charge transfer at a given overpotential. Architecture and surface engineering may influence these quantities by altering active-site density, interfacial electronic structure, and the density of recombination-active surface states.

In semiconductor photoelectrodes, the measured current depends not only on interfacial kinetics, but also on the supply of charge carriers to the surface. A better apparent kinetic response may therefore result from reduced recombination or improved charge extraction, rather than from higher catalytic activity of the surface itself. For this reason, Butler–Volmer-type analysis should be considered together with impedance data recorded

under illumination and with stability results. This helps distinguish charge-transfer limitations from recombination or transport effects. [30]

When one of the exponential terms becomes dominant, Butler-Volmer behaviour can be simplified to the Tafel form:

$$\eta = a + b\log(j) \tag{27}$$

where a is an intercept term and b is the Tafel slope. Tafel analysis is widely used because it provides a compact descriptor of how strongly current responds to changes in the overpotential. Within a photoelectrode system, a lower apparent Tafel slope may be associated with improved interfacial kinetics, but it can just as well arise from a change in the dominant regime, for example from charge-transfer limitation to transport limitation, or from the influence of series resistance and recombination. For this reason, Tafel slopes should not be used as stand-alone proof of better catalysis unless supporting evidence indicates that the same kinetic regime applies across the compared samples and that uncompensated resistance, mass-transport limitation, or gas-bubble coverage do not dominate the selected potential window. [31]

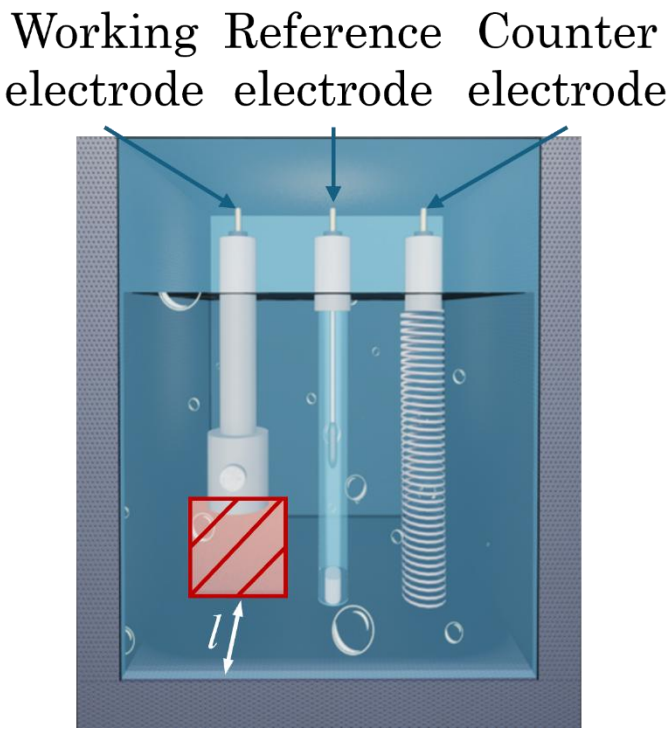

Figure 1.4. *Schematic representation of a standard three-electrode electrochemical/photoelectrochemical cell, showing the working, reference, and counter electrodes, together with the defined illuminated and immersed area of the working electrode and the main geometric parameters relevant to measurement reproducibility. Prepared by the author.*

1.4.3. Wavelength-resolved response and device-relevant efficiency metrics: IPCE, ABPE, STH, and Faradaic efficiency

Kinetic parameters alone are not enough to describe PEC performance, because they do not show directly how effectively light is converted into current or chemical products. For this reason, PEC analysis also includes wavelength-dependent measurements and efficiency parameters such as IPCE or ABPE. These values are useful when comparing different electrode structures, because they connect the photocurrent response with the illumination conditions and the applied bias. [28], [32]

The incident photon-to-current efficiency (IPCE) expresses the number of incident photons at a given wavelength that are converted into the collected current. In this work, IPCE is defined as:

$$IPCE(\lambda)(\%) = \frac{1240 j(\lambda)}{P(\lambda)\lambda} \times 100 \tag{28}$$

where $j(\lambda)$ is the photocurrent density measured at wavelength λ, and $P(\lambda)$ is the incident light power density at that same wavelength. IPCE is useful because it enables the examination of the wavelength-dependent response separately from the effects of broadband illumination. In this way, it gives a more detailed view of how effectively a given electrode converts absorbed or incident light into measurable current.

IPCE is a useful diagnostic tool because it can help determine whether the main limitation comes from light absorption, charge separation and collection, or losses at the interface. At the same time, the measured IPCE values are strongly affected by the experimental setup. Parameters such as beam size, alignment, chopping or lock-in conditions, and calibration of wavelength-dependent irradiance at the sample plane all matter. Because of this, reliable reporting requires clear definition of both the irradiance and the electrode area, especially for structured electrodes where scattering and the effective illuminated area may influence photon utilisation. [4], [32]

Applied bias photon-to-current efficiency (ABPE) connects photocurrent under bias to incident illumination intensity and reflects the efficiency of converting light into electrical power under an applied potential. The ABPE definition is given below.

$$\eta_{ABPE}(\%) = \frac{j(1.23 - V_{bias})}{P_{in}} \times 100 \tag{29}$$

where j is the photocurrent density at the applied bias, V_{bias} is the applied potential (typically vs RHE), 1.23 V corresponds to the thermodynamic water-splitting potential, and P_{in} is the incident light power density. Here, the metric combines current output with the applied bias and therefore provides a practical way to compare photoelectrode performance under the same illumination and electrolyte conditions.

ABPE is useful for comparing photoanodes tested under the same illumination and electrolyte conditions, because it includes both the photocurrent and the applied bias. However, the calculated value depends on how the potential is converted, how the current density is normalised, and which electrode area is used. For this reason, ABPE values should be reported together with the reference scale, usually RHE, the light intensity at the sample position, and the geometric or illuminated area used for the calculation. [4], [29]

The most demanding metric used for PEC water splitting is the solar-to-hydrogen (STH) efficiency. It relates the incident solar power directly to the chemical energy stored in the produced hydrogen, either under unbiased conditions or within a clearly defined device configuration. The STH expression is given below.

$$\eta_{STH}(\%) = \frac{j_{op} \times 1.23 \times FE}{P_{in}} \times 100 \tag{30}$$

where j_{op} is the operating current density under the relevant operating condition, and FE is the Faradaic efficiency for hydrogen evolution. In this case, the operating current density is only meaningful when it is linked to verified hydrogen production through an appropriate Faradaic-efficiency term.

In practice, any claim based on STH efficiency has to be validated carefully, because the relevant output is hydrogen produced as a chemical product, not photocurrent by itself. For that reason, the measurement should include clear information on the illumination spectrum and intensity, the active area, the method used for gas collection or product analysis, and whether any external bias was applied. STH values are therefore most convincing when they are reported together with explicit experimental conditions and direct quantification of the generated product. [4], [33], [34]

Faradaic efficiency (FE) is used to relate the measured charge to the amount of chemical product actually formed. It shows what part of the measured current is used for the desired reaction, for example hydrogen or oxygen evolution. The remaining current may come from side reactions, corrosion, or capacitive and transient processes. FE is defined as follows:

$$FE_{H_2}(\%) = \frac{2Fn(H_2)}{Q} \times 100 \tag{31}$$

where n_{H2} is the amount (moles) of hydrogen produced, Q is the total charge passed, and F is the Faraday constant. The factor of 2 in the hydrogen case reflects the two electrons required to produce one molecule of H_2.

Because FE depends on accurate product quantification, it must be paired with a clearly described analytical method, such as gas chromatography, calibrated volumetric collection, or dissolved-gas analysis, together with appropriate control tests. This is

especially important for photoelectrodes, because photocurrent may contain non-faradaic contributions and side reactions may occur depending on electrolyte composition and surface state. [35], [36]

Finally, IPCE, ABPE, STH, and FE are more informative when considered together rather than as separate values. IPCE shows the wavelength-dependent charge-collection behaviour, ABPE reflects power conversion under applied bias, and STH together with FE links the electrical response to confirmed chemical product formation. This combined view is particularly important for architecture-driven systems, because structural design may improve light utilisation while at the same time changing transport and interfacial kinetics. For that reason, more than one metric is needed to determine which factor is mainly responsible for the observed improvement. [27], [34], [37]

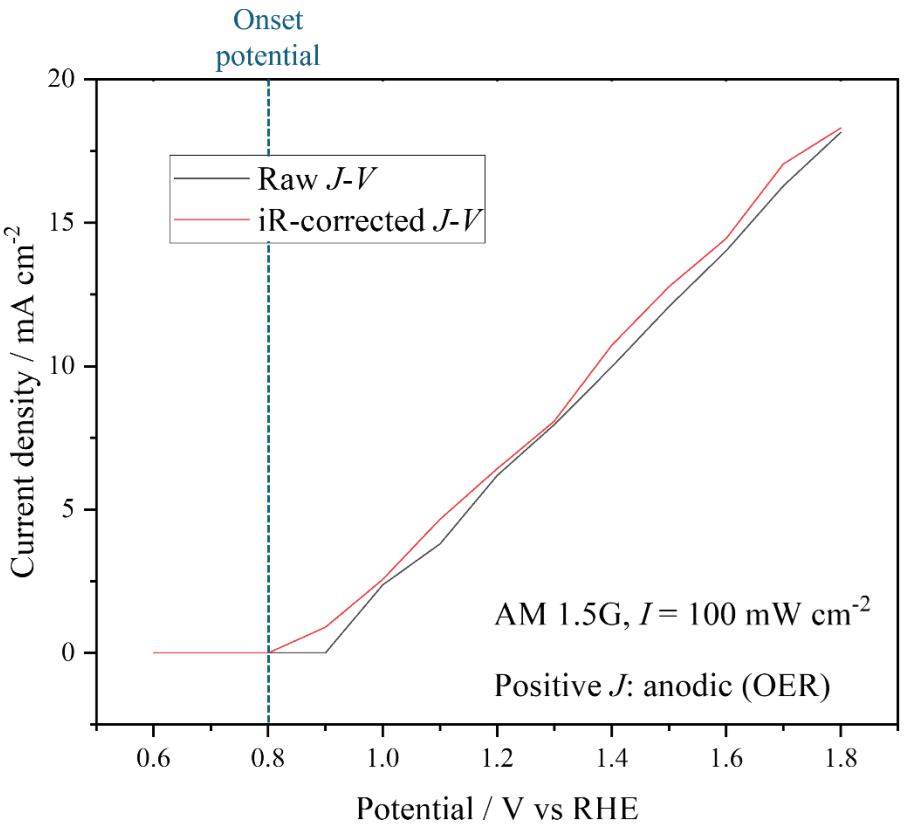

Figure 1.5. *Dark and illuminated current density-potential (j–E) curves used to illustrate photocurrent onset and the bias dependence of photoelectrode behaviour. Prepared by the author.*

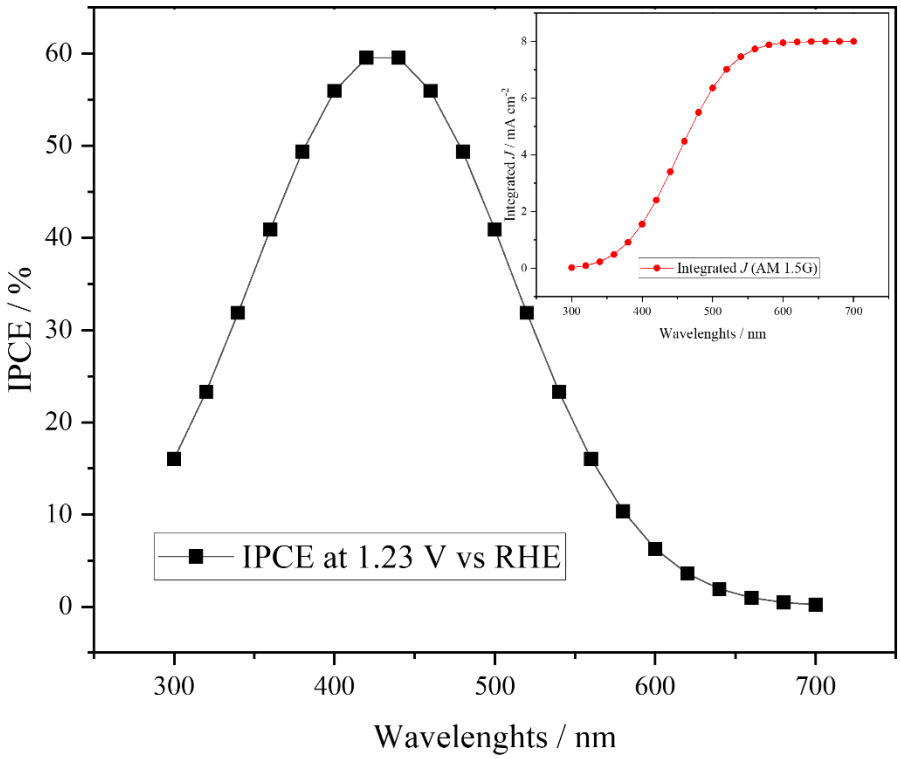

Figure 1.6. *AM 1.5G solar spectral distribution and the conceptual relationship between wavelength-resolved incident photon-to-current efficiency (IPCE) and the resulting photocurrent under broadband illumination. Prepared by the author*

1.5. Electrochemical diagnostics for photoelectrodes: impedance analysis and semiconductor parameters

Electrochemical methods are essential for separating the contributions of charge-transfer kinetics, resistive losses, and capacitive or space-charge effects in photoelectrode systems. Among these methods, electrochemical impedance spectroscopy (EIS) is especially useful because it probes the frequency-dependent response of the electrode–electrolyte interface and provides access to effective parameters associated with interfacial charge transfer, transport limitation, and non-ideal capacitive behaviour. [38], [39]

1.5.1. What EIS measures and why equivalent circuits are model-dependent

In EIS, the electrode is probed with a small AC signal applied around a chosen operating condition set by the potential and the illumination state. The resulting impedance response is then recorded over a range of frequencies. For photoelectrodes, measurements under illumination are often used to examine how interfacial charge-transfer resistance and

capacitive behaviour differ from the dark case. However, EIS cannot be interpreted independently of the model. The same dataset can often be fitted with more than one equivalent circuit and still appear acceptable, especially for porous or heterogeneous electrodes where several time constants may overlap. Because of that, fitted parameters are better treated as effective comparative values obtained within one consistent modelling approach, not as unique intrinsic constants of the material. [38], [39]

A Nyquist plot can be useful as a first visual guide, since semicircle-like features are often associated with charge-transfer processes combined with non-ideal capacitance, whereas low-frequency tails may point to mass-transport contributions or distributed interfacial behaviour. Simultaneously, porous and structured electrodes rarely behave as ideal RC systems. For this reason, the shape of the plot by itself is not sufficient for mechanistic interpretation. Such conclusions should be based on an explicit equivalent-circuit model and supported by additional evidence, for example illumination-dependent response, stability behaviour, and reproducible trends across the analysed sample series.

1.5.2. Constant phase element (CPE): why it appears and how to interpret it safely

A constant phase element (CPE) is commonly used when the capacitive response is non-ideal. This is often the case in photoelectrodes, since real electrode surfaces are heterogeneous. Factors such as roughness, porosity, variation in local reaction rates, and uneven current distribution can give rise to a distribution of time constants rather than a single ideal capacitance. The CPE expression used in this work is given below.

$$Z_{CPE} = \frac{1}{Q(j\omega)^n} \tag{32}$$

where Q is the CPE coefficient, ω is angular frequency, j is the imaginary unit, and n (with $0<n\leq1$) quantifies deviation from ideal capacitive behaviour.

The practical implication is that Q and n (or α) should not be treated as simple capacitance values. Instead, they describe the extent to which the interface deviates from ideal capacitive behavior.

When n is close to 1, the response becomes similar to that of an ideal capacitor. In contrast, lower n values indicate stronger dispersion and a greater degree of non-ideal behavior. For this reason, CPE parameters are better interpreted in a comparative way, using the same equivalent circuit, frequency range, and illumination conditions, rather than being taken directly as physical capacitances without proper conversion and justification. [40], [41]

For structured and porous photoelectrodes, a decrease in n is usually interpreted as a sign of stronger dispersion, which may indicate greater heterogeneity or changes in the

interfacial states. Variations in Q , on the other hand, may be related to differences in effective interfacial area, surface-state density, or capacitance contributions associated with the space-charge region. Because of this, CPE trends are more informative when discussed together with morphology, illumination response, and, where relevant, semiconductor analysis such as Mott-Schottky interpretation, rather than being considered on their own.

1.5.3. Practical use in this research: separating charge-transfer resistance from non-ideal capacitance

If one equivalent circuit is used in the same way for the full sample series, EIS becomes useful for distinguishing between resistive and capacitive parts of the response. In many PEC architectures, a decrease in the fitted charge-transfer resistance under illumination can be interpreted as a sign of improved interfacial charge transfer and/or greater availability of photogenerated carriers for the reaction at the interface. However, structured electrodes may at the same time modify effective area, roughness, and heterogeneity. For that reason, EIS should be interpreted within a broader set of evidence that also includes j-E response, stability behaviour, and optical data, rather than being used as a single decisive proof of the mechanism. [28], [42]

1.5.4. Mott-Schottky analysis: flat-band potential, donor density, and why nanostructured electrodes require sanity checks

Capacitance-potential measurements are often analysed with the Mott-Schottky approach in order to estimate semiconductor parameters such as flat-band potential and apparent donor density. The method assumes that, within a certain regime, the measured interfacial capacitance is dominated mainly by the space-charge capacitance of the semiconductor. Based on this, the Mott-Schottky relation used here is given below.

$$\frac{1}{C_{SC}^2} = \frac{2}{\varepsilon\varepsilon_0 e N_D}\left(V - V_{fb} - \frac{kT}{e}\right) \tag{33}$$

where C_{SC} is the space-charge capacitance, ε is the dielectric constant of the semiconductor, ε_0 is the vacuum permittivity, e is the elementary charge, N_D is the donor density for n-type semiconductors, V is the applied potential, V_{fb} is the flat-band potential, k is Boltzmann's constant, and T is temperature. In practical use, the inverse-square capacitance is plotted against the applied potential, and the linear part of that plot is then used to estimate the apparent donor density and the flat-band potential.

The extracted parameters are meaningful only when the underlying assumptions of the method are reasonably satisfied. In real photoelectrodes, capacitance dispersion, surface states, frequency dependence, and other non-ideal interface contributions may dominate the measured capacitance. For this reason, Mott-Schottky results should be interpreted cautiously and supported by basic sanity checks such as frequency sweeps, careful

assessment of the linear fitting range, and consistency with other electrochemical and spectroscopic evidence. [5], [6]

One important limitation is that, in nanostructured and porous photoanodes, the measured capacitance does not always represent the depletion capacitance of the semiconductor layer itself. It may also contain a strong contribution from the conducting substrate, penetration of the electrolyte into the structure, contact-related injection effects, or residual geometric capacitances that remain present even when the semiconductor is nominally depleted. Because of this, a Mott-Schottky plot may look linear and still produce unrealistic doping densities or misleading flat-band potential values. [43], [44]

From a practical point of view, the method is most dependable when the same frequency is used for the entire sample series, the linear region is chosen on a physical basis rather than simply because it looks straight, and the extracted parameters are checked against other observations such as photocurrent onset, illumination-dependent resistance changes from impedance analysis, and stability behaviour. When these conditions are met, Mott-Schottky analysis remains useful as a comparative method for tracing relative shifts in interfacial energetics within a controlled sample set. [45]

Finally, it is essential to recognise that structured architectures may introduce additional capacitance contributions, including surface-state capacitance, Helmholtz-layer effects, and geometric capacitances. Because these contributions may be frequency dependent, they can distort both the slope and the intercept of the Mott-Schottky plot. Reporting the measurement frequency, AC amplitude, and the circuit or modelling context used to derive capacitance is therefore necessary both for reproducibility and for mechanistic credibility. [38], [46]

1.5.5. Practical integration with EIS/CPE modelling in this work

In practice, the capacitance values used in Mott-Schottky analysis are often taken from impedance spectra or calculated from parameters obtained by equivalent-circuit fitting. When the interface exhibits non-ideal capacitive behaviour represented by a CPE, conversion from fitted CPE parameters to an effective capacitance must be performed consistently, and the resulting value should be interpreted as an effective quantity rather than as an ideal physical capacitance. For this reason, Mott-Schottky trends are best discussed together with EIS-derived resistive contributions and CPE behaviour under the same illumination and potential conditions, rather than being treated as an isolated measurement. [39], [41]

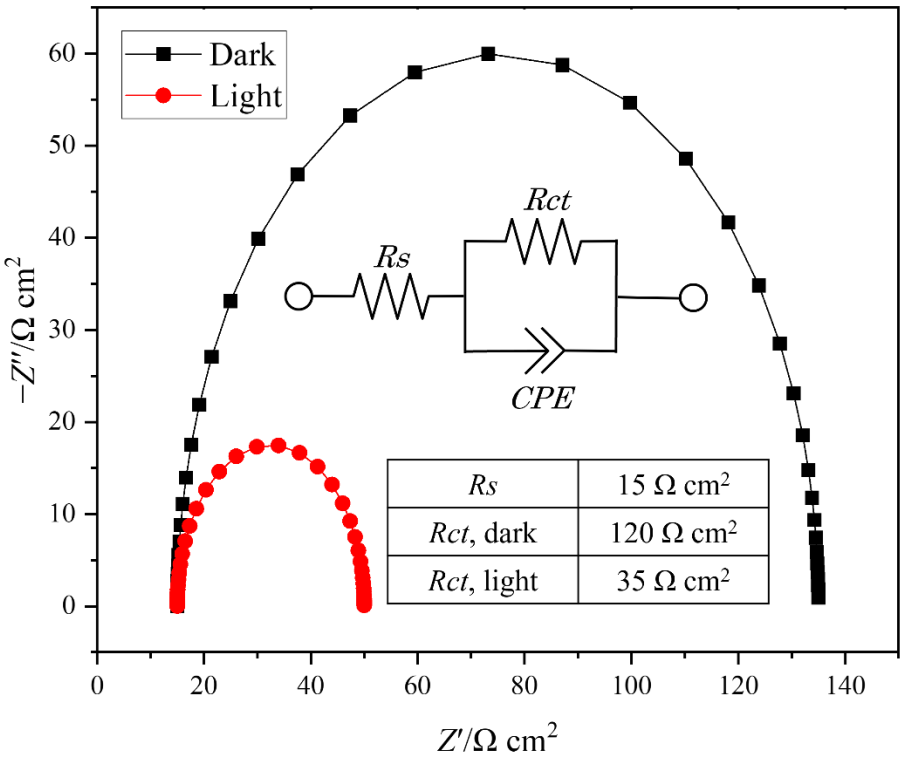

Figure 1.7. *Example Nyquist plot and a representative equivalent-circuit model used to interpret resistive and non-ideal capacitive contributions at the electrode-electrolyte interface in impedance spectroscopy. Prepared by the author.*

1.6. Summary and scope

This chapter outlined the conceptual and methodological basis used later to interpret both photocatalytic degradation experiments and photoelectrochemical water-splitting measurements from the same architecture-aware perspective. The main point is that light absorption creates non-equilibrium electron-hole pairs, but the measurable response depends on how many of these carriers avoid recombination, reach a reactive interface, and take part in interfacial charge transfer. For that reason, functional behaviour cannot be inferred from optical absorption alone, but has to be considered together with carrier fate, interface quality, and the transport limitations associated with the chosen architecture. [9], [10]

For photocatalytic water purification, the chapter discussed oxidation in aqueous media largely in terms of reactive oxygen species pathways and related them to practical issues such as oxygen availability, adsorption behaviour, and transport limitations arising from the physical format of the material. It also presented the quantitative tools used later for degradation analysis, namely UV-Vis concentration tracking, pseudo-first-order kinetics, and the Langmuir-Hinshelwood framework in its low- and high-coverage limits. These descriptors are used primarily for comparative analysis under controlled conditions, with the understanding that fitted values may be influenced not only by intrinsic photochemistry, but

also by adsorption and transport effects, especially in immobilised and highly porous systems. [18], [23]

For photoelectrochemistry, the chapter addressed water splitting by introducing the overall reaction together with the corresponding half-reactions, and by showing how thermodynamic reference points are related to kinetic demands through overpotential and kinetic models. It also presented the main device-relevant metrics used to connect light input with electrical and chemical output, namely IPCE, ABPE, STH, and Faradaic efficiency. At the same time, these metrics are only meaningful when the potential scale is reported consistently, the illuminated area is defined clearly, and product quantification is properly validated. [4], [37]

Finally, the chapter outlined the role of electrochemical diagnostics in identifying loss pathways and in supporting mechanistic interpretation. EIS together with equivalent-circuit modelling was introduced as a way to separate resistive contributions from non-ideal capacitive behaviour, including the response described by CPE elements. Mott-Schottky analysis was also discussed, but with clear caution in the case of nanostructured and porous electrodes, where capacitance dispersion and surface states may strongly influence the measured response. In this framework, fitted parameters are treated as effective comparative descriptors, and they are most meaningful when the modelling approach and measurement conditions are kept consistent across the analysed sample series. [6], [39]

The following chapter develops the state-of-the-art background required to position the investigated material platforms within current research. The literature review is organised around architecture-driven and interface-controlled strategies that address the limiting steps identified in Chapter 1, namely light utilisation in structured geometries, charge separation and transport across complex interfaces, and interfacial kinetics at semiconductor–electrolyte boundaries. Particular attention is given to immobilised and hierarchically structured systems, conformal coatings prepared by atomic layer deposition, laser-induced surface structuring, and hybrid interfaces that include conductive or catalytic components.In this way, the next chapter provides the necessary transition between photocatalytic degradation studies and PEC water-splitting analysis by placing them within a common mechanistic framework. It also provides the basis for later discussion of performance changes in terms of architecture, interface quality, and charge-utilisation pathways, instead of interpreting them through single parameters alone.

Subsequent chapters apply this framework to the investigated platforms and to the way their functional behaviour is evaluated. In the photocatalytic part, performance is interpreted with the help of adsorption-aware kinetic descriptors and with clear attention to the optical and transport limitations associated with the selected architecture. In the photoelectrochemical part, performance is discussed on the basis of device-level metrics and electrochemical diagnostics. Attention is also given to the potential scale used, the quality of

the measurements, and, when relevant, to whether the electrochemical response is confirmed by actual chemical product formation. Together, the following chapters show a consistent research line in which differences in performance are discussed mainly through architecture, interface quality, and charge-utilisation pathways, rather than through single isolated parameters.

Chapter 2. Literature Background on Architecture-Engineered TiO_2-Based Materials for Photocatalytic and Photoelectrochemical Use

2.1. TiO_2 as a benchmark photoactive oxide and the need for architecture-driven optimisation

Titanium dioxide has remained one of the key semiconductor materials in photocatalytic and photoelectrochemical research for decades. Its importance is not due to novelty, but to the fact that it combines physicochemical stability, broad synthetic versatility, low toxicity, relatively low cost, and compatibility with many different structural design strategies. Because of these features, TiO_2 has become not only one of the most intensively studied photoactive oxides, but also a model platform through which broader principles of light-driven semiconductor behaviour can be examined. In many respects, the development of modern photocatalysis and photoelectrochemistry has proceeded in parallel with the continuing reinterpretation of TiO_2-based systems, from classical particulate photocatalysts to thin films, nanotubular layers, fibrous composites, conformal coatings, heterostructures, and hierarchically organised electrode architectures. [47], [48], [49]

The long-standing research interest in TiO_2 is linked to its ability to absorb photons of sufficient energy and generate electron–hole pairs that may participate in redox processes. When irradiated with light whose energy exceeds its band-gap value, electrons are promoted from the valence band to the conduction band, leaving positively charged holes behind. The photogenerated carriers can then follow different pathways. They may recombine quickly, either in the bulk or at the surface, so that the absorbed energy is lost without producing useful chemical work. Alternatively, they may migrate to reactive interfaces, where they take part in oxidation and reduction reactions. Therefore, the behavior of TiO_2 is not controlled by light absorption alone. It also depends on the number of charge carriers generated, the number lost by recombination or trapping, the efficiency of the movement of the remaining charges through the material, and the rate at which they are transferred to adsorbed species or the electrolyte. This is why TiO_2 materials that appear similar in composition can still show very different photocatalytic or photoelectrochemical responses. [2], [9], [10]

The scientific value of TiO_2 lies partly in the fact that it is sufficiently well understood to serve as a benchmark system, yet sufficiently complex to remain an active subject of advanced research. On the one hand, it offers a comparatively well-established chemical platform with known crystalline polymorphs, widely discussed band positions, and a broad methodological literature. On the other hand, its functional behaviour remains highly sensitive to crystal structure, surface chemistry, synthesis route, defect distribution, morphology, and interface quality. This sensitivity makes TiO_2 especially useful for

investigating the influence of structural and interfacial engineering on photoinduced processes. In this sense, TiO_2 is not only a widely used photocatalyst. It also serves as a reference system for studying broader questions of semiconductor design, charge transport, interface control, and material architecture. [48], [50]

2.1.1. Fundamental properties of TiO_2 relevant to photoactivity

The practical use of TiO_2 in photocatalysis and photoelectrochemistry is rooted in several favourable physicochemical characteristics. First, TiO_2 remains chemically stable in many aqueous and oxidative environments, especially in comparison with narrower-band-gap semiconductors, which may suffer from photocorrosion or show poor long-term stability. This is particularly important in photoelectrochemical systems, where the material is often exposed at the same time to electrolyte, applied bias, and prolonged illumination. Second, TiO_2 is compatible with many different synthesis and processing methods, such as sol-gel preparation, hydrothermal growth, anodisation, thermal oxidation, sputtering, chemical vapour deposition, atomic layer deposition, electrospinning-based methods, and laser-assisted surface engineering. This synthetic flexibility allows TiO_2 to be incorporated into powders, coatings, membranes, fibres, and complex composite structures. Third, TiO_2, surface chemistry strongly affects its behaviour in aqueous systems. Surface hydroxyl groups and defect-related sites affect how TiO_2 interacts with water and adsorbed molecules. [7], [48], [51]

At the same time, TiO_2 also has clear limitations that arise from its electronic structure. Because its band gap is relatively wide, efficient excitation takes place mainly in the ultraviolet region. Since ultraviolet light represents only a small part of the solar spectrum, unmodified TiO_2 cannot make full use of visible sunlight without additional modification. This limitation has motivated a very large body of research on sensitisation, doping, heterostructure formation, plasmon-assisted strategies, and coupling with narrower-band-gap components. However, the wide band gap should not be viewed exclusively as a disadvantage because it is partly associated with the strong oxidative power of the photogenerated holes and the excellent chemical stability of the material. The challenge in TiO_2 research has therefore rarely been to replace the material completely, but rather to optimise or complement it in ways that preserve its advantages while lessening its built-in limitations [9], [50]

Another important issue is the recombination of charge carriers. TiO_2 may absorb light effectively, but the useful fraction of the generated electrons and holes can still remain low if recombination occurs before they take part in surface reactions or are extracted into an external circuit. Recombination may be promoted by bulk defects, grain boundaries, surface states, or poorly designed interfaces with other phases. For this reason, increasing light absorption by itself is often not enough to produce a real improvement in performance. A material may absorb more photons and still show only modest enhancement if its

architecture or interface quality does not support efficient carrier separation and transport. Consequently, much of the modern research on TiO_2 is not centred on absorption alone, but on the broader question of how absorbed energy is converted into usable interfacial charge. [10], [48]

2.1.2. Crystalline phases of TiO_2 and their functional significance

Titanium dioxide is found mainly in three crystalline polymorphs: anatase, rutile, and brookite. In the context of photocatalysis and photoelectrochemistry, however, anatase and rutile are discussed much more often than brookite. Anatase has usually been regarded as the more active phase in many suspended and nanostructured systems, whereas rutile is thermodynamically more stable and often becomes dominant after processing at higher temperatures. Brookite is also of scientific interest, but it is encountered less often because it is more difficult to synthesise and is less common in practical photoactive materials. [52], [53]

The higher activity often attributed to anatase has been explained through several factors, including favourable band-edge positions, lower recombination tendency in many cases, suitable charge-transport behaviour, and the fact that anatase is frequently obtained in nanostructured forms with high surface area. However, the common statement that “anatase is always better” is an oversimplification. The performance of anatase is therefore not fixed by the phase name alone. It depends on how the material is prepared, how crystalline it is, how many defects it contains, and what surface state is obtained after synthesis or post-treatment. Rutile should also not be dismissed as a weaker phase in every case. Rutile should not be treated only as the less active form of TiO_2. In photoelectrodes, mixed-phase oxides, or heat-treated coatings, it can be useful for more practical reasons: it may improve stability, help the coating contact the substrate, support charge transport, or change the optical response of the final structure. [48], [54]

The link between phase composition and performance becomes even more complicated in multiphase systems. Materials containing both anatase and rutile have often been reported to perform better than their single-phase counterparts. This is usually explained by improved charge separation at the phase boundaries, although the exact mechanism still depends on the material history and the structural context. In practice, the phase composition cannot be considered separately from morphology, grain connectivity, interface quality, and defect chemistry. For a dissertation centred on structure-property relationships, this is an important point: phase is relevant, but it does not determine performance on its own. [54], [55], [56]

A further complication arises in thin films and conformal coatings, where the phase present after deposition may differ from the phase desired during operation. For example, TiO_2 deposited by atomic layer deposition is often amorphous in the as-prepared state and requires thermal treatment to crystallise. The resulting phase and grain structure depend on

annealing temperature, atmosphere, film thickness, and substrate interaction. In these systems, phase transformation is not only a structural phenomenon but also part of the interface-engineering problem, because crystallisation may improve carrier transport while simultaneously changing stress, adhesion, roughness, and the density of reactive surface sites. [7], [52]

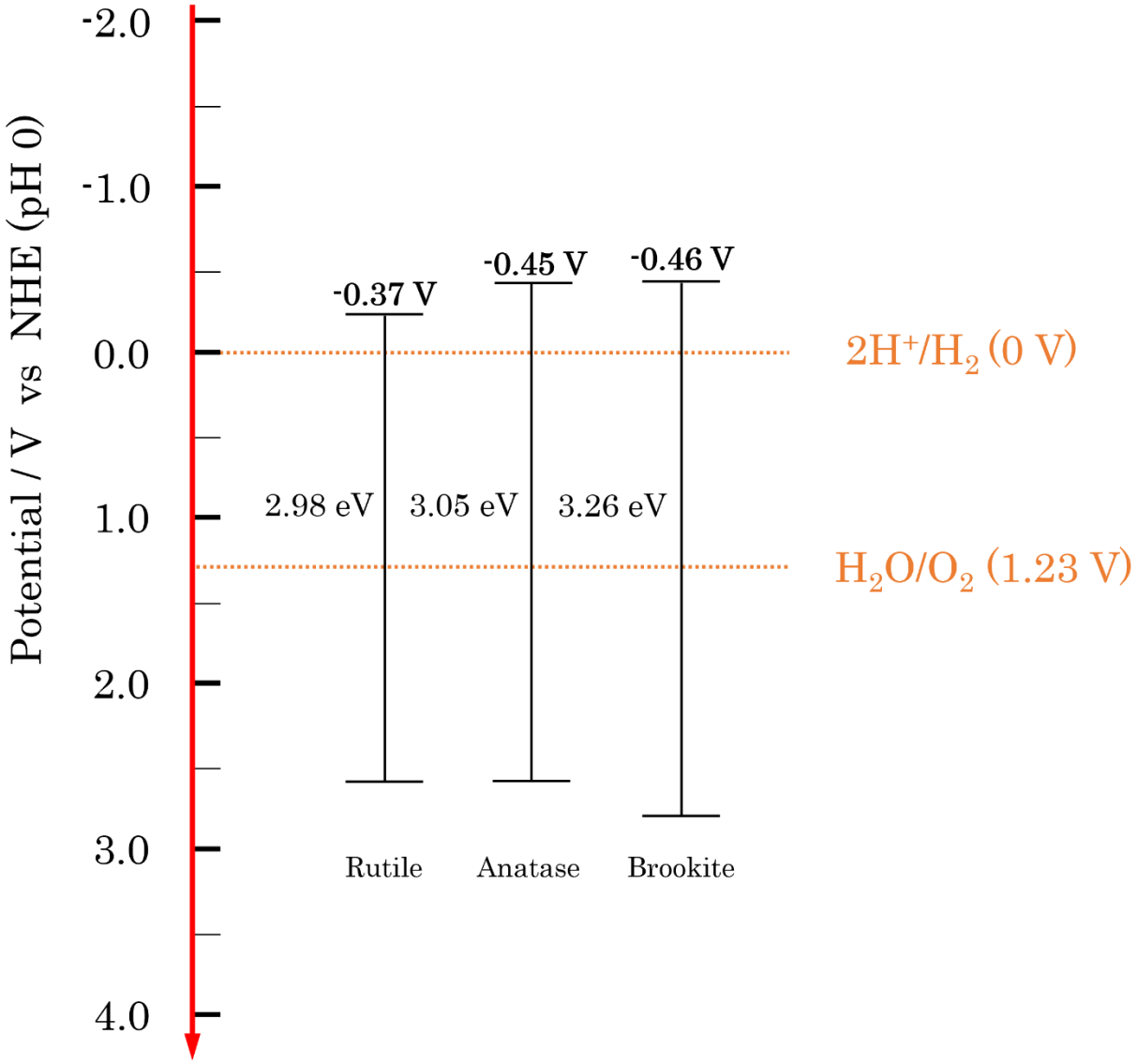

Figure 2.1. *Band-edge positions of the major TiO_2 polymorphs relative to the normal hydrogen electrode, together with their approximate band-gap energies. The scheme highlights the electronic differences between anatase, rutile, and brookite that are relevant to photocatalytic and photoelectrochemical behaviour. Adapted and redrawn by the author based on Ref.* [57].

2.1.3. TiO_2 in photocatalysis: opportunities and limitations

TiO_2 has been used in photocatalytic research for a long time, both as an active material and as a reference semiconductor. In dye-degradation studies, it is commonly chosen because it can oxidise organic molecules and because the dye concentration can be followed by UV-Vis spectroscopy. However, this type of test has to be interpreted with care. A decrease in the dye signal under illumination may result from photocatalytic degradation, but it may also be affected by adsorption, dye photosensitisation, or partial transformation of the dye molecule. For this reason, TiO_2-based photocatalytic results should not be discussed only in terms of activity, especially when structured or hybrid materials are compared. [1], [2]

One of the main advantages of TiO_2 in photocatalysis is that it can be prepared in several different morphological forms. It may be used as a high-surface-area powder, as a nanostructured film, as part of electrospun fibrous composites, or as a thin conformal coating deposited on mechanically stable supports. Each of these forms has its own strengths and limitations. In fundamental photocatalytic studies, TiO_2 is still often examined in powder form, mainly because this format exposes a large fraction of the material to the reaction medium and makes composition-based comparisons easier to carry out. Once the discussion shifts towards practical treatment, however, the same format becomes less favourable, since separation of the powder from water and its repeated reuse introduce obvious difficulties. Immobilised TiO_2 systems are easier to handle and can be integrated more readily into devices or continuous processes. Their performance, however, depends more strongly on how the system is arranged: how the liquid reaches the active surface, how well the surface is wetted, how light enters the structure, and how accessible the reactive sites remain. [15], [23]

These considerations show that the photocatalytic behaviour of TiO_2 depends not only on intrinsic semiconductor properties, but also on how the material is physically organised in the reaction environment. A powder suspension, a membrane-supported TiO_2 layer, and a TiO_2-coated structured metal substrate cannot be expected to behave identically even when their chemical composition is similar. The surrounding architecture affects the thickness of the diffusion boundary layer, the local distribution of light, the accessibility of surface hydroxyl groups, and the possibility of catalyst recovery after use. Therefore, a doctoral-level discussion of TiO_2 photocatalysis must go beyond simple activity values and address the full functional context in which the material operates [10]

2.1.4. TiO_2 in photoelectrochemistry

TiO_2 also has an important place in photoelectrochemical studies, but it is interpreted in a different way than in photocatalytic tests. In a photoanode, the main question is not only whether the material can absorb light and trigger a reaction at the surface, but whether the generated charges can be collected under applied bias and converted into photocurrent.

Therefore, TiO_2 is often used to study the effect of coating thickness, morphology, contact with the conductive support, and interface quality on charge extraction. Its wide band gap remains a limitation, because most of the absorbed light is in the ultraviolet range. Even with this limitation, TiO_2 is still a useful model system: it is stable, well understood, and can be deposited on different conductive substrates. [4], [37]

PEC testing is less forgiving of the material architecture than a typical slurry photocatalytic test. In a suspension, the catalyst particles function as separate units, and the measured response reflects the average behavior of the dispersed material. A photoelectrode cannot work in this way. The coating, support, surface, and electrolyte contact all have to function together. Light has to reach the active region, charges have to move into the substrate, and the electrolyte has to wet the surface in a stable way. Because of this, TiO_2 photoelectrodes are strongly affected by how the oxide is deposited, whether it forms a continuous layer, how it crystallises, and how well it follows the shape of the support. [7]

PEC testing is less forgiving than many slurry photocatalytic tests. In a powder suspension, many separate particles contribute to the final response, and small differences between them are averaged out. A photoelectrode works differently. The coating, support, electrolyte contact, and current pathway all have to function as one connected system. Light has to reach the active layer, charges have to move into the substrate, and the electrolyte has to contact the surface without the structure losing stability. Therefore, TiO_2 photoelectrodes are strongly affected by the deposition, crystallization, and adherence of the oxide to complex surface topographies. [4]

This is why TiO_2 remains useful in studies of structured and hierarchical photoelectrodes. Since its chemistry is relatively well known, changes in photocurrent can be discussed mainly in terms of architecture, interface quality, and charge transport, rather than being dominated by chemical instability or unclear degradation processes. In this role, TiO_2 provides a stable platform for examining how photoelectrode design affects performance. [7], [37], [50]

2.1.5. Why TiO_2 still matters in advanced materials research

Given the enormous amount of literature on TiO_2, it is reasonable to ask why this material still occupies such a central place in current research. The reason is that TiO_2 is no longer studied only as a simple photocatalyst or as an isolated oxide powder. More often, it is used as one part of a larger architecture. In this role, TiO_2 allows questions to be addressed that go beyond its basic photocatalytic activity. These include the behavior of thin oxide coatings on rough or hierarchical supports, the contact of TiO_2 with conductive phases, the effect of structured surfaces on light trapping and charge transport, and the incorporation of TiO_2 into immobilized membranes or heterostructures without losing stability. [50], [52]

In other words, the present relevance of TiO_2 lies in its role as an experimentally robust platform for exploring broader design principles in photoactive materials. This makes it possible to investigate morphology, interface engineering, deposition precision, support geometry, and functional immobilisation within a chemically familiar framework. This is especially important in a dissertation that seeks to connect several material formats under a common scientific logic. TiO_2 provides continuity across these formats while still allowing a sufficiently rich range of structural modification. [48]

Another important reason for the continued significance of TiO_2 is its methodological importance. Because TiO_2 has been studied so extensively, it offers a broad comparative background for interpreting new results. Improvements observed in TiO_2-based systems can therefore be discussed against a mature body of knowledge rather than in isolation. This is especially valuable in doctoral research, where the aim is not merely to report a locally improved material, but to position the findings within a broader scientific landscape. A well-chosen TiO_2-based study may thus contribute not only to application-oriented optimisation, but also to the critical refinement of how photocatalytic and photoelectrochemical performance are interpreted. [23]

2.1.6. From material selection to architecture-driven optimization

Although TiO_2 is often introduced as a benchmark semiconductor, the current direction of the field indicates that benchmark status alone is insufficient to achieve high functional performance. The central research question is no longer whether TiO_2 can act as a photocatalyst or photoelectrode, but how its intrinsic limitations can be addressed through structural and interfacial design. This shift in emphasis has led to the growing importance of architecture-driven optimisation as a central strategy in advanced TiO_2 research. [10]

Architecture-driven optimisation refers to the deliberate control of how the active material is organised across multiple length scales in order to influence light absorption, carrier transport, interfacial accessibility, and structural stability. In the case of TiO_2, this may include control over crystal-phase distribution, film thickness, surface roughness, pore structure, fibre arrangement, support topology, or the geometry of a hybrid interface. Such control is especially important because the effective diffusion length of photogenerated carriers is limited, which means that useful performance depends strongly on whether the material geometry supports rapid and directed transport before recombination occurs. [7]

This concept is important for both photocatalysis and photoelectrochemistry. In photocatalytic systems, architecture affects how reactants reach active sites, how strongly intermediates are adsorbed, how light enters and moves through the structure, and how easily the catalyst can be recovered after use. In photoelectrochemical systems, it also determines film continuity, electrical contact with the substrate, and the relation between optical absorption depth and the distance over which charges must be transported. For this reason,

architecture should not be regarded as a secondary feature introduced after material selection, but as one of the main factors shaping functional behaviour. [1], [4]

The move towards architecture-based strategies has also changed the way TiO_2 performance is interpreted. Earlier studies often compared materials mainly in terms of composition, crystallinity, or nominal band-gap value. More recent work shows that these features cannot be considered independently of geometry and interface quality. A thin TiO_2 film deposited on a hierarchically structured metal support, for example, cannot be judged in the same way as a high-surface-area nanopowder dispersed in suspension. Although both are chemically TiO_2, they operate under different conditions and are limited by different factors. As a result, the main scientific question is no longer simply what the material is, but how it is organised and how that organisation affects photoinduced processes. [23]

2.1.7. Relevance of TiO_2 to the present dissertation

Within the framework of this dissertation, TiO_2 has a central and unifying role. It is used not simply as a classical photocatalyst, but because it makes it possible to systematically examine how the structural hierarchy, interface quality, and immobilization strategy influence light-driven behavior across different material systems. The dissertation does not treat TiO_2 as an isolated composition to be incrementally improved. Rather, it uses TiO_2-based and TiO_2-related architectures to examine a broader scientific problem: how to design semiconductor systems in which the geometry of the support, the nature of the interface, and the organisation of the active phase favour more efficient utilisation of photogenerated charge carriers. [50]

This perspective is especially relevant for systems involving conformal oxide coatings on structured substrates, electrospun or membrane-like photocatalytic materials, and hybrid assemblies containing additional interfacially active or conductive components. In each case, TiO_2 serves as a chemically stable, conceptually coherent platform that permits the role of the architecture to be examined in a controlled manner. The scientific importance of TiO_2 in this dissertation therefore lies not only in its individual material properties, but also in its ability to connect different experimental formats under a common logic. [10]

TiO_2 serves both as a benchmark material and as a means of gaining broader insight. Its extensive presence in the literature provides a robust basis for comparison, and its compatibility with advanced fabrication methods makes it particularly suitable for investigating persistent questions in materials-oriented chemical research.The focus on TiO_2 is therefore not a conservative choice, but a strategic one, as it allows the dissertation to build a coherent argument around architecture-driven optimisation within a material system of clear scientific relevance. [51]

2.1.8. Concluding remarks

TiO_2 is still widely used in photocatalysis and photoelectrochemistry because it is stable, can be processed in many ways, and serves as a useful reference oxide. At the same time, its weaknesses, especially limited visible-light use and strong recombination of photogenerated charges, mean that good performance does not come automatically. It depends strongly on how the material is designed. For that reason, TiO_2 is best treated as a research platform for studying the effects of architecture, interfaces, and heterostructure design on photoactive behaviour, rather than as a complete solution by itself. [48], [58]

This understanding provides the foundation for the sections that follow. Once TiO_2 is considered from the perspective of structure-property-performance relationships, it becomes clear that the key challenge is not only to modify the semiconductor chemically, but also to organise it spatially in ways that support light utilisation, charge separation, interfacial transfer, and functional stability. The rationale for architecture-driven optimisation therefore emerges naturally from the intrinsic strengths and weaknesses of TiO_2 itself. [23]

2.2. Architecture-driven optimisation of semiconductor photoactive systems

The increasing complexity of modern photocatalytic and photoelectrochemical materials has made it clear that functional performance cannot be explained solely by composition, nominal band-gap value, or isolated surface-area measurements. In many cases, materials with very similar chemistry behave differently because the decisive factor is not only what the material is made of, but how it is organised across multiple length scales. This has led to the growing importance of architecture-driven optimisation as a central strategy in the design of photoactive semiconductor systems. [58]

In the broadest sense, architecture refers to the spatial arrangement of the active phase and its surrounding structural environment. This includes particle size and shape, film continuity and thickness, the porosity and tortuosity of membrane-like structures, the topology of supporting substrates, the organisation of fibres within nonwoven mats, the presence of hierarchical roughness, and the quality and distribution of internal interfaces in hybrid materials. These structural features shape light–material interaction, charge movement through the system, mass transport to and from active sites, and ultimately the behaviour observed under real experimental conditions. As a consequence, architecture is not a secondary feature added after chemical design, but one of the principal variables controlling the practical efficiency of light-driven processes. [23], [58]

The need for architecture-based design becomes especially evident when the limitations of semiconductor photoactivity are considered directly. In both photocatalysis and photoelectrochemistry, the useful fraction of absorbed light is determined not only by

the generation of electron–hole pairs, but also by the competition between productive interfacial transfer and different loss processes. Among these losses, recombination is especially important. Because the lifetime and diffusion length of photogenerated charge carriers are finite, any architecture that forces carriers to travel through poorly connected, defect-rich, or unnecessarily thick material is likely to exhibit reduced functional efficiency. Performance can also be improved without any chemical changes to the semiconductor. Sometimes, the main benefit comes from the way the material is arranged: the charges are generated closer to the surface, have a shorter path to travel, or can move more easily toward the collecting substrate or reactive interface before recombination takes over. [6], [10], [58]

2.2.1. Architecture as a multi-scale concept

One reason architecture has become such a useful concept in materials science is that it acts across more than one length scale at the same time. At the nanoscale, this may involve grain size, crystallite boundaries, surface defects, shell thickness, or the local arrangement of heterointerfaces. At the microscale, it covers features such as pore organisation, fibre diameter, roughness, and patterned surface topography. On larger scales, it extends to the membrane thickness, substrate geometry, interconnected transport pathways, mechanical stability, and the manner in which the material is built into a device or reactor system. A photoactive system therefore cannot be described adequately by a single structural parameter. Instead, its behaviour emerges from the interaction of architectural features distributed across multiple levels of organisation. [58]

This multi-scale view is important for the materials studied here, including electrospun composites, conformal coatings on structured supports, and laser-textured electrodes. In these systems, nanoscale features affect charge separation and surface reactions, while microscale geometry influences wetting, light distribution, and diffusion of reactants. Larger-scale features are also important because they determine whether the material can be handled, recovered, placed in a cell, and reused without causing serious damage. Therefore, the photoactive response is not controlled by one structural level alone. In this dissertation, architecture is treated as the combined organisation of the whole material system. [25], [58]

The multi-scale perspective also helps explain why many changes that appear promising at first do not necessarily lead to a robust improvement. A heterojunction introduced at the nanoscale, for example, may favour local charge separation, but the overall benefit can remain small if the final material becomes less accessible to the liquid phase or if electrical continuity is poor at the device level. In a similar way, greater roughness or porosity may increase the geometrical surface area, yet the final effect may still be unclear when this is accompanied by strong tortuosity, light shielding, or unstable wetting. For this reason, architecture-driven optimisation requires several effects to be balanced together, rather than one parameter being maximised on its own. [58], [59], [60], [61]

2.2.2. Influence of architecture on light management

Architecture matters partly because it changes how light enters and moves through the material. Useful charge generation depends not only on the intrinsic absorption of the semiconductor, but also on reflection losses, scattering, optical path length, penetration depth, and the position of the absorbing phase within the structure. Therefore, even materials with similar band structures can use incident light differently when their surface topography or internal geometry is different. [62], [63], [64]

Surface texturing, porosity, and hierarchical organisation can all change the optical response by lowering reflection and increasing the distance over which light interacts with the active phase. This becomes especially relevant when the semiconductor layer is thin or when the support geometry favours repeated scattering and light trapping. Micro- and nanoscale roughness can modify the angular distribution of reflected light, while periodic or semi-periodic surface structures may affect absorption through more complex optical phenomena. As a result, architecture can improve the probability that incoming photons are absorbed in regions from which generated carriers still have a realistic chance of reaching useful interfaces. [25], [62], [63], [64]

However, a more favourable optical response should not automatically be taken as evidence of better functional performance. One of the recurring weaknesses in the literature is the assumption that stronger absorption must also produce better photocatalytic or photoelectrochemical behaviour. In practice, absorption is only one step in a longer sequence. If the additional carriers generated in optically enhanced regions recombine before they can be used, the net gain may be much smaller than that suggested by the optical data alone. This is particularly relevant in rough or highly structured systems, where regions of enhanced light capture may also coincide with increased defect density or longer local transport pathways. For this reason, architecture-driven optimisation must consider light management together with transport and interfacial kinetics rather than as a stand-alone objective. [10], [23], [64]

Another important point is that optical design cannot be treated in the same way for all application formats. In photocatalytic membranes and fibrous mats, light penetration may depend on membrane thickness, fibre packing density, and local opacity introduced by fillers or deposited particles. In photoelectrochemical electrodes, the relationship between the depth of light absorption and the distance over which the generated charges must be extracted is particularly important. When photons are absorbed in regions from which carriers cannot travel efficiently to the collecting substrate or to the electrolyte interface, the architectural advantage in the optical response does not necessarily lead to higher photocurrent. [58], [65], [66], [67]

2.2.3. Architecture and charge-carrier transport

Charge transport is strongly affected by the way in which the material is built. After light absorption, electrons and holes can contribute to a reaction only if they can move from the place where they are generated to a reactive surface or collecting contact. If this path is too long, poorly connected, or rich in recombination sites, many of the carriers are lost before they can be used. [42], [68], [69]

For powders and loosely packed nanomaterials, transport occurs through a complicated network of grains, agglomerates, and surface states. A higher surface area may then be beneficial in one sense, because it provides more reactive sites, but at the same time it may create more grain boundaries and carrier traps. In thin films and conformal coatings, carrier transport depends strongly on film thickness, crystallinity, defect density, and the quality of contact with the underlying support. In electrospun or membrane-type systems, transport may additionally be influenced by the distribution of the active phase within a polymer or composite matrix and by the degree of connectivity between neighbouring fibres or deposited domains. [70], [71], [72], [73]

An important goal of architecture-driven optimisation is therefore to shorten the average transport distance between the site of charge generation and the site of charge use. This can be approached in several ways. Nanostructuring may reduce the path carriers must travel to reach the surface. Hierarchical supports may increase the active area without requiring excessively thick coatings. Directional architectures can support charge transport towards the electrode substrate, while conductive interphases or hybrid components may open additional pathways that help suppress recombination losses. However, these strategies are only beneficial when the final system remains structurally coherent and does not create new barriers or sources of instability. [68], [74], [75], [76]

This issue becomes especially significant in photoelectrochemical systems. A photoelectrode must maintain electronic continuity from the irradiated semiconductor surface to the current collector, while also preserving sufficient access of the electrolyte to the reactive interface. If the architecture compromises either of these conditions, photocurrent may remain low despite nominally favourable semiconductor properties. For this reason, optimisation of photoelectrodes often involves finding a balance between thickness, roughness, porosity, and interface continuity rather than maximising one feature alone. [42], [69], [77]

2.2.4. Surface accessibility, wetting, and mass transport

While optical behaviour and charge transport are central to semiconductor functionality, architecture also influences a third major aspect of performance: the physical accessibility of active interfaces to reactants and the efficiency of mass transport within the system. This aspect is especially important in photocatalysis, where the overall reaction rate

depends not only on carrier generation and separation, but also on the ability of molecules from the liquid or gaseous phase to reach active sites, adsorb appropriately, react, and then diffuse away as products or intermediates. [78], [79], [80]

In powder suspensions, mass transport is usually less problematic because the catalyst is dispersed in the solution and mixing helps reduce concentration gradients. However, aggregation or poor wetting can limit the accessibility of the catalyst surface. In immobilised systems, transport depends much more strongly on the material architecture. Pores, fibres, channels, and surface protrusions decide whether the reactants can enter the structure or mainly interact with the outer surface. Local wetting behaviour is equally important, because hydrophilic and hydrophobic regions affect liquid penetration, capillary flow, and the real contact area between the material and the solution. [61], [78], [81]

These factors become particularly important in membrane-type and electrospun photocatalysts. Although a fibrous membrane may appear open and offer a large geometric surface, the real transport conditions still depend on fibre diameter, packing density, the size of inter-fibre voids, roughness, and surface chemistry. When the fibres are packed too closely, inner regions may be difficult to access or may not be illuminated evenly. If wettability is poor, contact with the liquid phase may remain incomplete, and the measured activity can then appear lower than it really is or vary from one region of the membrane to another. By contrast, a better-organised structure can give a stronger response even with the same nominal composition, simply because the liquid can penetrate it more easily and reach more active regions. [78], [79], [80], [82]

For photoelectrodes, this balance is not easy to achieve. The oxide surface should be in contact with the electrolyte, but the coating must also stay continuous and well connected to the support. A rougher or more porous surface usually gives a larger contact area. At the same time, it can make the real working conditions less uniform. Some parts of the surface may be wetted less effectively, diffusion may be slower in narrow regions, and gas bubbles may remain attached during operation. These effects can influence the measured PEC response and should be considered together with the electrode structure. [82], [83], [84]

This also affects how the results should be interpreted. If an immobilised or hierarchical photocatalyst removes more pollutant or gives a higher photocurrent, the improvement does not have to come only from better electronic properties. It may also come from better wetting, stronger or more favourable adsorption, easier access of reactants, or faster removal of products from the surface. The improvement is still real, but its origin should not be assigned too quickly to band-structure changes or heterojunction effects alone. In architecture-controlled materials, several factors usually act simultaneously. [85], [86], [87], [88]

2.2.5. Connection to the diagnostics framework

The contrast between particulate and immobilised systems illustrates especially clearly why architecture must be treated as a core design variable. In particulate photocatalysis, the active material is usually dispersed in the liquid phase, which tends to maximise contact between reactants and the available surface while also providing a relatively high specific surface area. This makes the format useful for mechanistic studies and for comparing compositional effects, but it also brings practical drawbacks, especially when catalyst recovery and reuse become important. Moreover, performance metrics obtained in such systems may be difficult to translate directly into realistic treatment or device environments. [89], [90], [91]

Immobilised systems, including coated supports, fibrous membranes, porous substrates, and structured electrodes, are based on a different architectural approach. In these systems, the active material remains fixed in place, often as a continuous or partially continuous phase supported by a mechanically stable scaffold. This can make handling easier and improve integration into practical systems, but it also changes the main limitations that need to be considered. Surface accessibility no longer depends only on area, but also on geometry and wetting. Charge transport may become more directional and more strongly dependent on the substrate. Optical behaviour can also change as a result of thickness, support reflectivity, or hierarchical roughness. Thus, immobilisation is not simply a practical solution to a recovery problem. It fundamentally changes the way in which the photoactive material operates. [86], [92], [93], [94]

This distinction is highly important in architecture-engineered materials. Many of the systems considered in this work are intentionally immobilised or structurally organised rather than used as conventional suspended powders. Their evaluation must therefore reflect not only intrinsic semiconductor behaviour, but also the practical and mechanistic consequences of architectural fixation. A rigorous literature discussion should make this distinction explicit, because otherwise comparisons between different material formats risk becoming superficial or misleading. [86], [89], [95], [96]

2.2.6. Hierarchical structures as a response to competing requirements

One of the main difficulties in semiconductor design is that improving one feature can weaken another. A larger surface area gives more contact with the electrolyte and more places for interfacial reactions, but very fine structuring can also add defect sites or make the material less stable. A thicker layer may absorb more light, yet the charges formed deeper inside it have farther to travel before they reach a useful interface. A porous structure can help the solution enter the material, but poor connectivity may slow charge transport and reduce mechanical strength. A compact film gives better electrical contact with the substrate, although it exposes a smaller active area. Hierarchical structures are useful because they are

meant to balance these competing effects instead of optimising only one feature. [97], [98], [99]

Hierarchical architectures are useful because no single structural scale is able to satisfy all requirements of a photoactive material. The larger structure can give the material its shape, mechanical support, optical texture, or recoverable form. The smaller structure then controls the local contact between the semiconductor, the electrolyte, and the reacting species. For example, laser texturing can make the support interact more strongly with light and can also provide the deposited layer with a better surface for attachment. This is only useful, however, if the semiconductor coating remains continuous and does not become so thick that charge extraction is hindered.In fibrous membranes, the mat itself gives the material a usable form: it can be handled, removed from the solution, and used again. The finer structure then becomes important at the working surface, where it affects liquid penetration and access to the active regions. The main point is therefore not to make the material more complex for its own sake, but to arrange different length scales so that light harvesting, surface access, and charge transport work together. [7], [25], [26]

The success of hierarchical design depends on how effectively the different structural levels are integrated. If the nanoscale coating fails to conform to the microscale support, or if the porous membrane becomes inaccessible to the liquid phase, the expected advantages may not be realised. For this reason, hierarchy must be matched by suitable fabrication methods. This is why techniques such as atomic layer deposition, electrospinning, and femtosecond laser structuring are especially relevant. They provide different ways of controlling architecture across multiple scales while maintaining sufficient precision to produce reproducible and interpretable results. [61], [78], [100]

2.2.7. The relationship between architecture and interface quality

Architecture and interface quality are closely linked. In hybrid and structured systems, the way the material components are arranged defines not only the overall geometry, but also the character of the contacts through which charge carriers, reactants, and even mechanical stresses are transferred. A heterostructure can only work as well as the interface that connects its components, and a structured support becomes truly beneficial only when the active phase is integrated with it in a continuous and functionally meaningful manner. [42], [58], [101], [102]

In many photoactive materials, improved performance is often linked either to the addition of a second phase or to increased substrate roughness. On their own, however, these changes do not ensure a real benefit. When the interfacial contact is discontinuous, rich in defects, weakly attached, or unevenly distributed, the final system may show stronger recombination, lower stability, or a response that is difficult to interpret clearly. For this reason, architecture-driven optimisation cannot be considered separately from interface engineering. The geometry of the material defines where interfaces appear and how large

they are, whereas the fabrication route determines whether these interfaces act as effective transport pathways or instead become barriers. [10], [85], [101], [103]

This point is particularly important in systems based on conformal coatings on complex surfaces. When a structured support is modified with a thin semiconductor layer, the functional properties of the final material depend strongly on whether the coating follows the support topography uniformly and whether the buried interface remains electrically and mechanically coherent. In such cases, the architecture does not merely influence the amount of active area. It defines the conditions under which the semiconductor and support exchange charge. In this work, geometry and interface formation are therefore treated as inseparable aspects of one design problem. [7], [104], [105], [106]

2.2.8. Architecture and the interpretation of performance enhancement

A more cautious interpretation becomes necessary as the architecture of a photoactive system becomes more complex. Changes in photocatalytic degradation rate, photocurrent density, or optical absorption are often read as straightforward signs of improved semiconductor behaviour, even though several of these observables may be altered at the same time by the architecture of the system. A rougher or more porous surface, for instance, can trap more light, adsorb more dye, improve wetting, change the local concentration of reactants near the interface, and alter the number of exposed crystal facets. In a similar way, a conductive additive may assist electron extraction, but it may also change morphology and dispersion. A membrane may facilitate recovery while simultaneously introducing internal transport limitations. For this reason, improved performance in architectured systems is rarely the result of one factor alone. [18], [23], [61], [103]

This complexity should not be considered a weakness of architecture-based research. On the contrary, it shows how closely optical, electronic, and transport effects are connected in real materials. At the same time, it means that mechanistic claims need to be made with caution. Better dye removal in a hybrid membrane, for example, should not be automatically considered as evidence of improved charge separation if adsorption and wetting effects have not been considered. In the same way, a higher photocurrent from a structured electrode does not by itself demonstrate that a heterojunction is working optimally, since the observed change may also result from greater roughness or improved contact with the substrate. [12], [30], [79], [86]

Accordingly, architecture-driven optimisation must be accompanied by architecture-aware interpretation. This requires not only the measurement of activity or photocurrent, but also consideration of morphology, interfacial structure, optical behaviour, stability, and transport conditions. The most meaningful contributions in this field are those that do not merely present higher performance values, but explain how structural organisation leads to those values and under what limitations the conclusions remain valid. [32], [39], [80], [102]

2.2.9. Relevance of architecture-driven optimisation to the present dissertation

The concept of architecture-driven optimisation provides one of the main unifying ideas of this work. Although the materials investigated in the following chapters differ in composition, format, and application context, they are connected by a common focus on how the spatial organisation of the active phase influences light-driven behaviour. This includes hierarchically structured supports produced by laser processing, conformal oxide layers introduced by controlled deposition methods, electrospun and membrane-type photocatalytic systems, and hybrids incorporating additional interfacially active components. [7], [8], [25], [26]

In these systems, the main question is not only which material is used, but how its structure affects the final photocatalytic or photoelectrochemical response. Surface geometry, coating continuity, interface quality, active-site accessibility, charge transport, recombination, and stability all influence the result. For this reason, the work does not focus only on changing the chemical composition. It also considers how the material is built and how this affects its behaviour under illumination. [10], [42], [62], [102]

This approach is also useful for organising the thesis. The material systems studied here are not identical: they include TiO_2 coatings on structured titanium, hybrid oxide membranes, and laser-processed semiconductor supports. However, they can still be discussed using the same questions as above. How far do charges have to travel? How good is the interface? Can the liquid reach the active region? Does the structure help or hinder light use and transport? Therefore, architecture is not treated here as a separate topic. This is one of the main ways in which the different studies in this dissertation are connected. [23], [42], [58], [86]

2.2.10. Concluding remarks

Architecture has become a central concept in the design of photocatalytic and photoelectrochemical materials because it connects composition with function through the real geometry of the system. It determines how light is absorbed, how carriers move, how reactants reach active sites, how interfaces are formed, and how a material behaves when transferred from an idealised laboratory format to an immobilised or device-oriented configuration. For this reason, architecture-driven optimisation should not be viewed as an optional refinement of semiconductor design. In this work, it is treated as one of the principal routes through which meaningful performance improvement can be achieved. [23], [58], [79], [86]

This point is especially relevant for TiO_2-based systems. TiO_2 is stable and well known, but its performance depends strongly on how the material is arranged and connected to other components. This makes it a useful platform for studying the role of hierarchical supports, conformal coatings, membrane formats, and hybrid interfaces in photoinduced

processes. The following sections therefore focus on the main strategies used in this work: controlled thin-film deposition, laser structuring, hybridisation with functional additives, and immobilised photoactive architectures. [7], [25], [50], [79]

2.3. Atomic layer deposition as a tool for interface and thickness control in photoactive systems

Among the available methods for preparing thin semiconductor coatings, atomic layer deposition (ALD) has become especially important in photocatalytic and photoelectrochemical materials research. Its significance lies not only in its ability to produce highly uniform films, but also in the degree of control it offers over thickness, conformality, and interface formation on substrates of complex geometry. In systems where architecture strongly influences functional behaviour, this level of control is particularly valuable. [72], [107], [108]

Coating a flat surface is relatively simple. The real difficulty appears when the support is rough, porous, or strongly textured. In such cases, a deposited layer may cover only the outer surface, grow unevenly, or partly block the structure that was meant to be preserved. ALD is valuable because it can build the oxide layer directly along the shape of the support, including surfaces that are difficult to coat by more conventional methods. In this dissertation, ALD is therefore treated not only as a technique for producing thin films, but as a way to introduce the photoactive phase without losing the architectural function of the underlying material. [72], [100], [109]

The relevance of ALD to photoactive systems is closely connected with the fact that many key performance parameters depend on nanoscale control. In photocatalytic and photoelectrochemical materials, the thickness of the semiconductor layer, the continuity of coverage, the quality of contact with the substrate, and the distribution of interfacial defects can all affect charge-carrier transport, recombination probability, and long-term stability. [110], [111]

Small variations in these parameters may substantially alter the functional response, especially when the active layer is ultrathin or deposited on a hierarchically structured support. A deposition method that allows thickness to be increased in a predictable and highly controlled manner is therefore especially important in research aimed not only at establishing whether a material performs well, but also at understanding why it behaves in that way. [100], [107], [108]

2.3.1. General principles of atomic layer deposition (ALD)

Atomic layer deposition is based on alternating, self-limiting surface reactions between gaseous precursors and a reactive substrate surface. In a typical ALD cycle, the first precursor is introduced into the reactor and reacts with available surface groups until

saturation is reached. Excess precursors and gaseous by-products are then removed, usually by purging with an inert gas. A second precursor is then introduced and reacts only with the surface species formed during the previous half-cycle. After a second purge step, one complete growth cycle is achieved. By repeating this sequence, a film can be built up with angstrom-level or sub-nanometre-level control over thickness. [100], [107], [108]

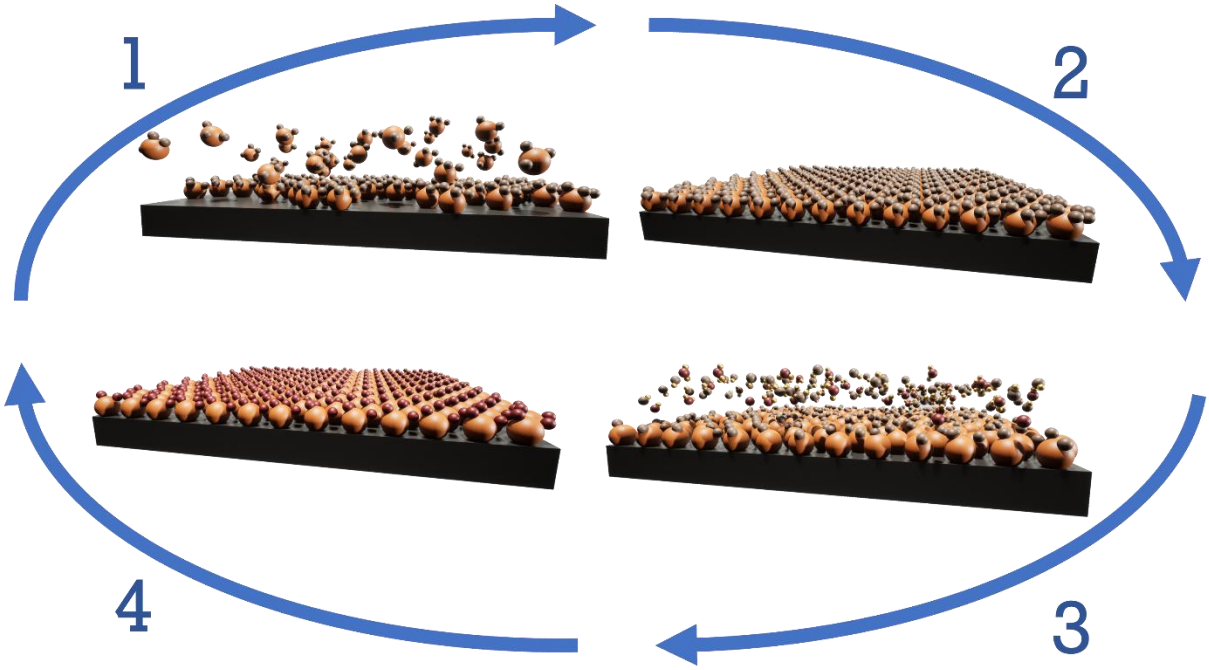

Figure 2.2. *TiO_2 ALD cycle carried out with $TiCl_4$ and H_2O: (1) the hydroxylated surface is exposed to $TiCl_4$, (2) unreacted $TiCl_4$ and volatile products are removed by purging, (3) H_2O is then pulsed to react with the modified surface and renew the hydroxyl termination, and (4) the chamber is purged once more before the sequence is repeated. Prepared by the author.*

The self-limiting character of each half-reaction is the defining advantage of ALD. Because the process depends on surface saturation rather than continuous gas-phase decomposition, growth is generally more uniform and reproducible than in many other vapour-phase deposition methods. This becomes particularly important when the substrate contains high-aspect-ratio features, internal porosity, or hierarchical roughness. Provided that the precursors can reach the accessible surface and the process conditions are appropriate, the deposited film can closely follow the substrate geometry. In photoactive materials, this is essential when the aim is to functionalise an architectured support without destroying or masking the structural features responsible for improved optical or interfacial behaviour. [72], [105], [107], [109], [112]

Another important characteristic of ALD is its ability to separate thickness control from many of the instabilities typical of less controlled deposition routes. Because the amount of material added in each cycle is limited by the number of reactive surface sites, film thickness can often be tuned very precisely through the number of cycles. This provides a valuable framework for systematic investigation of thickness-dependent phenomena, such as the transition from discontinuous islands to continuous coverage, the effect of thickness on crystallisation, or the balance between improved absorption and increased transport resistance. Such controlled variations are especially useful for studies on structure-property relationships. [71], [100], [110], [111], [113], [114]

2.3.2. Why ALD is attractive for photocatalytic and photoelectrochemical materials

The attractiveness of ALD in photoactive materials research arises from the fact that many performance-limiting steps occur at or near interfaces. In photocatalysis, the active surface must interact efficiently with adsorbed reactants while limiting charge recombination. In photoelectrochemistry, the semiconductor must be integrated with a substrate in a way that permits carrier transport to the external circuit while also maintaining a well-defined interface with the electrolyte. In both cases, uncontrolled roughness, partial coverage, excessive thickness, or buried interfacial defects can reduce the usefulness of an otherwise promising material. [7], [110], [115]

When the support is structured, coating becomes part of the design problem. The roughness, pores, or laser-made texture are there for a reason: they help the material interact with light, liquid, or the current collector. However, these advantages can be reduced if the coating is uneven. This is a possible drawback of dip-coating or sol-gel methods on complex surfaces, where the precursor may gather in some places, miss others, or change the shape of fine features during drying. ALD avoids this to a large extent because the oxide is built directly on the exposed surface. The coating can therefore be added without removing the role of the underlying architecture. [72], [100], [109]

This point is especially important when the substrate itself plays an active role in the final device. In a structured photoelectrode, the support is not simply a mechanical carrier. It may influence light trapping, geometric surface area, electrical contact, and local field distribution. If the deposition method fails to preserve the support architecture or produces a non-uniform buried interface, the final photoresponse may reflect deposition artefacts rather than the intended architectural design. The ability of ALD to coat such substrates with controlled uniformity therefore makes it highly valuable for the study of architecture-performance relationships. [7], [116], [117]

In photocatalytic systems, ALD can be used to give a support a function that it would not have on its own. A thin oxide layer can convert an inert or unstable surface into a photoactive surface, protect a sensitive material, or create an interface with another

semiconductor. Depending on the system, the ALD layer may act as the main active phase, a stabilising shell, or one part of a heterostructure. Because the layer thickness can be controlled quite precisely, it becomes easier to determine whether the observed effect comes mainly from the oxide chemistry, the support geometry, or the interface between them. [109], [110], [118], [119]

2.3.3. Thickness control as a functional design parameter

The thickness of the semiconductor layer in photoactive materials is not just a secondary parameter. In many cases, it determines whether the deposited film remains incomplete, acts as an effective active layer, or becomes thick enough to introduce transport limitations. Therefore, one of the main advantages of ALD is that it allows the thickness to be adjusted step by step with good reproducibility. [100], [110], [120]

If the deposited layer is too thin, the substrate may not be fully covered. The film can remain discontinuous and form separate islands instead of a uniform semiconducting layer. Pinholes or defect-rich regions may then control the response under electrochemical conditions. In photocatalytic tests, incomplete coverage can lead to uneven activity and unclear interfacial behaviour. In PEC measurements, exposed substrate areas may also affect the photocurrent and introduce additional reactions caused by direct contact between the substrate and the electrolyte. [72], [110], [116]

At the other extreme, films that are too thick can also become problematic. A thicker coating usually contains more light-absorbing material, but it also forces photogenerated carriers to travel farther before they reach the reactive interface or the current collector, which increases the chance of bulk recombination. Thick layers may additionally build up internal stress, lose conformality in the most difficult topographic regions, or become more prone to cracking and delamination after thermal treatment. For this reason, the link between thickness and performance is not linear. In most cases, there is an intermediate regime in which the coating is sufficiently complete and optically active, yet still thin enough to support efficient transport and good interfacial contact. [111], [121], [122]

For hierarchical supports, the thickness problem becomes even more important. A coating that is too thick can partly erase the benefit of the original geometry by smoothing sharp features or blocking access into the structure. A coating that is too thin causes a different problem, because the semiconductor layer may never become continuous enough to act as a stable active phase. In this respect, ALD is useful because it allows thickness to be varied systematically without changing either the substrate geometry or the deposition route. [58], [72], [100]

The thickness also affects the crystallization behavior. In many ALD-grown oxide systems, the transformation from amorphous to crystalline material depends on both annealing conditions and film thickness. Very thin coatings may crystallise differently from

thicker ones, and the resulting grain structure may influence carrier mobility, trap density, and surface reactivity. Consequently, the film thickness in ALD systems should not be considered only in geometrical terms. This is linked to phase evolution, defect structure, and interface development, all of which may influence the final photoresponse. [47], [71], [120]

2.3.4. Conformality on complex and hierarchical substrates

One of the main reasons ALD is used in advanced materials research is that it can coat substrates that are difficult to functionalise uniformly by more conventional methods. This is particularly relevant for hierarchical surfaces, porous membranes, microstructured metals, fibrous materials, and features with high aspect ratio. On such substrates, non-conformal deposition may lead to shadowing, pore blockage, local overgrowth, or thickness gradients, all of which make the results difficult to reproduce and interpret. [72], [109], [123]

In architecture-engineered systems, this becomes critical because the support already has a job to do. Its geometry is not only a surface on which the active phase is placed. The laser texture may help the material interact with light, the pores may allow liquid to pass through, and the fibre network may keep the active surface open to the solution. If the coating blocks these spaces or rounds off the features too much, the benefit of the original structure is reduced. Conformality is therefore important not because the coating looks more uniform, but because it helps the designed support continue to work after the active phase is added. [25], [79], [109]

ALD addresses this issue by allowing the material to be deposited in a layer-by-layer manner over the existing topology. Provided that the precursor exposure is sufficient and the process window is well chosen, the film can follow ridges, valleys, pores, and other surface features with relatively high fidelity. This makes ALD particularly valuable in studies where the aim is to determine how a structured support influences photoactivity after controlled oxide deposition. Without conformal coverage, it would be difficult to separate the effect of the support architecture from artefacts introduced by poor coating quality. [72], [100], [124]

Conformality is also closely linked to the reproducibility of comparative experiments. In research built around architecture-driven optimisation, it is often necessary to compare substrates that differ in roughness, periodicity, or geometry while keeping the deposited active phase as consistent as possible. ALD provides one of the best available frameworks for such comparisons because it minimises uncontrolled variation in coating thickness and coverage between differently structured samples. As a result, observed differences in behaviour can be attributed more confidently to the intended architectural variable rather than to inconsistencies in deposition. [100], [124], [125]

2.3.5. Interfacial quality and buried-interface control

In many photoactive systems, the most important interface is not the external surface exposed to light or electrolyte, but the buried interface between the semiconductor and its

supporting substrate. This interface governs adhesion, electrical contact, stress distribution, nucleation behaviour, and, in many cases, the ease with which photogenerated carriers can be extracted or transferred. However, it is often the least visible part of the material. For this reason, deposition methods that provide good control over the buried interface are especially valuable. [126], [127], [128]

ALD can improve interfacial quality in several respects. Because the earliest stages of growth are controlled by surface chemistry, the first deposited layers may form very close contact with the substrate. The self-limiting character of the process also helps reduce uncontrolled overgrowth and random island formation, which are more common in methods strongly affected by solution drying or non-uniform precursor decomposition. In addition, because the film grows gradually, it becomes possible to follow how the buried interface changes with increasing thickness, which is useful when distinguishing interface-dominated behaviour from behaviour that is more bulk-like. [72], [107], [110]

The quality of the buried interface is particularly important in photoelectrochemical systems. A photoactive oxide film may absorb light effectively, but the extracted photocurrent can still remain low if the electronic contact with the conductive substrate is poor. Voids at the interface, contamination, local delamination, or weak nucleation may all increase resistance and favour recombination. By contrast, an interface that is continuous and well adhered can improve charge collection and help the coating remain stable during electrochemical operation. This is one of the reasons why ALD is often chosen for oxide films used in photoelectrodes and related architectures. [116], [126], [127]

For photocatalytic coatings, interfacial quality also matters, even when current collection is not the primary function. The buried interface influences mechanical stability, resistance to delamination, and the way the active coating responds to thermal treatment or repeated wetting and drying cycles. In immobilised systems, these factors are especially important because a mechanically unstable active layer may gradually lose functionality even if its intrinsic photocatalytic properties are favourable. The value of ALD therefore lies not only in producing a good surface, but also in producing a robust and functionally meaningful internal contact. [129], [130], [131]

2.3.6. ALD-grown TiO_2 in photoactive systems

Titanium dioxide is one of the most extensively studied materials in ALD-based photoactive research. This is due partly to the availability of well-established precursor chemistries and partly to the central role of TiO_2 in photocatalysis and photoelectrochemistry more broadly. ALD-grown TiO_2 has been investigated as a photocatalytic thin film, photoanode coating, passivating or stabilizing shell, component of heterostructures, and conformal layer on textured or porous supports. [120], [132], [133]

One of the recurring themes in this literature is the distinction between as-deposited and thermally treated films. ALD TiO_2 is frequently amorphous immediately after deposition, depending on process temperature and precursor system. Although amorphous films may still show useful behaviour in some cases, many applications benefit from post-deposition annealing that induces crystallisation, often toward anatase or mixed-phase structures. Annealing can improve carrier transport, modify surface chemistry, and enhance photoresponse, but it may also change roughness, stress state, adhesion, and interaction with the support. Therefore, the behavior of ALD-grown TiO_2 should be regarded as the result of a combined deposition-crystallization process rather than deposition alone. [47], [117], [126], [130]

Another important point is that ALD-grown TiO_2 provides a particularly good platform for examining how thickness interacts with support geometry. Because the film can be deposited conformally over structured substrates, it becomes possible to investigate how a controlled amount of TiO_2 behaves when distributed over a microscopically or hierarchically modified surface. This type of system is highly relevant to architecture-focused work because it allows one to ask whether improved performance arises from the oxide itself, from the geometry of the support, or from the synergistic combination of both under conditions of good interface control. [72], [132], [134]

ALD TiO_2 is also useful as a reference system for more complex studies. Before adding heterojunctions, conductive phases, or more elaborate multi-step architectures, it is often important to establish how a controlled TiO_2 layer behaves on the selected support. Such baseline systems make later interpretation more reliable, because they help separate the effect of the oxide architecture itself from the influence of later modifications. This is especially useful in thesis work, where the scientific argument often develops more clearly when it moves from a simpler reference system to more advanced composite or hierarchical architectures. [110], [120], [128]

2.3.7. ALD in heterostructure and hybrid-system design

Beyond simple oxide coatings, ALD is also useful for building hybrid and heterostructured systems. Its main advantage here is the step-by-step control of layer growth, which allows different materials to be brought into contact in a reproducible way. This is important for core-shell structures, bilayers, passivation layers, thin interfacial modifiers, and coatings on conductive or structured supports. [110], [135], [136]

In such systems, the role of ALD is not limited to the deposition of an active semiconductor. It may also be used to tune band alignment indirectly through control of interface thickness, suppress unwanted interfacial reactions, stabilise a less robust underlying material, or create a thin barrier that modifies recombination pathways. For example, an ultrathin oxide layer introduced by ALD may reduce surface recombination or improve chemical stability without severely compromising transport, provided that its

thickness is carefully controlled. Similarly, a conformal layer may help convert a geometrically complex scaffold into a reproducible platform for further functionalisation. [127], [134], [135]

However, ALD-based heterostructures require careful interpretation. The method can change thickness, coverage, interface chemistry, and even wetting at the same time, so an observed improvement cannot always be linked to one mechanism only. A coated hybrid system may perform better because charge separation is improved, but the same result may also be influenced by stronger adhesion, lower defect exposure, changes in surface hydroxylation, or a more favourable morphology. For that reason, the value of ALD in heterostructure research lies not only in the control it offers, but also in the possibility of analysing carefully which variable is actually responsible for the functional change. [72], [108], [110], [137]

2.3.8. Limitations and interpretive challenges of ALD-based systems

ALD is useful mainly because it gives control, but this control is not unlimited. A 100 nm film, for example, requires many more cycles than a 10 nm film; therefore, thickness quickly becomes a question of process time. This is not critical for small laboratory samples, but it matters when the same approach is considered for larger surfaces or repeated fabrication. The shape of the support is another limitation. On an open surface, the precursor can reach the reaction sites more easily. In deep pores, narrow channels, or strongly tortuous structures, access is slower and the inner regions may not grow in the same way as the outer surface. Therefore, ALD conformality should be understood as a result of suitable process conditions, not as something guaranteed by the method itself. [72], [108], [138], [139]

Third, the apparent precision of ALD can sometimes encourage overinterpretation. A highly uniform film is not automatically an optimal film. If the selected thickness is unfavourable, if post-deposition treatment creates unwanted defects, or if the band positions of the deposited oxide do not suit the intended application, the resulting system may still perform poorly. Similarly, ALD may preserve substrate architecture very well, but this does not guarantee that the architecture itself is beneficial. In other words, although ALD provides control, it does not eliminate the need for sound material design. [100], [110], [116], [120]

The effect of ALD is also not always easy to separate into one clear cause. After deposition, the sample is no longer the same surface with only an added layer. The oxide coating may improve continuity, cover defect-rich regions, change wetting, alter crystallisation, or modify the local field at the interface. Any of these changes can affect the photocurrent or photocatalytic rate. Therefore, ALD-based systems are useful for studying mechanisms, but the improvement should be discussed as the result of several possible interfacial and structural changes, not as a single effect by default. [61], [71], [72], [110]

2.3.9. Relevance of ALD to the present dissertation

ALD is important in this dissertation because it enables the placement of TiO_2-based layers on structured supports with controlled thickness and coverage. In the studied systems, the coating is not just an added oxide film. It forms part of the working interface, where layer continuity, contact with the support, and the shape of the underlying structure all affect the photoactive response. This is why ALD is used when the support geometry itself is being tested, rather than treated only as a passive substrate. [72], [100], [108], [120]

The use of ALD also follows the architecture-based logic of the dissertation. It allows TiO_2-based coatings to be deposited on hierarchical surfaces without removing the shape of the support. This makes it possible to discuss the oxide layer, the support geometry, and the interface between them as connected parts of one system. The final response can then be considered in terms of several questions: what is caused by the coating itself, what comes from the structured support, and what depends on the quality of contact between the two factors. This is central to how the study interprets architecture-controlled photoactivity. [7], [72], [100]

Moreover, ALD contributes to the reproducibility and comparability of the studied materials. In research that includes different forms of structured or immobilised systems, it is essential to maintain high control over at least some fabrication variables. ALD provides this control by allowing the thickness to be tuned in a predictable manner and by reducing the uncontrolled variation in coverage quality. As a result, it supports not only material preparation, but also the interpretive discipline required for meaningful structure-property-performance analysis. [72], [100], [107], [139]

2.3.10. Concluding remarks

Atomic layer deposition has become one of the most important tools in the preparation of advanced photoactive materials because it enables precise control over thickness, conformality, and interface formation on substrates whose geometry would otherwise be difficult to functionalise reproducibly. In photocatalytic and photoelectrochemical research, where small structural differences can produce large functional consequences, this degree of control is especially valuable. ALD makes it possible to preserve the advantages of a structured support while introducing a semiconductor coating that is continuous enough to be functional and thin enough to remain transport-efficient. [72], [100], [108]

For TiO_2-based and related systems, ALD is especially useful because it allows one to examine, in a controlled way, how film thickness, crystallisation, buried-interface quality, and support architecture affect the final behaviour of the material. In this dissertation, its role is therefore not limited to deposition alone. ALD is used as a practical tool that connects structural design with functional response, so that geometry, interface formation, and active-

layer properties can be studied together within the same material system. [71], [72], [116], [120]

2.4. Laser-structured and hierarchical substrates for photoactive applications

The growing importance of architecture-driven optimisation has made surface and bulk structuring of substrates an increasingly significant part of modern photocatalytic and photoelectrochemical materials research. In many photoactive systems, the substrate is not merely a passive carrier of electrons. It can alter optical coupling, effective surface area, wetting, transport of mass, and mechanical stability, while in electrode systems it also affects electrical continuity and charge collection. Of the available structuring methods, laser processing has become especially useful because it allows the direct production of controlled micro-and nanoscale features on many kinds of materials without relying on masks, wet-chemical steps, or multistage lithographic processing. This is especially true for ultrafast laser processing, where high precision, minimal heat-affected zones, and rich morphology formation enable the creation of hierarchical surfaces with functionally relevant topology. [140], [141]

Laser structuring is attractive for photoactive materials because it changes the surface in a controlled and permanent way. The created texture can affect light interaction, surface area, wetting, and access to reactive sites. It also gives a defined base for later modification, for example by thin-film deposition or hybrid assembly. After a semiconductor layer is added, especially by a conformal method such as ALD, the support and the coating should no longer be treated separately. The support provides geometry, while the coating provides the photoactive interface. Their combined effect determines how the final material responds under photocatalytic or photoelectrochemical conditions. [142], [143]

2.4.1. Why structured substrates matter in photocatalysis and photoelectrochemistry

The importance of structured substrates in photoactive systems can be understood by considering the sequence of steps linking photon absorption to the functional output. In photocatalysis, the relevant output is the net rate of surface redox transformations driven by photogenerated carriers. In photoelectrochemistry, the output is the extraction of charges as photocurrent and their participation in electrochemical processes at the semiconductor-electrolyte interface. In both cases, performance is governed by the combined influence of optical absorption, charge separation, charge transport, interfacial transfer, and mass transport. The substrate structure can simultaneously affect several of these steps. [142]

From an optical point of view, surface texturing can lower specular reflection, increase diffuse scattering, and lengthen the effective light path inside the system. Thus, the probability of incident light being absorbed by the active layer may increase. Texturing can

also change the angular distribution of light in porous or hierarchical structures, which may promote additional light trapping through repeated scattering. Such effects become especially important when the semiconductor layer is thin or when the support has a strong refractive contrast relative to the surrounding medium. [144], [145]

From the geometric and interfacial point of view, structured substrates offer a larger effective area for coating growth and for surface reactions. At the same time, a larger area is only beneficial when reactants can still access it efficiently and when charge transport remains effective. In photocatalysis, a larger surface may favour adsorption and create more interfacial reaction sites, but this advantage can be offset if poorly wetted or weakly illuminated inner regions begin to impose diffusion limitations. In photoelectrochemistry, an increased area may strengthen the semiconductor-electrolyte interface, yet this advantage still has to be balanced against the need for continuous electrical contact and efficient extraction of photogenerated carriers. [146], [147]

The scientific value of structured substrates therefore lies not merely in producing a "rougher surface," but in providing a controllable design variable through which the coupling of optical, transport, and interfacial phenomena can be examined. This is particularly important in work that aims to develop a unified argument across several material formats, because structured substrates can serve as common platforms for analysing how architecture influences photoinduced behaviour. [142]

2.4.2. Ultrafast laser processing as a route to hierarchical architectures

Ultrafast laser processing, especially in the femtosecond regime, offers unusual possibilities for surface engineering because the energy is delivered faster than heat can diffuse through the material. As a result, the modification usually remains highly localised, which makes it possible to generate micro- and nanostructures while limiting bulk heating and unwanted damage to the surrounding material. Depending on the substrate, pulse energy, repetition rate, scanning strategy, and ambient conditions, this type of laser treatment can produce many different surface morphologies, including microgrooves, pits, ripples, and hierarchically rough structures that combine more than one structural scale. [140], [141]

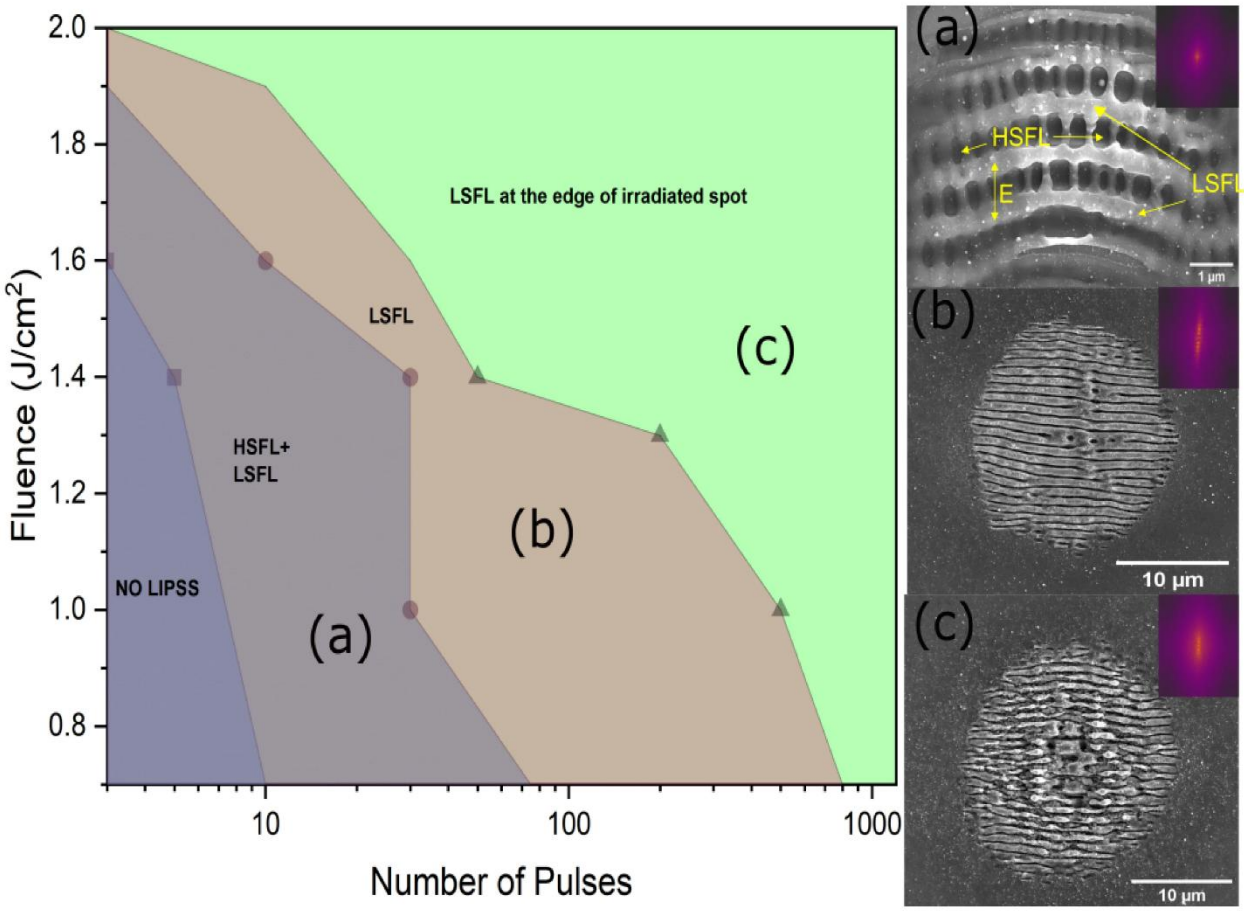

Figure 2.3. *Femtosecond-laser-induced periodic surface structures formed on silicon under different processing conditions. The images show how the surface morphology changes together with the corresponding structural regime. Reproduced from Ref.* [148]*, under the Creative Commons CC BY licence.*

A particularly important class of ultrafast-laser-induced features is the laser-induced periodic surface structures. These features typically appear as quasi-periodic patterns, with a period related to the laser wavelength and optical properties of the substrate. Different regimes are usually distinguished and are often described as low-spatial-frequency and high-spatial-frequency patterns. In practice, however, the resulting surface is often not a simple sinusoidal ripple, but part of a broader hierarchical texture that can include microscale ablation features, redeposited material, and nanoscale roughness. This complexity is important because it means that a laser-structured surface can modify light interaction and wetting behaviour through several mechanisms simultaneously. [149], [150]

For semiconductor and metallic supports, laser structuring can be considered as the preparation of the surface on which the active coating will later work. The texture produced by the laser affects not only light interaction, but also the way the next layer grows. It can influence whether the coating becomes continuous, how much material is needed to cover

the surface, and whether the final electrode remains accessible and stable. In this sense, laser processing does more than roughen the substrate. It defines the environment in which the film is deposited, the interface is formed, and the photoactive response develops. [143], [151]

2.4.3. Optical consequences of laser structuring

One of the main reasons for using laser structuring in photoactive materials is that it can change the optical response of the surface. Structured surfaces may lower reflection through graded refractive effects, promote multiple scattering, and increase effective absorption by extending the path of photons within the active layer or the structured architecture itself. Such effects are often discussed in connection with strongly absorbing, so-called “black” surfaces and with improved light trapping in photovoltaics and photoelectrodes. [144], [145]

For photocatalysis and photoelectrochemistry, however, the key issue is not simply whether the surface becomes optically darker, but whether such optical changes lead to more effective charge generation and use. A structured surface may absorb more light and still show no real functional improvement if recombination remains dominant or if the absorbed energy is concentrated in regions from which carriers cannot be extracted efficiently to a reactive interface. For this reason, optical enhancement has to be considered together with charge transport and interface-related factors. [142], [151]

Laser-induced periodic structures can also affect how light interacts with the surface. Their periodicity and surface relief may change scattering and absorption differently at different wavelengths. This makes the surface structure itself an important part of the optical design. However, an improved visible-range signal should be interpreted carefully. A change in reflectance does not by itself prove band-gap narrowing or a real shift of the absorption edge, because structured surfaces can also change the measured optical response through scattering and light-trapping effects. [149], [150]

This distinction is especially relevant in studies where laser processing is applied to semiconductor substrates such as silicon. In such cases, micro- and nanoscale structuring can greatly change reflectance and apparent optical absorption, producing strong differences in measured optical properties. The functional consequence, however, depends on whether the altered optical behaviour generates carriers that can be effectively used for interfacial reactions or electrical extraction. Optical data from structured substrates must therefore be connected to electrical or catalytic performance data and interpreted as part of the overall architecture-performance relationship. [144], [145]

2.4.4. Surface wetting, accessibility, and interfacial area

Laser structuring can also change the way the liquid meets the surface. This is important because photocatalysis and PEC operation both take place at a solid-liquid interface. The effect of structuring on wetting is not always the same. Depending on the

material, the texture produced by the laser, surface oxidation, and later treatment, the surface may become easier or harder to wet. This can change how much of the active area is really exposed to the solution. As a result, adsorption, local diffusion, boundary-layer thickness, and transport of reactants or products may all be affected. [146], [147]

In porous and membrane-based systems, wetting is not just a surface characteristic. It determines how deeply the liquid can penetrate into the structure, whether poorly refreshed regions remain inside it, and how uniformly reactants reach the active phase. In fibrous membranes and porous supports, capillary forces may help liquid penetration, whereas poor wetting can leave a significant part of the available surface effectively inactive. When a laser-structured substrate is later used as a support for a photoactive coating, its wetting behaviour becomes one of the factors governing the performance of the entire system. [146]

A larger interfacial area is often presented as one of the main advantages of surface texturing. In practice, however, the useful area is not the same as the geometric area. It depends on whether the semiconductor layer really follows the texture and whether the coated surface can still be reached by the electrolyte or pollutant solution. If the coating becomes too thick in recessed regions, or bridges over smaller features, part of the structured surface may stop contributing effectively. When the coating remains conformal, the original texture is preserved and the larger area can support more interfacial reactions. Therefore, laser structuring and the subsequent deposition step must be considered together, not as two independent stages. [72], [151]

2.4.5. Laser structuring as a scaffold for conformal coatings and hybrid interfaces

The value of laser structuring becomes much clearer when it is combined with a conformal deposition method such as atomic layer deposition. In that case, the laser is used to shape the scaffold, while ALD controls the composition and interface properties of the active layer. This is useful because the geometry of the support can be changed deliberately without losing good reproducibility of oxide thickness and coverage. [72], [100], [152]

When a conformal semiconductor layer is added to a laser-structured support, the benefit usually comes from several effects acting together. The textured support can increase the surface area and change the way light interacts with the material. The coating must closely follow this texture to maintain these advantages while forming a continuous photoactive layer. Good contact between the coating and the support is also important, especially in electrodes, where it can improve adhesion and help charges move into the current collector. In this type of system, the structure and the interface are not separate features. They work together to determine how effectively the material uses the generated charges. [105], [126], [151], [153]

However, the success of such strategies depends on process compatibility. Laser structuring may create redeposited material, microcracks, or compositional changes that influence coating nucleation. It may also generate extremely sharp features that are difficult to coat without thickness gradients if deposition conditions are not optimised. Laser structuring should therefore be understood as a way of creating a high-value scaffold, but one that requires careful subsequent processing and characterisation to ensure that the intended architecture is realised in the final functional system. [123], [149], [154], [155]

In hybrid materials, laser structuring can also affect where the added components actually end up. Conductive phases, co-catalysts, or layered materials may not spread in the same way on a flat surface and on a textured one. Local curvature, roughness, and wetting can make some regions collect more material than others. Because of this, the scaffold does more than increase surface area. It also shapes where heterointerfaces are formed in the final system. This is especially important in multi-component architectures, where the expected improvement depends on efficient interfacial charge transfer. [147], [156], [157], [158]

2.4.6. Structured metallic substrates and membrane-like supports in photoelectrochemistry

In photoelectrochemical systems, structured metallic supports are of interest because they combine strength, conductivity, and a surface geometry favourable for high-area interfaces. After deposition of a semiconductor oxide such as TiO_2, the support acts as the conductive backbone, whereas the oxide is responsible for photoresponse and interfacial redox activity. The final photocurrent then depends largely on the quality and continuity of the interface between these two parts. [100], [143], [159]

Hierarchical metallic membranes and porous supports offer additional advantages, such as high surface-to-volume ratio and the possibility of better mass transport. At the same time, they also bring specific challenges. The active coating must remain continuous throughout the entire structure, including the pores and internal surfaces; otherwise, electrical and chemical non-uniformities may start to control the response. The electrolyte must also reach the relevant active regions without producing stagnant zones or encouraging bubble accumulation. In addition, the entire structure has to remain stable during illumination and under electrochemical operating conditions. Hierarchical supports in PEC are therefore powerful but demanding architectures, and their successful use depends strongly on combining structuring with precise coating strategies. [72], [83], [84], [160]

Laser structuring can also be used to prepare metallic supports before the active coating is added. It can make the surface rougher in a controlled way, improve coating attachment, support nucleation, and change how light is coupled into the electrode. The important point, however, is not the texture alone. The structured scaffold must assist the entire photoelectrode, including light absorption, charge extraction, electrolyte contact, and

stability during operation. Therefore, laser-structured supports should be discussed as part of the full electrode architecture, not as separate modified surfaces. [151], [152], [161]

2.4.7. Mechanistic and interpretive considerations in laser-structured photoactive systems

A common difficulty with laser-structured photoactive materials is explaining why the performance changes. Laser treatment rarely changes only one feature. It can alter roughness, surface oxidation, defect density, wetting, and optical behaviour at the same time. For this reason, an improvement after laser structuring should not be assigned too quickly to one cause, such as larger surface area or stronger light absorption. The discussion has to consider which part of the photocatalytic or photoelectrochemical process is most likely affected by the new architecture, for example light use, charge transport, surface reaction, wetting, or mass transfer. [146], [149], [154], [162]

In photocatalysis, better performance may come from improved wetting and accessibility, stronger adsorption, more favourable light interaction, or changes in surface chemistry. In photoelectrochemistry, the improvement may instead be linked to better film adhesion, more efficient charge extraction through stronger interfacial contact, lower reflection, or a larger effective interface area. At the same time, laser processing can also introduce defects, and these may either improve activity by creating reactive sites or reduce performance by acting as recombination centres. For this reason, laser structuring should be regarded as a powerful but complex tool, whose final effect depends strongly on the material itself, the processing conditions, and the coating strategy used afterwards. [23], [147], [163]

It is also necessary to separate optical effects from real electronic changes. A structured surface can show lower reflectance or stronger apparent absorption simply because light is scattered, trapped, or reflected differently. This may appear as a change in the bandgap, although the electronic structure of the semiconductor may not necessarily change. Therefore, unless there is independent evidence for band-gap modification, such changes should be discussed mainly as light-management effects. This is especially important for laser-structured semiconductor supports, where reflectance can be strongly reduced even when the intrinsic absorption edge remains essentially unchanged. [15], [144], [149], [164]

2.4.8. Relevance of laser structuring to the present dissertation

Laser structuring plays an important role in the present dissertation because it provides a controlled route for introducing hierarchy into substrate architectures that are later functionalised with photoactive layers. In the investigated research, laser processing is not treated as a decorative roughening step, but as a deliberate strategy for creating scaffolds with modified optical behaviour, increased interfacial area, and altered accessibility that can support enhanced photocatalytic or photoelectrochemical function. [140], [165], [166], [167]

This is especially important when TiO_2 or related oxides are deposited conformally on complex supports. In these systems, the laser-made geometry is not removed by the coating step, but becomes part of the final photoactive structure. It can affect where light is absorbed, where interfaces are located, and how charges move towards the surface or current collector. For this reason, laser structuring is treated here as one of the main tools for controlling architecture, rather than only as a surface-roughening method. [72], [100], [168], [169]

Another reason for its relevance is that laser-structured surfaces provide an experimentally controllable variable through which structure-property-performance relationships can be studied. By comparing structured and unstructured substrates under otherwise comparable coating and testing conditions, it becomes possible to analyse how hierarchy influences photoactive behaviour. This supports the broader aim of the dissertation to develop a unified materials perspective across different photoactive formats, including structured supports, immobilised systems, and hybrid architectures. [23], [86], [165], [170]

2.4.9. Concluding remarks

Laser structuring, especially when performed with ultrafast pulses, provides a versatile method for creating hierarchical architectures of interest for photocatalysis and photoelectrochemistry. Such surface modification can change optical coupling, accessibility of the surface, wetting behaviour, and the effective interfacial area available for photoinduced reactions. Its value becomes particularly clear when it is combined with controlled deposition methods that retain the created geometry while adding a continuous semiconductor active layer. [140], [141], [165], [169]

At the same time, any enhancement associated with laser processing has to be interpreted carefully, because the treatment can change several parameters at once. The discussion should therefore relate performance changes to plausible mechanistic pathways, separate optical-coupling effects from genuine electronic modification, and take into account the way structuring interacts with the quality of the coating applied afterwards. When approached in this integrated manner, laser structuring is not only a route to better performance, but also a useful experimental strategy for examining architecture-driven design principles in photoactive materials. [15], [149], [164], [171]

2.5 Heterostructures and interface engineering for improved charge utilisation

In many semiconductor photocatalysts and photoelectrodes, the main problem is not only light absorption. The material may absorb photons, but the generated electrons and holes are often lost before they can be used. They can recombine through bulk defects, surface states, or poorly formed interfaces, and the absorbed energy then does not contribute to pollutant degradation, water splitting, or photocurrent. This is why heterostructures and

engineered interfaces are so important. By combining different phases in a controlled way, the material can direct charges along more favourable pathways, reduce recombination losses, and give the carriers a better chance of reaching the reactive interface. [172], [173], [174]

Heterostructures refer broadly to systems in which two or more materials are combined so that their electronic and interfacial properties interact in a functionally meaningful way. The goal is not simply to mix components, but to create contacts that control charge transfer. In photocatalysis, this increases the production of reactive species and enhances the oxidation or reduction rates. In photoelectrochemistry, it can improve charge extraction, shift onset potentials, reduce interfacial losses, and increase stability under bias. In both cases, the success of a heterostructure depends strongly on interface quality and on how the components are spatially organised within the architecture. [32], [175], [176]

2.5.1. Motivation for heterostructure design in photoactive systems

A key motivation for heterostructure engineering is that the processes limiting semiconductor performance are inherently interfacial. Even if a material generates charge carriers efficiently under illumination, those carriers must travel to and cross an interface in order to perform useful work. If the interface does not support effective separation and transfer, recombination dominates. The central challenge is therefore to create material systems in which the relevant interfaces promote directional carrier movement and minimise losses. [32], [173], [177]

For TiO_2-based materials, the reason for using heterostructures is easy to see. TiO_2 is stable and can be prepared by many routes, but on its own it uses mainly UV light and still loses many carriers through recombination. Because of this, TiO_2 is often placed in contact with another phase rather than treated as a complete system by itself. A second semiconductor may help to use a broader part of the spectrum. A conductive phase may provide an easier escape route for electrons. A core-shell or layered structure may separate the locations where charges are generated from those where they are consumed. A co-catalyst may improve a specific surface reaction. In all of these cases, the useful part is the interface, not just the added component. [48], [178], [179]

The literature shows that heterostructures can work well, but the reason for the improvement is not always clear. A stronger photocatalytic or photoelectrochemical response may come from better charge separation at the interface. It may also come from simpler effects, such as stronger adsorption, better wetting, a more favourable morphology, changes in surface defects, or different light scattering. In real hybrid materials, several of these effects can appear at the same time. For this reason, heterostructures should be discussed through the interface and the whole architecture, rather than explained automatically by charge separation alone. [22], [147], [172]

2.5.2. Concepts of charge separation at semiconductor interfaces

The basic concept behind many heterostructures is that an interface can create a driving force for charge separation by establishing an energetic preference for electrons and holes to reside in different regions of the system. In semiconductor-semiconductor junctions, this behaviour is often discussed in terms of band alignment. Depending on the relative positions of the conduction and valence bands, charge transfer can proceed in a direction that spatially separates electrons and holes, thereby reducing recombination probability. [175], [179]

A type-II heterojunction is often used to explain charge separation in coupled semiconductors. In this arrangement, electrons tend to move towards one component, while holes move towards the other. This separation can reduce recombination and make more carriers available at the interfaces. The drawback is that the carriers may end up at less favourable energy levels for the target redox reactions. For this reason, a type-II system can improve charge separation, but it may also lower the effective redox ability of the separated charges. [175], [180]

Another concept often discussed in this context is the Z-scheme or S-scheme approach, where the heterostructure is intended to retain strong redox ability while still promoting effective charge separation. In these systems, the lower-energy carriers recombine at the interface, whereas the more energetic electrons and holes remain available for surface redox reactions. Although this offers an attractive mechanistic picture, experimental confirmation usually requires particular care, since similar activity trends may arise from more than one mechanism. For that reason, discussion of such models in the literature should distinguish clearly between a conceptual interpretation and conclusions that are directly supported by structural or electrochemical evidence. [172], [181]

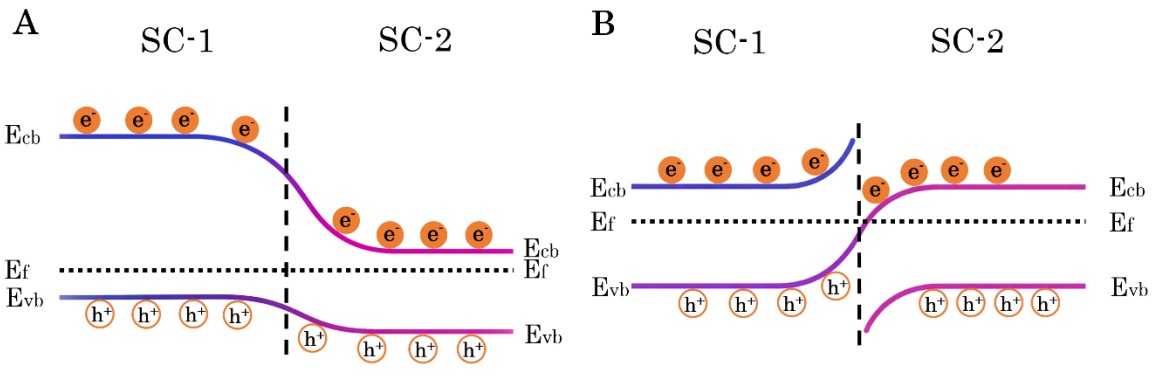

Type II-1 Type II-2 (Z-scheme)

Figure 2.4. *Schematic comparison of charge-carrier transfer pathways in (a) a type-II heterojunction and (b) a Z-scheme heterojunction. In the type-II configuration, electrons and holes accumulate in different semiconductors, promoting spatial separation but often reducing redox ability. In the Z-scheme configuration, interfacial recombination of the less energetic carriers preserves the strongly reducing electrons and strongly oxidising holes for photocatalytic or photoelectrochemical reactions. Adapted and redrawn by the author based on Ref.* [182]

Heterostructures are not limited to contacts between two semiconductors. They can also include metals, carbon-based phases, or other conductive interlayers. In such systems, the added phase may help collect electrons from the semiconductor, sometimes through Schottky-type behaviour, depending on the work-function difference and band bending at the interface. This can reduce recombination by moving electrons away from holes, leaving holes more available for oxidation reactions at the semiconductor surface. Conductive carbon, metal nanoparticles, and two-dimensional conductive phases can therefore influence charge dynamics even when they are not the main light-absorbing component. [8], [183], [184]

2.5.3. Interface engineering as the decisive factor

Although band-alignment concepts are useful, the literature also shows that the behaviour of heterostructures is often controlled less by the nominal electronic properties of the bulk phases than by the quality of the interface between them. That interface may contain defects, dangling bonds, contaminants, or regions with poor connectivity, all of which can serve as recombination centres. When contact between the phases is weak or incomplete, charge transfer may become inefficient and the system may behave more like a simple physical mixture than like a true functional junction. [48], [172], [182]

Interface engineering means controlling the contact between the different parts of a hybrid material, not only combining them in one sample. The manner in which one phase grows on another, the continuity of the contact, the number of defects at the boundary, and the local surface chemistry all affect the ease with which charges can cross the interface. This is why the preparation method matters. A heterostructure made by simple mixing may contain the right components, but only a small part of them may be in useful contact. In situ growth, conformal coating, or controlled deposition can give a more continuous junction and make charge transfer more effective. [7], [105], [113]

This becomes especially important when the material is built on a structured support or used in an immobilised form. A semiconductor layer on a rough or porous substrate may not have the same thickness everywhere, and poorly covered regions can become sites where recombination or resistance dominates. In fibrous membranes, the same problem appears in another form: additives must be distributed and connected well enough for charges to move through the composite. For this reason, a heterostructure is not defined only by which phases

are present. Its performance depends on where these phases are placed, how they touch each other, and whether the architecture allows the interface to work . [60], [75], [185]

2.5.4. Heterostructures in photocatalysis: adsorption, kinetics, and interpretive complexity

In studies of photocatalytic pollutant degradation, heterostructures are often examined by following dye decolourisation, mainly because the measurements are simple and suitable for quick comparison between samples. At the same time, dye-based tests are not straightforward to interpret. The strong adsorption of the dye on some components may lower the measured concentration, even when full oxidative decomposition has not occurred. In addition, some dyes can behave as photosensitisers under visible light, injecting electrons into the semiconductor and opening degradation pathways that are not directly related to the intrinsic light absorption of the semiconductor itself. The rate can also change for reasons that are not directly related to the charge separation. If the surface becomes rougher, more hydrophilic, or richer in adsorption sites, more pollutant may be held close to the active regions and the liquid may contact the material more effectively. Under these conditions, the measured degradation can increase even if the electronic separation of carriers has improved only modestly. [186], [187], [188]

In heterostructures that contain conductive additives or two-dimensional materials, the interpretation becomes even more complicated. Such conductive phases may indeed facilitate electron transport, but at the same time they can increase adsorption and introduce additional sites where reactions may occur. Hybrid systems may therefore show improved performance because of changes in pollutant capture rather than solely because of improved photocarrier utilisation. Photocatalytic enhancement in heterostructures should therefore be interpreted as the combined result of electronic, surface-chemical, and transport effects. [172], [189], [190]

This complexity does not reduce the value of heterostructure research. On the contrary, it highlights the need for careful design and characterisation. A stronger discussion becomes possible only when the observed performance is tied to independent signs that a functional interface has actually formed, for example changes in recombination-related spectroscopic features, modified impedance response, shifts in photoelectrochemical behaviour, or systematic effects of interface thickness and contact quality. When such evidence is combined with controlled comparisons that account for adsorption and morphology, interpretation of heterostructure behaviour becomes much more robust. [113], [172], [191]

2.5.5. Heterostructures in photoelectrochemistry: carrier extraction and interfacial kinetics

In photoelectrochemical systems, one of the main reasons for building heterostructures is to make charge extraction more effective, to limit recombination losses at the surface, and to create conditions more favourable for interfacial charge transfer. Since photoelectrochemistry operates with an external circuit, the design requirements are not the same as in photocatalysis. Here the architecture must support continuous electronic pathways from the semiconductor to the current collector and maintain stable contact with the electrolyte. Heterostructures are therefore often evaluated not only by photocurrent density, but also by onset potential, charge-transfer resistance, stability under bias, and behaviour under chopped illumination or transient conditions. [37], [191], [192]

One advantage of photoelectrochemical evaluation is that it can provide more direct insight into carrier transport and extraction than many photocatalytic tests. For example, changes in photocurrent may reflect improved charge separation or reduced recombination, although such interpretations still require caution. A higher photocurrent may also arise from increased roughness or a larger interfacial area rather than from improved junction behaviour. For this reason, interpretation of heterostructure effects in PEC also benefits from combining performance data with structural characterisation and impedance-based analysis. [191], [192], [193]

Heterostructures may also influence selectivity and stability in PEC operation. Even when photocurrent increases, long-term behaviour may deteriorate if the interface is unstable, if the conductive component oxidises, or if the junction degrades under prolonged illumination. This is particularly relevant in hybrid systems involving two-dimensional materials, surface terminations, or components sensitive to aqueous oxidation. Stability considerations are therefore an integral part of assessing heterostructures in photoelectrochemistry. [37], [194]

2.5.6. Heterostructure fabrication routes and the role of controlled deposition

The literature shows that heterostructure performance depends strongly on the fabrication route used to build the interface. Several broad approaches can be distinguished. [195]

In situ growth methods, in which one phase is formed directly on another, often produce better contact and more intimate interfaces than simple mixing. Examples include the hydrothermal growth of one oxide on a pre-existing support or the solvothermal deposition of a second semiconductor onto TiO_2. Such methods can yield strong junctions, but they may also introduce uncontrolled morphology changes and make it difficult to separate the effect of the interface from that of newly generated surface area or additional defect states. [196], [197]

Coating and deposition methods, such as sol-gel coating, electrophoretic deposition, sputtering, chemical vapour deposition, and atomic layer deposition, provide alternative ways of building such systems. Controlled deposition is particularly useful in architecture-driven research, because it can preserve the original geometry and at the same time make it possible to adjust thickness and coverage in a systematic way. ALD is especially important here, since it allows conformal coating of complex substrates and can produce well-defined interfaces in multilayer structures. This level of control becomes particularly valuable when the objective is to determine how heterojunction thickness, continuity, or interface quality influences the final performance. [72], [113], [198]

In polymer-based and electrospun systems, the fabrication route strongly affects how the hybrid phases are distributed and how well they remain connected. When conductive or semiconducting additives are dispersed uniformly and stay accessible, they may contribute in a beneficial way. If, however, they agglomerate, become trapped inside the fibres, or disturb fibre formation, they may not create functional transport pathways at all. In membrane architectures, this means that heterostructure formation is inseparable from the processing conditions and from the final spatial arrangement of the individual phases. [60], [75]

2.5.7. The interaction between heterostructures and architecture

Heterostructure design and architecture-driven optimisation are deeply linked. An interface can influence charge separation effectively only if it is positioned so that carriers can reach it and use it. The spatial distribution of heterointerfaces is therefore as important as their chemical identity. [77], [199]

In hierarchical electrodes, a conformal semiconductor coating can expose a large interfacial area. This area is useful only if charges and electrolyte can actually reach the right places. When the coating stays connected to the substrate and the electrolyte can access the active surface, the heterostructure may give a stronger photocurrent. If the layer is broken, poorly connected, or hidden inside regions that the electrolyte cannot reach well, the same heterostructure may contribute much less than expected. [199], [200], [201]

In fibrous and membrane-type photocatalysts, architecture influences how heterostructure components are exposed and how reactants interact with them. A hybrid system may show improved behaviour because the membrane captures pollutants more effectively, or because it brings reactants into closer proximity to reactive interfaces. At the same time, the membrane may introduce diffusion limitations that restrict the contribution of internal active sites. The functional value of a heterostructure must therefore always be interpreted within its architectural context. [26], [59], [202]

This is especially important when conductive two-dimensional phases are used. They can facilitate electron transport only when they are well connected and remain in contact

with the active semiconductor. If the flakes are isolated, poorly distributed, or buried inside the structure, their effect may be weak. The heterostructure therefore works only when the architecture allows connected charge pathways and accessible interfaces to form. [190], [203]

2.5.8. Relevance of heterostructure and interface engineering to the present research

Heterostructure formation and interface engineering are important in this work because they connect the material architecture with the final photoactive response. The systems studied here are not improved only by changing shape, roughness, or support geometry. Their behaviour also depends on how the different phases contact each other and how charges move across these contacts. This includes semiconductor-conductive interfaces, conformal oxide coatings on structured supports, and hybrid components introduced into immobilised architectures. In each case, the interface is treated as part of the design, not as a secondary boundary between materials. [190], [199], [202]

In the materials considered here, improved performance is expected mainly when a larger fraction of the photogenerated carriers reaches productive interfaces instead of being lost by recombination. This view is in line with the broader literature, where limited charge utilisation is often identified as one of the main bottlenecks in photoactive systems. At the same time, the present research also takes into account that hybridisation may influence adsorption, wetting, and transport, not only electronic behaviour. For this reason, interface-focused interpretation is treated as an important part of understanding the observed performance trends. [59], [77], [200]

Another important point is that the effectiveness of heterostructure strategies depends on how well they are integrated with the underlying architecture. The present research places strong emphasis on systems in which deposition and fabrication routes are chosen to preserve structural features and to form reproducible interfaces. This approach is consistent with the broader literature trend toward combining precise fabrication methods with architecture-controlled design in order to achieve more reliable performance enhancement. [199], [202]

2.5.9. Concluding remarks

Heterostructures and engineered interfaces represent powerful strategies for improving photocatalytic and photoelectrochemical materials because they address one of the key limitations of semiconductor systems: inefficient utilisation of photogenerated charge carriers. By designing interfaces that promote separation and directional transfer, it becomes possible to reduce recombination and increase the fraction of carriers available for surface reactions or electrical extraction. [77], [199]

At the same time, the literature also shows that the improved behaviour of heterostructures is rarely caused by one factor alone. Architecture, adsorption, wetting,

morphology, and stability may all contribute to the final trend that is observed. Therefore, meaningful design and interpretation require attention not only to electronic alignment but also to interface quality, spatial arrangement of the phases, and the operating environment of the material. [59], [190], [200]

This point leads into the following sections, where the main material formats used in this dissertation are discussed in more detail. These include conductive and two-dimensional phases such as MXenes, fibrous immobilised photocatalysts, and structured supports modified by controlled deposition methods. The focus remains the same in each case: how the chosen components and architecture affect charge transfer, accessibility, stability, and the final photoactive response. [26], [190], [202]

2.6. MXene-containing hybrid systems in photocatalysis and photoelectrochemistry

The rapid growth of research on two-dimensional materials has strongly influenced the development of hybrid systems for photocatalysis and photoelectrochemistry. Within this broader development, MXenes have become especially interesting as composite components, since they bring together high electrical conductivity, chemically active surfaces, and a form that can be introduced into many kinds of hybrid architectures. In many photoactive systems, the main limitation is not the generation of charge carriers, but their efficient separation and utilisation before recombination occurs. Conductive and interfacially active two-dimensional phases can, in principle, reduce these losses by providing favourable pathways for electron transport, improving interfacial charge transfer, and modifying surface interactions with reactants. This is the main reason why MXenes have been explored extensively as functional additives and interphases in TiO_2-based and related photoactive materials. [204], [205], [206], [207]

MXenes are usually obtained by selectively etching MAX phases, that is, layered ternary carbides or nitrides, and then delaminating the etched product to produce nanosheets. Their general formula is commonly written as $M_{n+1}X_nT_x$, where M is an early transition metal, X is carbon and/or nitrogen, and Tx denotes surface terminations, most often including –O, –OH, and –F. Among different MXenes, $Ti_3C_2T_x$ is the one most often used in photoactive systems. This is mainly because it is relatively accessible, electrically conductive, hydrophilic, and compatible with many oxide materials. Its layered structure also provides many places where it can contact semiconductors, polymer matrices, or adsorbed molecules. This is useful for building hybrid interfaces, but it also makes the material sensitive to preparation conditions and exposure to water, oxygen, or light. For this reason, $Ti_3C_2T_x$ should not be treated as a fixed conductive additive. Its surface chemistry and stability have to be considered when its role in charge transfer is discussed. [208], [209], [210]

2.6.1. Motivation for using MXenes in photoactive systems

The motivation for incorporating MXenes into photocatalytic or photoelectrochemical materials can be grouped into several broad functional expectations.

First, MXenes can act as conductive electron acceptors and transport pathways. In an illuminated semiconductor, electrons and holes are generated simultaneously. If one type of carrier can be extracted or delocalised more efficiently, the probability of recombination decreases and the other carrier has a greater chance of participating in interfacial reactions. In many hybrid systems, the MXene is expected to accept photogenerated electrons from the semiconductor and facilitate their transport toward reactive sites or a current collector, thereby improving overall charge utilisation. [211], [212], [213]

Second, MXenes are not only conductive sheets. Their surface is chemically active because it contains termination groups such as –O, –OH, and –F. These groups can affect how MXene disperses in water or polar solvents, how it attaches to oxide surfaces, and how nanoparticles or thin coatings grow on it. This is important because a hybrid material can work as a heterostructure only when the phases are in real contact, not just mixed together. In this sense, MXene surface chemistry can help create the close interfaces required for charge transfer. [205], [214], [215]

Third, MXene may also affect the way the dye solution interacts with the material. In photocatalytic tests, a lower dye concentration does not always mean that degradation alone has improved. Part of the dye may be retained near the active surface, especially when the material has more adsorption sites or becomes easier to wet. MXene can contribute to both effects. In membrane-type photocatalysts, this may allow the solution to reach more of the internal active regions. For this reason, improved dye removal after MXene addition should be discussed with caution, since adsorption, wetting, and access to the catalytic surface may contribute together with charge-transfer effects. [22], [147], [216]

Fourth, MXenes can also affect the formation of the composite, not only its performance after preparation. This is especially relevant for electrospun fibres and membranes. The addition of MXene may change the conductivity and viscosity of the spinning solution, the stability of the dispersion, and the way solid phases are distributed inside the fibers. Because of this, MXene can influence the final membrane structure as well as its performance-related properties, including permeability, capillary wetting, and surface roughness. [217], [218], [219]

These points show that MXene usually does more than one thing in a composite. It can affect charge transport, surface chemistry, adsorption, wetting, and even the way the material forms during preparation. This is part of its value, but it also makes the results harder to interpret. When the performance improves after MXene addition, the reason may

not be a single electronic effect. This may be due to several changes acting together. [220], [221], [222]

2.6.2. Surface chemistry and terminations: functional benefit and interpretive challenge

One important feature of MXenes is their surface termination. Unlike graphene-like carbon materials, MXene sheets usually carry functional groups introduced during synthesis, and these groups strongly affect their behaviour in composites. They influence hydrophilicity, dispersion in polar media, attachment to oxide surfaces, and the electronic character of the interface. In photoactive systems this can be useful, because the terminated surface helps MXene form close contact with TiO_2 or other oxides through hydrogen bonding, coordination-type interactions, or related surface contacts. In this way, the surface chemistry of MXene contributes not only to processing, but also to the quality of the heterointerface. [215], [220], [223]

However, the chemistry of the surface terminations is also one of the main sources of variability. Different synthesis batches may produce MXenes with different terminal group proportions, oxidation levels, and flake dimensions. In addition, processing steps such as sonication, drying, thermal treatment, or contact with oxygen-containing water can gradually change the surface chemistry. Because of this, the same MXene may not behave identically from one study to another. In research focused on reliable structure-performance relationships, such variability has to be addressed either by careful characterisation of the material or by designing comparisons in a way that limits uncontrolled differences. [221], [224], [225], [226]

Surface terminations also affect the electronic role of MXenes. Although MXenes are generally highly conductive, their work function and interfacial energetics depend on termination composition and surface state. This can influence whether the MXene acts as an efficient electron sink or whether the interface behaves less favourably. The electronic contribution of MXenes should therefore not be assumed automatically, but considered in relation to how the material is processed and how it contacts the semiconductor. [220], [222], [223]

2.6.3. Charge transfer and recombination suppression in MXene-semiconductor hybrids

One of the most frequently cited mechanisms for performance improvement in MXene-containing photoactive systems is enhanced charge separation. In this mechanistic picture, photogenerated electrons transfer from the semiconductor to the MXene, which acts as an electron acceptor because of its conductive nature and favourable interfacial energetics. Once electrons are transferred, they are less likely to recombine with holes in the semiconductor. The remaining holes can then participate in oxidation reactions, for example

in the generation of hydroxyl radicals in photocatalytic systems or in oxidation processes at a photoanode surface. [213], [220], [223]

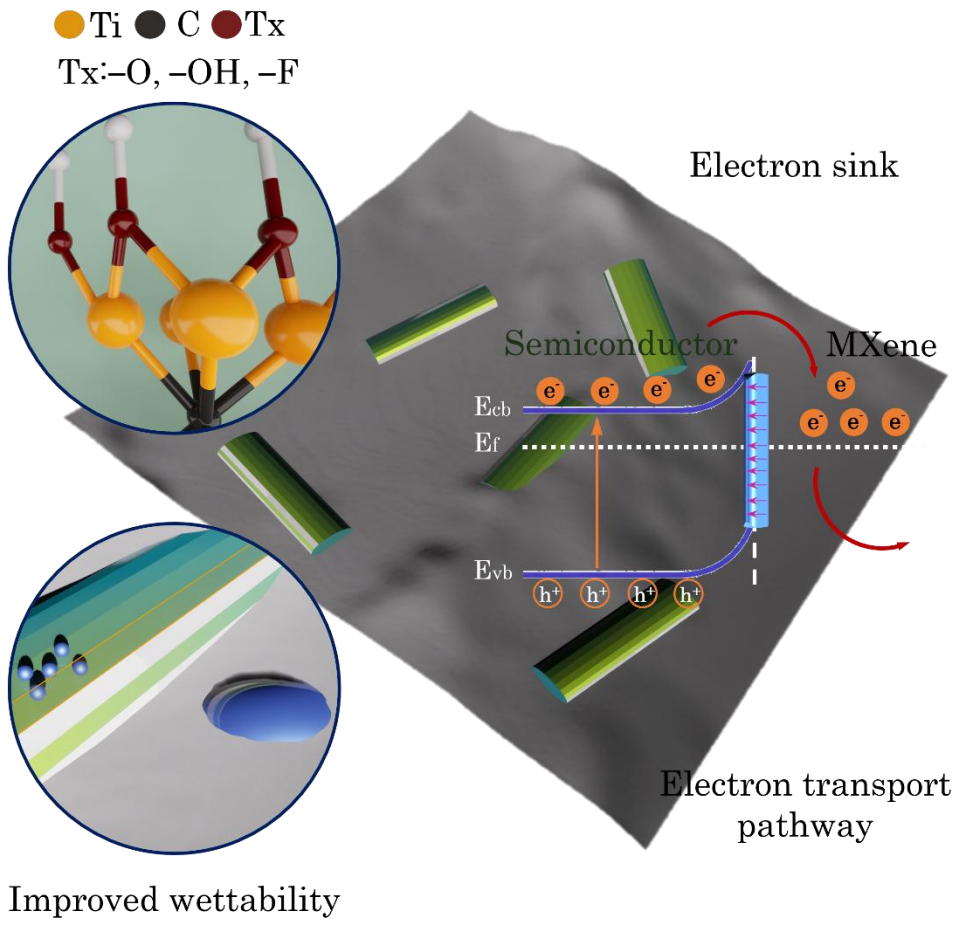

Figure 2.5. *$Ti_3C_2T_x$ MXene as a functional component in semiconductor hybrids. The MXene sheets, bearing terminal groups such as –O, –OH, and –F, are shown as the interfacial phase that can assist electron transfer and influence liquid wetting. Adapted and redrawn by the author based on Refs.* [227], [228], [229]

Such a mechanism is reasonable in many systems, especially when MXene is well connected to the semiconductor and the architecture does not hinder the transport. At the same time, “improved charge separation” is usually not measured directly, but concluded from the overall behaviour of the system together with supporting spectroscopic or electrochemical observations. In photoelectrochemical measurements, lower charge-transfer resistance or higher photocurrent can indicate better charge extraction. At the same time, these changes may also be influenced by roughness, surface area, wetting, or the way the active phases are connected. For this reason, MXenes should be discussed as components that can improve charge utilisation, but not as proof of a single mechanism by themselves.

The interpretation has to follow the evidence provided by the structural, electrochemical, and stability results. [23], [191], [222]

The distribution of MXenes within the composite is equally important. Its function as a transport pathway becomes more realistic when the sheets form a connected conductive network and remain in good contact with the semiconductor interface. In contrast, if the flakes remain isolated or are embedded in a polymer matrix without effective contact with the active semiconductor domains, their electronic role may be weak, even though they can still affect adsorption or the overall structure. For this reason, the performance of MXene-based hybrids depends strongly on the architecture of the composite, not simply on the fact that MXene is present. [218], [219], [221]

2.6.4. MXenes in photocatalytic pollutant degradation: adsorption, wetting, and practical relevance

In photocatalytic pollutant degradation, MXene-containing hybrids have often been reported to exhibit enhanced apparent kinetics. Several factors can contribute to this behaviour. [230]

One of the first changes is often observed in the way pollutants bind to the material. This is especially true for dyes, which may interact with a surface through electrostatic attraction, π–π association, or coordination-type contact. Because MXenes are both hydrophilic and chemically active, they can change not only how much pollutant is adsorbed, but also how quickly this uptake occurs. As a result, the concentration can drop more rapidly at the beginning of the experiment, and the local amount of pollutant near reactive sites may become higher. This may be helpful from the point of view of pollutant removal, but it also makes mechanistic interpretation more difficult, since adsorption-related concentration changes can be mistaken for true catalytic improvement. For this reason, when MXene-enhanced dye removal is evaluated, adsorption equilibria, dark-adsorption steps, and apparent rate constants should be interpreted with caution. [231], [232]

Wetting effects are also significant. In immobilised photocatalysts such as membranes, improved wetting can increase the effective active area exposed to solution and reduce the presence of air pockets or poorly contacted regions. MXene incorporation may enhance hydrophilicity and water permeability, thereby improving mass transport and performance even without substantial changes in intrinsic semiconductor charge dynamics. In this sense, MXene addition may improve the functional operation of the architecture rather than only the electronic properties of the semiconductor. [233]

These considerations are especially important in research aimed at developing practically relevant photocatalysts. Immobilised systems such as membranes are intended to provide ease of recovery and reuse, which remains a major limitation of powder catalysts. If MXene integration improves membrane wetting, stability, and reusability while also

supporting charge transfer, the overall system becomes more attractive for realistic treatment scenarios. At the same time, practical relevance also requires attention to long-term behaviour, since MXenes may undergo gradual oxidation in aqueous environments. [219], [225]

2.6.5. MXenes in electrospun fibres and membrane composites

MXenes can be introduced into hybrid photoactive materials in several ways, and electrospun fibres or nonwoven membranes are among the more convenient formats for doing so. A fibrous membrane provides an open and flexible scaffold with a large exposed area and interconnected free space between fibres. When MXene is incorporated into such a system, it does more than simply change the composition, because it may also affect electrical transport and the behaviour of the surface. The way in which it is introduced depends on the final structure that is intended for the material. MXene may be present already in the spinning mixture, it may be introduced together with semiconductor components during preparation of the composite, or it may be deposited afterwards onto the formed fibrous network. In each case, the final effect depends not only on the presence of MXene itself, but also on where it ends up in the structure and how well it remains connected to the photoactive phase. [219]

MXenes can influence fibre formation through their effect on solution conductivity and rheology. Changes in solution conductivity can affect jet stability and fibre diameter, while dispersion quality determines whether MXenes remain evenly distributed or agglomerate. The final distribution of MXene within or on the fibre surface determines whether its contribution is expressed mainly through electronic transport pathways, adsorption and wetting, or mechanical reinforcement. [218]

In photoactive fibre composites, the position of MXene relative to the semiconductor phase is highly important. When MXene is located at interfaces where it can accept electrons and remain connected with other conductive pathways, it may help limit recombination and improve the use of photogenerated carriers. If it is present in the structure but remains electronically isolated, its effect is more likely to appear through stronger adsorption or changes in surface wetting. In both situations, adding MXene can change how the membrane works in practice by affecting pollutant uptake, light penetration, and the possibility of repeated use. [234]

Electrospun membranes also make clear a broader point: in hybrid photoactive systems, transport processes often become one of the main limiting factors. Diffusion of pollutants through the membrane, penetration of the liquid phase, and the way light is distributed within the fibrous mat can all affect the apparent kinetics. For this reason, the performance of MXene-containing fibrous photocatalysts should be interpreted as the result of a coupled system in which architecture, mass transport, and interfacial charge processes act together. [235]

2.6.6. MXene stability, oxidation, and durability under operational conditions

One important issue in photoactive systems containing MXenes is their chemical stability, especially when the material is used in water and under oxidative conditions. Many MXenes, including $Ti_3C_2T_x$, are known to change gradually in such environments, particularly in the presence of dissolved oxygen, at higher temperature, or during longer storage. Under illumination and during photocatalytic operation, these changes may become even more significant. As a consequence, conductivity, surface chemistry, and interfacial behaviour may all evolve with time, which means that the functional role originally attributed to the MXene may also shift during use. [225]

This does not mean that MXenes are unsuitable for photoactive systems. It means, rather, that their use has to be considered together with the experimental timescale and with possible changes in the material during operation. In some situations, partial oxidation may lead to the formation of TiO_2-like species on the MXene surface and thus create new interfaces that affect performance. In other situations, oxidation may weaken the conductive network and reduce the intended benefit for charge transport. For this reason, stability assessment should not be treated as a secondary issue, but as an essential part of evaluating MXene-based photoactive systems. [226]

In photoelectrochemical environments, stability considerations can be even more critical because electrodes may operate for extended periods under bias. Potential cycling, local pH changes at the electrode surface, and oxidative holes can all influence the durability of MXene-containing interfaces. Long-term tests and post-operation characterisation are therefore particularly important when durable enhancement is attributed to MXene incorporation. [236]

From a research point of view, stability challenges may also be used constructively to design more durable architectures. When MXene sheets are protected by suitable placement within the composite, by coating approaches, or by stabilising interfaces, their beneficial contribution may persist for longer operating times. If, on the other hand, they are left directly exposed to aggressive environments, performance may change during use and the interpretation of results becomes less straightforward. In this sense, durability becomes another design parameter, alongside conductivity and interface engineering. [237]

2.6.7. Interpretation of performance enhancement in MXene hybrids

MXene-containing systems are difficult to interpret because the additive can change several things at once. If the photocatalytic rate increases, improved charge separation may be part of the reason, but it is not the only possible explanation. The material may also adsorb more dye, wet more easily, or distribute the active phases in a more favourable way. A similar caution is needed in PEC measurements. A higher photocurrent may point to better charge extraction, but it may also be helped by stronger film contact, increased roughness, or a

larger active area. For this reason, MXene should be discussed as a component that can influence the whole architecture, rather than as an additive with one fixed function. [238], [239], [240]

A stronger interpretation usually depends on several observations being read together. Morphological analysis is needed to show how the phases are distributed and whether good contact is actually formed. Optical analysis helps to determine whether the observed changes originate from intrinsic absorption effects or mainly from geometry. Further insight may be obtained from impedance and transient measurements, which can help show whether the interface has changed and whether recombination behaviour has shifted, while stability tests indicate whether the observed improvement is maintained over longer operation. When these different results point in the same direction, the introduction of MXene can be discussed more convincingly as a way of improving charge utilisation in architectured systems. [39], [239], [241]

At the same time, MXene should not be treated as a guaranteed improvement. Its effect depends on the semiconductor, the preparation route, the working medium, and the way the composite is built. If too much MXene is added, it may shade the semiconductor or cover active surface sites. If the sheets aggregate, the contact with the active phase may become poorer and the sample-to-sample behaviour less reproducible. Therefore, MXene content has to be optimised together with the processing conditions. A larger amount does not automatically mean better photocatalytic or photoelectrochemical performance. [240], [242], [243]

2.6.8. Relevance of MXene-containing systems to the present research

MXene-containing hybrids are relevant here because they bring together several ideas discussed earlier: interface design, architecture control, and better use of photogenerated charges. In the systems considered in this dissertation, MXenes are not treated only as conductive fillers. Their role depends on how they contact oxide semiconductors, how they are distributed in the structure, and whether they help or hinder access to the active interface. In this way, MXene becomes part of the architecture itself, influencing both charge behaviour and the working surface of the material. [238], [239], [240]

The integration of MXenes into structured or membrane-like systems is especially consistent with the research focus on practical formats. In immobilised photocatalysts, improved wetting, adsorption, and transport can be as important as electronic effects. MXenes provide a route to influence these properties while also potentially improving charge separation. At the same time, their chemical dynamics under aqueous conditions require careful evaluation of stability and of the evolving nature of hybrid interfaces. This perspective supports a more realistic understanding of how conductive two-dimensional components operate within complex photoactive materials. [39], [241], [242]

2.6.9. Concluding remarks

MXenes have become attractive components in photocatalytic and photoelectrochemical hybrid materials because they bring together high electrical conductivity, chemically active surfaces, and broad compatibility with different semiconductors and composite designs. Once introduced into such systems, they may help the generated charges to be used more effectively by supporting electron extraction and transport. At the same time, they can also influence adsorption, wetting behaviour, and the microstructural organisation of the material, especially in immobilised architectures. [215], [243]

At the same time, MXene-based enhancement must be interpreted carefully because their multifunctionality can produce performance changes through several coupled mechanisms. In addition, stability and oxidation behaviour under aqueous and oxidative conditions remain important considerations for practical application and long-term operation. When these factors are treated systematically, MXene-containing systems provide a valuable platform for studying how conductive two-dimensional phases can be integrated into architecture-engineered photoactive materials. [172], [221]

2.7. Electrospun and membrane-type photocatalysts: immobilisation, transport effects, and functional design

For real use in water treatment and related environmental applications, photocatalytic systems are often limited as much by process and materials-handling issues as by the chemistry of the catalyst itself. Many powdered photocatalysts may show high apparent activity in laboratory experiments, yet their use in practice becomes more difficult because they have to be separated from the treated water, part of the material may be lost, and repeated reuse is not always straightforward. These constraints have motivated extensive research on immobilised photocatalysts in the form of coatings, monoliths, foams, meshes, porous scaffolds, and membrane-type systems. Among these approaches, electrospun fibrous membranes have attracted particular attention because they combine high geometric surface area, interconnected porosity, and structural flexibility with the possibility of incorporating multiple functional components within a single architecture. [73], [244]

In membrane-type photocatalysts, the material is designed not only to be photoactive, but also to act as a structurally organised platform through which the reacting solution can interact with the active surface in a controlled manner. This shifts the design problem from a purely composition-centred question to a coupled systems question involving catalyst distribution, reactant access, light interaction with the membrane, and the mechanical behaviour of the architecture during repeated use. As a result, membrane-type photocatalysts must be analysed through a combination of semiconductor photophysics and transport-aware materials engineering. [59], [245]

2.7.1. Why immobilisation matters: from powder catalysts to recoverable architectures

A large part of photocatalytic work is still carried out with powders, since this format puts a substantial fraction of the material in direct contact with the solution and is convenient for comparing materials of different composition. In a well-mixed suspension, reactants can reach the particles efficiently, and concentration changes can be followed easily by optical measurements. At the same time, this format is not easy to transfer directly into practical operation. After treatment, the catalyst has to be separated from the liquid, usually by filtration, sedimentation, or related steps, which makes the process more complicated and more costly. If recovery is incomplete, part of the catalyst may be lost and secondary contamination can also become an issue. In addition, fine powders may agglomerate, lose dispersibility, or undergo surface changes over repeated cycles, making long-term performance less predictable. [246], [247]

Immobilised photocatalysts address these issues by fixing the active phase onto a recoverable support or within an organised architecture that can be removed easily from the medium. This can improve reusability and simplify integration into flow-through reactors or modular treatment systems. At the same time, immobilisation changes the operating conditions of the catalyst. In immobilised photocatalysts, part of the active surface may be harder to reach, transport inside the structure may become slower, and light may not penetrate the material uniformly. For this reason, they should not be judged only by direct mass-based comparison with powders. They work in a different format. Their value also depends on whether they are stable, easy to handle, reusable, and able to treat the solution effectively under conditions closer to practical use. [248], [249]

From a research perspective, the transition from powders to immobilised architectures is not merely a practical adjustment. It also opens new scientific questions concerning how geometry, wetting, diffusion pathways, and structural hierarchy influence the observed kinetics of photocatalytic processes. This is especially important in research aimed at developing architecture-driven design principles. Membrane-type photocatalysts provide an experimentally rich platform in which mass transport and surface accessibility become controllable variables rather than uncontrolled experimental artefacts. [59], [249], [250], [251]

2.7.2. Electrospinning as a versatile route to fibrous photocatalytic membranes

Electrospinning is widely used to produce fibrous membranes whose fibre diameters can range from the micrometre scale down to a few tens of nanometres, depending on the properties of the solution and on the applied processing conditions. In this technique, a polymer solution or precursor mixture is driven from a nozzle in a strong electric field. The resulting charged jet is stretched while the solvent evaporates, and this finally leads to

continuous fibres that are collected in the form of a nonwoven mat. By varying solution viscosity, conductivity, surface tension, flow rate, and applied voltage, electrospinning allows substantial control over fibre diameter, morphology, and membrane thickness. [252], [253]

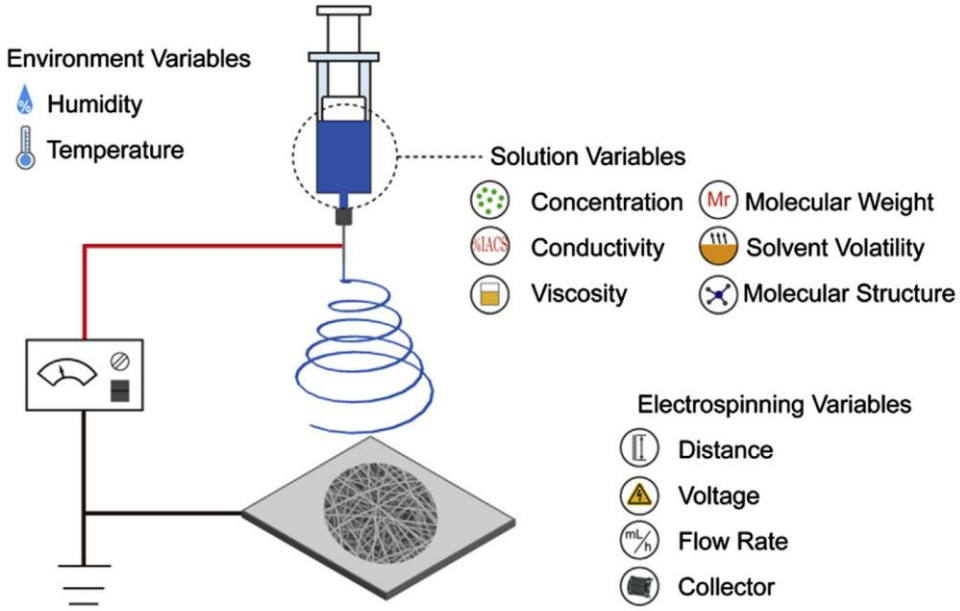

Figure 2.6. *Schematic representation of the electrospinning process together with the main parameters that influence fibre formation and membrane morphology, including solution properties, environmental conditions, and electrospinning settings. Reproduced from Ref.* [254] *with permission from Elsevier.*

A strong advantage of electrospinning is that it allows the membrane composition to be changed during fabrication, not only after the fibres are made. Nanoparticles, semiconductor powders, metal salts, precursor compounds, or two-dimensional additives can be added directly to the spinning solution. The fibres can also be modified later by coating, impregnation, or deposition. Depending on the system, the electrospun mat may remain as a polymer support carrying the photocatalyst, or it may be converted by heat treatment into inorganic or carbon-based fibres. This flexibility makes electrospinning useful for photocatalytic membranes, because the chemical composition and the fibrous architecture can be adjusted together. [245], [255]

Electrospun membranes also have structural advantages for photocatalysis. Their porous fibre network can let water pass through or spread across the material more easily than in a dense film. The fibres provide a large exposed surface, while the open spaces between them can help reactants reach active regions. At the same time, a continuous membrane is easier to handle, remove from solution, and reuse. This makes electrospun

systems attractive not only because of their activity, but also because they offer a practical immobilised format. [73], [256]

2.7.3. Architectures of electrospun photocatalytic membranes

The architecture of electrospun photocatalytic membranes can vary widely depending on how the active phase is introduced and where it is located relative to the fibre surface. Several general configurations are commonly encountered. [257]

In one common design, semiconductor particles are placed inside the polymer fibres. This can help keep the particles fixed in the membrane and reduce material loss during use. The drawback is that not all of the photocatalyst may remain available to the solution. If much of the active phase is trapped inside the polymer, the reaction can only occur where light, water, and pollutant molecules still reach it. For this reason, the performance of such fibres depends strongly on particle exposure at the surface, polymer permeability, and the quality of contact between the active phase and the reacting medium. [258]

A second configuration involves decorating fibre surfaces with semiconductor particles or coatings. This can improve accessibility of active sites because the particles remain exposed to light and reactants, but it may also introduce challenges related to adhesion and long-term stability. If surface-deposited particles detach during use, performance may decrease over time and the practical advantages of immobilisation may be lost. [202]

A third option is to make core-shell or multilayer fibres, where the different components are placed in separate parts of the fibre. This can be useful because each part can have a different role. For example, the core may provide mechanical support, while the outer layer provides the photoactive surface. In another design, a conductive inner phase may help charge transport, while the semiconductor shell remains in contact with the solution. These architectures can improve stability and charge movement, but only if the processing is well controlled and the layers are formed as intended. [259]

In all of these configurations, two factors become especially important: how the active phase is distributed and how thick the membrane is. If the membrane is too thin, the available active area may be limited and the structure may lack sufficient mechanical stability. If it becomes too thick, light may penetrate less effectively and transport through the membrane may become restricted. For this reason, membrane design has to balance activity with accessibility, permeability, and structural robustness. [26], [245]

2.7.4. Light distribution and optical effects in fibrous membranes

Light interacts with electrospun membranes in a way that differs markedly from dispersed powders. In powder suspensions, individual particles are often exposed to light more independently, although scattering and turbidity still affect how photons are

distributed. In a fibrous membrane, by contrast, light passes through a structured network made up of fibres, voids, and particles that may be embedded or deposited on the surface. The resulting optical environment is therefore more complex, with scattering, reflection, and absorption taking place at the same time. [65], [260]

Membrane thickness and the degree of fibre packing have a strong effect on how deeply light can penetrate into the structure. When the fibres are packed too closely, or when the membrane contains a large amount of opaque material, the upper part may absorb or scatter most of the incoming light, so the deeper regions remain only weakly illuminated. In that case, part of the internal active phase may be used inefficiently. A membrane of more moderate thickness and with a more open porous structure, by contrast, may allow light to distribute more evenly and thus improve effective use of the active material. [65], [261]

Fibre diameter also affects the way light behaves inside the membrane. Nanofibres may increase scattering and provide a larger surface area, whereas microfibres may allow deeper light penetration and a lower pressure drop in flow-through systems. Surface roughness or additional hierarchical features on the fibres can further modify optical interaction. This shows that photocatalytic membranes are intrinsically dependent on architecture, and that optical design has to be considered together with transport and surface accessibility. [260], [262]

An important interpretive consequence is that improved photocatalytic performance in a fibrous membrane may reflect more favourable light utilisation arising from geometry rather than a change in intrinsic semiconductor properties. When membrane-based systems are compared, it is therefore useful to relate activity trends to structural parameters such as membrane thickness, fibre diameter distribution, and, where relevant, optical transmission or reflectance characteristics. [65]

2.7.5. Mass transport, wetting, and boundary-layer effects

A membrane changes the conditions of the photocatalytic test. In a stirred powder suspension, the catalyst particles are dispersed in the liquid, so dye molecules and dissolved oxygen can reach them more directly. A membrane is fixed, and the solution must enter or pass along its internal fibre network. For that reason, pore size, fibre packing, wettability, and tortuous pathways become part of the reaction environment. The measured activity may therefore depend not only on the semiconductor and its charge behaviour, but also on how easily the solution reaches the active regions and how quickly products can leave them. [201], [263]

Wetting is one of the key factors in membrane operation. When the membrane is not wetted well enough, water may enter the structure unevenly and part of the material may remain effectively inactive. If hydrophilicity is improved, capillary penetration can become easier and the contact area available to the liquid can increase. Because of this, apparent

activity may change strongly even when the semiconductor content stays nearly the same. This becomes particularly important in composite membranes, where added components can markedly alter the surface chemistry. [147], [264]

Boundary-layer effects may also play an important role in membrane photocatalysis. The degradation rate depends not only on the activity of the catalyst itself, but also on how efficiently pollutant molecules are transported to the active sites. When this transport is slow, the measured kinetics may be governed more by diffusion than by the intrinsic photocatalytic reactivity of the material. Under such conditions, increasing the semiconductor loading does not necessarily lead to a proportional improvement, because the system is already limited by mass transport. This creates an important limitation for interpretation: comparisons between photocatalytic membranes need to take geometry and transport conditions into account, rather than assuming that the observed differences reflect kinetic factors alone. [263], [265]

The interplay between transport and reaction is also relevant for the design of flow-through systems. Although membranes offer the possibility of continuous treatment, their performance depends on residence time, flow distribution, pressure drop, and stability under flow. For this reason, meaningful evaluation of membrane photocatalysts often requires more than batch degradation tests. It also benefits from analysis of reuse behaviour, mechanical stability, and performance under conditions closer to the intended application. [92], [266]

2.7.6. Adsorption versus photocatalytic conversion: interpretive discipline

A membrane can lower the measured dye concentration even before photocatalytic conversion is considered, because its chemistry, porosity, and added functional phases may already promote strong uptake of the pollutant from solution. As a result, dye concentration may drop noticeably already in the dark, before illumination is applied. This is useful from the point of view of pollutant capture, but it should not be confused with chemical transformation. After the light is switched on, the adsorbed dye may undergo degradation, may desorb back into solution, or may be converted into intermediates with different optical absorption. [267], [268], [269]

When dye-based systems are used to evaluate membrane photocatalysts, the experiments have to be designed and interpreted with particular care. Reaching adsorption-desorption equilibrium in the dark, reporting the extent of dark adsorption, and checking whether decolourisation reflects actual mineralisation or only disruption of the chromophore all make the conclusions more reliable. In the same way, rate constants should not be interpreted without considering whether the measured behaviour is governed by the reaction itself or instead by adsorption and transport effects. [269], [270], [271]

Immobilised photocatalysts can change the role of adsorption compared with powders. A membrane may hold pollutant molecules close to the active surface, which can make removal appear more efficient. However, if adsorption is strong, the first drop in

concentration may mainly reflect uptake by the membrane rather than photocatalytic conversion. For this reason, adsorption has to be included in the discussion of membrane behaviour, but it should not be confused with photocatalytic activity when the mechanism is interpreted. [267], [268]

2.7.7. Hybridisation and multifunctionality in electrospun photocatalytic membranes

Electrospun membranes are well suited to hybrid design because several components can be incorporated into one fibrous architecture. In these systems, TiO_2 is often combined with other oxides, conductive additives, or two-dimensional materials to modify not only charge utilisation, but also adsorption and wetting behaviour. Conductive phases may act as routes for electron transport and in this way help to limit recombination, while additional semiconductors may create heterojunctions that modify charge separation and the spectral response. The polymer used to build the membrane can likewise influence hydrophilicity, mechanical behaviour, and stability. For this reason, membrane photocatalysts are better viewed as multifunctional systems rather than as simple carriers of a single active phase. [190], [202], [272], [273]

However, this multifunctional character also makes the design more difficult. Introducing additional components can increase complexity and, if dispersion is poor or fibre formation becomes unstable, reproducibility may suffer. A high loading of particles may lead to bead formation, fibre breakage, or uneven distribution within the membrane. Some additives may also shield the material from light or reduce the exposed semiconductor surface by covering active sites. For this reason, the design of hybrid membranes has to balance functional benefits against structural integrity and accessibility. [245], [274], [275]

Another important design dimension is reusability. One of the main motivations for immobilisation is the possibility of reusing the photocatalyst over multiple cycles without major loss of material or performance. Hybrid components may improve initial activity but may also introduce long-term stability problems if they leach, oxidise, or degrade under irradiation. Research on hybrid membranes therefore benefits from stability testing and post-use characterisation to confirm that observed enhancement is sustained rather than merely transient. [91], [276], [277]

2.7.8. Stability, durability, and practical constraints

A photocatalytic membrane has to remain usable under the conditions in which it is tested. It is placed in water, exposed to light, mixed or flowed over, removed, and often used again. During this process, the polymer may swell, soften, become brittle, or change at the surface. The active particles may also be lost if they are not held firmly in the fibre network. There is also a chemical risk: reactive species formed during photocatalysis can attack the polymer close to the catalytic sites, not only the pollutant. For this reason, the first

degradation result is not enough to judge the membrane. Its structure, particle retention, and repeated-use stability have to be considered together with photocatalytic activity. [278], [279], [280]

In many systems, the polymer matrix is chosen mainly for mechanical support and chemical resistance, while the photoactive phase is responsible for the functional response. Even so, polymers that are relatively stable may still degrade during prolonged exposure to reactive radicals, especially under oxidative photocatalytic conditions. Possible ways to limit this include selecting more resistant polymers, designing architectures in which radicals are consumed close to the semiconductor surface, and building composites that reduce attack on the polymer backbone. This shows that the design of membrane photocatalysts has to address not only photoactivity, but also long-term compatibility of the materials. [281], [282]

Practical limitations also include fouling and blockage when membranes are used in more realistic water-treatment conditions. Natural organic matter, dissolved salts, and suspended contaminants may change membrane behaviour, lower permeability, and alter interactions at the surface. Although laboratory studies often rely on relatively clean model solutions, any move towards practical application requires these effects to be taken into account explicitly. For this reason, membrane-photocatalysis research becomes most meaningful when laboratory performance is discussed together with questions of stability, reuse, and integration into a broader treatment system. [92], [283]

2.7.9. Relevance of membrane photocatalysts to the present research

Electrospun and membrane-type photocatalysts are relevant to the present research because they represent a practical and architecturally rich format for implementing semiconductor photoactivity. In the investigated systems, immobilisation is treated not as a minor practical step, but as a structural design strategy that changes how light, reactants, and charge carriers interact. Membrane architectures make it possible to examine questions of accessibility, wetting, and transport directly alongside more classical semiconductor considerations such as recombination and interface quality. [249], [272]

The inclusion of electrospun hybrid membranes also supports the broader aim of linking photocatalysis and photoelectrochemistry through a common materials perspective. Both fields involve the same fundamental challenge of converting absorbed photon energy into usable interfacial charge. Membranes provide a platform in which architecture and interface engineering can be used to improve charge utilisation and practical functionality. At the same time, they highlight the importance of transport and operational format in determining observed performance. [265], [284]

In this sense, membrane photocatalysts contribute to an integrated understanding of photoactive materials design. They show that performance is not determined solely by

intrinsic material properties, but also by how those properties are expressed within an organised structure capable of operating in a realistic environment. [285]

2.7.10. Concluding remarks

Electrospun and membrane-type photocatalysts are attractive mainly because they avoid one of the practical problems of powders: after use, the material can be removed from the solution and used again. The fibre network also gives a large surface and open pores, and different active components can be introduced into the membrane during or after fabrication. However, such systems do not work only because of their composition. Their activity depends on whether light reaches the active regions, whether the liquid wets the fibres, whether pollutants and oxygen can move through the structure, and whether the membrane remains stable during use. For this reason, membrane photocatalysis has to be discussed as an architecture-dependent process, not simply as powder photocatalysis fixed onto a support. [92], [249]

For this reason, the design and evaluation of membrane photocatalysts require an integrated approach that treats photophysics, interface engineering, and transport as coupled aspects of a single system. This perspective is consistent with the broader architecture-driven framework developed throughout this chapter and provides the basis for linking immobilised photocatalytic platforms with structured photoelectrochemical architectures and hybrid interfaces discussed in the subsequent sections. [58], [199], [249], [272]

2.8. Linking photocatalysis and photoelectrochemistry: shared principles and format-dependent constraints

In the literature, photocatalysis and photoelectrochemistry are usually discussed separately, largely because the experiments are carried out in different ways and the results are expressed through different kinds of performance data. In photocatalysis, attention is usually focused on the rate of chemical conversion under illumination, typically in batch or flow systems. In photoelectrochemistry, the main signal is the extraction of photogenerated charge in the form of electrical current under controlled electrochemical conditions. Even so, both are based on the same underlying physical principles. In each case, the process begins with light absorption in a semiconductor, followed by generation of electron-hole pairs, competition between recombination and separation, transport of carriers to the relevant interfaces, and finally interfacial charge transfer to chemical species. The practical distinction lies in how the carriers are used and in how the system constrains transport and reaction pathways. [174], [286], [287]

Because photocatalysis and photoelectrochemistry are both governed by the same basic semiconductor processes, considering them within one research framework can give a broader view than treating them as unrelated subjects. This is particularly important in work focused on architecture-driven design. Changes in morphology, interface quality, and

structural hierarchy often affect several steps of the overall process at once, although the relative importance of those steps is not the same in photocatalytic and photoelectrochemical systems. Looking at both fields together therefore makes it easier to distinguish effects that arise from carrier dynamics and interfacial kinetics themselves from those that depend mainly on the operating format. [58], [288]

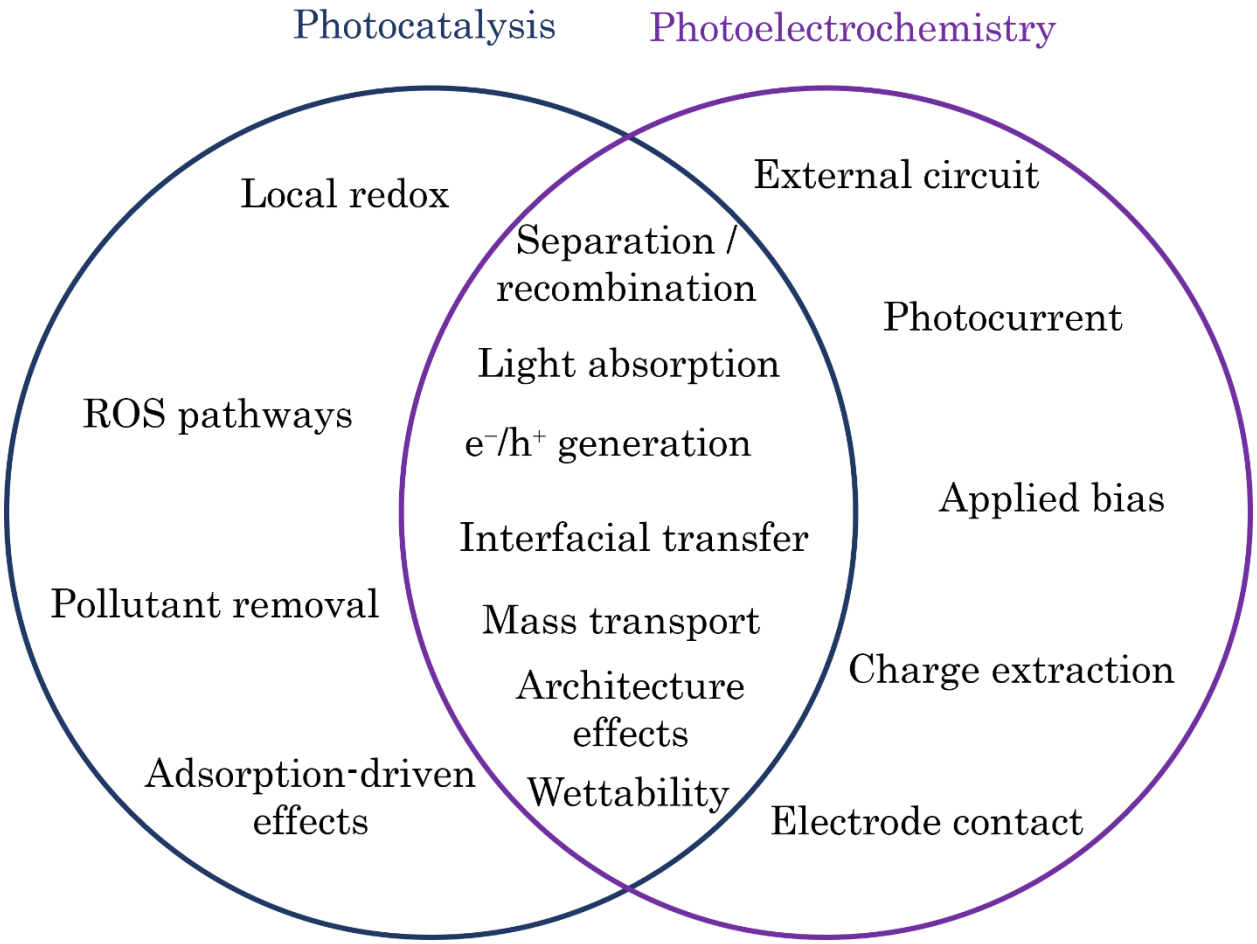

Figure 2.7. *Conceptual overlap between photocatalysis and photoelectrochemistry, showing their shared semiconductor basis and their main format-dependent features. Prepared by the author.*

2.8.1. Common physical basis: generation and fate of photogenerated charge carriers

In both photocatalysis and photoelectrochemistry, the first step is absorption of light by the semiconductor and the generation of electron-hole pairs. What matters next is what happens to those carriers. If recombination takes place, the absorbed energy is dissipated without useful effect, for example as heat or luminescence. If the charges are separated and reach the relevant interfaces, they can participate in redox reactions. In this sense, both fields

are limited by the same basic competition between carrier loss through recombination and their productive use in interfacial charge transfer. [193], [289]

The same design ideas appear in photocatalysis and photoelectrochemistry, but they do not mean exactly the same thing in both cases. In both formats, the material first has to deal with the same problem: light creates electrons and holes, and many of them are lost before they reach a useful interface. This is why heterostructures, conductive additives, defect control, crystallinity, and coating thickness are all important. Architecture adds another level to this issue. It can bring the active interface closer to where charges are formed, improve contact with the liquid, or give the material a more usable shape. The difference is what happens afterwards. In photocatalysis, the final result is affected by the solution itself, including adsorption, wetting, oxygen access, and diffusion of the pollutant. In photoelectrochemistry, the structure also has to stay connected to the current collector and work under applied bias. For this reason, the same material strategy can connect the two fields, but the explanation has to follow the way the system is actually tested. [195], [290]

2.8.2. Key operational difference: where charges go and how they are used

The main difference between photocatalysis and photoelectrochemistry is where the generated charges are used. In photocatalysis, there is no external circuit. Electrons and holes are usually consumed at or near the semiconductor surface, where they react with adsorbed molecules, water, oxygen, or other dissolved species. Because of this, the result depends strongly on the immediate surface environment. Adsorption, surface hydroxyl groups, oxygen availability, and diffusion of reactants or products can all affect how efficiently the generated charges are converted into chemical change. [291], [292]

In photoelectrochemistry, by contrast, at least one type of carrier is extracted through an external circuit. For a photoanode, electrons are transported to the current collector and through the circuit, while holes participate in oxidation at the semiconductor-electrolyte interface. For a photocathode, the situation is reversed. Because the system includes external bias and a defined electrode architecture, carrier extraction becomes a major limiting factor. The semiconductor must therefore remain electrically integrated with a conductive substrate, and the interface with the electrolyte must support stable and efficient charge transfer. Film continuity, substrate contact, and electrical resistance consequently play a stronger role than in many photocatalytic tests. [42], [141], [286]

This difference also affects how materials are evaluated. A photocatalyst may show high apparent activity because of favourable adsorption and surface reactivity even when long-range carrier transport is poor, since carriers are consumed locally at the surface. A photoelectrode, in contrast, requires more stringent transport pathways because carriers must reach the current collector efficiently. The same material can therefore behave differently depending on whether it is used as a suspended photocatalyst, an immobilised membrane, or a thin-film electrode. [32], [185]

2.8.3. Format-dependent transport constraints

Because photocatalysis and photoelectrochemistry impose different transport requirements, architecture optimisation must be evaluated in a format-dependent manner. [199], [201]

In photocatalysis, the movement of molecules can be just as important as the semiconductor itself. In powder suspensions, stirring and dispersion decide how easily pollutant molecules and oxygen reach the catalyst surface. In immobilised systems, especially membranes, the situation is more restricted. The solution has to wet the material, enter the pores, and move through the fibre network, while light also has to reach the active regions. Even a good semiconductor will contribute only partly if it is hidden inside poorly wetted or poorly illuminated parts of the membrane. For this reason, mass transport and light penetration should be treated together when discussing how much of the active phase is really used. [249], [265], [272]

In photoelectrochemistry, the architecture has to do more than expose a semiconductor to light. The material is connected to a current collector, so the charges produced under illumination must be able to move through the solid part of the electrode before they are lost by recombination. At the same time, the electrolyte still has to reach the active surface. This creates a compromise. A thicker coating may absorb more light, but it can also make charge collection less efficient. A textured support may give more surface area, but it can also make the coating thickness, resistance, and electrolyte access less uniform. For this reason, a PEC electrode works best when the active layer remains accessible to the electrolyte and is also well connected to the substrate. [32], [37], [58], [141]

This helps explain why photocatalytic and PEC performance do not necessarily improve in the same way. A modification that is beneficial in one case may have only a limited effect in the other. For example, a conductive additive may help electrons leave the semiconductor more easily, but that benefit can remain barely visible in photocatalysis when the measured behaviour is still dominated by adsorption or by the chemistry of the surface. By contrast, a surface modification that improves adsorption and wetting may markedly enhance photocatalysis, while giving little benefit in PEC operation if charge extraction through the solid remains the main limitation. For this reason, considering the two fields together is useful, because it helps separate design features that address general carrier-related limitations from those whose benefit is mainly tied to a specific operating format. [174], [293]

2.8.4. Comparing performance metrics and their interpretation

Another difference is the type of result that is taken as “performance”. In photocatalysis, this is often the decrease of dye concentration during irradiation, expressed as colour removal, degradation efficiency, or an apparent kinetic constant. Such values are

useful, but they belong to the whole test, not only to the catalyst. They can change with adsorption time, starting concentration, light geometry, catalyst amount, stirring, and diffusion conditions. In dye experiments, colour loss also needs caution, because it does not necessarily mean complete mineralisation of the molecule. Sensitisation and intermediate products may also affect the measured signal. For this reason, photocatalytic results should be read as experiment-dependent values, rather than as fixed properties of the material itself. [86], [268], [294]

In photoelectrochemical work, performance is usually discussed on the basis of quantities such as photocurrent density, onset potential, incident photon-to-current efficiency, applied-bias photon-to-current efficiency, and chronoamperometric stability. These parameters can provide useful information about charge extraction and behaviour at the interface, but they do not lend themselves to a simple direct interpretation. A higher photocurrent, for instance, does not automatically mean that chemical conversion or fuel production has increased. A stronger current response does not by itself show that photoelectrochemical conversion has become more efficient. Some of the measured signal may still come from side reactions or capacitive charging, so Faradaic efficiency cannot be claimed unless the reaction products are analysed directly. The same caution applies to rougher electrodes, where photocurrent may increase simply because the interface area is larger, even though charge separation in the semiconductor itself has not improved. For this reason, PEC metrics, just like photocatalytic ones, have to be interpreted in relation to architecture, interface design, and operating conditions. [295], [296], [297]

Using both tests makes the discussion less dependent on a single measurement. Photocatalysis shows the behaviour of the material in solution, where dye uptake, wetting, oxygen supply, light penetration, and diffusion can all affect the apparent conversion. PEC measurements examine another part of the same system by following how efficiently charges are extracted under applied bias. In this sense, the two approaches are complementary. Agreement between them supports a charge-utilisation explanation, while disagreement suggests that other factors, such as transport, surface accessibility, optical effects, film continuity, or electrical contact, may be involved. [298], [299], [300]

2.8.5. Architecture-driven design principles that connect photocatalysis and PEC

A key advantage of linking photocatalysis and PEC is that certain architecture-driven design principles can be examined across both formats, even though the metrics differ. [174]

Light management is a useful link between photocatalysis and PEC, but it should not be treated as a benefit by itself. A textured or hierarchical surface can lower reflection and increase the time that light spends inside the material. This may help create more charge carriers near useful interfaces in photocatalysis, or increase absorption in a photoelectrode. The important question is what happens to those carriers afterwards. If they recombine

before reaching the surface or the current collector, stronger absorption does not improve the real function of the material. For this reason, optical improvement has value only when it is matched with short transport paths, continuous charge-collection routes, and interfaces that can actually use the generated carriers. [299], [301]

Short transport distances are another principle common to both fields. In photocatalysis, the generated carriers have to reach the surface quickly, whereas in PEC systems they must be transported efficiently to the surface and/or to the current collector. Thin films, conformal coatings, nanostructured surfaces, and hierarchical scaffolds can all help shorten the path that carriers need to travel. At the same time, there is no single universal definition of a “short” transport distance, because it depends on factors such as diffusion length, defect density, and recombination at interfaces.. For this reason, architectural optimisation is most effective when the sites of carrier generation remain close to the interfaces where those carriers are either collected or used in reaction. [302], [303]

Interface engineering is an important issue in both photocatalysis and photoelectrochemistry. In photocatalytic systems, the nature of the surface interface strongly influences whether charge carriers are used in reactions that generate active species or are instead lost by recombination. In PEC systems, much depends on what happens where the semiconductor meets the electrolyte. What happens at this boundary has a direct effect on both the onset of photocurrent and the final efficiency of the system, since it is here that band bending is established and interfacial charge-transfer reactions take place. For that reason, the quality and continuity of interfaces become important in both photocatalysis and photoelectrochemistry, especially when hybrid materials are involved. When deposition is well controlled and junctions are formed properly, recombination losses can be reduced and charge transfer can become more efficient. If the interfaces are poorly formed, they may instead become the dominant source of loss. [304], [305]

Immobilisation is another point where photocatalysis and PEC come close to each other. In photocatalysis, membranes, coated substrates, and other fixed formats move the material away from powder suspensions and closer to a usable device. In PEC, the material is already fixed as an electrode, so the same issues appear from the beginning. In both cases, the architecture has to do more than hold the active phase. It must allow wetting, transport through or across the structure, mechanical stability, and repeated operation. For this reason, immobilisation is not only a practical choice. It is part of how the photoactive system performs. [96], [295]

2.8.6. How photocatalysis and PEC complement each other in research interpretation

Reading photocatalysis and PEC results together can strengthen the conclusions, because each approach highlights a different part of the same charge-carrier behaviour. [96]

Photocatalysis emphasises chemical outcomes in complex aqueous environments, where adsorption, diffusion, and surface chemistry strongly influence the results. It therefore reflects practical behaviour well, but often provides only limited direct insight into carrier transport and extraction pathways. [49], [298]

PEC makes it possible to examine charge extraction and interfacial behaviour under controlled bias conditions. Because the generated charges have to be collected as current, this approach can reveal transport-related limitations that may remain less obvious in photocatalytic tests. Additional insight may come from measurements such as impedance spectroscopy, transient photocurrent response, and potential-dependent analysis, which can help to identify changes in interfacial resistance and recombination behaviour. Even so, PEC results on their own are not enough to define chemical-conversion efficiency unless they are supported by direct product analysis. [192], [241], [306], [307]

When both approaches are used and interpreted within a consistent materials framework, they can provide a more complete understanding of how architecture and interface engineering influence photoactive behaviour. For example, if a structured material shows improved photocatalytic degradation together with improved photocurrent response, this supports the view that charge utilisation has improved rather than only adsorption effects. If photocatalytic performance improves clearly while the PEC response changes only slightly, this may indicate that the main gain in the photocatalytic format comes from adsorption and wetting, whereas charge extraction still remains one of the limiting steps in PEC operation. Conversely, if PEC improves without strong photocatalytic improvement, it may indicate that electrical extraction pathways have improved while surface redox pathways or adsorption behaviour in photocatalysis remain limiting. [16], [23], [37]

2.8.7. Relevance to the present research framework

Linking photocatalysis and photoelectrochemistry is central to the present research framework because the investigated materials and architectures span both formats and are unified by the concept of architecture-controlled charge utilisation. Structured substrates, conformal oxide coatings, hybrid interfaces, and immobilised membrane platforms all influence the same fundamental processes, but they do so under different constraints depending on whether the system is tested as a photocatalyst or as a photoelectrode. [37], [58], [308]

This combined perspective supports a more coherent interpretation of the publication-based results presented later. It provides a conceptual basis for explaining why architecture-driven design is expected to influence both pollutant degradation and photoelectrochemical behaviour, while also recognising that improvements must be interpreted in relation to format-dependent limitations. In this way, different material platforms can be connected through shared principles rather than treated as unrelated studies. [174], [309]

Furthermore, discussing photocatalysis and PEC together helps avoid an overly narrow explanation of performance changes. If trends are compared across both formats, it becomes easier to see whether the improvement is more likely related to charge use, transport and accessibility, optical effects, or surface chemistry. This makes the interpretation stronger and supports the chapter's main argument that architecture and interfaces have to be considered together. [23], [272]

2.8.8. Concluding remarks

Photocatalysis and photoelectrochemistry start from the same semiconductor processes, but the material is tested in different ways. In photocatalysis, the response is followed through chemical change in the solution, so adsorption, wetting, diffusion, and access of reactants to the surface can strongly influence the apparent kinetics. In photoelectrochemistry, the material has to work as an electrode. The generated charges must be extracted under applied bias, which makes film continuity, substrate contact, interfacial resistance, and stable electrolyte access especially important. [37], [287], [292]

Photocatalysis and PEC are considered together in this dissertation because the same design idea can be tested in two different ways. A structured support, a conformal oxide layer, a hybrid interface, or an immobilised membrane may improve one part of the process, but its real role depends on the operating format. In photocatalysis, these features influence how light, water, oxygen, and pollutants reach the active surface. In PEC, they must also allow the generated charges to move through the electrode and be collected under bias. This comparison helps bring the publication results into one line of discussion, centred on how architecture and interface quality affect the use of photogenerated charges in different photoactive systems. [58], [72], [96]

2.9. Open problems, literature gaps, and reporting pitfalls in photoactive materials research

The literature on photocatalysis and photoelectrochemistry has grown very quickly, and under laboratory conditions many material systems appear to perform better than earlier ones. At the same time, this large body of work has also made a number of recurring weaknesses easier to recognise. Results are often difficult to compare, and mechanistic explanations are sometimes stated with greater certainty than the available evidence supports. This problem does not arise only from the way experiments are performed. It also lies in the way data are reported, in the limited separation of overlapping effects, and in the fact that stability and true chemical conversion are not always verified in a sufficiently rigorous way. Identifying these gaps is important because they define the research space in which architecture-driven design can provide meaningful progress. They also clarify what kinds of evidence are needed for reliable interpretation of performance improvements, especially in complex structured and hybrid systems. [16], [23], [37]

In TiO_2-based and related photoactive systems, a better number does not explain itself. Faster dye removal or higher photocurrent only shows that the system has changed. The reason may be improved charge separation, but it may also be better light trapping, larger exposed surface, stronger adsorption, easier wetting, or better contact between phases. This is why such results have to be interpreted together with the structure of the material and the way the experiment was performed. Dye tests are especially sensitive, because colour loss can include adsorption or sensitisation. PEC results also depend strongly on how potentials, illuminated area, light intensity, efficiency values, and product formation are reported. Stability must also be considered, since structured and hybrid materials may change during use. In this dissertation, architecture is therefore treated not as an automatic advantage, but as something that must preserve accessible interfaces, continuous contact, structural stability, and useful charge transfer. [22], [58], [309]

2.9.1. Conflation of optical enhancement with intrinsic electronic modification

After structuring, a material may reflect less light, but this does not mean by itself that the semiconductor absorbs differently at the electronic level. In rough, porous, or periodic surfaces, part of the incident light is simply redirected many times inside the structure instead of returning directly to the detector. The spectrum can therefore suggest stronger absorption even when the absorption edge of the semiconductor is unchanged. For this reason, in this dissertation such changes are treated mainly as an effect of surface geometry, unless they are supported by additional evidence for band-structure modification. [144], [149]

This point is especially important for laser-structured systems. Laser-made micro- and nanoscale features can strongly reduce reflectance, so the optical change may look very convincing. However, lower reflectance does not by itself prove that the semiconductor has changed electronically. The important question is whether the additional light interaction leads to carriers that are actually separated and used. If recombination still dominates, the optical improvement may give only a small functional benefit. For this reason, one recurring problem in the literature is that light-coupling effects are not always separated clearly from real changes in semiconductor electronic structure. [149], [193]

A similar problem appears in hybrid systems when added components also affect the optical response. Conductive phases, carbon-based materials, or two-dimensional additives may increase absorption in the visible range, but this does not necessarily mean that the semiconductor is generating more useful photocarriers. In some cases, the added absorption may be largely parasitic. In such cases, improved optical absorption may not correlate with improved photocatalytic or PEC performance and can even reduce performance through light shielding of the semiconductor. Thus, the literature reveals a need for architecture-aware optical interpretation, where optical changes are evaluated together with evidence of

charge utilisation rather than being treated as independent proof of functional improvement. [15], [310]

2.9.2. Adsorption, photosensitisation, and the interpretation of dye degradation

Dye degradation is often used because it is simple to run and easy to follow by UV-Vis spectroscopy. It gives a fast way to compare samples, but the result is not always straightforward. A lower dye concentration during illumination may come from oxidative degradation, but it may also include adsorption on the material, desorption during the test, changes in dye aggregation, or formation of products with different absorption bands. Dyes can also take part in the photochemical process themselves. Some of them absorb visible light and inject electrons into the semiconductor, even when the semiconductor is not strongly excited in that range. In such cases, the observed visible-light response may be partly dye-sensitised rather than caused only by intrinsic excitation of the photocatalyst. [12], [22], [270]

In membrane and hybrid photocatalysts, the concentration curve does not describe only the semiconductor reaction. It describes the behaviour of the whole material in contact with the dye solution. A fibrous or MXene-containing structure may retain part of the dye while illumination is already taking place, so adsorption, diffusion, and photooxidation can overlap. For this reason, the results are discussed here as dye-removal behaviour, with photocatalytic degradation assigned only where the experimental controls justify it. [12], [22], [73]

Another limitation is that colour loss is not always checked against deeper chemical conversion. In many dye-degradation studies, the disappearance of the main absorption band is treated as the main result, although this may only show disruption of the chromophore. Full mineralisation is not required in every study, but some distinction between decolourisation and broader oxidative breakdown is still important for environmental interpretation. This is especially true when adsorption or dye sensitisation may contribute to the observed response. For this reason, dye-removal data are stronger when they are supported by additional evidence on the degradation pathway or conversion products. [16], [268]

2.9.3. Separation of surface-area effects from genuine charge-utilisation improvement

In nanostructured and hierarchical materials, higher surface area is often taken as a reason for better activity. In some cases this is correct, but it is not a complete explanation. More surface may simply give the dye more places to adsorb and more contact points with the solution. The measured activity can therefore increase even if charge separation or carrier transport has not improved much. At the same time, a material with a smaller surface area

may still work efficiently if charges are collected more easily and the interface is better organised. Surface area is therefore important, but it should not be used as the only explanation for improved performance. [23], [174], [297]

Surface-area and roughness changes are often reported, but their meaning is not always clear. A rougher or more developed surface can give a stronger photocatalytic response simply because more interface is exposed. In PEC measurements the same problem appears as a larger electrochemically active area or roughness factor: the photocurrent may increase partly because there is more working surface, not necessarily because carrier separation or transport inside the semiconductor has improved. For this reason, geometric enhancement should be separated from mechanistic enhancement. A higher signal caused mainly by larger area should not be presented as direct evidence of better charge-carrier behaviour. [39], [241], [311]

In structured electrodes and membranes, a change in surface area usually brings other changes with it. A rougher surface may expose more active sites, but it can also change how light is reflected, how the liquid wets the material, and how easily reactants move through the structure. Because of this, a higher activity or photocurrent should not be assigned too quickly to better charge utilisation. It may partly come from geometry itself. This is why controlled sample series are important in architecture-driven work: when thickness, coverage, and interface quality are kept as comparable as possible, the role of the structure can be judged more reliably. [39], [308], [312]

2.9.4. Incomplete control and reporting of interface quality in hybrid and structured systems

A heterostructure is only useful if the interface actually works. Placing two phases in one material does not guarantee this. The phases may be present, but if they meet only poorly, or if the boundary between them is defective, charges may still recombine before they can be separated. This is also important for coated structured supports. A textured substrate can help with surface area and light interaction, but these advantages depend on the quality of the oxide layer placed on it. If the coating is incomplete, weakly attached, or uneven in thickness, the hidden contact between the coating and the support may become a place where losses occur rather than a functional junction. [72], [195], [313]

The weak point in many hybrid and structured systems is that the interface is taken for granted. Showing TiO_2, MXene, ZnO, or another phase by XRD, Raman, or XPS only proves that the components are present. It does not prove that they touch each other in the right way. In porous or hierarchical architectures this becomes critical, because the coating has to follow a difficult surface, not a flat one. If some regions are uncovered, overfilled, weakly attached, or electrically disconnected, the measured response may be controlled by these imperfections rather than by the intended design. Therefore, the interface has to be

treated as a real structural feature of the material, not just as an assumed boundary between two detected phases. [39], [241], [289]

Controlled methods such as ALD can reduce this problem because they give better control over coverage and reproducibility. Still, ALD does not remove the need for careful interpretation. The final interface also depends on the chosen thickness, possible post-treatment, crystallinity of the deposited layer, and the defects introduced or passivated during growth. For this reason, interface quality remains one of the main variables in structured photoactive systems. If it is not discussed directly, it can easily become a hidden source of ambiguity in the explanation of performance trends. [100], [113], [304]

2.9.5. Stability, durability, and evolving material state under operation

Initial performance describes only the material before it has been tested. Once the system is exposed to light, electrolyte, stirring, flow, or applied bias, its surface and interfaces may change. Active components can detach, pores or surface sites can become blocked, polymer supports can age, and electrode contacts can be altered during operation. Stability testing is therefore part of the performance assessment itself. It shows whether the measured response is a lasting feature of the working material or only the behaviour of the freshly prepared sample. [278], [314]

This is especially important for hybrid systems that contain chemically active or unstable components. Conductive phases and two-dimensional materials may change during contact with water, oxygen, light, or reactive species. MXenes are a clear example, because oxidation can change their conductivity, surface chemistry, and contact with the semiconductor over time. Such changes may reduce performance, but they may also create new interfacial conditions that change the response in a less predictable way. Without stability testing, it is difficult to know whether the observed enhancement belongs to a stable material system or only to an early stage of its operation. [221], [225]

Another stability-related gap is that many studies focus on activity trends while providing limited evidence of the post-operation structural state. Yet for mechanistic interpretation it is often essential to know whether the material remains chemically and structurally similar after testing. Without such confirmation, performance changes may be explained incorrectly, especially if the material evolves during operation. Stability assessment together with post-test characterisation therefore represents a major gap that must be addressed when designing practical architecture-engineered photoactive systems. [39], [278]

2.9.6. Comparability and reporting limitations in photocatalysis

Photocatalytic results can be difficult to compare even when each experiment is done correctly. The measured rate depends on the whole testing setup, not only on the photocatalyst. Lamp intensity, spectrum, reactor geometry, catalyst amount, pollutant

concentration, pH, and oxygen level can all change the degradation curve. Because of this, rate constants or final degradation percentages are most useful inside one controlled sample series. Across different studies, they should be compared only with caution, unless the experimental conditions are clearly similar. [315], [316]

In photocatalysis, the way the test is reported can strongly affect how the result is understood. Naming the lamp or giving its nominal power is not enough, because the reaction depends on the light that actually reaches the sample: its intensity, spectral range, and path through the reactor. Adsorption has a similar effect on interpretation. If the dark stage is not reported clearly, especially for membranes, pollutant uptake can be mixed with photocatalytic removal. The final rate may then describe the behaviour of the whole test system rather than the intrinsic activity of the material. [269], [317]

Activity is also reported in different ways, which makes comparison harder. Some studies give only the percentage of dye removed after a chosen irradiation time, while others calculate an apparent rate constant. The kinetic model used is not always justified, even though pseudo-first-order or pseudo-second-order fitting may describe different limiting situations. This becomes especially important for complex architectures, where diffusion, wetting, and access to active sites can affect the shape of the kinetic curve. For this reason, inconsistent reporting is a real limitation in the literature, because it makes it difficult to compare materials systematically rather than only within one experimental series. [298]

2.9.7. Comparability and reporting limitations in photoelectrochemistry

PEC performance is also sensitive to the way the experiment is set up. A photocurrent value is not determined by the electrode material alone. It can change with light intensity, illuminated area, electrolyte composition, pH, reference-electrode scale, scan rate, and the prior condition of the surface. For this reason, similar photoelectrodes may appear to perform differently simply because they were measured under different conditions. Photocurrent should therefore be treated mainly as a charge-extraction signal. To claim efficient chemical conversion, it has to be supported by product detection, Faradaic efficiency, and stability data. [32], [39], [42]

Photocurrent is an important PEC descriptor, but it cannot explain the electrode by itself. A higher current may mean better charge extraction, but it may also reflect lower resistance, different active area, improved light access, or a more favourable measurement geometry. For this reason, PEC discussion should include impedance, stability, and clear reporting of potentials. Values measured with different reference electrodes must be converted to the same scale before comparison. The illumination setup also has to be defined, since front-side and back-side irradiation, exposed area, and light intensity can change the response even for the same electrode. [4], [39]

In structured electrodes, a higher photocurrent does not necessarily mean that the semiconductor itself has become more efficient. Part of the increase may come from rougher morphology, larger electrochemically active area, or better exposure of the surface to the electrolyte. For this reason, photocurrent trends should be discussed together with the architecture of the electrode and, where possible, with impedance results that indicate changes in charge transfer or resistance. The issue is not that photocurrent data are unimportant, but that they need supporting evidence before a clear mechanism can be assigned. [241], [311]

2.9.8. Limited integration between photocatalysis and PEC as complementary evaluation tools

Photocatalysis and PEC look at the same photoactive material from different sides. Photocatalysis shows whether light exposure leads to chemical change in the solution, but the result can be mixed with adsorption, wetting, and mass transport. PEC follows charge extraction more directly, but photocurrent does not by itself prove efficient product formation. When both types of data are considered together, the interpretation becomes less one-sided. It becomes easier to judge whether the improvement is mainly related to charge use, interface quality, transport, or the architecture of the material. [23], [37], [309]

When a structured material is examined in only one working format, its behaviour is easy to overread. Faster dye removal from a membrane does not necessarily identify the role of charge transfer, because adsorption, wetting, and internal transport may contribute to the same trend. A higher photocurrent from a structured electrode also does not fully define the mechanism, since area, electrolyte access, and electrical contact may all influence the response. This is why photocatalytic and PEC measurements are most useful when they are used together. They help test whether the architecture improves the use of photogenerated charges, or mainly changes the environment in which those charges are generated and consumed. [22], [39], [73], [241]

2.9.9. Summary of key gaps relevant to architecture-engineered TiO_2-based systems

The gaps and pitfalls outlined above can be summarised as several interrelated needs that define meaningful progress in architecture-engineered photoactive materials: [22], [37], [149], [311]

1. Clear separation of optical coupling effects from intrinsic electronic modification, especially in structured and laser-processed systems.
2. Systematic treatment of adsorption and photosensitisation in dye-degradation studies, particularly in membrane and hybrid materials.

3. Separating improvements caused mainly by larger surface area from those related to better charge utilisation, using supporting electrochemical and spectroscopic evidence.
4. Explicit attention to interface quality and coating continuity, especially in heterostructures and structured supports where local defects can dominate behaviour.
5. Robust stability assessment and post-operation characterisation, especially for systems involving dynamic components such as two-dimensional conductive phases.
6. Improved reporting and comparability of experimental conditions, including illumination parameters and potential-reference conventions.
7. Use of complementary evaluation frameworks that integrate photocatalytic and PEC perspectives in order to strengthen mechanistic interpretation.

These points define not only limitations in existing work, but also opportunities for systematic research. Architecture-driven design provides a promising route for improving photoactive systems, but its success depends on controlling and interpreting the coupled roles of geometry, interface quality, transport, and stability. [58]

2.10 Research strategy and positioning of the present work relative to the identified gaps

The points discussed above show that improved performance is not enough unless the reason for it is also examined. In structured and hybrid materials, a higher activity or photocurrent has to be related to the real form of the system: the geometry that was created, the continuity of the coating, the quality of the interfaces, the access of liquid and light, and the stability during use. This is especially important for TiO_2-based systems, because TiO_2 does not have one fixed role. It may act as a thin coating, a photoactive membrane component, part of a heterostructure, or the active layer of a photoelectrode. For this reason, this dissertation treats architecture as the common link between the studied materials and uses both photocatalytic and PEC testing to understand how structure and interfaces affect the final response. [23], [37], [58]

TiO_2 is used in this work in several different forms, and these forms cannot be treated as interchangeable. A compact coating, a layer on a laser-textured support, a membrane component, and a phase combined with a conductive additive all place the oxide in a different environment. The same material may therefore show a different response because the coating continuity, interface contact, liquid access, light distribution, and carrier path are different. This is why the discussion pays attention not only to TiO_2 itself, but also to how it is built into the final structure. [22], [149], [249]

2.10.1. Architecture-driven design as the organising research principle

The research is structured around the idea that architecture can be engineered at multiple length scales in order to improve both functional performance and practical relevance. This includes:

- Micro- and nanoscale surface structuring to influence light interaction, wettability, and accessible interfacial area.
- Hierarchical scaffolds and membranes to create immobilised photoactive formats that are recoverable and suitable for repeated use.
- Thin-film and conformal coatings to introduce photoactive oxides onto complex supports while preserving the underlying geometry.
- Hybrid and heterostructured interfaces to guide charge carriers towards productive transfer pathways and suppress recombination.

By treating these elements as parts of one strategy, the research does not present each improvement as a separate effect. Instead, it uses the different material systems to examine the same broader question: how the spatial organisation of the active phase, support, and interfaces affects performance in different photoactive formats.

This design principle also supports a consistent interpretation of results. Because architecture can influence optical behaviour, adsorption, wetting, and transport simultaneously, the research emphasises comparisons in which the structural variable is introduced deliberately and evaluated in relation to the full set of coupled effects it can produce. In this way, architecture serves not only as a route to improved performance, but also as a framework for more disciplined mechanism-oriented interpretation. [15], [249]

2.10.2. Controlled interface formation through thin-film deposition and reproducible platforms

A rough or porous support is useful only after the active layer has been placed on it properly. Until then, the geometry is only a potential advantage. If TiO_2 does not cover the surface evenly, or if the contact with the scaffold is poor, the system being tested is no longer just a structured support with an active coating. It is also a material with local coating defects. In this work, this point is treated seriously. The deposition step is therefore used not only to introduce the semiconductor, but also to make the contact between the active phase and the support as controlled as possible**.** [72], [100]

Conformal thin-film deposition is useful here because it allows the oxide layer to be added without losing the shape of the support. On complex or hierarchical surfaces, this makes it possible to control the coating thickness and coverage more reliably. The same scaffold can then be compared with different oxide thicknesses, while the main geometry

remains largely unchanged. This is important because it helps separate what comes from the structured substrate from what comes from the deposited oxide layer. It also makes the sample series easier to compare, since performance changes are less likely to result from random coating differences. [100], [105], [113]

This controlled-interface strategy is not limited to the deposition step itself. It also shapes the way the research is organised. Simpler reference systems are considered first, then coating thickness, post-treatment, and interface quality are adjusted before moving to more complex architectures or hybrid combinations. This stepwise approach makes the interpretation safer, because the effect of each change can be followed more clearly instead of introducing many variables at once. [23]

2.10.3. Using structured substrates to study optical coupling without overclaiming electronic modification

In this work, laser treatment is used mainly to shape the surface. The textured substrate may reflect less light, hold light for longer, or expose the coating to the solution in a different way. These changes can improve the measured response, but they are not taken as proof that the semiconductor band structure has changed. A band-structure change is discussed only when there is evidence for it beyond the optical effect caused by the surface texture. [144], [149]

In this approach, lower reflectance is treated first as a result of the surface structure, not as direct evidence of band-gap narrowing. A textured support can change where light goes, how long it remains in the material, and how the active layer is exposed at the interface. These effects can improve performance, but they are different from a true electronic modification of the semiconductor. For this reason, optical changes are interpreted together with the role of the architecture. This is especially important when structured supports are combined with conformal coatings or hybrid layers, because improved light use is valuable only if the interface also supports charge separation and transport. [15], [193]

2.10.4. Addressing adsorption and transport effects in immobilised photocatalytic systems

One major weakness in many photocatalytic studies is that pollutant removal is not always separated clearly from photocatalytic degradation. This is especially problematic in dye tests, where adsorption or dye sensitisation can strongly affect the early part of the experiment. The issue becomes even more important for immobilised membranes, because these materials can adsorb dye and at the same time create slower, less uniform transport inside the structure**.** [12], [73], [270]

In this work, membrane photocatalysts are treated as whole working systems, not only as supports carrying an active phase. Their response depends on adsorption, wetting, diffusion, light access, and the way the membrane is handled during testing. For this

reason, the discussion does not rely only on apparent kinetic constants. It also considers how immobilisation changes access to the active regions, how dark adsorption affects the starting point of the reaction, and how reuse, fibre arrangement, and membrane thickness influence the observed behaviour. [249], [269], [272]

This approach also gives immobilised photocatalysts a more practical meaning. Immobilisation is not treated only as a way to recover the catalyst after the test. It is considered as a way to build a defined material format, where liquid access, transport paths, and exposure of the active surface can be controlled. This makes it easier to discuss membrane-type catalysts on their own terms, rather than comparing them directly with powders. It also helps interpret hybrid composites more carefully, because any improvement can be related not only to composition, but also to how the architecture affects accessibility and transport. [249], [258]

2.10.5. Positioning hybrid interfaces as charge-utilisation strategies rather than universal “enhancement” claims

Hybrid and heterostructured materials are often described as automatically better, but this is not always justified. Their improved response may come from several effects at once, including morphology, adsorption, wetting, light shielding, or real charge-transfer improvement. In this work, hybrid interfaces are therefore treated as tools whose value depends on how well the phases contact each other and how they are placed within the architecture. They are useful only when they help the generated charges move or react more effectively, rather than simply adding another component to the system. [15], [195]

In practical terms, this means that conductive additives and two-dimensional phases are considered not as guaranteed enhancers but as components whose role must be established within the composite architecture. Their potential to act as electron acceptors, transport pathways, or interfacial modifiers is evaluated in relation to their distribution, contact quality, and stability under operating conditions. This approach is especially relevant for MXene-containing systems, where chemical evolution in aqueous environments can modify conductivity and functional behaviour over time. [190], [221], [225]

This positioning helps keep the interpretation more controlled. Performance changes are not assigned to one simple explanation, such as “better charge transfer”, unless the structure and interface support it. Instead, the results are read through the combined effects of architecture, contact quality, accessibility, and charge utilisation. [23]

2.10.6. Complementary evaluation across photocatalysis and photoelectrochemistry

The interpretation in this work is not based on one performance signal alone. Dye-degradation data are read as the behaviour of the whole material in an illuminated solution, where reaction, adsorption, wetting, and diffusion may occur together. PEC data are used as

a separate check of how easily photogenerated charges leave the electrode and cross the interface. Since photocurrent is not the same as product yield, it is not used alone as proof of conversion efficiency. The two datasets are therefore combined to judge whether the improvement is mainly linked to charge utilisation, surface access, transport, or contact between phases. [37], [286]

In this work, photocatalytic and PEC measurements are used as two views of how architecture affects charge use. If both dye-degradation behaviour and PEC response improve, the case for better carrier utilisation becomes stronger. If the trends do not match, the difference is also useful: it may show that photocatalysis is being limited by adsorption, wetting, or transport, while PEC is more sensitive to charge extraction and interfacial resistance. In this way, the two types of testing help connect the different material formats within one architecture-based interpretation, rather than treating each result as an isolated performance value. [272], [298]

2.10.7. How the publication set addresses the identified gaps

The research outcomes presented in the publication part of the dissertation are structured as connected case studies that collectively address the major gaps identified in the literature.

Structured substrates are useful in this work mainly as controlled light-management platforms. They make it possible to discuss changes in reflectance, scattering, and optical coupling without automatically treating them as band-gap modification.

Conformal oxide coatings address the interface problem more directly. The question here is whether the active oxide can be deposited on a complex scaffold while keeping both the scaffold geometry and a continuous contact region.

Immobilised fibrous membranes bring the discussion closer to practical photocatalysis, but they also add transport-related limitations. Their performance is read together with dye uptake, wetting, diffusion through the membrane, and accessibility of the active regions.

Hybrid systems containing conductive or two-dimensional phases are used to test whether added components can really support charge utilisation. Their role is not assumed from their presence alone. It depends on where they are located, how well they contact the semiconductor, and whether they remain stable during operation.

Together, these studies form a coherent architecture-driven research programme rather than a collection of independent optimisations. They demonstrate how structured and hybrid systems can be designed and interpreted in a way that is consistent with the needs of reproducibility, mechanism-aware analysis, and practical relevance.

2.10.8. Concluding remarks and transition to the publication-based chapters

The literature discussed in this chapter shows that photocatalytic and PEC behaviour is shaped by several connected processes rather than by composition alone. Optical response, charge transport, interface quality, accessibility, adsorption, and stability all affect the measured performance. It also shows that improvement can be difficult to assign when the material architecture is not well controlled, when the interface is only assumed, or when adsorption and durability are not considered carefully. [22], [23], [37]

The present research addresses these limitations by using architecture as the main organising principle. The focus is placed on controlled interface formation, structured and immobilised material formats, and evaluation by both photocatalytic and PEC methods. In this way, the work aims not only to improve performance, but also to make the observed changes easier to interpret and more relevant for future practical use.

On this basis, the next chapter presents the publications that form the main research output of the dissertation. Each paper is introduced by a short contextual note explaining the problem addressed, the architecture tested, and its contribution to the broader aim of understanding charge utilisation in TiO_2-based and related photoactive systems.

Chapter 3. Overview of the publication-based research and integration within a unified framework

The research presented in this dissertation is based on four peer-reviewed publications. These publications are reproduced at the end of the thesis file in their published form, but they are not treated here as separate and disconnected research outputs. Instead, Chapter 3 explains how they form one coherent research direction centred on architecture-engineered semiconductor nanocomposites for photocatalytic and photoelectrochemical applications.

The purpose of this chapter is therefore not to repeat the full experimental details already available in the published papers. Its role is to show how the individual studies are connected, how they address the main objective of the dissertation, and how they contribute to the broader interpretation developed in Chapters 1 and 2. Particular attention is given to the relationship between material architecture, interface quality, light utilisation, charge separation, transport limitations, and operational stability.

The publications deal with four different systems: laser-structured Si/MXene/TiO_2 surfaces, electrospun PID/TiO_2/WO_3/MXene membranes, $ZnFe_2O_4$/ZnO core-shell nanofibres, and structured Ti-TiO_2 photoanodes. They are not connected by one identical composition. They are connected by the way the active material is arranged and joined with its support or neighbouring phase. In each case, the question is whether this arrangement helps the semiconductor use light more effectively, separate and move charges, and interact with the reaction environment under irradiation.

In this dissertation, the published papers contain the full experimental details and results. The thesis text is used to connect those papers and explain their place in the overall study. For this reason, the following sections do not summarise each article step by step. They show how each publication contributes to the common research direction.

3.1. Integrated research objective and research logic

The integrated objective of the dissertation was to determine how architecture-controlled design can improve the photocatalytic and photoelectrochemical behaviour of TiO_2-based and related semiconductor nanocomposites. The central assumption was that the performance of such systems is not determined by chemical composition alone. Instead, it depends on how the active material is organised, how interfaces are formed, how light enters and interacts with the structure, and how photogenerated charge carriers are transported and used at reactive boundaries.

This connection can be seen already in the Si/MXene/TiO_2 study. There, the laser-structured silicon was not used only as a substrate, but as the element that defined the surface geometry and light interaction. MXene and ALD-grown TiO_2 were then added to give the structured surface its conductive and photocatalytic functions. In the PID/TiO_2/WO_3/MXene study, the electrospun membrane was important not only as a support, but as the working photocatalyst form, where wetting, transport through the fibre mat, exposure of active regions, and contact between components all affected the response. The $ZnFe_2O_4$/ZnO nanofibre publication showed the same idea in a PEC oxide heterostructure, where the core-shell arrangement and annealing-driven interdiffusion influenced the visible-light behaviour. Finally, the Ti-TiO_2 membrane study combined laser-shaped titanium with ALD TiO_2 to obtain a binder-free hierarchical photoelectrode, in which the texture, oxide thickness, coating continuity, and charge-transfer behaviour had to be considered together.

The publications therefore represent different experimental answers to the same broader problem. Each study examines a different way of organising semiconductor materials so that light absorption, charge separation, charge transport, and interfacial reaction pathways become more favourable. The material formats are different, but the underlying principle is the same: architecture is treated as a functional design parameter rather than as a secondary morphological feature.

This approach also creates a link between photocatalysis and photoelectrochemistry. In photocatalytic dye degradation, the useful response is followed mainly through the removal of an organic model pollutant from solution. In PEC water splitting, the response is followed through photocurrent, impedance behaviour, photoconversion efficiency, and wavelength-dependent charge extraction. These two testing formats are different, but they are governed by related physical processes. In both cases, the material must absorb light, generate charge carriers, limit recombination, transport charges to the interface, and support interfacial redox reactions.

For this reason, the dissertation does not treat photocatalysis and PEC as isolated research areas. Instead, they are used as complementary ways of examining how architecture and interfaces affect photoinduced processes. Photocatalytic experiments show how structured and immobilised materials behave in contact with polluted water under irradiation. PEC measurements provide more direct insight into charge extraction, interfacial resistance, and electrode behaviour under applied bias. Taken together, these approaches provide a broader basis for interpreting the role of architecture in semiconductor nanocomposites.

The dissertation follows one main line of work. The materials are first given a defined form, whether by laser structuring, electrospinning, ALD growth, or heterostructure formation. After that, their structure, composition, optical behaviour, and electrochemical properties are examined in relation to the intended function. Photocatalytic and PEC tests

are then used not only to compare activity, but also to understand how the chosen material form affects charge generation, transport, interface contact, and final utilisation.

This approach is important because a higher degradation efficiency or photocurrent density is treated as a starting point, not as a complete explanation. The functional result is read together with the structure of the sample, the quality of the interface, and the conditions under which the material works. Adsorption, wetting, light scattering, surface access, coating thickness, and stability may all influence the measured response. In this way, the publication set supports a careful interpretation of semiconductor photoactivity, where performance trends are connected with the real working architecture of each system.

3.2. Relationship to open problems and methodological positioning

The publication set responds to several problems that appear repeatedly in photocatalytic and PEC materials research. Optical changes are not always easy to separate from real electronic improvement. Dye-degradation results can be affected by adsorption, wetting, and transport. Hybrid interfaces may also change during operation, especially when chemically dynamic components are used. At the same time, improved performance is often explained too quickly by composition alone. The studies included in this dissertation address these issues by focusing on how the material is built, how the interfaces are formed, and how these factors influence the final photoactive response.

Optical enhancement is treated carefully in the two laser-structured studies. A stronger optical response does not automatically mean that the semiconductor band structure has changed. In textured systems, part of the effect can come simply from the way the surface redirects and traps incoming light. This is the case for both the Si/MXene/TiO_2 and Ti-TiO_2 systems, where laser processing created organised surface features before the active components were introduced. The improved response is therefore discussed first in relation to surface architecture and light management. The TiO_2 layer, and MXene in the silicon-based system, are then considered through their interfacial role rather than as evidence that the optical change comes only from intrinsic electronic modification.

A second issue is the role of adsorption and mass transport in photocatalytic dye degradation. In immobilised systems, especially membranes and fibrous materials, a decrease in dye concentration may be affected not only by photocatalytic conversion, but also by adsorption, wetting, diffusion into the structure, and accessibility of active sites. This is particularly relevant for the PID/TiO_2/WO_3/MXene membrane system, where the fibrous architecture improves practical handling and reusability, but also introduces transport-related factors that must be considered when interpreting the degradation results. For this reason, the photocatalytic response is treated as the behaviour of a complete membrane architecture rather than as a simple property of the oxide additives alone.

A third problem concerns the interface itself. In many hybrid systems it is tempting to explain the result by band alignment, but band alignment only describes the possible direction of charge transfer. It does not show whether the two phases are actually joined well enough for that transfer to occur. The contact may be incomplete, defect-rich, chemically unstable, or different from one region of the material to another. This point is addressed in the dissertation through several examples. In the Si/MXene/TiO_2 system, ALD is used to form TiO_2 on a structured hybrid surface. In the $ZnFe_2O_4$/ZnO fibres, the interface forms during annealing as Fe and Zn species intermix. In the Ti-TiO_2 membrane photoelectrode, the contact between the laser-shaped Ti support and the ALD TiO_2 layer is treated as a key part of the PEC response, not only as a boundary between two materials.

The fourth issue is the durability of the functional architecture. A material that performs well only in the first test may still have limited practical relevance. Therefore, the included publications consider stability and repeated operation where possible. In the electrospun PID/TiO_2/WO_3/MXene membrane study, reuse tests show how activity changes during repeated dye degradation cycles. In the Ti-TiO_2 membrane study, post-operation structural analysis is used to assess whether the hierarchical electrode remains stable after PEC testing. These examples support the broader view that stability must be discussed together with architecture, because surface blockage, oxidation, coating integrity, and interface changes may all affect long-term performance.

The dissertation does not take one measurement as enough to explain the material response. Dye degradation is considered together with optical and spectroscopic results, and PEC data are read together with impedance, Mott-Schottky analysis, IPCE, ABPE, and structural characterisation. This is important because each measurement can be misleading when used alone. A higher photocurrent may result from better charge extraction, but also from larger area or improved contact. Faster dye removal may involve photocatalysis, but also adsorption or transport. Lower PL intensity or stronger absorbance may support better charge behaviour, but they do not prove the full mechanism by themselves. For this reason, the discussion is based on how different measurements point in the same direction, rather than on a single performance indicator.

The four publications are not used to show the same effect four times. They show how different material formats change the conditions under which a semiconductor works. In one case, the important issue may be liquid access to a membrane. In another, it may be coating continuity, contact with the support, or charge extraction through an electrode. Each study is therefore read according to its own experimental form. The connection between them is simpler: in every case, the active phase has to be placed and connected in a way that allows photogenerated charges to be used before they recombine.

In this sense, the methodological contribution of the dissertation is not limited to the fabrication of new materials. It also lies in the way the results are read. The same general

principle is applied across the publications: performance enhancement should be connected to structural, optical, chemical, and interfacial evidence, and possible alternative explanations should be acknowledged where the data do not allow one mechanism to be isolated completely.

3.3. Publication map and contribution to the integrated framework

The dissertation is based on four peer-reviewed publications that together form the experimental foundation of the work. The full papers are reproduced at the end of the thesis file in the publication section, where each article is preceded by an individual contextual introduction. In the present chapter, they are discussed only as parts of one integrated research framework.

The order of the publications in the dissertation follows the scientific logic of the work rather than only the chronological order of publication. The sequence moves from structured photocatalytic surfaces, through immobilised fibrous photocatalytic membranes, towards heterostructured and hierarchical photoelectrochemical systems. This arrangement helps to show that the dissertation is not a collection of separate studies, but a connected research path built around architecture-controlled photoactivity.

Publication 1 deals with a silicon surface that was first organised by laser treatment and then modified with MXene and ALD TiO_2. This study is used in the dissertation to show how a flat semiconductor support can be turned into a more functional photocatalytic surface. The nanoripples mainly change the surface geometry and optical response. The TiO_2 layer gives the surface an oxide coating suitable for photocatalysis, while MXene introduces an additional conductive contact between the structured support and the oxide phase. The dye-degradation improvement is therefore read as the result of this combined surface construction, rather than as a simple consequence of adding one extra component.

Publication 2 shifts the discussion to an immobilised membrane system. In this study, electrospun polyimide fibres were modified with TiO_2, WO_3, and $Ti_3C_2T_x$ MXene for photocatalytic water purification. The membrane gives the photocatalyst a recoverable form, while the oxide nanowires provide the photoactive domains and MXene adds a conductive component at the hybrid interface. The study is important because the result cannot be explained only by the presence of these components. In a fibrous membrane, dye degradation also depends on how the liquid wets the mat, how easily dye reaches the active regions, how the components are distributed inside the fibres, and whether the membrane can be reused.

Publication 3 deals with $ZnFe_2O_4$/ZnO core-shell nanofibres prepared by co-axial electrospinning and thermal treatment. This work is included as a heterostructured oxide system with visible-light photoelectrochemical response. Its importance lies in the use of fibrous core-shell architecture to bring together two oxide phases with different optical and

electronic roles. The final structure is also affected by Fe/Zn interdiffusion during annealing, which means that the photoelectrochemical behaviour cannot be explained only by the idealised starting core-shell design. This publication contributes to the dissertation by extending the discussion beyond TiO_2-based systems and by showing how fibrous geometry, oxide heterostructure formation, and phase interaction influence PEC response.

Publication 4 is the final study because it brings the work back to TiO_2 in a PEC electrode format. The system is based on titanium membranes shaped by femtosecond laser ablation and then coated with TiO_2 by ALD. The laser step gives the Ti support a hierarchical surface and improves light interaction, while ALD makes it possible to add TiO_2 with controlled thickness. This allowed thinner and thicker oxide layers to be compared on the same type of scaffold, so the effect of coating thickness, crystallinity, and Ti/TiO_2 contact could be discussed more clearly. The study shows how a metallic support and a controlled oxide layer can be combined into a binder-free photoelectrode for water-splitting measurements.

Taken together, the publications cover four different ways of building a photoactive material: a laser-structured Si surface modified with TiO_2 and MXene, a fibrous polymer/oxide/MXene membrane for dye degradation, a $ZnFe_2O_4$/ZnO core-shell fibre system for visible-light PEC response, and a laser-shaped Ti membrane coated with ALD TiO_2 for water splitting. The systems are different, but they all test the same point. A semiconductor does not work only because of its composition. Its response also depends on where the active phase is placed, how it contacts conductive or supporting components, how the surface is exposed to light and liquid, and how the interfaces are formed inside the final architecture.

Although each publication uses a different system, all four are connected by the same scientific question. They ask how the organisation of the material influences the use of light and the fate of photogenerated charge carriers. In some cases, the architectural contribution is mainly optical, as in light trapping by laser-structured surfaces. In other cases, it is related mainly to interface quality, coating continuity, or heterostructure formation. In the fibrous systems, the architecture also controls practical aspects such as wetting, accessibility, mass transport, and recoverability.

The publication map leads to the main point of the thesis. In photocatalytic and PEC nanocomposites, composition explains only part of the response. The same phase can behave differently when it is placed in another geometry, connected to another component, or tested in another format. For this reason, the results are discussed through the whole working system: the active phase, conductive elements, support structure, interface contact, and operating conditions.

This section also clarifies the role of the individual introductions placed before each full paper in the final publication section. Those introductions provide the detailed paper-by-

paper context, including motivation, working hypothesis, architecture concept, main results, interpretation, limitations, and author contribution. The present chapter provides the broader map, while the final publication section preserves the full published record and explains the place of each paper within the dissertation.

3.4. Integration of the publications into one research narrative

Although The publications included in this dissertation are connected by a common research narrative based on architecture-controlled photoactivity. Each paper investigates a different material system, but all of them address the same broader problem: how the useful response of a semiconductor material can be improved by controlling not only its composition, but also its geometry, interface quality, and operating format.

The first publication introduces the idea that surface architecture can directly influence photocatalytic behaviour. In the SiNR/MXene/TiO_2 system, the laser-induced nanoripple structure provides an organised substrate that improves light interaction through surface structuring and light trapping. The ALD-grown TiO_2 layer gives the system a chemically stable oxide interface, while MXene contributes to interfacial charge transfer. The importance of this study within the dissertation is that it shows how photocatalytic enhancement can arise from the combination of optical, chemical, and electronic effects within one structured surface.

The second publication is based on electrospun PID membranes containing TiO_2, WO_3, and MXene. This is a different type of photocatalyst, because the active phases are fixed inside a fibrous mat instead of being used as a powder or a flat coating. The membrane can be removed from solution and reused, but its structure also affects the test itself. Liquid has to wet the fibres, dye has to reach the active regions, and light has to pass through the mat. For this reason, the photocatalytic response is read as the behaviour of the whole membrane system, not only as the effect of TiO_2, WO_3, or MXene separately.

The third publication introduces $ZnFe_2O_4$/ZnO core-shell nanofibres as a PEC system. It is included not because it repeats the TiO_2 work, but because it shows the same problem in another oxide material. The fibre has to keep two phases in contact, and this contact is partly formed during annealing, when Fe and Zn species interdiffuse. As a result, the final PEC behaviour depends on more than the presence of ZnO and $ZnFe_2O_4$. It depends on the fibre shape, the core-shell arrangement, and the interface produced during heat treatment. This study therefore connects the fibrous-material part of the dissertation with the PEC discussion.

The fourth publication concerns the Ti-TiO_2 membrane photoelectrode. Unlike the earlier systems, this work starts from a metallic titanium membrane that already serves as the current collector. Femtosecond laser ablation is used to give this membrane a hierarchical surface, and ALD is then used to cover it with TiO_2 of controlled thickness. The result is a

binder-free PEC platform in which the support, the photoactive oxide, and the charge-collection pathway are part of the same structure. For this reason, the study is placed at the end of the publication sequence.

The publications are arranged to show the main forms in which the photoactive materials were studied. The first work concerns a modified silicon surface, where laser structuring, TiO_2 deposition, and MXene addition are combined. The second work changes the format to an electrospun membrane, so the photocatalyst is considered as a recoverable fibrous material rather than a loose or flat system. The third and fourth works move to PEC electrodes, first through $ZnFe_2O_4$/ZnO core-shell fibres and then through Ti-TiO_2 membranes prepared from structured titanium. Although the systems differ, they are connected by the same practical issue: the active phase has to be placed in a form that allows contact with light, the reaction medium, and, where relevant, the current collector.

The publications show that improved performance is usually not caused by one feature alone. Laser structuring changes the surface in several ways at once: it can reduce reflection, increase surface development, and modify contact with the liquid or electrolyte. ALD also has more than one role, because the TiO_2 layer has to be continuous, sufficiently thin or thick for the intended function, properly crystallised, and well connected to the support. MXene is similar in this respect. It may support charge transfer, but only if it is well distributed, in contact with the oxide, and stable during operation. Electrospun membranes add still another set of effects, since the fibre network helps with recovery and reuse but also controls wetting, diffusion, and access to active regions. For this reason, the results are interpreted as the behaviour of complete material systems, rather than as the effect of a single component or property.

This integrated reading allows the dissertation to move beyond a simple comparison of activity values. The main conclusion from the publication set is not only that one sample performs better than another, but that the final behaviour of semiconductor nanocomposites depends on the full architecture in which the active phase operates. Light absorption, charge separation, interfacial transfer, surface accessibility, and stability are not independent variables. They are coupled through the way the material is built.

For this reason, the publications are treated in the dissertation as complementary evidence for one central argument. Architecture is not only a descriptive feature of the material. It is a functional design parameter that determines how efficiently photogenerated charge carriers are produced, separated, transported, and used in photocatalytic or photoelectrochemical processes.

3.5. Author contribution and role in the included publications

The publications included in this dissertation were prepared as collaborative research works, but the author’s contribution to them was direct and substantial. Across the

publication set, the author participated in the development of the research concept, experimental work, material preparation, functional testing, data interpretation, visualisation, and manuscript preparation. The author's role was therefore not limited to technical assistance, but was connected with the central experimental and interpretive tasks that form the basis of the dissertation.

In the study on highly regular laser-induced silicon nanoripples modified with MXene and ALD-grown TiO_2, the author contributed to the investigation of the structured photocatalytic system and to the interpretation of its functional behaviour. This work was important for establishing the role of laser-induced surface architecture, TiO_2 coating, and MXene-assisted interfacial charge transfer in photocatalytic dye degradation. Within the dissertation, the author's contribution to this publication is connected with the development and analysis of the structured photocatalytic platform and with the preparation of the research output included in the thesis.

In the publication on electrospun polyimide nanofibres modified with TiO_2, WO_3, and $Ti_3C_2T_x$ MXene, the author contributed to fabrication, investigation, methodology, data curation, and preparation of the original draft. This contribution is especially relevant to the dissertation because the study represents the immobilised membrane-type photocatalyst within the publication set. The author's work was connected with the preparation and analysis of the hybrid fibrous architecture, evaluation of its photocatalytic behaviour, and interpretation of the relationship between membrane structure, oxide/MXene modification, and dye degradation performance.

In the study on $ZnFe_2O_4$/ZnO core-shell nanofibres, the author's contribution was connected with the fabrication of the core-shell structures, photoelectrochemical characterisation, data analysis, and preparation of the draft manuscript. This work is important in the dissertation because it extends the architecture-driven approach to a related metal-oxide heterostructure with visible-light PEC response. The author's role therefore covered both the experimental development of the fibrous oxide system and the interpretation of its photoelectrochemical behaviour.

In the publication on hierarchically structured Ti-TiO_2 membranes fabricated by femtosecond laser ablation and ALD, the author contributed to investigation, formal analysis, visualisation, and preparation of both the original and revised manuscript. This study is one of the central elements of the dissertation because it combines laser-generated hierarchical architecture with controlled TiO_2 deposition for PEC water splitting. The author's contribution was therefore directly connected with the preparation, analysis, and interpretation of the binder-free Ti-TiO_2 membrane photoanode.

Taken together, these contribution statements show that the author was actively involved in the main scientific tasks required for the dissertation. These tasks included the fabrication and modification of semiconductor architectures, photocatalytic and

photoelectrochemical testing, interpretation of structural and functional results, and preparation of the published manuscripts. The author's work therefore covered the essential stages of the research process, from material design and experimental realisation to the scientific explanation of the observed behaviour.

The collaborative character of the publications is also important to acknowledge. Several experimental and analytical tasks were carried out together with co-authors who provided expertise in laser processing, electrospinning, electron microscopy, surface analysis, photoelectrochemical testing, and materials characterisation. However, the author's contribution remained central to the research direction presented in the dissertation, especially in relation to architecture-engineered photocatalytic and photoelectrochemical systems.

Within the dissertation, the author's contribution covered the main stages of the included studies: experimental design, material fabrication, characterisation, functional testing, data analysis, and manuscript preparation. A further part of this work was to place the individual results within the broader interpretation used in the thesis, where the role of architecture, interface quality, and charge utilisation is considered across the different material systems.

3.6. How the publication section is organised and introduced

The full publications are reproduced at the end of the dissertation in a separate publication section. This arrangement was chosen in order to keep the main thesis text focused on synthesis and interpretation, while still preserving the complete published record on which the dissertation is based. The publications therefore function as the documented experimental foundation of the thesis, whereas the preceding chapters explain the scientific background, research logic, and integrated meaning of the results.

Each reproduced paper is introduced by a short contextual note. These notes are not meant to summarise the full article or repeat the experimental section. They are included to guide the reader through the publication part of the dissertation: why the paper is placed there, which architectural idea it represents, and how its results contribute to the common aim of the thesis.

Each contextual introduction follows the same general structure. First, the scientific problem and motivation of the publication are briefly introduced. Second, the research objective and working hypothesis are stated. Third, the material architecture is described in relation to the design concept of the dissertation. Fourth, the main results are summarised with emphasis on those findings that are most relevant to the thesis framework. Fifth, the results are interpreted in terms of architecture, interface quality, light utilisation, charge transfer, transport effects, and stability. Finally, the main limitations or open questions are identified, together with the author's contribution to the work.

This structure was used to make the publication section more coherent. Without these introductions, the reproduced papers would remain formally connected to the dissertation, but the reader would have to reconstruct their relationship to the main thesis objective independently. The contextual notes therefore act as a bridge between the integrated discussion in the main text and the full published papers placed at the end of the thesis file.

The introductions also help avoid unnecessary repetition. Detailed experimental procedures, complete characterisation results, figure-by-figure discussion, and full reference lists remain in the published articles themselves. The introductory notes focus only on the role of each publication within the dissertation. In this way, the publication section becomes more than an archive of papers, but it does not interrupt the main flow of the thesis with repeated article-level details.

The publications are placed in an order that follows the change in material format. The section begins with a laser-structured Si/MXene/TiO_2 photocatalytic surface. It then moves to electrospun PID/TiO_2/WO_3/MXene membranes, where the photocatalyst is used in an immobilised fibrous form. The next publication presents $ZnFe_2O_4$/ZnO core-shell nanofibres as a related oxide system for PEC studies. The section ends with Ti-TiO_2 membrane photoanodes, where laser-structured titanium and ALD-grown TiO_2 are combined for PEC water splitting.

With this organisation, the thesis text and the publication section have different roles. The main chapters explain the background, the research idea, and the connection between the studied systems. The publication section gives the full peer-reviewed papers on which the experimental part is based. In this way, the dissertation can be read as a single connected work, while the original publications remain included in full at the end.

3.7. Transition to the publication chapters

The preceding sections have shown how the included publications are connected within one research framework. Although the papers differ in material system, fabrication route, and testing method, they all address the same central issue: how architecture and interface quality influence the behaviour of semiconductor nanocomposites under photocatalytic or photoelectrochemical conditions.

The publication section is organised around four experimental systems. The first is a laser-structured Si/MXene/TiO_2 surface used for photocatalytic degradation. The second is an electrospun PID/TiO_2/WO_3/MXene membrane, where the photocatalyst is fixed in a recoverable fibrous form. The third is a $ZnFe_2O_4$/ZnO core-shell nanofibre system examined under visible-light PEC conditions. The fourth is a Ti-TiO_2 membrane photoelectrode prepared by femtosecond laser ablation of titanium followed by ALD growth of TiO_2.

The sequence shows how the work changes from one material form to another. It begins with a structured surface for photocatalysis, continues with a recoverable electrospun

membrane, and then moves to PEC electrodes. These systems are different, but they are read in the same way: the active phase has to be placed where light can reach it, where charges can move away from it, and where the solution or electrolyte can contact it. This is the link between the publications.

The full published papers are presented in the final publication section of the thesis. Each paper is preceded by an individual contextual introduction prepared by the author. These introductions explain the motivation of the study, the architectural concept being tested, the main results relevant to the dissertation, the interpretation of the findings within the common framework, and the limitations or open questions that remain.

The publication section should therefore be read as the experimental basis of the dissertation. The papers contain the peer-reviewed research results, while the short introductions explain how each study connects with the argument developed in the previous chapters. Taken together, they support the main conclusion of the thesis: semiconductor nanocomposites cannot be understood through composition alone. Their performance depends on how composition, geometry, interfaces, light use, transport, and stability come together in the working material.

Chapter 4. Introductions to the publications included in the dissertation

The following chapter introduces the peer-reviewed publications on which the dissertation is based. These introductions are included in the main body of the thesis because their purpose is interpretive rather than documentary. They explain how each publication fits into the overall research framework, what scientific problem it addresses, which architectural concept is tested, and how the main findings contribute to the thesis objective.

The published articles are not inserted in full at this point of the dissertation. They are collected at the end of the thesis in their original published form, together with the author contribution statements and the relevant publication documents. This keeps the main body of the dissertation reserved for the connecting discussion: how the studies relate to each other, how the results are interpreted, and how they support the overall scientific argument. The full papers then serve as the documented peer-reviewed basis for the experimental work.

Each publication introduction follows the same general structure. First, the scientific context and motivation of the study are presented. Second, the research objective and working hypothesis are stated. Third, the material architecture is described in relation to the design strategy of the dissertation. Fourth, the most important results are summarised, with emphasis on their relevance to the thesis framework. Fifth, the findings are interpreted in terms of architecture, interface quality, light utilisation, charge transfer, transport effects, and stability. Finally, the main limitations and open questions are identified.

The introductions are ordered by the function of the systems rather than by publication date. The chapter first presents the photocatalytic part of the work, beginning with the Si/MXene/TiO_2 structured surface and then moving to the PID/TiO_2/WO_3/MXene electrospun membrane. It then turns to the photoelectrochemical part, represented by $ZnFe_2O_4$/ZnO core-shell nanofibres and the Ti–TiO_2 membrane photoelectrode. This order helps the reader follow the change from pollutant degradation systems to water-splitting photoelectrodes, while keeping the common focus on architecture, interfaces, and charge utilisation.

These introductions should therefore be read as part of the scientific argument of the thesis. They connect the individual papers with the broader dissertation framework before the complete published articles are presented at the end of the thesis. In this way, the reader first receives the author’s integrated interpretation of the publication set and then the formal publication record on which the dissertation is based.

4.1. Highly regular laser-induced periodic silicon surface modified by MXene and ALD TiO_2 for organic pollutants degradation

Reference:

A. Lys, I. Gnilitskyi, E. Coy, M. Jancelewicz, O. Gogotsi, I. Iatsunskyi, *Highly regular laser-induced periodic silicon surface modified by MXene and ALD TiO_2 for organic pollutants degradation*, Applied Surface Science 640 (2023) 158336.
DOI: 10.1016/j.apsusc.2023.158336
Journal impact factor: 6.9
Ministerial points: 140

4.1.1 Context and motivation

The removal of dye pollutants from water is not only a question of decolourisation, but of changing the organic molecules that remain in the solution. This makes semiconductor photocatalysis a useful approach, because irradiation can create reactive charge carriers at the solid-liquid interface and drive surface redox reactions. TiO_2 is a suitable reference material for such work because it is stable in water, relatively low in toxicity, and has a well-known photocatalytic response. At the same time, its use as a single-phase photocatalyst is limited. Most of its excitation occurs under ultraviolet light, and many of the generated carriers are lost through recombination before they can take part in surface reactions.

One way to improve the behaviour of TiO_2-based photocatalysts is to combine the active oxide with a structured support that can improve light interaction and provide a more favourable architecture for charge separation. Silicon is attractive in this respect because it is abundant, well understood, and can be structured with high precision. At the same time, bare silicon is not sufficiently stable under photocatalytic and aqueous conditions, which means that surface protection and interface control are required.

Laser-induced periodic surface structures provide a useful route for producing regular surface architectures without relying on complex lithographic processing. In this publication, highly regular silicon nanoripples were used as a structured platform. Their role was not only to support the active material, but also to improve light interaction through scattering and light trapping. The system was further modified with $Ti_3C_2T_x$ MXene and ALD-grown TiO_2 in order to combine optical, conductive, and chemical functions within one hybrid photocatalytic architecture.

This publication starts the dissertation from a modified silicon surface. The laser treatment gives the substrate a regular nanoripple morphology. TiO_2 is deposited by ALD to create the photocatalytic oxide layer, and MXene is added as a conductive phase at the interface. The study is used to show that the dye-degradation response depends on how these parts are arranged on the surface, not only on the presence of TiO_2 or MXene.

4.1.2 Research objective and working hypothesis

The objective of the study was to fabricate SiNR/MXene/TiO_2 photocatalytic surfaces and evaluate their activity in rhodamine 6G degradation. The main comparison was made between SiNR/TiO_2 and SiNR/MXene/TiO_2 samples, in order to determine whether $Ti_3C_2T_x$ MXene provides an additional improvement within the same laser-structured silicon/TiO_2 platform.

The working hypothesis was that the SiNR/MXene/TiO_2 surface would improve rhodamine 6G degradation because MXene would change the way the structured silicon support and the TiO_2 coating communicate electronically. The silicon nanoripples were used to increase the interaction of light with the surface, and the ALD-grown TiO_2 layer provided the photocatalytic oxide phase. The role of $Ti_3C_2T_x$ was to create a more conductive contact at the SiNR/TiO_2 interface, so that photogenerated charges could be transferred more efficiently instead of recombining. The expected improvement was therefore connected with the interface created between SiNR, MXene, and TiO_2.

4.1.3 Materials and architecture concept

The study was carried out on laser-formed silicon nanoripples rather than on flat silicon. This surface gave the material a regular texture for light interaction and served as the base for the hybrid photocatalytic layer. $Ti_3C_2T_x$ MXene was introduced onto the rippled silicon before TiO_2 was deposited by ALD. The obtained SiNR/MXene/TiO_2 surface was then tested in rhodamine 6G degradation.

ALD was chosen so that TiO_2 could be added without losing the nanoripple texture already formed on silicon and modified with MXene. The coating had to remain thin and continuous enough to follow this surface, because the structure itself was part of the photocatalytic design. In the final SiNR/MXene/TiO_2 system, the optical effect of the rippled silicon, the conductive contact introduced by MXene, and the stable oxide surface provided by TiO_2 were therefore considered together rather than separately.

The material was therefore not designed as a simple mixture of components. It was designed as a layered and structured photocatalytic surface in which geometry, conductivity, and surface chemistry were combined. This makes the publication directly relevant to the architecture-driven approach of the dissertation.

4.1.4 Key results and main contribution

The SiNR/MXene/TiO_2 surface showed a much stronger photocatalytic response than the SiNR/TiO_2 reference. In the publication, the degradation efficiency of the ternary system was about 2.6 times higher. This increase was not assigned only to the presence of MXene. It was discussed in relation to the whole structured interface, including stronger

light interaction, improved charge separation, and the conductive role of MXene between the silicon nanoripples and the TiO_2 coating.

The optical results showed that the ternary architecture absorbed light over a broad spectral range. This behaviour was linked to the laser-patterned silicon surface, which contributed to light trapping and lower effective reflectance losses. At the same time, the MXene-containing system showed features consistent with improved charge-carrier separation and reduced recombination.

The main contribution of the publication lies in demonstrating that a highly regular laser-induced silicon surface can be converted into a more effective photocatalytic platform through MXene modification and ALD TiO_2 coating. In the context of the dissertation, this work provides the first example of how surface architecture, conformal oxide deposition, and conductive two-dimensional materials can be combined to improve photocatalytic dye degradation.

4.1.5 Interpretation within the research framework

The results of this publication are interpreted in the dissertation as an example of architecture-controlled photocatalytic enhancement. The improved behaviour of the SiNR/MXene/TiO_2 system should not be assigned only to the presence of TiO_2 or only to MXene. Instead, it results from the way the three components are organised within one structured system.

The silicon nanoripples changed the optical conditions at the surface by increasing interaction with incident light. The TiO_2 coating supplied the photocatalytic oxide interface and also helped stabilise the silicon-based structure. MXene was included as a conductive phase that could assist charge transfer across the interface and limit recombination. The improved response was therefore interpreted as the result of these elements working in one surface architecture, rather than as the effect of a single component.

At the same time, the result should be interpreted with caution. Dye degradation experiments may be affected by adsorption, dye sensitisation, surface wetting, and light distribution. Therefore, the increased degradation efficiency is best understood as the response of the full SiNR/MXene/TiO_2 architecture under the applied experimental conditions, rather than as a simple intrinsic property of one component.

4.1.6 Limitations and open questions

This result should be kept within the scope of the test that was performed. The MXene-containing surface showed better removal of R6G than the SiNR/TiO_2 reference, which confirms the benefit of the hybrid architecture for this model photocatalytic reaction. At the same time, the experiment does not allow the full reaction pathway to be separated into adsorption, sensitisation, and radical oxidation contributions. For that reason, the result

is used here as evidence of improved dye-degradation performance, while more detailed pathway assignment would require additional control experiments.

Second, the state of MXene after use remains an open question. $Ti_3C_2T_x$ may change in water under illumination, especially in an oxidative photocatalytic environment. Such changes could alter the MXene/TiO_2 contact and reduce, or modify, its conductive role in the hybrid surface. Longer cycling tests, together with post-reaction analysis of the SiNR/MXene/TiO_2 surface, would be needed to check whether the interface remains stable during operation.

Third, this study shows the benefit of the SiNR/MXene/TiO_2 surface, but it does not allow each contribution to be separated completely. The nanoripple geometry, TiO_2 layer, and MXene-containing interface were changed as one surface system, so the higher activity should be treated as the response of this combined architecture. A clearer separation would need additional series in which only one parameter is changed at a time, such as MXene amount, TiO_2 thickness, or ripple geometry.

Overall, this publication establishes the first step in the dissertation's research narrative. It shows that laser-structured surfaces can be used not only as supports, but as active architectural elements that influence light utilisation and photocatalytic behaviour.

4.1.7 Author contribution and role in the publication

The author contributed to the investigation, analysis, visualisation, and preparation of the manuscript. Within the context of the dissertation, the author's role was connected with the evaluation and interpretation of the structured SiNR/MXene/TiO_2 photocatalytic system, including the relationship between surface architecture, TiO_2 coating, MXene modification, and photocatalytic degradation behaviour. The author was also involved in presenting the results in the form of a peer-reviewed publication and in connecting the findings with the broader architecture-driven research framework developed in this thesis.

4.2. Electrospun Polyimide Nanofibers Modified with Metal Oxide Nanowires and MXene for Photocatalytic Water Purification

Reference:

A. Lys, V. Myndrul, M. Pavlenko, B. Anastaziak, P. Holec, K. Vodseďálková, E. Coy, M. Bechelany, I. Iatsunskyi, *Electrospun Polyimide Nanofibers Modified with Metal Oxide Nanowires and MXene for Photocatalytic Water Purification*, Nanomaterials 15 (2025) 1371.
DOI: 10.3390/nano15171371
Journal impact factor: 4.3
Ministerial points: 100

4.2.1 Context and motivation

Photocatalytic water purification is commonly studied using powder photocatalysts, because powders usually provide high surface area and good contact with the pollutant solution. However, this format also creates practical problems. After the process, the catalyst has to be separated from treated water, and repeated use may become difficult. Immobilised photocatalysts offer a possible solution to this problem because they can be recovered more easily and used in repeated cycles.

At the same time, immobilisation changes the way a photocatalyst works. In a membrane or film, the active material is no longer fully dispersed in the solution. Therefore, the observed photocatalytic response may depend not only on the chemical composition of the active phases, but also on wetting, diffusion of the dye solution, access to active sites, light penetration, and the distribution of the photoactive components inside the structure.

Electrospun nanofibrous membranes are useful in this context because they combine high surface area with a self-supporting and recoverable form. Their open fibrous network can provide access for the liquid phase while allowing the material to be handled as a membrane rather than as a powder. For this reason, electrospun membranes are attractive for photocatalytic water purification, especially when the active components can be incorporated into the fibre network in a controlled way.

This publication examines a hybrid membrane based on electrospun polyimide nanofibres modified with TiO_2, WO_3, and $Ti_3C_2T_x$ MXene. Within the dissertation, the study is important because it shifts the discussion from structured rigid surfaces to flexible immobilised photocatalytic membranes. It shows that the membrane itself should be treated as a functional architecture, not only as a passive support for the oxide particles.

4.2.2 Research objective and working hypothesis

The objective of the study was to prepare polyimide electrospun membranes containing TiO_2, WO_3 nanowires, and $Ti_3C_2T_x$ MXene, and to evaluate them in photocatalytic degradation of rhodamine 6G under simulated solar irradiation. The study focused on this material as a hybrid fibrous membrane, where the active components are immobilised in one recoverable photocatalytic structure rather than used as a dispersed powder.

The working hypothesis was that the membrane would benefit from bringing the oxide phases and MXene into one fibrous structure. TiO_2 and WO_3 were used as the photoactive oxide components responsible for light-induced charge generation and surface oxidation reactions. MXene was introduced as a conductive two-dimensional phase that could improve contact between components and support charge transfer within the hybrid membrane. The expected improvement was therefore connected not only with the

composition of the membrane, but also with how the oxide and MXene phases were distributed and exposed inside the electrospun fibre network.

The polyimide scaffold was expected to provide a stable membrane format that could be handled and reused more easily than powder photocatalysts. Therefore, the expected improvement was not connected only with the presence of TiO_2, WO_3, or MXene separately, but with their organisation inside a fibrous immobilised architecture.

4.2.3 Materials and architecture concept

The study was based on a polyimide membrane produced by electrospinning. The membrane was used to keep the photocatalytic material in a fixed fibrous form instead of a powder suspension. TiO_2 and WO_3 nanowires formed the oxide fraction of the composite, while $Ti_3C_2T_x$ MXene was added as the conductive component. In this system, the fibre mat was part of the photocatalyst itself, because it affected how the active phases were distributed, connected, and exposed to the dye solution.

The architecture can be understood as a hybrid fibrous network in which several functional elements operate together. The polyimide fibres provide the recoverable membrane form. The oxide nanowires introduce photoactive regions where light-induced charge carriers can be generated and used for photocatalytic reactions. MXene provides electronic communication between the components and may help reduce recombination losses.

This design is directly connected with the main thesis framework because it combines material composition with immobilised architecture. The photocatalyst is not simply a mixture of oxide and MXene particles. It is a structured membrane in which fibre morphology, additive distribution, wetting, light access, and interfacial contact influence the final behaviour.

4.2.4 Key results and main contribution

The results showed that PID-based nanofibrous hybrids can work as immobilised photocatalysts under simulated solar light. Among the tested samples, the membrane containing TiO_2, WO_3, and $Ti_3C_2T_x$ MXene gave the best response, removing about 74% of rhodamine 6G after 90 min of irradiation. This result indicates that the combined oxide/MXene composition was more effective when fixed within the electrospun fibre network.

The higher activity was connected with changes in optical and charge-carrier behaviour. The MXene-containing membranes absorbed light over a broader range and showed weaker photoluminescence emission. This was taken to indicate lower recombination and more effective charge separation in the hybrid fibre system, most likely due to better interfacial charge transfer between the oxide phases and MXene.

The publication also tested the membrane over repeated photocatalytic cycles. The PID/TiO_2/WO_3/MXene sample kept most of its activity after five uses, although the removal efficiency decreased slightly. This point is important for the dissertation because the membrane was not only active under irradiation, but could also be recovered and reused, which is one of the main advantages of the immobilised fibrous format.

The main contribution of this publication is the demonstration of a recoverable hybrid photocatalytic membrane based on electrospun polyimide fibres containing oxide nanowires and MXene. In the dissertation, this study is important because it shows that immobilised photocatalysts cannot be discussed only through their composition. The membrane form also affects how the dye solution wets the material, how easily active regions are reached, and how the sample behaves during repeated use.

4.2.5 Interpretation within the research framework

Within the dissertation, this publication is important because it changes the photocatalyst from a dispersed material into a fixed fibrous membrane. This changes the interpretation of the result. The measured activity depends not only on the TiO_2/WO_3/MXene composition, but also on how the membrane wets, how the dye solution enters the fibre network, and how much of the active material remains exposed during irradiation. The study is therefore discussed as a membrane-based photocatalytic system, where composition and material form have to be considered together.

The fibrous membrane changes the way the photocatalyst works during the test. The dye solution has to wet the fibre mat, pass through or along its pores, and reach the oxide-containing regions. Light also has to penetrate the membrane far enough to activate these regions. These points are important because the catalyst is fixed in one structure rather than freely dispersed in the solution.

The oxide components form the photoactive part of the membrane, while MXene is considered as the conductive phase that may help electron transfer and limit recombination. Its role, however, cannot be judged only from its presence in the composite. It also depends on how well MXene is distributed, how closely it contacts the oxide domains, whether it affects light absorption, and whether it remains stable in water under oxidative photocatalytic conditions.

The publication therefore supports one of the main points of the thesis: a photocatalytic membrane should not be judged only by which active phases it contains. Its response also depends on the way the membrane is built: the polymer scaffold, fibre structure, oxide/MXene contact, movement of the dye solution through the material, and stability during reuse.

4.2.6 Limitations and open questions

The PID/TiO_2/WO_3/MXene membrane performed well in the R6G test, but the result should be read as dye removal by an electrospun membrane system. In such a material, the dye can be removed from solution in more than one way: by photocatalytic degradation under irradiation and by retention within the fibre network. The porous structure and large accessible surface of the membrane make this adsorption contribution important, so it should be considered together with the photocatalytic response rather than ignored.

Second, the behaviour of MXene after repeated photocatalytic use still needs to be verified. $Ti_3C_2T_x$ can be sensitive to water, light, and oxidative species, so its surface and conductivity may change during operation. If this happens, the contact between MXene and the oxide phases may also change, which would affect the charge-transfer role assigned to it. Longer reuse tests, together with post-reaction analysis of the membrane, would help determine whether the MXene/oxide interface remains stable over time.

Third, the membrane was not yet optimised as a structure. The fibre size, membrane thickness, and amount of TiO_2, WO_3, and MXene can change the result as much as the choice of components themselves. A membrane that is too thick or compact may block light and slow dye movement through the fibre mat. Poor distribution of the additives may also leave the oxides and MXene poorly connected. For future work, the loading should be adjusted carefully, because too much additive can cause aggregation, light shielding, and irregular fibres, while too little may give too few active contacts for efficient photocatalysis.

These limitations do not weaken the main contribution of the study, but they show that immobilised hybrid photocatalysts require careful optimisation. Their performance is controlled by a balance between photoactivity, transport, accessibility, and stability.

4.2.7 Author contribution and role in the publication

The author contributed to the synthesis of the hybrid electrospun membranes, investigation, methodology, data curation, interpretation of the results, and preparation of the original draft of the publication. Within the dissertation framework, the author's role was directly connected with the preparation, evaluation, and interpretation of the PID/TiO_2/WO_3/MXene membrane system as an immobilised photocatalytic architecture.

In particular, the author was involved in producing the membrane materials and analysing how the incorporation of TiO_2, WO_3, and $Ti_3C_2T_x$ MXene affected the structure and photocatalytic behaviour of the fibrous system. This contribution was important because the publication is not only about the activity of individual components, but about the fabrication and interpretation of a complete recoverable membrane platform.

The author's work helped connect the experimental results with the broader thesis argument that fibrous photocatalytic membranes are not only passive supports for active

phases. In this study, the membrane response is interpreted through the whole fibrous system: membrane morphology, oxide/MXene contact, charge-transfer behaviour, wetting, dye access, and stability during repeated use all contribute to the final photocatalytic performance.

4.3. Core-shell nanofibers of $ZnFe_2O_4$/ZnO for enhanced visible-light photoelectrochemical performance

Reference:

A. Lys, V. Zabolotnii, M. Čaplovičová, I. Tepliakova, A. Berzins, M. Sahul, Ľ. Čaplovič, A. Pogrebnjak, I. Iatsunskyi, R. Viter, *Core-shell nanofibers of $ZnFe_2O_4$/ZnO for enhanced visible-light photoelectrochemical performance*, Journal of Alloys and Compounds 984 (2024) 173885.
DOI: 10.1016/j.jallcom.2024.173885
Journal impact factor: 6.3
Ministerial points: 100

4.3.1 Context and motivation

In PEC water splitting, the electrode has to absorb light and then move the generated charges to the right interface before they recombine. This is a demanding requirement for wide-band-gap oxides such as ZnO. They are stable and can be processed relatively easily, but most of their optical response is limited to the UV region. As a result, ZnO alone cannot use the visible part of solar irradiation efficiently, even though this part represents a large fraction of the available light.

Visible-light response can be improved by moving from a single oxide to an oxide heterostructure. In this study, $ZnFe_2O_4$ was used to introduce absorption in the visible range, while ZnO remained part of the system as a stable oxide phase. The important point was the core-shell fibre form, because it placed the two oxides in direct contact along a continuous nanofibre architecture. This arrangement was expected to support charge separation more effectively than the individual oxides and to give a stronger PEC response under visible illumination.

Electrospun fibres are well suited for this type of PEC material because they give a continuous oxide network with a large exposed surface. Co-axial electrospinning adds further control, since different precursors can be introduced into the core and shell parts of the fibre before calcination. After annealing, however, the final oxide structure does not always reproduce the starting core-shell design exactly. Fe and Zn species may diffuse between regions during heat treatment, so the final fibre has to be understood as a thermally formed heterostructure rather than a perfectly separated core and shell.

Within the dissertation, this publication extends the discussion to a non-TiO_2 oxide system. Its relevance is not only the use of ZnO and $ZnFe_2O_4$, but the way these phases are organised in a fibrous electrode. The PEC behaviour is shaped by the nanofibre morphology, the core-shell precursor arrangement, the phase changes produced during annealing, and the ability of the final heterostructure to respond to visible light. In this way, the study broadens the thesis discussion while keeping the same focus on architecture, interface formation, and charge utilisation.

4.3.2 Research objective and working hypothesis

This study was designed to obtain a $ZnFe_2O_4$/ZnO fibrous oxide system from co-axial electrospinning and annealing. The prepared fibres were examined structurally, optically, and photoelectrochemically in order to see whether the core-shell-derived arrangement of the two oxides could support a visible-light PEC response.

The working hypothesis was that the combination of $ZnFe_2O_4$ and ZnO within a core-shell nanofibre architecture would improve the use of visible light and support more effective charge separation at the oxide interface. $ZnFe_2O_4$ was expected to contribute visible-light absorption, while ZnO was expected to provide a stable oxide phase and support charge transport. The core-shell geometry was expected to increase interfacial contact between the two oxide components and provide a continuous fibrous pathway favourable for PEC operation.

At the same time, the study recognised that the final structure could be affected by Fe/Zn interdiffusion during annealing. Therefore, the working concept was not only based on an ideal core-shell model, but also on understanding how the real annealed oxide architecture controls optical and PEC behaviour.

4.3.3 Materials and architecture concept

The investigated material was prepared using co-axial electrospinning. Separate precursor solutions were used for the core and shell, containing iron and zinc salts in polymeric matrices. After electrospinning, the obtained precursor fibres were thermally treated to remove the polymer and convert the inorganic precursors into oxide phases.

The intended architecture was a $ZnFe_2O_4$/ZnO core-shell nanofibre system. In this design, the fibrous morphology provides a high-surface-area pathway for interaction with the electrolyte, while the oxide heterostructure introduces an interface for charge separation. The core-shell format is important because it spatially organises the two oxide components and increases the probability of contact between them along the fibre length.

Characterisation showed that the final material should be understood as a real annealed heterostructure rather than as a perfectly sharp core-shell arrangement. Fe/Zn interdiffusion during heat treatment affected phase formation and the final oxide distribution.

This point is important for the dissertation because it shows that architecture is not only defined by the initial synthesis design, but also by the transformations that occur during post-treatment.

4.3.4 Key results and main contribution

The study confirmed the formation of ZnO and $ZnFe_2O_4$ phases in the electrospun nanofibres. Structural and spectroscopic characterisation showed that the final architecture was strongly influenced by interdiffusion during annealing. This interdiffusion helped form the $ZnFe_2O_4$/ZnO heterostructured system, but it also made the boundary between the core and shell less idealised than in a simple schematic model.

The optical analysis showed visible-light absorption associated with the $ZnFe_2O_4$-containing heterostructure. This was important because it addressed one of the main limitations of ZnO-based photoelectrodes, namely the restriction of absorption mainly to the UV range. The fibrous heterostructure therefore provided a route towards broader spectral utilisation.

Photoelectrochemical measurements demonstrated a clear response under visible-light illumination. The material showed improved PEC behaviour compared with reference oxide configurations, and the response was discussed in relation to charge separation, heterointerface formation, and the fibrous architecture of the electrode.

The main contribution of the publication lies in demonstrating that co-axial electrospinning can be used to produce fibrous $ZnFe_2O_4$/ZnO oxide heterostructures with visible-light PEC activity. Within the dissertation, this study broadens the research framework by showing that architecture-driven improvement is not limited to TiO_2, but can also be applied to related metal-oxide systems where heterostructure formation and fibrous morphology control the photoelectrochemical response.

4.3.5 Interpretation within the research framework

Within the dissertation, this publication is interpreted as a bridge between immobilised fibrous photocatalysts and structured PEC photoelectrodes. Like the PID-based membrane system, it uses an electrospun fibrous architecture. However, its function is evaluated through photoelectrochemical measurements rather than dye degradation. This makes it useful for connecting the photocatalytic and PEC parts of the thesis.

The $ZnFe_2O_4$/ZnO system shows that the architecture is created during both fibre formation and annealing. The electrospun fibre gives the material its accessible shape, but the useful heterostructure appears only after the oxide phases form and contact each other during heat treatment. In the final material, the fibre morphology affects electrolyte access, while the $ZnFe_2O_4$/ZnO interface affects visible-light response and charge separation. The PEC behaviour therefore depends on how these two parts of the structure develop together.

A key point is that the co-axial fibre is not the final architecture, but the route used to obtain it. During annealing, Fe- and Zn-containing regions can mix, react, and form the final oxide phases. The $ZnFe_2O_4$/ZnO system therefore has to be interpreted from the structure after heat treatment, including phase distribution, crystallinity, and the real contact between the oxides. This is important for the dissertation because it shows that architecture is not defined only by the synthesis scheme, but by what is actually formed in the final material.

The publication also provides a complementary example to the TiO_2-based studies. While TiO_2 remains the main reference oxide of the dissertation, the $ZnFe_2O_4$/ZnO system shows how other metal-oxide combinations can be used to address visible-light response and charge separation. It therefore strengthens the broader discussion of related semiconductor architectures.

4.3.6 Limitations and open questions

Although the publication shows visible-light PEC activity, the important structure is the one formed after annealing. The co-axial fibre only provides the initial placement of the Fe- and Zn-containing precursors. During heat treatment, these species partly redistribute, and the final $ZnFe_2O_4$/ZnO contact develops inside the fibre. This is beneficial for creating an oxide heterointerface, but it also means that the original boundary between the two regions cannot be treated as sharp. Therefore, the PEC behaviour should be interpreted through the annealed phase distribution and oxide contact, rather than through an idealised core-shell model.

Second, further optimisation of the precursor ratios, fibre diameter, annealing temperature, and annealing time would be useful. These parameters could influence phase composition, crystallinity, defect density, and the degree of interdiffusion. Better control over these factors may improve the balance between visible-light absorption and charge transport.

Third, longer PEC stability tests would be needed to judge how durable the nanofibre electrode is during operation. The material shows a promising photoelectrochemical response, but this does not yet show how it behaves under extended illumination and electrolyte contact. Continuous testing would help determine whether the oxide fibre structure remains stable and whether the photocurrent can be maintained over longer operating times.

Finally, the electrode surface could be further developed by adding a suitable cocatalyst or by applying an additional surface modification. This would be aimed at the reaction interface rather than at light absorption alone. In a PEC electrode, even when charges are generated and separated, slow transfer to the electrolyte can still limit the final

response. A cocatalyst could help lower these interfacial kinetic losses and improve the conversion of photogenerated carriers into the desired reaction.

4.3.7 Author contribution and role in the publication

The author contributed to the synthesis and fabrication of the $ZnFe_2O_4$/ZnO core-shell nanofibre structures, as well as to their photoelectrochemical characterisation, data analysis, interpretation of the results, and preparation of the draft manuscript. Within the dissertation framework, the author's role was directly connected with producing and evaluating the fibrous oxide heterostructure as a visible-light-responsive PEC architecture.

In particular, the author was involved in preparing the core-shell nanofibre system by co-axial electrospinning and in analysing how the synthesis route, annealing treatment, oxide phase formation, and Fe/Zn interdiffusion affected the final material structure. This contribution is important because the publication does not only test a ready-made material, but examines how the fabricated fibrous heterostructure develops and how this real architecture controls the PEC response.

The author's work also included connecting the experimental findings with the broader dissertation argument that semiconductor photoactivity depends not only on oxide composition, but also on the architecture actually obtained after synthesis and thermal treatment. In this publication, that means interpreting the PEC behaviour through the combined effects of fibrous morphology, $ZnFe_2O_4$/ZnO heterostructure formation, visible-light absorption, and interfacial charge separation.

4.4. Hierarchically Structured Ti-TiO_2 Membranes Fabricated by Femtosecond Laser Ablation and Atomic Layer Deposition for Enhanced Photoelectrochemical Water Splitting

Reference:

A. Lys, I. Gnilitskyi, E. Coy, M. Jancelewicz, M. Bechelany, I. Iatsunskyi, *Hierarchically Structured Ti-TiO_2 Membranes Fabricated by Femtosecond Laser Ablation and Atomic Layer Deposition for Enhanced Photoelectrochemical Water Splitting*, ACS Applied Materials & Interfaces 17 (2025) 43390–43402.
DOI: 10.1021/acsami.5c07488
Journal impact factor: 8.2
Ministerial points: 200

4.4.1. Context and motivation

In PEC water splitting, the photoelectrode has to do several things at once. It must absorb light, keep the generated charges separated, move them through the solid phase, and maintain stable contact with the electrolyte. TiO_2 is a useful material for this type of system because it is stable, inexpensive, and relatively safe. However, it absorbs mainly UV light,

and many of the generated carriers are lost through recombination or slow transport before they can contribute to the electrochemical reaction.

For this reason, improvement of TiO_2-based photoelectrodes cannot rely only on changing chemical composition. The architecture of the electrode is also important. A structured support can increase light trapping, enlarge the effective surface area, improve electrolyte contact, and create more favourable pathways for charge extraction. In parallel, a controlled semiconductor coating can improve interface quality and define the active surface of the electrode.

This publication addresses the problem through a Ti-TiO_2 membrane photoelectrode. The titanium membrane was first structured by femtosecond laser ablation, which produced a hierarchical conductive scaffold without the need for a binder. TiO_2 was then deposited by ALD, allowing the oxide layer to cover the structured metal surface with controlled thickness. In the dissertation, this study is important because the PEC response is considered as the result of the Ti scaffold and TiO_2 coating acting as one electrode system. The discussion therefore focuses on how the laser-made hierarchy, oxide thickness, coating continuity, and Ti/TiO_2 interface influence light use and charge transfer.

4.4.2. Research objective and working hypothesis

The objective of the study was to fabricate Ti-TiO_2 membrane photoanodes by first structuring titanium with femtosecond laser ablation and then growing TiO_2 by ALD. The work compared TiO_2 coatings of different thickness on the same type of hierarchical Ti scaffold in order to determine how the oxide layer affects morphology, optical response, crystallinity, charge-transfer behaviour, and PEC water-splitting performance.

Two TiO_2 coating thicknesses were investigated: approximately 10 nm and approximately 100 nm. This comparison was important because it allowed the role of oxide thickness and structural development to be examined while keeping the same laser-structured titanium support.

The working hypothesis was that the PEC response of the Ti-TiO_2 membrane would be determined by the balance between the laser-made scaffold and the ALD oxide layer. The hierarchical titanium support was expected to improve light interaction and provide direct electrical connection. The TiO_2 coating was expected to supply the photoactive surface, but its thickness had to be optimised. A thicker layer could be favourable because of improved crystallinity and absorption, but only if it did not create excessive transport losses or recombination before the charges reached the Ti/TiO_2 interface.

4.4.3. Materials and architecture concept

The investigated system was based on titanium foil processed by femtosecond laser ablation. The laser treatment produced a highly ordered array of micro-pyramidal structures

and transformed the flat titanium foil into a structured membrane-like scaffold. This geometry is important because it creates a binder-free electrode architecture rather than a conventional particle-based film deposited on a flat conductive substrate.

The laser-structured titanium scaffold was subsequently coated with TiO_2 by ALD using $TiCl_4$ and H_2O as precursors. ALD was used to deposit the oxide on the three-dimensional Ti surface while keeping control over the layer thickness. Two coatings were prepared for comparison: 250 cycles produced an approximately 10 nm TiO_2 layer, whereas 2500 cycles produced an approximately 100 nm layer.

In this system, the titanium membrane and the TiO_2 coating have to be considered together. The laser-treated Ti surface provides the developed conductive scaffold, while ALD places the oxide directly onto that geometry. As a result, the electrode response depends not only on the properties of TiO_2, but also on how the oxide is connected to the structured metal surface. Coating continuity, electrolyte access, and charge extraction through the Ti scaffold are therefore central to the interpretation of the PEC behaviour.

4.4.4. Key results and main contribution

The laser-structured titanium membrane showed very low reflectance over a broad spectral range. This optical behaviour was attributed mainly to the hierarchical microstructure, which promotes light trapping and multiple reflections within the surface architecture. This result is important because it shows that the support geometry itself contributes to light management before the semiconductor coating is even considered.

The thickness of the ALD TiO_2 layer was one of the main factors controlling the electrode behaviour. The 10 nm coating was too thin to form a well-developed crystalline oxide layer and remained mostly amorphous, so its effect on the PEC response was limited. The 100 nm coating gave a clearer anatase contribution and a more complete TiO_2 structure. This change in the oxide layer was reflected directly in the photoelectrochemical measurements, where the thicker coating showed the stronger response.

Among the tested samples, the 100 nm TiO_2 coating gave the strongest PEC response. The photocurrent reached about 27 $\mu A\ cm^{-2}$ at 1.4 V vs NHE, with an IPCE of about 31% at 275 nm and an ABPE roughly three times higher than for the uncoated structured Ti membrane. In the dissertation, these results are used mainly to show the effect of the electrode design. The value of the system lies in combining a laser-structured Ti scaffold with a controlled ALD TiO_2 layer, producing a binder-free photoelectrode whose improved response can be linked to the developed surface geometry and better oxide formation.

The main contribution of the publication lies in demonstrating a freestanding Ti-TiO_2 membrane photoanode fabricated by a laser-assisted ALD strategy. Within the dissertation, this study provides the strongest example of how surface geometry, oxide thickness,

crystallinity, interface quality, and charge-transfer behaviour can be integrated into one photoelectrochemical platform.

4.4.5. Interpretation within the research framework

Within the dissertation, this publication is the clearest PEC example of the architecture-based approach. The higher response is not explained simply by the presence of TiO_2. It comes from the prepared Ti-TiO_2 electrode as a whole: the laser-made titanium scaffold, the conformal oxide coating, and the interface between them. The 100 nm TiO_2 layer was especially important because its better-developed structure and crystallinity improved the way charges were used during PEC operation.

The laser-structured titanium scaffold is mainly responsible for the optical and geometrical contribution. Its pyramidal architecture reduces reflectance, increases interaction with incident light, and provides a larger effective area for contact with the electrolyte. At the same time, the metallic titanium support provides a conductive pathway for charge extraction.

The ALD TiO_2 layer is the part of the electrode that determines the semiconductor response, but this depends on how the layer develops during deposition. The 10 nm coating confirmed that TiO_2 was present, but it did not yet provide a sufficiently developed oxide structure for strong PEC behaviour. The 100 nm coating gave a more effective photoactive layer, with clearer crystallinity and better continuity on the structured Ti scaffold. Its stronger response is therefore connected with the quality of the formed oxide layer and its contact with titanium, rather than with TiO_2 deposition alone.

This publication also supports one of the main methodological arguments of the dissertation: photocurrent should not be interpreted alone. The PEC behaviour was discussed together with structural characterisation, optical analysis, impedance behaviour, IPCE, ABPE, Mott-Schottky analysis, and stability-related observations. This combined interpretation makes the work directly connected to the thesis framework developed in Chapters 1 and 2.

4.4.6. Limitations and open questions

This study improves the way TiO_2 is used in a photoelectrode, but it does not change the nature of TiO_2 itself. The laser-made hierarchy gives the electrode a more favourable surface for light interaction and electrolyte contact, and ALD allows the oxide layer to be placed on this surface in a controlled way. However, the active semiconductor remains TiO_2, so the response is still mainly governed by UV excitation. For this reason, further development should focus on modifying the oxide part of the system, for example by introducing dopants, forming a heterostructure, or adding a phase that can use visible light more effectively.

Second, the TiO_2 thickness still needs more precise optimisation. In this study, the 100 nm layer gave a better PEC response than the 10 nm layer, showing that a more developed oxide coating was beneficial. However, increasing the thickness further would not necessarily improve the electrode. At some point, a thicker TiO_2 layer could make charge transport longer, increase recombination, or add resistive losses. For this reason, the useful thickness window should be defined more carefully in future work.

Third, the durability of the Ti-TiO_2 membrane still needs to be followed over longer operation. The post-test characterisation reported in the study shows that the electrode remains stable after the applied PEC measurements. However, hierarchical electrodes may change slowly during longer exposure to light, bias, and electrolyte. Small changes in the TiO_2 layer, surface chemistry, or Ti/TiO_2 contact may only become visible after extended operation. For this reason, future work should include longer continuous PEC tests together with structural and chemical analysis after use.

Finally, the next improvement should probably be made at the surface where the PEC reaction actually occurs. The Ti-TiO_2 membrane already gives a useful electrode form, with a structured metal scaffold and a directly grown oxide layer. However, charge transfer from TiO_2 to the electrolyte may still be slow, especially for oxygen evolution. A cocatalyst or very thin interfacial layer could be used to make this step easier. The important condition is that this added layer should not hide the laser-made surface, block electrolyte contact, or weaken the direct connection between TiO_2 and the titanium scaffold.

4.4.7. Author contribution and role in the publication

The author contributed to the investigation, formal analysis, visualisation, interpretation of the results, and preparation of both the original and revised manuscript. Within the dissertation framework, the author's role was connected with the analysis and interpretation of the hierarchical Ti-TiO_2 membrane photoanodes and their photoelectrochemical behaviour.

In particular, the author was involved in examining how the femtosecond-laser-structured titanium scaffold and ALD-grown TiO_2 coatings affected morphology, light trapping, surface chemistry, oxide crystallinity, charge-transfer behaviour, and PEC performance. This contribution is important because the publication is not only about reporting a TiO_2-coated electrode, but about interpreting a complete binder-free photoelectrode architecture in which support geometry and oxide-layer properties act together.

The author's work helped place the results of this publication within the wider argument of the dissertation. The Ti-TiO_2 membrane is not discussed only as a photoanode with improved photocurrent, but as a system where several factors act together. The geometry of the titanium support, the quality and thickness of the TiO_2 coating, charge

transfer across the metal/oxide and oxide/electrolyte interfaces, and stability during PEC operation all shape the final response. For this reason, the publication provides a suitable closing point for the publication sequence, since it brings together the main design principles developed throughout the dissertation.

Chapter 5. General conclusions and future perspectives

5.1. General conclusions

The work presented in this dissertation focused on architecture-engineered semiconductor nanocomposites for photocatalytic and photoelectrochemical applications. The central aim was to examine how the behaviour of TiO_2-based and related metal-oxide systems can be improved by controlling not only chemical composition, but also support geometry, surface structure, interface quality, immobilisation strategy, and charge-transfer pathways.

The results collected across the publications show that architecture was part of the working function of the materials, not only their external morphology. The photocatalytic and photoelectrochemical responses were not determined by composition alone. They depended on how each structure affected light interaction, charge separation, carrier transport, access to the reaction interface, and stability during use. In this way, the publication set supports the main thesis argument that material performance must be understood through the complete architecture of the system.

The SiNR/MXene/TiO_2 study shows that the structured surface itself takes part in the photocatalytic response. The regular silicon nanoripples changed the way light was used at the surface, while ALD made it possible to place TiO_2 on this geometry in a controlled way. MXene introduced an additional electronic pathway between the structured substrate and the oxide layer. For this reason, the improved degradation behaviour is better interpreted as the result of the complete SiNR/MXene/TiO_2 surface architecture, rather than as the effect of silicon, MXene, or TiO_2 considered separately.

The electrospun PID/TiO_2/WO_3/MXene membrane showed that immobilised photocatalysis cannot be reduced to the presence of active phases in a polymer support. The membrane form affected how the material was used, recovered, and exposed to the dye solution. The TiO_2/WO_3/MXene combination improved the photoactive part of the system, mainly through stronger light absorption and more favourable charge separation. However, the final response also depended on the fibrous PID network, including wetting, adsorption, access to oxide-rich regions, and transport of the solution through the membrane.

The $ZnFe_2O_4$/ZnO nanofibre study moved the discussion away from TiO_2-only architectures and introduced another oxide system for PEC operation. Its importance lies in the link between fibre geometry, visible-light absorption, and the formation of a $ZnFe_2O_4$/ZnO interface. The study also showed that the final electrode is not simply the structure planned during co-axial electrospinning. Annealing changes the precursor fibre through phase formation and Fe/Zn interdiffusion. For this reason, the PEC response has to

be discussed on the basis of the annealed material itself, especially the real phase distribution, crystallinity, and oxide-oxide contact formed after thermal treatment.

The hierarchically structured Ti-TiO_2 membrane study is the most complete PEC example in the dissertation. The electrode was built by combining a laser-structured titanium membrane with an ALD-grown TiO_2 layer, without using a binder. Femtosecond laser processing gave the titanium a developed surface that improved light interaction, while ALD allowed TiO_2 to be deposited with controlled thickness on this complex geometry.

The comparison between 10 nm and 100 nm TiO_2 layers showed that the PEC response was controlled by the state of the oxide layer, not only by its presence. The thicker coating gave a more developed TiO_2 structure, with improved crystallinity and more effective charge-transfer behaviour. This study therefore confirms one of the main points of the dissertation: hierarchical geometry and controlled semiconductor interfaces can work together in a single photoelectrode architecture.

Taken together, the publications show that improved performance in semiconductor photocatalysts and photoelectrodes is rarely the result of a single factor. In the systems studied here, enhancement was governed by the interaction between optical effects, surface accessibility, interfacial charge transfer, material stability, and the physical format of the material. For this reason, the dissertation supports the view that photocatalytic and photoelectrochemical materials should be designed and evaluated as integrated architectures.

The thesis also shows that photocatalysis and photoelectrochemistry can be used as complementary ways of examining photoactive semiconductor materials. Dye-degradation tests show how a material behaves during pollutant removal under irradiation, but the result is not always governed only by photocatalysis. Adsorption, dye sensitisation, wetting, and transport through the structure may also affect the measured removal. PEC measurements give a clearer view of charge extraction and interfacial losses, although they are also influenced by electrode geometry, electrolyte contact, applied bias, and stability during operation. Taken together, these two approaches give a wider picture of how material architecture affects light-driven processes.

A further conclusion is that the methods used in the dissertation should not be seen only as preparation techniques. Each of them was used to control a particular part of the material function. Femtosecond laser structuring shaped the surface and improved light interaction. ALD allowed TiO_2 and other oxide layers to be deposited with controlled thickness and good coverage on complex supports. Electrospinning gave the materials a recoverable fibrous form, which is important for membrane photocatalysis. Heterostructure formation and MXene addition were used to modify charge separation and interfacial transport. Together, these methods show how fabrication can be used as a way to design the working behaviour of photocatalysts and photoelectrodes.

Overall, the dissertation shows that TiO_2-based and related semiconductor nanocomposites work best when several material functions are developed together. Light use, chemical stability, surface accessibility, charge transfer, and durability during operation cannot be separated completely from one another. The results therefore support an integrated design approach, where composition, morphology, and interface quality are treated as connected parts of the same photocatalytic or photoelectrochemical system.

5.2. Future perspectives

The results presented in this dissertation suggest several directions for future work. One of the most important is a clearer separation of photocatalytic degradation from adsorption and possible dye-sensitisation effects. This is particularly relevant for immobilised membranes and MXene-containing hybrids, where the measured decrease in dye concentration may be influenced by dye uptake, surface interactions, and absorption of light by the dye itself. Future studies should therefore use a wider range of pollutant models and, where possible, include mineralisation measurements and analysis of degradation intermediates.

Second, future work should examine whether the developed architectures remain stable during longer operation. This is important for both photocatalytic membranes and PEC electrodes. In MXene-containing systems, $Ti_3C_2T_x$ may gradually oxidise or change its surface terminations in water under illumination, which could affect its conductivity and its contact with the oxide phases. In hierarchical photoelectrodes, prolonged exposure to light, electrolyte, and applied bias may influence the surface morphology, the oxide coating, or the metal/oxide interface. Therefore, longer photocatalytic and PEC stability tests should be combined with post-operation structural, chemical, and electrochemical analysis.

Third, the next step is to tune the physical design of the membranes and electrodes more carefully. In the electrospun systems, small changes in fibre size, membrane thickness, porosity, and additive content can change how the liquid enters the mat, how light reaches the active regions, and how well the oxide and MXene phases contact each other. These parameters should therefore be varied deliberately, rather than treated only as fabrication outcomes.

A similar issue applies to ALD-coated photoelectrodes. The TiO_2 layer has to be thick enough to form a useful photoactive coating, but not so thick that charge extraction becomes more difficult. Crystallinity, defects, coating continuity, and contact with the support all need to be balanced together. Future optimisation should therefore look for the range where the architecture still supports light absorption, charge transport, and interfacial transfer at the same time.

Fourth, the next improvement could come from the surface chemistry of the photoelectrode. Even if the architecture helps with light trapping and charge collection, the

oxygen-evolution reaction can still be slow at the semiconductor/electrolyte boundary. A cocatalyst or a very thin interfacial layer could help at this point by making hole transfer to the electrolyte easier and lowering charge-transfer resistance.

Such modification should be introduced in a way that respects the architecture already created by laser structuring and ALD. The main value of the Ti-TiO_2 membrane lies in its binder-free conductive scaffold, conformal oxide coverage, and developed surface relief. A cocatalyst or additional interfacial layer should therefore not replace these features or cover them excessively. Its role should be limited to improving the reaction side of the electrode, especially charge transfer during oxygen evolution. In this form, the modified photoelectrode could gain better interfacial kinetics while still keeping the advantages of the original design: light trapping, electrolyte access, direct charge collection through the titanium scaffold, and mechanical stability.

Finally, the architecture-driven strategy developed in this thesis could be extended to other semiconductor systems and application formats. The same principles may be useful for designing visible-light-active photocatalysts, integrated photoelectrodes, flow-through photocatalytic membranes, and hybrid systems combining light absorption, charge transport, and catalytic functionality. The most promising future direction is therefore not only to search for new compositions, but to design complete working architectures in which composition, geometry, interfaces, and operating environment are considered together from the beginning.

Scientific achievements and professional development

List of publications

1. *Enhancing the Hydrogen Storage Properties of A_xB_y Intermetallic Compounds by Partial Substitution: A Short Review*
   Andrii Lys, Julien O. Fadonougbo, Mohammad Faisal, Jin-Yoo Suh, Young-Su Lee, Jae-Hyeok Shim, Jihye Park and Young Whan Cho
   Hydrogen,1(1), 38-63, 2020
   doi.org/10.3390/hydrogen1010004
2. *Highly regular laser-induced periodic silicon surface modified by MXene and ALD TiO_2 for organic pollutants degradation*
   Andrii Lys, Iaroslav Gnilitskyi, Emerson Coy, Mariusz Jancelewicz, Oleksiy Gogotsi, Igor Iatsunskyi
   Applied Surface Science, 640, 158336, 2023
   doi.org/10.1016/j.apsusc.2023.158336
3. *Core-shell nanofibers of $ZnFe_2O_4$/ZnO for enhanced visible-light photoelectrochemical performance*
   Andrii Lys, Viktor Zabolotnii, Mária Čaplovičová, Iryna Tepliakova, Agris Berzin, Martin Sahul, Ľubomír Čaplovič, Alexander Pogrebnjak, Igor Iatsunskyi, Roman Viter
   Journal of Alloys and Compounds, 984, 173885, 2024
   doi.org/10.1016/j.jallcom.2024.173885
4. *Ag, Cu, and Se-doped ultrasmall iron oxide colloidal gels: Revealing potential for photo/electrochemical applications*
   Olena Ivashchenko, Artur Jędrzak, **Andrii Lys**, Karol Załęski, Sylwia Różańska, Jacek Różański, Emerson Coy Igor Iatsunskyi
   Applied Surface Science, 673, 160916, 2024
   doi.org/10.1016/j.apsusc.2024.160916
5. *Hierarchically Structured Ti-TiO_2 Membranes Fabricated by Femtosecond Laser Ablation and Atomic Layer Deposition for Enhanced Photoelectrochemical Water Splitting*
   Andrii Lys, Iaroslav Gnilitskyi, Emerson Coy, Mariusz Jancelewicz, Mikhael Bechelany, Igor Iatsunskyi
   ACS Applied Materials & Interfaces, 17(30), 43390-43402, 2025
   doi.org/10.1021/acsami.5c07488
6. *Electrospun Polyimide Nanofibers Modified with Metal Oxide Nanowires and MXene for Photocatalytic Water Purification*
   Andrii Lys, Valerii Myndrul, Mykola Pavlenko, Błażej Anastaziak, Pavel Holec,

Kateřina Vodseďálková, Emerson Coy, Mikhael Bechelany, Igor Iatsunskyi
Nanomaterials 2025, 15(17), 1371, 2025
doi.org/10.3390/nano15171371

Funded project

PRELUDIUM 23, National Science Centre, Poland, project no. 2024/53/N/ST5/02538. Principal investigator. Project title: Enhanced photocatalytic hydrogen production via nanoscale engineering of N-doped metal oxide heterostructures and metal oxide/metal nitride heterostructures.

Participation in research projects

M-ERA.NET 2021 call, Mem4BoTiReg, project no. M-ERA.NET3/2021 /63/Mem4BoTiReg/2023 – project led by Prof. dr. hab. Igor Iatsunskyi; research work related to nanomaterial characterisation.

POLTAJ12/2024/56/DOPASENS/2025 – project led by Prof. dr. hab. Igor Iatsunskyi; research work related to nanomaterial characterisation.

International mobility and secondment visits

- 2022, Czech Republic, Nanopharma a.s.
  Two-month scientific training carried out within the framework of the HORIZON 2020 RISE project
- 2023, Latvia, 3D Strong Ltd.
  Six-month scientific training carried out within the framework of the HORIZON 2020 RISE project.
- 2024, Lithuania, Vilnius University, and Czech Republic, RESPILON company
  Two-month scientific training carried out within the framework of the ESCULAPE project.
- 2024, Italy, Polish Academy of Sciences, Scientific Centre in Rome
  Three-day workshop: Light-responsive nanomaterials for biomedical applications.
- 2025, France, INSERM; Portugal, BIOFABICS – 3D Biotissue Analogues; Czech Republic, RESPILON Group
  Three-month scientific training carried out within the framework of the ESCULAPE project.
- 2026, Czech Republic, RESPILON Group
  One-month scientific training carried out within the framework of the ESCULAPE project.

Conference presentations and dissemination activities

1. A. Lys, I. Iatsunskyi, “Substitutional effects in intermetallic compounds for hydrogen storage”, NanoTech Poland 2022, 12th International Conference, 1–3 June 2022, Poznań, Poland. Poster presentation.
2. A. Lys, R. Viter, I. Iatsunskyi, “Novel $ZnFe_2O_4$/ZnO core-shell nanofibers with promising photoelectrochemical properties for water splitting applications”, NanoTech Poland 2023, 13th International Conference, 14–16 June 2023, Poznań, Poland. Poster presentation.
3. A. Lys, I. Hanif, I. Iatsunskyi, “Novel 1D ZnO nanomaterials with promising photoelectrochemical properties for biosensing and water splitting applications”, AMPERE NMR School 2023, 18–24 June 2023, Zakopane, Poland. Poster presentation.
4. A. Lys, I. Iatsunskyi, “1D electrospun nanocomposite nanofibers for efficient photocatalytic applications”, NanoTech Poland 2024, 14th International Conference, 5–7 June 2024, Poznań, Poland. Oral presentation.
5. A. Lys, M. Pavlenko, I. Iatsunskyi, “Electrospun biodegradable PLA membranes enhanced with bioactive nanoparticles and BMP-2 for advanced bone and tissue regeneration”, 8th International Conference on Multifunctional, Hybrid and Nanomaterials, 3–6 March 2025, Montpellier, France. Poster presentation.
6. A. Lys, M. Pavlenko, I. Iatsunskyi, “Bioactive electrospun nanofiber membranes for dental tissue engineering and regeneration”, 2025 International Conference on Biofabrication, 14–17 September 2025, Warsaw, Poland. Poster presentation.
7. A. Lys, I. Iatsunskyi, “Laser-structured and ALD-coated titanium membranes: a robust platform for solar-driven hydrogen production”, 5th International Workshop on Functional Nanostructured Materials, FuNaM-5, 24–26 September 2025, Kraków, Poland. Poster presentation.
8. A. Lys, M. Jancelewicz I. Iatsunskyi, “Atomic Layer Deposition of ZnO/TiO_2 Thin-Film Heterostructures for Water Splitting”, NanoTech Poland 2026 & NIBS 15th International Conference, 8–11 June 2026, Poznań, Poland

References

[1] U. Hübner *et al.*, "Advanced oxidation processes for water and wastewater treatment – Guidance for systematic future research," *Heliyon*, vol. 10, no. 9, p. e30402, May 2024, doi: 10.1016/j.heliyon.2024.e30402.

[2] M. R. Hoffmann, S. T. Martin, W. Choi, and D. W. Bahnemann, "Environmental Applications of Semiconductor Photocatalysis," *Chem. Rev.*, vol. 95, no. 1, pp. 69–96, Jan. 1995, doi: 10.1021/cr00033a004.

[3] A. Fujishima and K. Honda, "Electrochemical Photolysis of Water at a Semiconductor Electrode," *Nature*, vol. 238, no. 5358, pp. 37–38, Jul. 1972, doi: 10.1038/238037a0.

[4] O. J. Alley *et al.*, "Best Practices in PEC Water Splitting: How to Reliably Measure Solar-to-Hydrogen Efficiency of Photoelectrodes," *Front. Energy Res.*, vol. 10, p. 884364, Oct. 2022, doi: 10.3389/fenrg.2022.884364.

[5] A. Hankin, F. E. Bedoya-Lora, J. C. Alexander, A. Regoutz, and G. H. Kelsall, "Flat band potential determination: avoiding the pitfalls," *J. Mater. Chem. A*, vol. 7, no. 45, pp. 26162–26176, 2019, doi: 10.1039/C9TA09569A.

[6] K. Sivula, "Mott–Schottky Analysis of Photoelectrodes: Sanity Checks Are Needed," *ACS Energy Lett.*, vol. 6, no. 7, pp. 2549–2551, Jul. 2021, doi: 10.1021/acsenergylett.1c01245.

[7] A. T. Sivagurunathan, S. Adhikari, and D.-H. Kim, "Strategies and implications of atomic layer deposition in photoelectrochemical water splitting: Recent advances and prospects," *Nano Energy*, vol. 83, p. 105802, May 2021, doi: 10.1016/j.nanoen.2021.105802.

[8] T. R. Seling, M. Songsart-Power, A. K. Shringi, J. Paudyal, F. Yan, and T. B. Limbu, "Ti3C2Tx MXene-Based Hybrid Photocatalysts in Organic Dye Degradation: A Review," *Molecules*, vol. 30, no. 7, p. 1463, Mar. 2025, doi: 10.3390/molecules30071463.

[9] S. Lettieri, M. Pavone, A. Fioravanti, L. Santamaria Amato, and P. Maddalena, "Charge Carrier Processes and Optical Properties in TiO2 and TiO2-Based Heterojunction Photocatalysts: A Review," *Materials*, vol. 14, no. 7, p. 1645, Mar. 2021, doi: 10.3390/ma14071645.

[10] R. Qian *et al.*, "Charge carrier trapping, recombination and transfer during TiO2 photocatalysis: An overview," *Catalysis Today*, vol. 335, pp. 78–90, Sep. 2019, doi: 10.1016/j.cattod.2018.10.053.

[11] A. A. Tountas *et al.*, "Light-harvesting properties of photocatalyst supports—no photon left behind," *npj Comput Mater*, vol. 10, no. 1, p. 239, Oct. 2024, doi: 10.1038/s41524-024-01409-0.

[12] M. Rochkind, S. Pasternak, and Y. Paz, "Using Dyes for Evaluating Photocatalytic Properties: A Critical Review," *Molecules*, vol. 20, no. 1, pp. 88–110, Dec. 2014, doi: 10.3390/molecules20010088.

[13] A. D. Walter *et al.*, "Adsorption and self-sensitized, visible-light photodegradation of rhodamine 6G and crystal violet by one-dimensional lepidocrocite titanium oxide," *Matter*, vol. 6, no. 11, pp. 4086–4105, Nov. 2023, doi: 10.1016/j.matt.2023.09.008.

[14] M. Sachs, E. Pastor, A. Kafizas, and J. R. Durrant, "Evaluation of Surface State Mediated Charge Recombination in Anatase and Rutile TiO_2," *J. Phys. Chem. Lett.*, vol. 7, no. 19, pp. 3742–3746, Oct. 2016, doi: 10.1021/acs.jpclett.6b01501.

[15] G. D. Gesesse, A. Gomis-Berenguer, M.-F. Barthe, and C. O. Ania, "On the analysis of diffuse reflectance measurements to estimate the optical properties of amorphous porous carbons and semiconductor/carbon catalysts," *Journal of Photochemistry and Photobiology A: Chemistry*, vol. 398, p. 112622, Jul. 2020, doi: 10.1016/j.jphotochem.2020.112622.

[16] A. Mills, C. Hill, and P. K. J. Robertson, "Overview of the current ISO tests for photocatalytic materials," *Journal of Photochemistry and Photobiology A: Chemistry*, vol. 237, pp. 7–23, Jun. 2012, doi: 10.1016/j.jphotochem.2012.02.024.

[17] International Organization for Standardization, *Fine ceramics (advanced ceramics, advanced technical ceramics) — Determination of photocatalytic activity of surfaces in an aqueous medium by degradation of methylene blue*, ISO 10678:2024, Geneva, Switzerland., 2024. Accessed: Apr. 28, 2026. [Online]. Available: https://www.iso.org/standard/86490.html

[18] D. F. Ollis, "Kinetics of Photocatalyzed Reactions: Five Lessons Learned," *Front. Chem.*, vol. 6, p. 378, Aug. 2018, doi: 10.3389/fchem.2018.00378.

[19] C. Turchi, "Photocatalytic degradation of organic water contaminants: Mechanisms involving hydroxyl radical attack," *Journal of Catalysis*, vol. 122, no. 1, pp. 178–192, Mar. 1990, doi: 10.1016/0021-9517(90)90269-P.

[20] V. V. Guliants, “Structure–reactivity relationships in oxidation of C4 hydrocarbons on supported vanadia catalysts,” *Catalysis Today*, vol. 51, no. 2, pp. 255–268, Jun. 1999, doi: 10.1016/S0920-5861(99)00049-8.

[21] S. E. Braslavsky, “Glossary of terms used in photochemistry, 3rd edition (IUPAC Recommendations 2006),” *Pure and Applied Chemistry*, vol. 79, no. 3, pp. 293–465, Jan. 2007, doi: 10.1351/pac200779030293.

[22] M. N. Chong, B. Jin, C. W. K. Chow, and C. Saint, “Recent developments in photocatalytic water treatment technology: A review,” *Water Research*, vol. 44, no. 10, pp. 2997–3027, May 2010, doi: 10.1016/j.watres.2010.02.039.

[23] J. Schneider *et al.*, “Understanding TiO_2 Photocatalysis: Mechanisms and Materials,” *Chem. Rev.*, vol. 114, no. 19, pp. 9919–9986, Oct. 2014, doi: 10.1021/cr5001892.

[24] A. Mills and S. Le Hunte, “An overview of semiconductor photocatalysis,” *Journal of Photochemistry and Photobiology A: Chemistry*, vol. 108, no. 1, pp. 1–35, Jul. 1997, doi: 10.1016/S1010-6030(97)00118-4.

[25] J. Bonse, J. Krüger, S. Höhm, and A. Rosenfeld, “Femtosecond laser-induced periodic surface structures,” *Journal of Laser Applications*, vol. 24, no. 4, p. 042006, Sep. 2012, doi: 10.2351/1.4712658.

[26] D. Pathak, A. Sharma, D. P. Sharma, and V. Kumar, “A review on electrospun nanofibers for photocatalysis: Upcoming technology for energy and environmental remediation applications,” *Applied Surface Science Advances*, vol. 18, p. 100471, Dec. 2023, doi: 10.1016/j.apsadv.2023.100471.

[27] R. H. Coridan *et al.*, “Methods for comparing the performance of energy-conversion systems for use in solar fuels and solar electricity generation,” *Energy Environ. Sci.*, vol. 8, no. 10, pp. 2886–2901, 2015, doi: 10.1039/C5EE00777A.

[28] X. Shi, L. Cai, M. Ma, X. Zheng, and J. H. Park, “General Characterization Methods for Photoelectrochemical Cells for Solar Water Splitting,” *ChemSusChem*, vol. 8, no. 19, pp. 3192–3203, Oct. 2015, doi: 10.1002/cssc.201500075.

[29] M. Qureshi and K. Takanabe, “Insights on Measuring and Reporting Heterogeneous Photocatalysis: Efficiency Definitions and Setup Examples,” *Chem. Mater.*, vol. 29, no. 1, pp. 158–167, Jan. 2017, doi: 10.1021/acs.chemmater.6b02907.

[30] S. Anantharaj, S. Noda, M. Driess, and P. W. Menezes, “The Pitfalls of Using Potentiodynamic Polarization Curves for Tafel Analysis in Electrocatalytic Water Splitting,” *ACS Energy Lett.*, pp. 1607–1611, Mar. 2021, doi: 10.1021/acsenergylett.1c00608.

[31] O. Van Der Heijden, S. Park, R. E. Vos, J. J. J. Eggebeen, and M. T. M. Koper, “Tafel Slope Plot as a Tool to Analyze Electrocatalytic Reactions,” *ACS Energy Lett.*, vol. 9, no. 4, pp. 1871–1879, Apr. 2024, doi: 10.1021/acsenergylett.4c00266.

[32] H. Dotan, K. Sivula, M. Grätzel, A. Rothschild, and S. C. Warren, “Probing the photoelectrochemical properties of hematite (α-Fe_2O_3) electrodes using hydrogen peroxide as a hole scavenger,” *Energy Environ. Sci.*, vol. 4, no. 3, pp. 958–964, 2011, doi: 10.1039/C0EE00570C.

[33] A. J. Cowan and J. R. Durrant, “Long-lived charge separated states in nanostructured semiconductor photoelectrodes for the production of solar fuels,” *Chem. Soc. Rev.*, vol. 42, no. 6, pp. 2281–2293, 2013, doi: 10.1039/C2CS35305A.

[34] H. Dotan, N. Mathews, T. Hisatomi, M. Grätzel, and A. Rothschild, “On the Solar to Hydrogen Conversion Efficiency of Photoelectrodes for Water Splitting,” *J. Phys. Chem. Lett.*, vol. 5, no. 19, pp. 3330–3334, Oct. 2014, doi: 10.1021/jz501716g.

[35] Z. Chen, H. N. Dinh, and E. Miller, *Photoelectrochemical Water Splitting: Standards, Experimental Methods, and Protocols*. in SpringerBriefs in Energy. New York, NY: Springer New York, 2013. doi: 10.1007/978-1-4614-8298-7.

[36] N. Dutta, D. Bagchi, G. Chawla, and S. C. Peter, “A Guideline to Determine Faradaic Efficiency in Electrochemical CO_2 Reduction,” *ACS Energy Lett.*, vol. 9, no. 1, pp. 323–328, Jan. 2024, doi: 10.1021/acsenergylett.3c02362.

[37] M. G. Walter *et al.*, “Solar Water Splitting Cells,” *Chem. Rev.*, vol. 110, no. 11, pp. 6446–6473, Nov. 2010, doi: 10.1021/cr1002326.

[38] M. E. Orazem and B. Tribollet, *Electrochemical Impedance Spectroscopy*, 1st ed. Wiley, 2017. doi: 10.1002/9781119363682.

[39] A. Ch. Lazanas and M. I. Prodromidis, “Electrochemical Impedance Spectroscopy─A Tutorial,” *ACS Meas. Sci. Au*, vol. 3, no. 3, pp. 162–193, Jun. 2023, doi: 10.1021/acsmeasuresciau.2c00070.

[40] G. J. Brug, A. L. G. Van Den Eeden, M. Sluyters-Rehbach, and J. H. Sluyters, “The analysis of electrode impedances complicated by the presence of a constant phase element,” *Journal of Electroanalytical Chemistry and Interfacial Electrochemistry*, vol. 176, no. 1–2, pp. 275–295, Sep. 1984, doi: 10.1016/S0022-0728(84)80324-1.

[41] C. H. Hsu and F. Mansfeld, "*Technical Note:* Concerning the Conversion of the Constant Phase Element Parameter Y into a Capacitance," *Corrosion*, vol. 57, no. 9, pp. 747–748, Sep. 2001, doi: 10.5006/1.3280607.

[42] L. M. Peter, "Energetics and kinetics of light-driven oxygen evolution at semiconductor electrodes: the example of hematite," *J Solid State Electrochem*, vol. 17, no. 2, pp. 315–326, Feb. 2013, doi: 10.1007/s10008-012-1957-3.

[43] S. Ravishankar, J. Bisquert, and T. Kirchartz, "Interpretation of Mott–Schottky plots of photoanodes for water splitting," *Chem. Sci.*, vol. 13, no. 17, pp. 4828–4837, 2022, doi: 10.1039/D1SC06401K.

[44] F. Fabregat-Santiago, G. Garcia-Belmonte, J. Bisquert, P. Bogdanoff, and A. Zaban, "Mott-Schottky Analysis of Nanoporous Semiconductor Electrodes in Dielectric State Deposited on SnO[sub 2](F) Conducting Substrates," *J. Electrochem. Soc.*, vol. 150, no. 6, p. E293, 2003, doi: 10.1149/1.1568741.

[45] K. Gelderman, L. Lee, and S. W. Donne, "Flat-Band Potential of a Semiconductor: Using the Mott–Schottky Equation," *J. Chem. Educ.*, vol. 84, no. 4, p. 685, Apr. 2007, doi: 10.1021/ed084p685.

[46] H. Shooshtari Gugtapeh, A. H. Aghaii, and A. Simchi, "Mott–Schottky Analysis in Semiconductor Electrochemistry: A Practical Guide with Hands-On Experiments," *J. Chem. Educ.*, vol. 102, no. 8, pp. 3567–3574, Aug. 2025, doi: 10.1021/acs.jchemed.5c00522.

[47] M. G. Ambartsumov, V. A. Tarala, E. V. Medyanik, V. V. Kovalenko, and O. M. Chapura, "Post-annealing microstructural evolution of titanium dioxide thin films grown by thermal and plasma-enhanced atomic layer deposition," *Applied Surface Science*, vol. 714, p. 164419, Dec. 2025, doi: 10.1016/j.apsusc.2025.164419.

[48] M. A. Henderson, "A surface science perspective on TiO2 photocatalysis," *Surface Science Reports*, vol. 66, no. 6–7, pp. 185–297, Jun. 2011, doi: 10.1016/j.surfrep.2011.01.001.

[49] F. R. Amalia, B. Ohtani, and E. Kowalska, "Spectrophotometric analysis: Challenge for a reliable evaluation of photocatalytic activity under visible light irradiation," *Journal of Photochemistry and Photobiology C: Photochemistry Reviews*, vol. 64, p. 100701, Aug. 2025, doi: 10.1016/j.jphotochemrev.2025.100701.

[50] U. Diebold, "The surface science of titanium dioxide," *Surface Science Reports*, vol. 48, no. 5–8, pp. 53–229, Jan. 2003, doi: 10.1016/S0167-5729(02)00100-0.

[51] A. Fujishima, T. N. Rao, and D. A. Tryk, "Titanium dioxide photocatalysis," *Journal of Photochemistry and Photobiology C: Photochemistry Reviews*, vol. 1, no. 1, pp. 1–21, Jun. 2000, doi: 10.1016/S1389-5567(00)00002-2.

[52] D. A. H. Hanaor and C. C. Sorrell, "Review of the anatase to rutile phase transformation," *J Mater Sci*, vol. 46, no. 4, pp. 855–874, Feb. 2011, doi: 10.1007/s10853-010-5113-0.

[53] C. Günnemann, C. Haisch, M. Fleisch, J. Schneider, A. V. Emeline, and D. W. Bahnemann, "Insights into Different Photocatalytic Oxidation Activities of Anatase, Brookite, and Rutile Single-Crystal Facets," *ACS Catal.*, vol. 9, no. 2, pp. 1001–1012, Feb. 2019, doi: 10.1021/acscatal.8b04115.

[54] D. C. Hurum, A. G. Agrios, K. A. Gray, T. Rajh, and M. C. Thurnauer, "Explaining the Enhanced Photocatalytic Activity of Degussa P25 Mixed-Phase TiO_2 Using EPR," *J. Phys. Chem. B*, vol. 107, no. 19, pp. 4545–4549, May 2003, doi: 10.1021/jp0273934.

[55] S. Cong and Y. Xu, "Explaining the High Photocatalytic Activity of a Mixed Phase TiO_2 : A Combined Effect of O_2 and Crystallinity," *J. Phys. Chem. C*, vol. 115, no. 43, pp. 21161–21168, Nov. 2011, doi: 10.1021/jp2055206.

[56] X. Jiang *et al.*, "Anatase and rutile in evonik aeroxide P25: Heterojunctioned or individual nanoparticles?," *Catalysis Today*, vol. 300, pp. 12–17, Feb. 2018, doi: 10.1016/j.cattod.2017.06.010.

[57] D. R. Eddy *et al.*, "Heterophase Polymorph of TiO2 (Anatase, Rutile, Brookite, TiO2 (B)) for Efficient Photocatalyst: Fabrication and Activity," *Nanomaterials*, vol. 13, no. 4, p. 704, Feb. 2023, doi: 10.3390/nano13040704.

[58] C. Jiang, S. J. A. Moniz, A. Wang, T. Zhang, and J. Tang, "Photoelectrochemical devices for solar water splitting – materials and challenges," *Chem. Soc. Rev.*, vol. 46, no. 15, pp. 4645–4660, 2017, doi: 10.1039/C6CS00306K.

[59] P. Argurio, E. Fontananova, R. Molinari, and E. Drioli, "Photocatalytic Membranes in Photocatalytic Membrane Reactors," *Processes*, vol. 6, no. 9, p. 162, Sep. 2018, doi: 10.3390/pr6090162.

[60] M. Barrande, R. Bouchet, and R. Denoyel, "Tortuosity of Porous Particles," *Anal. Chem.*, vol. 79, no. 23, pp. 9115–9121, Dec. 2007, doi: 10.1021/ac071377r.

[61] D. Quéré, “Wetting and Roughness,” *Annu. Rev. Mater. Res.*, vol. 38, no. 1, pp. 71–99, Aug. 2008, doi: 10.1146/annurev.matsci.38.060407.132434.

[62] E. Yablonovitch, “Statistical ray optics,” *J. Opt. Soc. Am.*, vol. 72, no. 7, p. 899, Jul. 1982, doi: 10.1364/JOSA.72.000899.

[63] R. Mupparapu, K. Vynck, T. Svensson, M. Burresi, and D. S. Wiersma, “Path length enhancement in disordered media for increased absorption,” *Opt. Express*, vol. 23, no. 24, p. A1472, Nov. 2015, doi: 10.1364/OE.23.0A1472.

[64] X. Zhang and S. John, “Photonic crystal light trapping for photocatalysis,” *Opt. Express*, vol. 29, no. 14, p. 22376, Jul. 2021, doi: 10.1364/OE.427218.

[65] T. Blachowicz and A. Ehrmann, “Optical Properties of Electrospun Nanofiber Mats,” *Membranes*, vol. 13, no. 4, p. 441, Apr. 2023, doi: 10.3390/membranes13040441.

[66] S. A. Heredia Deba, B. A. Wols, D. R. Yntema, and R. G. H. Lammertink, “Advanced ceramics in radical filtration: TiO2 layer thickness effect on the photocatalytic membrane performance,” *Journal of Membrane Science*, vol. 672, p. 121423, Apr. 2023, doi: 10.1016/j.memsci.2023.121423.

[67] Z. Vilamova *et al.*, “Enhancing photocatalytic g-C3N4/PVDF membranes through new insights into the preparation methods,” *Polymer*, vol. 307, p. 127238, Jul. 2024, doi: 10.1016/j.polymer.2024.127238.

[68] S. Kment *et al.*, “Photoanodes based on TiO_2 and α-Fe_2O_3 for solar water splitting – superior role of 1D nanoarchitectures and of combined heterostructures,” *Chem. Soc. Rev.*, vol. 46, no. 12, pp. 3716–3769, 2017, doi: 10.1039/C6CS00015K.

[69] P. Zhang, L. Gao, X. Song, and J. Sun, “Micro- and Nanostructures of Photoelectrodes for Solar-Driven Water Splitting,” *Advanced Materials*, vol. 27, no. 3, pp. 562–568, Jan. 2015, doi: 10.1002/adma.201402477.

[70] F. Fabregat-Santiago, G. Garcia-Belmonte, I. Mora-Seró, and J. Bisquert, “Characterization of nanostructured hybrid and organic solar cells by impedance spectroscopy,” *Phys. Chem. Chem. Phys.*, vol. 13, no. 20, p. 9083, 2011, doi: 10.1039/c0cp02249g.

[71] V. Miikkulainen, M. Leskelä, M. Ritala, and R. L. Puurunen, “Crystallinity of inorganic films grown by atomic layer deposition: Overview and general trends,” *Journal of Applied Physics*, vol. 113, no. 2, p. 021301, Jan. 2013, doi: 10.1063/1.4757907.

[72] V. Cremers, R. L. Puurunen, and J. Dendooven, “Conformality in atomic layer deposition: Current status overview of analysis and modelling,” *Applied Physics Reviews*, vol. 6, no. 2, p. 021302, Jun. 2019, doi: 10.1063/1.5060967.

[73] M. B. Chabalala, N. N. Gumbi, B. B. Mamba, M. Z. Al-Abri, and E. N. Nxumalo, “Photocatalytic Nanofiber Membranes for the Degradation of Micropollutants and Their Antimicrobial Activity: Recent Advances and Future Prospects,” *Membranes*, vol. 11, no. 9, p. 678, Aug. 2021, doi: 10.3390/membranes11090678.

[74] K. Shankar *et al.*, “Recent Advances in the Use of TiO_2 Nanotube and Nanowire Arrays for Oxidative Photoelectrochemistry,” *J. Phys. Chem. C*, vol. 113, no. 16, pp. 6327–6359, Apr. 2009, doi: 10.1021/jp809385x.

[75] S. Kirkpatrick, “Percolation and Conduction,” *Rev. Mod. Phys.*, vol. 45, no. 4, pp. 574–588, Oct. 1973, doi: 10.1103/RevModPhys.45.574.

[76] D. Stauffer and A. Aharony, *Introduction To Percolation Theory*, 0 ed. Taylor & Francis, 2018. doi: 10.1201/9781315274386.

[77] A. Vilanova, P. Dias, T. Lopes, and A. Mendes, “The route for commercial photoelectrochemical water splitting: a review of large-area devices and key upscaling challenges,” *Chem. Soc. Rev.*, vol. 53, no. 5, pp. 2388–2434, 2024, doi: 10.1039/D1CS01069G.

[78] E. W. Washburn, “The Dynamics of Capillary Flow,” *Phys. Rev.*, vol. 17, no. 3, pp. 273–283, Mar. 1921, doi: 10.1103/PhysRev.17.273.

[79] M. Binazadeh, J. Rasouli, S. Sabbaghi, S. M. Mousavi, S. A. Hashemi, and C. W. Lai, “An Overview of Photocatalytic Membrane Degradation Development,” *Materials*, vol. 16, no. 9, p. 3526, May 2023, doi: 10.3390/ma16093526.

[80] R. Xu, S. Qin, T. Lu, S. Wang, J. Chen, and Z. He, “Engineering Photocatalytic Membrane Reactors for Sustainable Energy and Environmental Applications,” *Catalysts*, vol. 15, no. 10, p. 947, Oct. 2025, doi: 10.3390/catal15100947.

[81] J. T. Gostick, M. A. Ioannidis, M. W. Fowler, and M. D. Pritzker, “Wettability and capillary behavior of fibrous gas diffusion media for polymer electrolyte membrane fuel cells,” *Journal of Power Sources*, vol. 194, no. 1, pp. 433–444, Oct. 2009, doi: 10.1016/j.jpowsour.2009.04.052.

[82] K. C. Kim, X. Lin, and C. Li, “Structural design of the electrospun nanofibrous membrane for membrane distillation application: a review,” *Environ Sci Pollut Res*, vol. 29, no. 55, pp. 82632–82659, Nov. 2022, doi: 10.1007/s11356-022-23066-w.

[83] A. Angulo, P. Van Der Linde, H. Gardeniers, M. Modestino, and D. Fernández Rivas, “Influence of Bubbles on the Energy Conversion Efficiency of Electrochemical Reactors,” *Joule*, vol. 4, no. 3, pp. 555–579, Mar. 2020, doi: 10.1016/j.joule.2020.01.005.

[84] F. Sepahi, R. Verzicco, D. Lohse, and D. Krug, “Mass transport at gas-evolving electrodes,” *J. Fluid Mech.*, vol. 983, p. A19, Mar. 2024, doi: 10.1017/jfm.2024.51.

[85] C. S. Turchi and D. F. Ollis, “Comment. Photocatalytic reactor design: an example of mass-transfer limitations with an immobilized catalyst,” *J. Phys. Chem.*, vol. 92, no. 23, pp. 6852–6853, Nov. 1988, doi: 10.1021/j100334a070.

[86] A. Visan, J. R. Van Ommen, M. T. Kreutzer, and R. G. H. Lammertink, “Photocatalytic Reactor Design: Guidelines for Kinetic Investigation,” *Ind. Eng. Chem. Res.*, vol. 58, no. 14, pp. 5349–5357, Apr. 2019, doi: 10.1021/acs.iecr.9b00381.

[87] S. Ahmadi, J. M. Quimbayo, V. B. K. Yaah, S. B. De Oliveira, and S. Ojala, “A critical review on combining adsorption and photocatalysis in composite materials for pharmaceutical removal: Pros and cons, scalability, TRL, and sustainability,” *Energy Nexus*, vol. 17, p. 100396, Mar. 2025, doi: 10.1016/j.nexus.2025.100396.

[88] J. Zhang, L. Li, and H. Li, “Adsorption-Controlled Wettability and Self-Cleaning of TiO_2,” *Langmuir*, vol. 39, no. 17, pp. 6188–6200, May 2023, doi: 10.1021/acs.langmuir.3c00324.

[89] A. Manassero, M. L. Satuf, and O. M. Alfano, “Photocatalytic reactors with suspended and immobilized TiO2: Comparative efficiency evaluation,” *Chemical Engineering Journal*, vol. 326, pp. 29–36, Oct. 2017, doi: 10.1016/j.cej.2017.05.087.

[90] M. F. J. Dijkstra, E. C. B. Koerts, A. A. C. M. Beenackers, and J. A. Wesselingh, “Performance of immobilized photocatalytic reactors in continuous mode,” *AIChE Journal*, vol. 49, no. 3, pp. 734–744, Mar. 2003, doi: 10.1002/aic.690490317.

[91] A. Y. Shan, T. I. Mohd. Ghazi, and S. A. Rashid, “Immobilisation of titanium dioxide onto supporting materials in heterogeneous photocatalysis: A review,” *Applied Catalysis A: General*, vol. 389, no. 1–2, pp. 1–8, Dec. 2010, doi: 10.1016/j.apcata.2010.08.053.

[92] H. M. Samuel, C. A. Mecha, N. Kipchumba, and Z. A. Suliman, “Recent advances in photocatalytic membrane reactors, technological readiness and progress towards industrial scale adoption,” *Journal of Water Process Engineering*, vol. 80, p. 109172, Dec. 2025, doi: 10.1016/j.jwpe.2025.109172.

[93] K. Azrague, E. Puechcostes, P. Aimar, M. Maurette, and F. Benoitmarquie, “Membrane photoreactor (MPR) for the mineralisation of organic pollutants from turbid effluents,” *Journal of Membrane Science*, vol. 258, no. 1–2, pp. 71–77, Aug. 2005, doi: 10.1016/j.memsci.2005.02.027.

[94] A. H. Oleiwi, A. R. Jabur, and Q. F. Alsalhy, “Electrospinning technology in water treatment applications: Review article,” *Desalination and Water Treatment*, vol. 322, p. 101175, Apr. 2025, doi: 10.1016/j.dwt.2025.101175.

[95] M. E. Leblebici, G. D. Stefanidis, and T. Van Gerven, “Comparison of photocatalytic space-time yields of 12 reactor designs for wastewater treatment,” *Chemical Engineering and Processing: Process Intensification*, vol. 97, pp. 106–111, Nov. 2015, doi: 10.1016/j.cep.2015.09.009.

[96] K. P. Sundar and S. Kanmani, “Progression of Photocatalytic reactors and it’s comparison: A Review,” *Chemical Engineering Research and Design*, vol. 154, pp. 135–150, Feb. 2020, doi: 10.1016/j.cherd.2019.11.035.

[97] S. Reghunath, D. Pinheiro, and S. D. Kr, “A review of hierarchical nanostructures of TiO2: Advances and applications,” *Applied Surface Science Advances*, vol. 3, p. 100063, Mar. 2021, doi: 10.1016/j.apsadv.2021.100063.

[98] W. Zhang, Y. Tian, H. He, L. Xu, W. Li, and D. Zhao, “Recent advances in the synthesis of hierarchically mesoporous TiO2 materials for energy and environmental applications,” *National Science Review*, vol. 7, no. 11, pp. 1702–1725, Nov. 2020, doi: 10.1093/nsr/nwaa021.

[99] Z. Ren, Y. Guo, C.-H. Liu, and P.-X. Gao, “Hierarchically nanostructured materials for sustainable environmental applications,” *Front. Chem.*, vol. 1, 2013, doi: 10.3389/fchem.2013.00018.

[100] S. M. George, “Atomic Layer Deposition: An Overview,” *Chem. Rev.*, vol. 110, no. 1, pp. 111–131, Jan. 2010, doi: 10.1021/cr900056b.

[101] H. Sudrajat and M. Nobatova, “Heterojunction photocatalysts: where are they headed?,” *RSC Appl. Interfaces*, vol. 2, no. 3, pp. 599–619, 2025, doi: 10.1039/D5LF00037H.

[102] S. J. A. Zaidi *et al.*, “Interfaces in Atomic Layer Deposited Films: Opportunities and Challenges,” *Small Science*, vol. 3, no. 10, p. 2300060, Oct. 2023, doi: 10.1002/smsc.202300060.

[103] X. He, T. Kai, and P. Ding, “Heterojunction photocatalysts for degradation of the tetracycline antibiotic: a review,” *Environ Chem Lett*, vol. 19, no. 6, pp. 4563–4601, Dec. 2021, doi: 10.1007/s10311-021-01295-8.

[104] R. L. Puurunen, “Surface chemistry of atomic layer deposition: A case study for the trimethylaluminum/water process,” *Journal of Applied Physics*, vol. 97, no. 12, p. 121301, Jun. 2005, doi: 10.1063/1.1940727.

[105] J. W. Elam, D. Routkevitch, P. P. Mardilovich, and S. M. George, “Conformal Coating on Ultrahigh-Aspect-Ratio Nanopores of Anodic Alumina by Atomic Layer Deposition,” *Chem. Mater.*, vol. 15, no. 18, pp. 3507–3517, Sep. 2003, doi: 10.1021/cm0303080.

[106] X. Zhou *et al.*, “Interface engineering of the photoelectrochemical performance of Ni-oxide-coated n-Si photoanodes by atomic-layer deposition of ultrathin films of cobalt oxide,” *Energy Environ. Sci.*, vol. 8, no. 9, pp. 2644–2649, 2015, doi: 10.1039/C5EE01687H.

[107] M. Leskelä and M. Ritala, “Atomic Layer Deposition Chemistry: Recent Developments and Future Challenges,” *Angew Chem Int Ed*, vol. 42, no. 45, pp. 5548–5554, Nov. 2003, doi: 10.1002/anie.200301652.

[108] R. W. Johnson, A. Hultqvist, and S. F. Bent, “A brief review of atomic layer deposition: from fundamentals to applications,” *Materials Today*, vol. 17, no. 5, pp. 236–246, Jun. 2014, doi: 10.1016/j.mattod.2014.04.026.

[109] T. Onn, R. Küngas, P. Fornasiero, K. Huang, and R. Gorte, “Atomic Layer Deposition on Porous Materials: Problems with Conventional Approaches to Catalyst and Fuel Cell Electrode Preparation,” *Inorganics*, vol. 6, no. 1, p. 34, Mar. 2018, doi: 10.3390/inorganics6010034.

[110] N. K. R. Eswar, S. A. Singh, and J. Heo, “Atomic layer deposited photocatalysts: comprehensive review on viable fabrication routes and reactor design approaches for photo-mediated redox reactions,” *J. Mater. Chem. A*, vol. 7, no. 30, pp. 17703–17734, 2019, doi: 10.1039/C9TA04780H.

[111] P. O. Oviroh, R. Akbarzadeh, D. Pan, R. A. M. Coetzee, and T.-C. Jen, “New development of atomic layer deposition: processes, methods and applications,” *Science and Technology of Advanced Materials*, vol. 20, no. 1, pp. 465–496, Dec. 2019, doi: 10.1080/14686996.2019.1599694.

[112] S. Ng, R. Zazpe, J. Rodriguez-Pereira, J. Michalička, J. M. Macak, and M. Pumera, “Atomic layer deposition of photoelectrocatalytic material on 3D-printed nanocarbon structures,” *J. Mater. Chem. A*, vol. 9, no. 18, pp. 11405–11414, 2021, doi: 10.1039/D1TA01467F.

[113] R. L. Puurunen and W. Vandervorst, “Island growth as a growth mode in atomic layer deposition: A phenomenological model,” *Journal of Applied Physics*, vol. 96, no. 12, pp. 7686–7695, Dec. 2004, doi: 10.1063/1.1810193.

[114] J. Bisquert, “Physical electrochemistry of nanostructured devices,” *Phys. Chem. Chem. Phys.*, vol. 10, no. 1, pp. 49–72, 2008, doi: 10.1039/B709316K.

[115] X. Shen *et al.*, “Comprehensive Evaluation for Protective Coatings: Optical, Electrical, Photoelectrochemical, and Spectroscopic Characterizations,” *Front. Energy Res.*, vol. 9, p. 799776, Jan. 2022, doi: 10.3389/fenrg.2021.799776.

[116] T. Moehl, J. Suh, L. Sévery, R. Wick-Joliat, and S. D. Tilley, “Investigation of (Leaky) ALD TiO_2 Protection Layers for Water-Splitting Photoelectrodes,” *ACS Appl. Mater. Interfaces*, vol. 9, no. 50, pp. 43614–43622, Dec. 2017, doi: 10.1021/acsami.7b12564.

[117] M. Hannula, H. Ali-Löytty, K. Lahtonen, E. Sarlin, J. Saari, and M. Valden, “Improved Stability of Atomic Layer Deposited Amorphous TiO_2 Photoelectrode Coatings by Thermally Induced Oxygen Defects,” *Chem. Mater.*, vol. 30, no. 4, pp. 1199–1208, Feb. 2018, doi: 10.1021/acs.chemmater.7b02938.

[118] X. Wang, Z. Zhao, C. Zhang, Q. Li, and X. Liang, “Surface Modification of Catalysts via Atomic Layer Deposition for Pollutants Elimination,” *Catalysts*, vol. 10, no. 11, p. 1298, Nov. 2020, doi: 10.3390/catal10111298.

[119] S. S. Mali, C. S. Shim, H. K. Park, J. Heo, P. S. Patil, and C. K. Hong, “Ultrathin Atomic Layer Deposited TiO_2 for Surface Passivation of Hydrothermally Grown 1D TiO_2 Nanorod Arrays for Efficient Solid-State Perovskite Solar Cells,” *Chem. Mater.*, vol. 27, no. 5, pp. 1541–1551, Mar. 2015, doi: 10.1021/cm504558g.

[120] J.-P. Niemelä, G. Marin, and M. Karppinen, “Titanium dioxide thin films by atomic layer deposition: a review,” *Semicond. Sci. Technol.*, vol. 32, no. 9, p. 093005, Sep. 2017, doi: 10.1088/1361-6641/aa78ce.

[121] M. Heikkilä, E. Puukilainen, M. Ritala, and M. Leskelä, “Effect of thickness of ALD grown TiO2 films on photoelectrocatalysis,” *Journal of Photochemistry and Photobiology A: Chemistry*, vol. 204, no. 2–3, pp. 200–208, May 2009, doi: 10.1016/j.jphotochem.2009.03.019.

[122] O. M. E. Ylivaara *et al.*, “Mechanical and optical properties of as-grown and thermally annealed titanium dioxide from titanium tetrachloride and water by atomic layer deposition,” *Thin Solid Films*, vol. 732, p. 138758, Aug. 2021, doi: 10.1016/j.tsf.2021.138758.

[123] S. O. Kucheyev *et al.*, “Mechanisms of Atomic Layer Deposition on Substrates with Ultrahigh Aspect Ratios,” *Langmuir*, vol. 24, no. 3, pp. 943–948, Feb. 2008, doi: 10.1021/la7018617.

[124] J. Yim, E. Verkama, J. A. Velasco, K. Arts, and R. L. Puurunen, “Conformality of atomic layer deposition in microchannels: impact of process parameters on the simulated thickness profile,” *Phys. Chem. Chem. Phys.*, vol. 24, no. 15, pp. 8645–8660, 2022, doi: 10.1039/D1CP04758B.

[125] F. Gao, S. Arpiainen, and R. L. Puurunen, “Microscopic silicon-based lateral high-aspect-ratio structures for thin film conformality analysis,” *Journal of Vacuum Science & Technology A: Vacuum, Surfaces, and Films*, vol. 33, no. 1, p. 010601, Jan. 2015, doi: 10.1116/1.4903941.

[126] J. Saari, H. Ali-Löytty, M. Honkanen, A. Tukiainen, K. Lahtonen, and M. Valden, “Interface Engineering of TiO_2 Photoelectrode Coatings Grown by Atomic Layer Deposition on Silicon,” *ACS Omega*, vol. 6, no. 41, pp. 27501–27509, Oct. 2021, doi: 10.1021/acsomega.1c04478.

[127] D. H. Wi *et al.*, “Impact of the Atomic Structure at the $BiVO_4$ /TiO_2 Interface on the Electronic Properties and Performance of $BiVO_4$ /TiO_2 Photoanodes,” *J. Am. Chem. Soc.*, vol. 147, no. 34, pp. 30851–30862, Aug. 2025, doi: 10.1021/jacs.5c07695.

[128] B. Gupta *et al.*, “Recent Advances in Materials Design Using Atomic Layer Deposition for Energy Applications,” *Adv Funct Materials*, vol. 32, no. 3, p. 2109105, Jan. 2022, doi: 10.1002/adfm.202109105.

[129] A. I. Abdulagatov *et al.*, “$Al_2 O_3$ and TiO_2 Atomic Layer Deposition on Copper for Water Corrosion Resistance,” *ACS Appl. Mater. Interfaces*, vol. 3, no. 12, pp. 4593–4601, Dec. 2011, doi: 10.1021/am2009579.

[130] J.-H. Kim, H.-J. Kil, S. Lee, J. Park, and J.-W. Park, “Interfacial Delamination at Multilayer Thin Films in Semiconductor Devices,” *ACS Omega*, vol. 7, no. 29, pp. 25219–25228, Jul. 2022, doi: 10.1021/acsomega.2c02122.

[131] A. H. Behroozi, V. Vatanpour, L. Meunier, M. Mehrabi, and E. H. Koupaie, “Membrane Fabrication and Modification by Atomic Layer Deposition: Processes and Applications in Water Treatment and Gas Separation,” *ACS Appl. Mater. Interfaces*, p. acsami.2c22627, Mar. 2023, doi: 10.1021/acsami.2c22627.

[132] F. Dvorak *et al.*, “One-dimensional anodic TiO2 nanotubes coated by atomic layer deposition: Towards advanced applications,” *Applied Materials Today*, vol. 14, pp. 1–20, Mar. 2019, doi: 10.1016/j.apmt.2018.11.005.

[133] R. Zazpe *et al.*, “Atomic Layer Deposition for Coating of High Aspect Ratio TiO_2 Nanotube Layers,” *Langmuir*, vol. 32, no. 41, pp. 10551–10558, Oct. 2016, doi: 10.1021/acs.langmuir.6b03119.

[134] A. Lys, I. Gnilitskyi, E. Coy, M. Jancelewicz, M. Bechelany, and I. Iatsunskyi, “Hierarchically Structured Ti-TiO_2 Membranes Fabricated by Femtosecond Laser Ablation and Atomic Layer Deposition for Enhanced Photoelectrochemical Water Splitting,” *ACS Appl. Mater. Interfaces*, vol. 17, no. 30, pp. 43390–43402, Jul. 2025, doi: 10.1021/acsami.5c07488.

[135] A. S. Alotabi *et al.*, “A Comprehensive Review of the Role of Overlayers in Photocatalytic Overall Water Splitting and Related Reactions,” *Chem. Rev.*, vol. 126, no. 5, pp. 2801–2845, Mar. 2026, doi: 10.1021/acs.chemrev.5c00326.

[136] D. Ma *et al.*, “Rational design of CdS@ZnO core-shell structure via atomic layer deposition for drastically enhanced photocatalytic H2 evolution with excellent photostability,” *Nano Energy*, vol. 39, pp. 183–191, Sep. 2017, doi: 10.1016/j.nanoen.2017.06.047.

[137] D. A. Karajz and I. M. Szilágyi, “Review of photocatalytic ZnO nanomaterials made by atomic layer deposition,” *Surfaces and Interfaces*, vol. 40, p. 103094, Aug. 2023, doi: 10.1016/j.surfin.2023.103094.

[138] D. Muñoz-Rojas and J. MacManus-Driscoll, “Spatial atmospheric atomic layer deposition: a new laboratory and industrial tool for low-cost photovoltaics,” *Mater. Horiz.*, vol. 1, no. 3, pp. 314–320, 2014, doi: 10.1039/C3MH00136A.

[139] D. Muñoz-Rojas, V. H. Nguyen, C. Masse De La Huerta, S. Aghazadehchors, C. Jiménez, and D. Bellet, “Spatial Atomic Layer Deposition (SALD), an emerging tool for energy materials. Application to new-generation photovoltaic devices and transparent conductive materials,” *Comptes Rendus. Physique*, vol. 18, no. 7–8, pp. 391–400, Sep. 2017, doi: 10.1016/j.crhy.2017.09.004.

[140] K. Sugioka and Y. Cheng, “Ultrafast lasers—reliable tools for advanced materials processing,” *Light Sci Appl*, vol. 3, no. 4, pp. e149–e149, Apr. 2014, doi: 10.1038/lsa.2014.30.

[141] J. Kwon, S. Ko, H. Kim, H. J. Park, C. Lee, and J. Yeo, “Recent advances in vacuum- and laser-based fabrication processes for solar water-splitting cells,” *Mater. Chem. Front.*, vol. 8, no. 11, pp. 2322–2340, 2024, doi: 10.1039/D3QM01336G.

[142] X. Sheng, T. Xu, and X. Feng, “Rational Design of Photoelectrodes with Rapid Charge Transport for Photoelectrochemical Applications,” *Advanced Materials*, vol. 31, no. 11, p. 1805132, Mar. 2019, doi: 10.1002/adma.201805132.

[143] D. Bialuschewski *et al.*, “Laser-Textured Metal Substrates as Photoanodes for Enhanced PEC Water Splitting Reactions,” *Adv Eng Mater*, vol. 20, no. 9, p. 1800167, Sep. 2018, doi: 10.1002/adem.201800167.

[144] A. Polman and H. A. Atwater, “Photonic design principles for ultrahigh-efficiency photovoltaics,” *Nature Mater*, vol. 11, no. 3, pp. 174–177, Mar. 2012, doi: 10.1038/nmat3263.

[145] X. Liu, P. R. Coxon, M. Peters, B. Hoex, J. M. Cole, and D. J. Fray, “Black silicon: fabrication methods, properties and solar energy applications,” *Energy Environ. Sci.*, vol. 7, no. 10, pp. 3223–3263, 2014, doi: 10.1039/C4EE01152J.

[146] A. O. Ijaola *et al.*, “Wettability Transition for Laser Textured Surfaces: A Comprehensive Review,” *Surfaces and Interfaces*, vol. 21, p. 100802, Dec. 2020, doi: 10.1016/j.surfin.2020.100802.

[147] G. Liu, W. S. Y. Wong, M. Kraft, J. W. Ager, D. Vollmer, and R. Xu, “Wetting-regulated gas-involving (photo)electrocatalysis: biomimetics in energy conversion,” *Chem. Soc. Rev.*, vol. 50, no. 18, pp. 10674–10699, 2021, doi: 10.1039/D1CS00258A.

[148] H. Vaghasiya and P.-T. Miclea, “Investigating Laser-Induced Periodic Surface Structures (LIPSS) Formation in Silicon and Their Impact on Surface-Enhanced Raman Spectroscopy (SERS),” *Optics*, vol. 4, no. 4, pp. 538–550, Oct. 2023, doi: 10.3390/opt4040039.

[149] J. Bonse and S. Gräf, “Maxwell Meets Marangoni—A Review of Theories on Laser-Induced Periodic Surface Structures,” *Laser & Photonics Reviews*, vol. 14, no. 10, p. 2000215, Oct. 2020, doi: 10.1002/lpor.202000215.

[150] C. Florian, S. V. Kirner, J. Krüger, and J. Bonse, “Surface functionalization by laser-induced periodic surface structures,” *Journal of Laser Applications*, vol. 32, no. 2, p. 022063, May 2020, doi: 10.2351/7.0000103.

[151] M. Liang *et al.*, “Femtosecond laser mediated fabrication of micro/nanostructured TiO2- photoelectrodes: Hierarchical nanotubes array with oxygen vacancies and their photocatalysis properties,” *Applied Catalysis B: Environmental*, vol. 277, p. 119231, Nov. 2020, doi: 10.1016/j.apcatb.2020.119231.

[152] F. D. Ince and T. Özel, “Laser surface texturing of materials for surface functionalization: A holistic review,” *Surface and Coatings Technology*, vol. 498, p. 131818, Feb. 2025, doi: 10.1016/j.surfcoat.2025.131818.

[153] A. Samanta, W. Huang, H. Chaudhry, Q. Wang, S. K. Shaw, and H. Ding, “Design of Chemical Surface Treatment for Laser-Textured Metal Alloys to Achieve Extreme Wetting Behavior,” *ACS Appl. Mater. Interfaces*, vol. 12, no. 15, pp. 18032–18045, Apr. 2020, doi: 10.1016/j.surfcoat.2021.127219.

[154] S. Nolte *et al.*, “Ablation of metals by ultrashort laser pulses,” *J. Opt. Soc. Am. B*, vol. 14, no. 10, p. 2716, Oct. 1997, doi: 10.1364/JOSAB.14.002716.

[155] D. J. Förster, B. Jäggi, A. Michalowski, and B. Neuenschwander, “Review on Experimental and Theoretical Investigations of Ultra-Short Pulsed Laser Ablation of Metals with Burst Pulses,” *Materials*, vol. 14, no. 12, p. 3331, Jun. 2021, doi: 10.3390/ma14123331.

[156] E. R. Moldovan *et al.*, “Wettability and Surface Roughness Analysis of Laser Surface Texturing of AISI 430 Stainless Steel,” *Materials*, vol. 15, no. 8, p. 2955, Apr. 2022, doi: 10.3390/ma15082955.

[157] Z. Zhang, T. Zhao, M. Liu, and L. Jiang, “Superwetting Catalysts: Principle, Design, and Synthesis,” *Advanced Materials*, vol. 37, no. 51, p. 2506058, Dec. 2025, doi: 10.1002/adma.202506058.

[158] Z. Wang, Y. Liu, and V. M. Linkov, “The influence of catalyst layer morphology on the electrochemical performance of DMFC anode,” *Journal of Power Sources*, vol. 160, no. 1, pp. 326–333, Sep. 2006, doi: 10.1016/j.jpowsour.2006.01.056.

[159] G. Stelmacovich and S. Pylypenko, “Characterization of Porous Transport Layers Towards the Development of Efficient Proton Exchange Membrane Water Electrolysis,” *ChemElectroChem*, vol. 11, no. 20, p. e202400377, Oct. 2024, doi: 10.1002/celc.202400377.

[160] Y. Liu, Q. Diankai, Z. Xu, P. Yi, and L. Peng, “Comprehensive Analysis of the Gradient Porous Transport Layer for the Proton-Exchange Membrane Electrolyzer,” *ACS Appl. Mater. Interfaces*, vol. 16, no. 36, pp. 47357–47367, Sep. 2024, doi: 10.1021/acsami.4c00006.

[161] D. Kuczyńska-Zemła, A. Sotniczuk, M. Pisarek, A. Chlanda, and H. Garbacz, “Corrosion behavior of titanium modified by direct laser interference lithography,” *Surface and Coatings Technology*, vol. 418, p. 127219, Jul. 2021, doi: 10.1016/j.surfcoat.2021.127219.

[162] Z. Liu, T. Niu, Y. Lei, and Y. Luo, “Metal surface wettability modification by nanosecond laser surface texturing: A review,” *Biosurface and Biotribology*, vol. 8, no. 2, pp. 95–120, Jun. 2022, doi: 10.1049/bsb2.12039.

[163] R. Said *et al.*, “Navigating the complexities of electrocatalytic water splitting: a critical examination of pitfalls and considerations in performance evaluation,” *Electrochemistry Communications*, vol. 182, p. 108094, Jan. 2026, doi: 10.1016/j.elecom.2025.108094.

[164] D. M. Callahan, J. N. Munday, and H. A. Atwater, “Solar Cell Light Trapping beyond the Ray Optic Limit,” *Nano Lett.*, vol. 12, no. 1, pp. 214–218, Jan. 2012, doi: 10.1021/nl203351k.

[165] S. Sharma *et al.*, “Review of Laser-Based Surface Nanotexturing for Enhanced Light Absorption and Photoelectrochemical Water Splitting,” *ACS Appl. Nano Mater.*, vol. 7, no. 16, pp. 18367–18378, Aug. 2024, doi: 10.1021/acsanm.3c04083.

[166] T. Fox *et al.*, “Single-step Production of Photocatalytic Surfaces via Direct Laser Interference Patterning of Titanium,” *ChemNanoMat*, vol. 9, no. 10, p. e202300314, Oct. 2023, doi: 10.1002/cnma.202300314.

[167] J. Bonse and S. Gräf, “Ten Open Questions about Laser-Induced Periodic Surface Structures,” *Nanomaterials*, vol. 11, no. 12, p. 3326, Dec. 2021, doi: 10.3390/nano11123326.

[168] T. Giannakis *et al.*, “Enhancing the Photocatalytic Activity of Immobilized TiO2 Using Laser-Micropatterned Surfaces,” *Applied Sciences*, vol. 14, no. 7, p. 3033, Apr. 2024, doi: 10.3390/app14073033.

[169] M. Zou *et al.*, “Preparation and photocatalytic properties of TiO2 based on burst-mode femtosecond laser and anodization,” *Optical Materials*, vol. 159, p. 116649, Feb. 2025, doi: 10.1016/j.optmat.2025.116649.

[170] K. Bronnikov *et al.*, “Highly Regular Laser-Induced Periodic Surface Structures on Titanium Thin Films for Photonics and Fiber Optics,” *ACS Appl. Mater. Interfaces*, vol. 16, no. 50, pp. 70047–70056, Dec. 2024, doi: 10.1021/acsami.4c15455.

[171] M. Qiao *et al.*, “Femtosecond Laser Induced Phase Transformation of TiO_2 with Exposed Reactive Facets for Improved Photoelectrochemistry Performance,” *ACS Appl. Mater. Interfaces*, vol. 12, no. 37, pp. 41250–41258, Sep. 2020, doi: 10.1021/acsami.0c10026.

[172] H. Kisch, “Semiconductor Photocatalysis—Mechanistic and Synthetic Aspects,” *Angew Chem Int Ed*, vol. 52, no. 3, pp. 812–847, Jan. 2013, doi: 10.1002/anie.201201200.

[173] Y. Tachibana, L. Vayssieres, and J. R. Durrant, “Artificial photosynthesis for solar water-splitting,” *Nature Photon*, vol. 6, no. 8, pp. 511–518, Aug. 2012, doi: 10.1038/nphoton.2012.175.

[174] T. Hisatomi, J. Kubota, and K. Domen, “Recent advances in semiconductors for photocatalytic and photoelectrochemical water splitting,” *Chem. Soc. Rev.*, vol. 43, no. 22, pp. 7520–7535, Jan. 2014, doi: 10.1039/C3CS60378D.

[175] L. Zhang and M. Jaroniec, “Toward designing semiconductor-semiconductor heterojunctions for photocatalytic applications,” *Applied Surface Science*, vol. 430, pp. 2–17, Feb. 2018, doi: 10.1016/j.apsusc.2017.07.192.

[176] J. A. Seabold and K.-S. Choi, “Efficient and Stable Photo-Oxidation of Water by a Bismuth Vanadate Photoanode Coupled with an Iron Oxyhydroxide Oxygen Evolution Catalyst,” *J. Am. Chem. Soc.*, vol. 134, no. 4, pp. 2186–2192, Feb. 2012, doi: 10.1021/ja209001d.

[177] M. Grätzel, “Photoelectrochemical cells,” *Nature*, vol. 414, no. 6861, pp. 338–344, Nov. 2001, doi: 10.1038/35104607.

[178] W. Xu, J. S. Kong, Y.-T. E. Yeh, and P. Chen, “Single-molecule nanocatalysis reveals heterogeneous reaction pathways and catalytic dynamics,” *Nature Mater*, vol. 7, no. 12, pp. 992–996, Dec. 2008, doi: 10.1038/nmat2319.

[179] J. Low, J. Yu, M. Jaroniec, S. Wageh, and A. A. Al-Ghamdi, “Heterojunction Photocatalysts,” *Advanced Materials*, vol. 29, no. 20, p. 1601694, May 2017, doi: 10.1002/adma.201601694.

[180] Y. Yuan *et al.*, “A review of metal oxide-based Z-scheme heterojunction photocatalysts: actualities and developments,” *Materials Today Energy*, vol. 21, p. 100829, Sep. 2021, doi: 10.1016/j.mtener.2021.100829.

[181] J. Low, C. Jiang, B. Cheng, S. Wageh, A. A. Al-Ghamdi, and J. Yu, “A Review of Direct Z-Scheme Photocatalysts,” *Small Methods*, vol. 1, no. 5, p. 1700080, May 2017, doi: 10.1002/smtd.201700080.

[182] L. Zhang and M. Jaroniec, “Toward designing semiconductor-semiconductor heterojunctions for photocatalytic applications,” *Applied Surface Science*, vol. 430, pp. 2–17, Feb. 2018, doi: 10.1016/j.apsusc.2017.07.192.

[183] S. Linic, U. Aslam, C. Boerigter, and M. Morabito, “Photochemical transformations on plasmonic metal nanoparticles,” *Nature Mater*, vol. 14, no. 6, pp. 567–576, Jun. 2015, doi: 10.1038/nmat4281.

[184] Y. Zhang *et al.*, “Surface-Plasmon-Driven Hot Electron Photochemistry,” *Chem. Rev.*, vol. 118, no. 6, pp. 2927–2954, Mar. 2018, doi: 10.1021/acs.chemrev.7b00430.

[185] J.-M. Herrmann, “Heterogeneous photocatalysis: fundamentals and applications to the removal of various types of aqueous pollutants,” *Catalysis Today*, vol. 53, no. 1, pp. 115–129, Oct. 1999, doi: 10.1016/S0920-5861(99)00107-8.

[186] E. Kusiak-Nejman, A. Sienkiewicz, A. Wanag, P. Rokicka-Konieczna, and A. W. Morawski, “The Role of Adsorption in the Photocatalytic Decomposition of Dyes on APTES-Modified TiO2 Nanomaterials,” *Catalysts*, vol. 11, no. 2, p. 172, Jan. 2021, doi: 10.3390/catal11020172.

[187] J. Diaz-Angulo, I. Gomez-Bonilla, C. Jimenez-Tohapanta, M. Mueses, M. Pinzon, and F. Machuca-Martinez, “Visible-light activation of TiO2 by dye-sensitization for degradation of pharmaceutical compounds,” *Photochem Photobiol Sci*, vol. 18, no. 4, pp. 897–904, Apr. 2019, doi: 10.1039/c8pp00270c.

[188] S. Khan, T. Noor, N. Iqbal, and L. Yaqoob, “Photocatalytic Dye Degradation from Textile Wastewater: A Review,” *ACS Omega*, vol. 9, no. 20, pp. 21751–21767, May 2024, doi: 10.1021/acsomega.4c00887.

[189] S. P.-G. Khumalo, D. Lokhat, C. J.-T. Anwar, and H. Reddy, “Synthesis of Iron on Carbon Foam for Use in the Removal of Phenol from Aqueous Solutions,” *Molecules*, vol. 28, no. 3, p. 1272, Jan. 2023, doi: 10.3390/molecules28031272.

[190] X. Li *et al.*, “Applications of MXene ($Ti_3 C_2 T_x$) in photocatalysis: a review,” *Mater. Adv.*, vol. 2, no. 5, pp. 1570–1594, 2021, doi: 10.1039/D0MA00938E.

[191] D. Klotz, D. A. Grave, H. Dotan, and A. Rothschild, “Empirical Analysis of the Photoelectrochemical Impedance Response of Hematite Photoanodes for Water Photo-oxidation,” *J. Phys. Chem. Lett.*, vol. 9, no. 6, pp. 1466–1472, Mar. 2018, doi: 10.1021/acs.jpclett.8b00096.

[192] L. M. Peter, A. B. Walker, T. Bein, A. G. Hufnagel, and I. Kondofersky, “Interpretation of photocurrent transients at semiconductor electrodes: Effects of band-edge unpinning,” *Journal of Electroanalytical Chemistry*, vol. 872, p. 114234, Sep. 2020, doi: 10.1016/j.jelechem.2020.114234.

[193] S. R. Pendlebury *et al.*, “Correlating long-lived photogenerated hole populations with photocurrent densities in hematite water oxidation photoanodes,” *Energy Environ. Sci.*, vol. 5, no. 4, pp. 6304–6312, 2012, doi: 10.1039/C1EE02567H.

[194] C. Ros, N. M. Carretero, J. David, J. Arbiol, T. Andreu, and J. R. Morante, “Insight into the Degradation Mechanisms of Atomic Layer Deposited TiO_2 as Photoanode Protective Layer,” *ACS Appl. Mater. Interfaces*, vol. 11, no. 33, pp. 29725–29735, Aug. 2019, doi: 10.1021/acsami.9b05724.

[195] H. Wang *et al.*, “Semiconductor heterojunction photocatalysts: design, construction, and photocatalytic performances,” *Chem. Soc. Rev.*, vol. 43, no. 15, p. 5234, Jul. 2014, doi: 10.1039/C4CS00126E.

[196] S. Wen and Y. Huang, “Fabrication of Ag3PO4/g-C3N4 heterojunction photocatalyst via in-situ growth and its photocatalytic performance,” *PLoS One*, vol. 20, no. 12, p. e0337123, Dec. 2025, doi: 10.1371/journal.pone.0337123.

[197] R. Boroujerdi, A. Abdelkader, and R. Paul, “State of the Art in Alcohol Sensing with 2D Materials,” *Nano-Micro Lett.*, vol. 12, no. 1, p. 33, Dec. 2020, doi: 10.1007/s40820-019-0363-0.

[198] L. J. Falling *et al.*, “The ladder towards understanding the oxygen evolution reaction,” *Current Opinion in Electrochemistry*, vol. 30, p. 100842, Dec. 2021, doi: 10.1016/j.coelec.2021.100842.

[199] J. C. Bui, E. W. Lees, L. M. Pant, I. V. Zenyuk, A. T. Bell, and A. Z. Weber, “Continuum Modeling of Porous Electrodes for Electrochemical Synthesis,” *Chem. Rev.*, vol. 122, no. 12, pp. 11022–11084, Jun. 2022, doi: 10.1021/acs.chemrev.1c00901.

[200] B. Tjaden, D. J. L. Brett, and P. R. Shearing, “Tortuosity in electrochemical devices: a review of calculation approaches,” *International Materials Reviews*, vol. 63, no. 2, pp. 47–67, Feb. 2018, doi: 10.1080/09506608.2016.1249995.

[201] T.-T. Nguyen, A. Demortière, B. Fleutot, B. Delobel, C. Delacourt, and S. J. Cooper, “The electrode tortuosity factor: why the conventional tortuosity factor is not well suited for quantifying transport in porous Li-ion battery electrodes and what to use instead,” *npj Comput Mater*, vol. 6, no. 1, p. 123, Aug. 2020, doi: 10.1038/s41524-020-00386-4.

[202] H. S. Zakria, M. H. D. Othman, R. Kamaludin, S. H. Sheikh Abdul Kadir, T. A. Kurniawan, and A. Jilani, “Immobilization techniques of a photocatalyst into and onto a polymer membrane for photocatalytic activity,” *RSC Adv.*, vol. 11, no. 12, pp. 6985–7014, 2021, doi: 10.1039/D0RA10964A.

[203] E. Chang *et al.*, “Percolation mechanism and effective conductivity of mechanically deformed 3-dimensional composite networks: Computational modeling and experimental verification,” *Composites Part B: Engineering*, vol. 207, p. 108552, Feb. 2021, doi: 10.1016/j.compositesb.2020.108552.

[204] M. Naguib *et al.*, “Two-Dimensional Nanocrystals Produced by Exfoliation of $Ti_3 AlC_2$,” *Advanced Materials*, vol. 23, no. 37, pp. 4248–4253, Oct. 2011, doi: 10.1002/adma.201102306.

[205] B. Anasori, M. R. Lukatskaya, and Y. Gogotsi, “2D metal carbides and nitrides (MXenes) for energy storage,” *Nat Rev Mater*, vol. 2, no. 2, p. 16098, Jan. 2017, doi: 10.1038/natrevmats.2016.98.

[206] V.-H. Nguyen *et al.*, “Novel Architecture Titanium Carbide (Ti3C2Tx) MXene Cocatalysts toward Photocatalytic Hydrogen Production: A Mini-Review,” *Nanomaterials*, vol. 10, no. 4, p. 602, Mar. 2020, doi: 10.3390/nano10040602.

[207] X. Xie and N. Zhang, “Positioning MXenes in the Photocatalysis Landscape: Competitiveness, Challenges, and Future Perspectives,” *Adv Funct Materials*, vol. 30, no. 36, p. 2002528, Sep. 2020, doi: 10.1002/adfm.202002528.

[208] M. Naguib *et al.*, “Two-Dimensional Transition Metal Carbides,” *ACS Nano*, vol. 6, no. 2, pp. 1322–1331, Feb. 2012, doi: 10.1021/nn204153h.

[209] M. Ghidiu, M. R. Lukatskaya, M.-Q. Zhao, Y. Gogotsi, and M. W. Barsoum, “Conductive two-dimensional titanium carbide ‘clay’ with high volumetric capacitance,” *Nature*, vol. 516, no. 7529, pp. 78–81, Dec. 2014, doi: 10.1038/nature13970.

[210] C. J. Zhang *et al.*, “Oxidation Stability of Colloidal Two-Dimensional Titanium Carbides (MXenes),” *Chem. Mater.*, vol. 29, no. 11, pp. 4848–4856, Jun. 2017, doi: 10.1021/acs.chemmater.7b00745.

[211] S. Tang, W. Qiu, S. Xiao, Y. Tong, and S. Yang, “Harnessing hierarchical architectures to trap light for efficient photoelectrochemical cells,” *Energy Environ. Sci.*, vol. 13, no. 3, pp. 660–684, 2020, doi: 10.1039/C9EE02986A.

[212] J. Low, L. Zhang, T. Tong, B. Shen, and J. Yu, “TiO2/MXene Ti3C2 composite with excellent photocatalytic CO2 reduction activity,” *Journal of Catalysis*, vol. 361, pp. 255–266, May 2018, doi: 10.1016/j.jcat.2018.03.009.

[213] C. Peng *et al.*, “Photocatalysis over MXene-based hybrids: Synthesis, surface chemistry, and interfacial charge kinetics,” *APL Materials*, vol. 9, no. 7, p. 070703, Jul. 2021, doi: 10.1063/5.0055711.

[214] I. Persson *et al.*, “On the organization and thermal behavior of functional groups on $Ti_3 C_2$ MXene surfaces in vacuum,” *2D Mater.*, vol. 5, no. 1, p. 015002, Oct. 2017, doi: 10.1088/2053-1583/aa89cd.

[215] Y. Gogotsi and B. Anasori, “The Rise of MXenes,” *ACS Nano*, vol. 13, no. 8, pp. 8491–8494, Aug. 2019, doi: 10.1021/acsnano.9b06394.

[216] I. Ihsanullah, “MXenes (two-dimensional metal carbides) as emerging nanomaterials for water purification: Progress, challenges and prospects,” *Chemical Engineering Journal*, vol. 388, p. 124340, May 2020, doi: 10.1016/j.cej.2020.124340.

[217] N. Bhardwaj and S. C. Kundu, “Electrospinning: A fascinating fiber fabrication technique,” *Biotechnology Advances*, vol. 28, no. 3, pp. 325–347, May 2010, doi: 10.1016/j.biotechadv.2010.01.004.

[218] M. Carey and M. W. Barsoum, “MXene polymer nanocomposites: a review,” *Materials Today Advances*, vol. 9, p. 100120, Mar. 2021, doi: 10.1016/j.mtadv.2020.100120.

[219] W. Wu, X. Li, Y. Liu, Z. Liu, Y. Wang, and T. Jiao, “Electrospun MXene-based nanofibrous membranes: Multifunctional integration, challenges, and emerging applications,” *Progress in Organic Coatings*, vol. 208, p. 109480, Nov. 2025, doi: 10.1016/j.porgcoat.2025.109480.

[220] T. Schultz *et al.*, “Surface Termination Dependent Work Function and Electronic Properties of $Ti_3C_2T_x$ MXene,” *Chem. Mater.*, vol. 31, no. 17, pp. 6590–6597, Sep. 2019, doi: 10.1021/acs.chemmater.9b00414.

[221] T. Habib *et al.*, “Oxidation stability of Ti3C2Tx MXene nanosheets in solvents and composite films,” *npj 2D Mater Appl*, vol. 3, no. 1, p. 8, Feb. 2019, doi: 10.1038/s41699-019-0089-3.

[222] V. Nesterova, V. Korostelev, and K. Klyukin, “Unveiling the Role of Termination Groups in Stabilizing MXenes in Contact with Water,” *J. Phys. Chem. Lett.*, vol. 15, no. 13, pp. 3698–3704, Apr. 2024, doi: 10.1021/acs.jpclett.4c00045.

[223] L. Xu, T. Wu, P. R. C. Kent, and D. Jiang, “Interfacial charge transfer and interaction in the MXene / Ti O 2 heterostructures,” *Phys. Rev. Materials*, vol. 5, no. 5, p. 054007, May 2021, doi: 10.1103/PhysRevMaterials.5.054007.

[224] S. Doo *et al.*, “Mechanism and Kinetics of Oxidation Reaction of Aqueous $Ti_3C_2T_x$ Suspensions at Different pHs and Temperatures,” *ACS Appl. Mater. Interfaces*, vol. 13, no. 19, pp. 22855–22865, May 2021, doi: 10.1021/acsami.1c04663.

[225] W. Cao *et al.*, “A review of how to improve Ti3C2Tx MXene stability,” *Chemical Engineering Journal*, vol. 496, p. 154097, Sep. 2024, doi: 10.1016/j.cej.2024.154097.

[226] K. P. Marquez *et al.*, “Understanding the Chemical Degradation of $Ti_3C_2T_x$ MXene Dispersions: A Chronological Analysis,” *Small Science*, p. 2400150, Jun. 2024, doi: 10.1002/smsc.202400150.

[227] F. Shahzad *et al.*, “Electromagnetic interference shielding with 2D transition metal carbides (MXenes),” *Science*, vol. 353, no. 6304, pp. 1137–1140, Sep. 2016, doi: 10.1126/science.aag2421.

[228] A. Grzegórska *et al.*, “Enhanced photocatalytic activity of accordion-like layered Ti3C2 (MXene) coupled with Fe-modified decahedral anatase particles exposing {1 0 1} and {0 0 1} facets,” *Chemical Engineering Journal*, vol. 426, p. 130801, Dec. 2021, doi: 10.1016/j.cej.2021.130801.

[229] J. Shen *et al.*, “Built-in electric field induced CeO2/Ti3C2-MXene Schottky-junction for coupled photocatalytic tetracycline degradation and CO2 reduction,” *Ceramics International*, vol. 45, no. 18, pp. 24146–24153, Dec. 2019, doi: 10.1016/j.ceramint.2019.08.123.

[230] Y. Ibrahim *et al.*, “A review of MXenes as emergent materials for dye removal from wastewater,” *Separation and Purification Technology*, vol. 282, p. 120083, Feb. 2022, doi: 10.1016/j.seppur.2021.120083.

[231] M. Jeon *et al.*, “A review on MXene-based nanomaterials as adsorbents in aqueous solution,” *Chemosphere*, vol. 261, p. 127781, Dec. 2020, doi: 10.1016/j.chemosphere.2020.127781.

[232] Y. Zhang, L. Wang, N. Zhang, and Z. Zhou, “Adsorptive environmental applications of MXene nanomaterials: a review,” *RSC Adv.*, vol. 8, no. 36, pp. 19895–19905, 2018, doi: 10.1039/C8RA03077D.

[233] A. Khosla *et al.*, “Emergence of MXene and MXene–Polymer Hybrid Membranes as Future- Environmental Remediation Strategies,” *Advanced Science*, vol. 9, no. 36, p. 2203527, Dec. 2022, doi: 10.1002/advs.202203527.

[234] R. Imsong, F. U. Ahmed, and D. Dhar Purkayastha, “Tailoring MXene-based electrospun membranes with spindle-like structures for multifunctional oily wastewater treatment,” *Chemical Engineering Journal*, vol. 520, p. 165721, Sep. 2025, doi: 10.1016/j.cej.2025.165721.

[235] A. Sun *et al.*, “Assembly of MXene/ZnO heterojunction onto electrospun poly(arylene ether nitrile) fibrous membrane for favorable oil/water separation with high permeability and synergetic antifouling performance,” *Journal of Membrane Science*, vol. 663, p. 120933, Dec. 2022, doi: 10.1016/j.memsci.2022.120933.

[236] A. Lee, M. Shekhirev, M. Anayee, and Y. Gogotsi, “Multi-year study of environmental stability of Ti3C2Tx MXene films,” *Graphene and 2D mater*, vol. 9, no. 1–2, pp. 77–85, Jun. 2024, doi: 10.1007/s41127-024-00076-8.

[237] T. Peng, R. Wu, B. Wang, T. Liskiewicz, and S. Shi, “Long-Term Storage of Ti3C2Tx Aqueous Dispersion with Stable Electrochemical Properties,” *Materials*, vol. 17, no. 22, p. 5414, Nov. 2024, doi: 10.3390/ma17225414.

[238] K. Takanabe, “Addressing fundamental experimental aspects of photocatalysis studies,” *Journal of Catalysis*, vol. 370, pp. 480–484, Feb. 2019, doi: 10.1016/j.jcat.2018.10.006.

[239] F. E. Bedoya-Lora, I. Holmes-Gentle, and A. Hankin, “Electrochemical techniques for photoelectrode characterisation,” *Current Opinion in Green and Sustainable Chemistry*, vol. 29, p. 100463, Jun. 2021, doi: 10.1016/j.cogsc.2021.100463.

[240] S. S. Emmanuel *et al.*, “MXenes as sustainable functional nanomaterials for photocatalytic degradation of dye pollutants: Performance, effect of process parameters, stability and re-useability evaluation – A critical review,” *Sustainable Materials and Technologies*, vol. 46, p. e01683, Dec. 2025, doi: 10.1016/j.susmat.2025.e01683.

[241] C. Plank *et al.*, “A review on the distribution of relaxation times analysis: A powerful tool for process identification of electrochemical systems,” *Journal of Power Sources*, vol. 594, p. 233845, Feb. 2024, doi: 10.1016/j.jpowsour.2023.233845.

[242] M. S. I. Nasri, M. F. R. Samsudin, A. A. Tahir, and S. Sufian, “Effect of MXene Loaded on g-C3N4 Photocatalyst for the Photocatalytic Degradation of Methylene Blue,” *Energies*, vol. 15, no. 3, p. 955, Jan. 2022, doi: 10.3390/en15030955.

[243] L. Xiu, Z. Wang, M. Yu, X. Wu, and J. Qiu, “Aggregation-Resistant 3D MXene-Based Architecture as Efficient Bifunctional Electrocatalyst for Overall Water Splitting,” *ACS Nano*, vol. 12, no. 8, pp. 8017–8028, Aug. 2018, doi: 10.1021/acsnano.8b02849.

[244] A. H. Zyoud *et al.*, “Raw clay supported ZnO nanoparticles in photodegradation of 2-chlorophenol under direct solar radiations,” *Journal of Environmental Chemical Engineering*, vol. 8, no. 5, p. 104227, Oct. 2020, doi: 10.1016/j.jece.2020.104227.

[245] A. M. Nasir *et al.*, “Recent progress on fabrication and application of electrospun nanofibrous photocatalytic membranes for wastewater treatment: A review,” *Journal of Water Process Engineering*, vol. 40, p. 101878, Apr. 2021, doi: 10.1016/j.jwpe.2020.101878.

[246] A. Nait Ajjou, “Aqueous-phase catalytic oxidation, transfer hydrogenation, reductive amination and hydration reactions,” *Catalysis Today*, vol. 247, pp. 177–181, Jun. 2015, doi: 10.1016/j.cattod.2014.06.020.

[247] J. C. Espíndola, R. O. Cristóvão, A. Mendes, R. A. R. Boaventura, and V. J. P. Vilar, “Photocatalytic membrane reactor performance towards oxytetracycline removal from synthetic and real matrices: Suspended vs immobilized TiO2-P25,” *Chemical Engineering Journal*, vol. 378, p. 122114, Dec. 2019, doi: 10.1016/j.cej.2019.122114.

[248] Z. Xing *et al.*, “Recent advances in floating TiO2-based photocatalysts for environmental application,” *Applied Catalysis B: Environmental*, vol. 225, pp. 452–467, Jun. 2018, doi: 10.1016/j.apcatb.2017.12.005.

[249] D. Wood, S. Shaw, T. Cawte, E. Shanen, and B. Van Heyst, “An overview of photocatalyst immobilization methods for air pollution remediation,” *Chemical Engineering Journal*, vol. 391, p. 123490, Jul. 2020, doi: 10.1016/j.cej.2019.123490.

[250] H. Ma *et al.*, “A facile approach to enhance performance of PVDF-matrix nanocomposite membrane via manipulating migration behavior of graphene oxide,” *Journal of Membrane Science*, vol. 590, p. 117268, Nov. 2019, doi: 10.1016/j.memsci.2019.117268.

[251] M. Wang, W. Zhen, B. Tian, J. Ma, and G. Lu, “The inhibition of hydrogen and oxygen recombination reaction by halogen atoms on over-all water splitting over Pt-TiO2 photocatalyst,” *Applied Catalysis B: Environmental*, vol. 236, pp. 240–252, Nov. 2018, doi: 10.1016/j.apcatb.2018.05.031.

[252] Z.-M. Huang, Y.-Z. Zhang, M. Kotaki, and S. Ramakrishna, “A review on polymer nanofibers by electrospinning and their applications in nanocomposites,” *Composites Science and Technology*, vol. 63, no. 15, pp. 2223–2253, Nov. 2003, doi: 10.1016/S0266-3538(03)00178-7.

[253] A. Greiner and J. H. Wendorff, “Electrospinning: A Fascinating Method for the Preparation of Ultrathin Fibers,” *Angew Chem Int Ed*, vol. 46, no. 30, pp. 5670–5703, Jul. 2007, doi: 10.1002/anie.200604646.

[254] Y.-Z. Long, X. Yan, X.-X. Wang, J. Zhang, and M. Yu, “Electrospinning,” in *Electrospinning: Nanofabrication and Applications*, Elsevier, 2019, pp. 21–52. doi: 10.1016/B978-0-323-51270-1.00002-9.

[255] Y. Xing *et al.*, “Electrospun Ceramic Nanofibers for Photocatalysis,” *Nanomaterials*, vol. 11, no. 12, p. 3221, Nov. 2021, doi: 10.3390/nano11123221.

[256] Y. Liao, C.-H. Loh, M. Tian, R. Wang, and A. G. Fane, “Progress in electrospun polymeric nanofibrous membranes for water treatment: Fabrication, modification and applications,” *Progress in Polymer Science*, vol. 77, pp. 69–94, Feb. 2018, doi: 10.1016/j.progpolymsci.2017.10.003.

[257] A. Rianjanu, “Recent Advances in Electrospun Nanofiber Membranes for Dye Filtration: A Focused Mini-Review,” *Environmental Chemistry and Safety*, vol. 1, no. 2, p. 9600018, Sep. 2025, doi: 10.26599/ECS.2025.9600018.

[258] M. Samadi and A. Z. Moshfegh, “Recent Developments of Electrospinning-Based Photocatalysts in Degradation of Organic Pollutants: Principles and Strategies,” *ACS Omega*, vol. 7, no. 50, pp. 45867–45881, Dec. 2022, doi: 10.1021/acsomega.2c05624.

[259] H. Jiang, L. Wang, and K. Zhu, “Coaxial electrospinning for encapsulation and controlled release of fragile water-soluble bioactive agents,” *Journal of Controlled Release*, vol. 193, pp. 296–303, Nov. 2014, doi: 10.1016/j.jconrel.2014.04.025.

[260] S. C. Lee, “Radiative transfer through a fibrous medium: Allowance for fiber orientation,” *Journal of Quantitative Spectroscopy and Radiative Transfer*, vol. 36, no. 3, pp. 253–263, Sep. 1986, doi: 10.1016/0022-4073(86)90073-7.

[261] T. Linder, T. Löfqvist, E. L. G. Wernersson, and P. Gren, “Light scattering in fibrous media with different degrees of in-plane fiber alignment,” *Opt. Express*, vol. 22, no. 14, p. 16829, Jul. 2014, doi: 10.1364/OE.22.016829.

[262] A. Y. Mikheev, Y. M. Shlyapnikov, I. L. Kanev, A. V. Avseenko, and V. N. Morozov, “Filtering and optical properties of free standing electrospun nanomats from nylon-4,6,” *European Polymer Journal*, vol. 75, pp. 317–328, Feb. 2016, doi: 10.1016/j.eurpolymj.2016.01.001.

[263] C. Regmi, S. Lotfi, J. C. Espíndola, K. Fischer, A. Schulze, and A. I. Schäfer, “Comparison of Photocatalytic Membrane Reactor Types for the Degradation of an Organic Molecule by TiO2-Coated PES Membrane,” *Catalysts*, vol. 10, no. 7, p. 725, Jun. 2020, doi: 10.3390/catal10070725.

[264] F. Zhu *et al.*, “Photocatalytic PAN Nanofibrous Membrane through Anchoring a Nanoflower-Branched CoAl-LDH@PANI Heterojunction for Organic Hazards Degradation and Oil-Containing Emulsified Wastewater Separation,” *Langmuir*, vol. 40, no. 28, pp. 14368–14383, Jul. 2024, doi: 10.1021/acs.langmuir.4c00980.

[265] M. D. L. M. Ballari, R. Brandi, O. Alfano, and A. Cassano, “Mass transfer limitations in photocatalytic reactors employing titanium dioxide suspensions,” *Chemical Engineering Journal*, vol. 136, no. 1, pp. 50–65, Feb. 2008, doi: 10.1016/j.cej.2007.03.028.

[266] F. R. Pomilla *et al.*, “CO_2 to Liquid Fuels: Photocatalytic Conversion in a Continuous Membrane Reactor,” *ACS Sustainable Chem. Eng.*, vol. 6, no. 7, pp. 8743–8753, Jul. 2018, doi: 10.1021/acssuschemeng.8b01073.

[267] A. Haleem, A. Shafiq, S.-Q. Chen, and M. Nazar, “A Comprehensive Review on Adsorption, Photocatalytic and Chemical Degradation of Dyes and Nitro-Compounds over Different Kinds of Porous and Composite Materials,” *Molecules*, vol. 28, no. 3, p. 1081, Jan. 2023, doi: 10.3390/molecules28031081.

[268] J. Marugán, M.-J. López-Muñoz, R. Van Grieken, and J. Aguado, “Photocatalytic Decolorization and Mineralization of Dyes with Nanocrystalline TiO_2 /SiO_2 Materials,” *Ind. Eng. Chem. Res.*, vol. 46, no. 23, pp. 7605–7610, Nov. 2007, doi: 10.1021/ie070093u.

[269] A. Dougan-Bacha, J. E. Cox, and S. K. St. Angelo, “Decoupling Adsorption and Photocatalysis: Addressing the Dark Adsorption Pitfall in Catalyst Ranking,” *ACS Omega*, vol. 11, no. 2, pp. 2289–2296, Jan. 2026, doi: 10.1021/acsomega.5c09004.

[270] S. Gonuguntla, R. Kamesh, U. Pal, and D. Chatterjee, “Dye sensitization of TiO2 relevant to photocatalytic hydrogen generation: Current research trends and prospects,” *Journal of Photochemistry and Photobiology C: Photochemistry Reviews*, vol. 57, p. 100621, Dec. 2023, doi: 10.1016/j.jphotochemrev.2023.100621.

[271] H. D. Tran, D. Q. Nguyen, P. T. Do, and U. N. P. Tran, “Kinetics of photocatalytic degradation of organic compounds: a mini-review and new approach,” *RSC Adv.*, vol. 13, no. 25, pp. 16915–16925, 2023, doi: 10.1039/D3RA01970E.

[272] Y. Shi, J. Huang, G. Zeng, W. Cheng, and J. Hu, “Photocatalytic membrane in water purification: is it stepping closer to be driven by visible light?,” *Journal of Membrane Science*, vol. 584, pp. 364–392, Aug. 2019, doi: 10.1016/j.memsci.2019.04.078.

[273] H. Khan, M. G. Rigamonti, G. S. Patience, and D. C. Boffito, “Spray dried TiO2/WO3 heterostructure for photocatalytic applications with residual activity in the dark,” *Applied Catalysis B: Environmental*, vol. 226, pp. 311–323, Jun. 2018, doi: 10.1016/j.apcatb.2017.12.049.

[274] B. Sun *et al.*, “Advances in three-dimensional nanofibrous macrostructures via electrospinning,” *Progress in Polymer Science*, vol. 39, no. 5, pp. 862–890, May 2014, doi: 10.1016/j.progpolymsci.2013.06.002.

[275] W. Yuan and K.-Q. Zhang, “Structural Evolution of Electrospun Composite Fibers from the Blend of Polyvinyl Alcohol and Polymer Nanoparticles,” *Langmuir*, vol. 28, no. 43, pp. 15418–15424, Oct. 2012, doi: 10.1021/la303312q.

[276] M. Zhang, Y. Yang, X. An, and L. Hou, “A critical review of g-C3N4-based photocatalytic membrane for water purification,” *Chemical Engineering Journal*, vol. 412, p. 128663, May 2021, doi: 10.1016/j.cej.2021.128663.

[277] W.-W. Wang, C.-Z. Man, C.-M. Zhang, L. Jiang, Y. Dan, and T.-P. Nguyen, “Stability of poly(l-lactide)/TiO2 nanocomposite thin films under UV irradiation at 254 nm,” *Polymer Degradation and Stability*, vol. 98, no. 4, pp. 885–893, Apr. 2013, doi: 10.1016/j.polymdegradstab.2013.01.003.

[278] S. S. Chin, K. Chiang, and A. G. Fane, “The stability of polymeric membranes in a TiO2 photocatalysis process,” *Journal of Membrane Science*, vol. 275, no. 1–2, pp. 202–211, Apr. 2006, doi: 10.1016/j.memsci.2005.09.033.

[279] S. Singh, H. Mahalingam, and P. K. Singh, “Polymer-supported titanium dioxide photocatalysts for environmental remediation: A review,” *Applied Catalysis A: General*, vol. 462–463, pp. 178–195, Jul. 2013, doi: 10.1016/j.apcata.2013.04.039.

[280] L. Chen, P. Xu, and H. Wang, “Photocatalytic membrane reactors for produced water treatment and reuse: Fundamentals, affecting factors, rational design, and evaluation metrics,” *Journal of Hazardous Materials*, vol. 424, p. 127493, Feb. 2022, doi: 10.1016/j.jhazmat.2021.127493.

[281] E. Yousif and R. Haddad, “Photodegradation and photostabilization of polymers, especially polystyrene: review,” *SpringerPlus*, vol. 2, no. 1, p. 398, Dec. 2013, doi: 10.1186/2193-1801-2-398.

[282] M. T. Tsehaye, S. Velizarov, and B. Van Der Bruggen, “Stability of polyethersulfone membranes to oxidative agents: A review,” *Polymer Degradation and Stability*, vol. 157, pp. 15–33, Nov. 2018, doi: 10.1016/j.polymdegradstab.2018.09.004.

[283] P. Le-Clech, V. Chen, and T. A. G. Fane, “Fouling in membrane bioreactors used in wastewater treatment,” *Journal of Membrane Science*, vol. 284, no. 1–2, pp. 17–53, Nov. 2006, doi: 10.1016/j.memsci.2006.08.019.

[284] M. Schleuning, I. Y. Ahmet, R. Van De Krol, and M. M. May, “The role of selective contacts and built-in field for charge separation and transport in photoelectrochemical devices,” *Sustainable Energy Fuels*, vol. 6, no. 16, pp. 3701–3716, 2022, doi: 10.1039/D2SE00562J.

[285] S. Mozia, “Photocatalytic membrane reactors (PMRs) in water and wastewater treatment. A review,” *Separation and Purification Technology*, vol. 73, no. 2, pp. 71–91, Jun. 2010, doi: 10.1016/j.seppur.2010.03.021.

[286] K. Sivula and R. Van De Krol, “Semiconducting materials for photoelectrochemical energy conversion,” *Nat Rev Mater*, vol. 1, no. 2, p. 15010, Jan. 2016, doi: 10.1038/natrevmats.2015.10.

[287] A. Kudo and Y. Miseki, “Heterogeneous photocatalyst materials for water splitting,” *Chem. Soc. Rev.*, vol. 38, no. 1, pp. 253–278, 2009, doi: 10.1039/B800489G.

[288] S. Shen, S. A. Lindley, X. Chen, and J. Z. Zhang, “Hematite heterostructures for photoelectrochemical water splitting: rational materials design and charge carrier dynamics,” *Energy Environ. Sci.*, vol. 9, no. 9, pp. 2744–2775, 2016, doi: 10.1039/C6EE01845A.

[289] S. Corby, R. R. Rao, L. Steier, and J. R. Durrant, “The kinetics of metal oxide photoanodes from charge generation to catalysis,” *Nat Rev Mater*, vol. 6, no. 12, pp. 1136–1155, Aug. 2021, doi: 10.1038/s41578-021-00343-7.

[290] H. Dotan *et al.*, “Resonant light trapping in ultrathin films for water splitting,” *Nature Mater*, vol. 12, no. 2, pp. 158–164, Feb. 2013, doi: 10.1038/nmat3477.

[291] B. Ohtani and S. Nishimoto, “Effect of surface adsorptions of aliphatic alcohols and silver ion on the photocatalytic activity of titania suspended in aqueous solutions,” *J. Phys. Chem.*, vol. 97, no. 4, pp. 920–926, Jan. 1993, doi: 10.1021/j100106a018.

[292] Y. Nosaka and A. Y. Nosaka, “Generation and Detection of Reactive Oxygen Species in Photocatalysis,” *Chem. Rev.*, vol. 117, no. 17, pp. 11302–11336, Sep. 2017, doi: 10.1021/acs.chemrev.7b00161.

[293] J. Z. Bloh, “A Holistic Approach to Model the Kinetics of Photocatalytic Reactions,” *Front. Chem.*, vol. 7, p. 128, Mar. 2019, doi: 10.3389/fchem.2019.00128.

[294] A. Sivakumar, B. Murugesan, A. Loganathan, and P. Sivakumar, “A review on decolourisation of dyes by photodegradation using various bismuth catalysts,” *Journal of the Taiwan Institute of Chemical Engineers*, vol. 45, no. 5, pp. 2300–2306, Sep. 2014, doi: 10.1016/j.jtice.2014.07.003.

[295] J. Antonio Abarca, G. Díaz-Sainz, I. Merino-Garcia, A. Irabien, and J. Albo, “Photoelectrochemical CO2 electrolyzers: From photoelectrode fabrication to reactor configuration,” *Journal of Energy Chemistry*, vol. 85, pp. 455–480, Oct. 2023, doi: 10.1016/j.jechem.2023.06.032.

[296] S. B. A. Hamid, S. J. Teh, C. W. Lai, S. Perathoner, and G. Centi, “Applied bias photon-to-current conversion efficiency of ZnO enhanced by hybridization with reduced graphene oxide,” *Journal of Energy Chemistry*, vol. 26, no. 2, pp. 302–308, Mar. 2017, doi: 10.1016/j.jechem.2016.11.006.

[297] A. C. Guler, J. Antos, M. Masar, M. Urbanek, M. Machovsky, and I. Kuritka, “Comprehensive evaluation of photoelectrochemical performance dependence on geometric features of ZnO nanorod electrodes,” *Nanoscale Adv.*, vol. 5, no. 11, pp. 3091–3103, 2023, doi: 10.1039/D3NA00089C.

[298] X. Zhan *et al.*, “Investigation of the reaction kinetics of photocatalytic pollutant degradation under defined conditions with inkjet-printed TiO_2 films – from batch to a novel continuous-flow microreactor,” *React. Chem. Eng.*, vol. 5, no. 9, pp. 1658–1670, 2020, doi: 10.1039/D0RE00238K.

[299] B. Liu *et al.*, “Back-illuminated photoelectrochemical flow cell for efficient CO2 reduction,” *Nat Commun*, vol. 13, no. 1, p. 7111, Nov. 2022, doi: 10.1038/s41467-022-34926-x.

[300] F. Matter and M. Niederberger, “The Importance of the Macroscopic Geometry in Gas-Phase Photocatalysis,” *Advanced Science*, vol. 9, no. 13, p. 2105363, May 2022, doi: 10.1002/advs.202105363.

[301] F. Matter and M. Niederberger, “Optimization of Mass and Light Transport in Nanoparticle-Based Titania Aerogels,” *Chem. Mater.*, vol. 35, no. 19, pp. 7995–8008, Oct. 2023, doi: 10.1021/acs.chemmater.3c01218.

[302] J. Deng, Y. Su, D. Liu, P. Yang, B. Liu, and C. Liu, “Nanowire Photoelectrochemistry,” *Chem. Rev.*, vol. 119, no. 15, pp. 9221–9259, Aug. 2019, doi: 10.1021/acs.chemrev.9b00232.

[303] C. Tuc Altaf *et al.*, “Efficiency enhancement in photoelectrochemical water splitting: Defect passivation and boosted charge transfer kinetics of zinc oxide nanostructures via chalcopyrite/chalcogenide mix sensitization,” *Phys. Rev. Materials*, vol. 5, no. 12, p. 125403, Dec. 2021, doi: 10.1103/PhysRevMaterials.5.125403.

[304] M. G. Sendeku *et al.*, “Frontiers in Photoelectrochemical Catalysis: A Focus on Valuable Product Synthesis,” *Advanced Materials*, vol. 36, no. 21, p. 2308101, May 2024, doi: 10.1002/adma.202308101.

[305] C. Zhou *et al.*, “Enhancing photoelectrochemical CO2 reduction with silicon photonic crystals,” *Front. Chem.*, vol. 11, p. 1326349, Dec. 2023, doi: 10.3389/fchem.2023.1326349.

[306] D. Cardenas-Morcoso, A. Bou, S. Ravishankar, M. García-Tecedor, S. Gimenez, and J. Bisquert, “Intensity-Modulated Photocurrent Spectroscopy for Solar Energy Conversion Devices: What Does a Negative Value Mean?,” *ACS Energy Lett.*, vol. 5, no. 1, pp. 187–191, Jan. 2020, doi: 10.1021/acsenergylett.9b02555.

[307] T. Paltrinieri, L. Bondi, V. Đerek, B. Fraboni, E. D. Głowacki, and T. Cramer, “Understanding Photocapacitive and Photofaradaic Processes in Organic Semiconductor Photoelectrodes for Optobioelectronics,” *Adv Funct Materials*, vol. 31, no. 16, p. 2010116, Apr. 2021, doi: 10.1002/adfm.202010116.

[308] N. D. Mohamad, Z. M. Zaki, and A. Amir, “Mechanisms of enhanced oxidative degradation of tetrachloroethene by nano-magnetite catalysed with glutathione,” *Chemical Engineering Journal*, vol. 393, p. 124760, Aug. 2020, doi: 10.1016/j.cej.2020.124760.

[309] K. Sivula and R. Van De Krol, “Erratum: Semiconducting materials for photoelectrochemical energy conversion,” *Nat Rev Mater*, p. 16010, Feb. 2016, doi: 10.1038/natrevmats.2016.10.

[310] A. Lys, I. Gnilitskyi, E. Coy, M. Jancelewicz, O. Gogotsi, and I. Iatsunskyi, “Highly regular laser-induced periodic silicon surface modified by MXene and ALD TiO2 for organic pollutants degradation,” *Applied Surface Science*, vol. 640, p. 158336, Dec. 2023, doi: 10.1016/j.apsusc.2023.158336.

[311] C. L. Bentley, M. Kang, and P. R. Unwin, “Nanoscale Surface Structure–Activity in Electrochemistry and Electrocatalysis,” *J. Am. Chem. Soc.*, vol. 141, no. 6, pp. 2179–2193, Feb. 2019, doi: 10.1021/jacs.8b09828.

[312] J. Zhai *et al.*, “A review of recent development in the enhancement mechanism of catalytic membranes for wastewater treatment,” *Environmental Functional Materials*, vol. 4, no. 1, pp. 79–98, Apr. 2025, doi: 10.1016/j.efmat.2025.02.004.

[313] Y. Wang *et al.*, “Rational design of defect metal oxide/covalent organic frameworks Z-scheme heterojunction for photoreduction CO2 to CO,” *Applied Catalysis B: Environmental*, vol. 327, p. 122419, Jun. 2023, doi: 10.1016/j.apcatb.2023.122419.

[314] S. Vanka, G. Zeng, T. G. Deutsch, F. M. Toma, and Z. Mi, “Long-Term Stability Metrics of Photoelectrochemical Water Splitting,” *Front. Energy Res.*, vol. 10, p. 840140, May 2022, doi: 10.3389/fenrg.2022.840140.

[315] Md. A. Hoque and M. I. Guzman, “Photocatalytic Activity: Experimental Features to Report in Heterogeneous Photocatalysis,” *Materials*, vol. 11, no. 10, p. 1990, Oct. 2018, doi: 10.3390/ma11101990.

[316] J. M. Buriak, P. V. Kamat, and K. S. Schanze, “Best Practices for Reporting on Heterogeneous Photocatalysis,” *ACS Appl. Mater. Interfaces*, vol. 6, no. 15, pp. 11815–11816, Aug. 2014, doi: 10.1021/am504389z.

[317] E. Asenath-Smith, E. K. Ambrogi, L. C. Moores, S. D. Newman, and J. A. Brame, “Leveraging chemical actinometry and optical radiometry to reduce uncertainty in photochemical research,” *Journal of Photochemistry and Photobiology A: Chemistry*, vol. 372, pp. 279–287, Mar. 2019, doi: 10.1016/j.jphotochem.2018.12.024.

List of figures

purging, (3) H_2O is then pulsed to react with the modified surface and renew the hydroxyl termination, and (4) the chamber is purged once more before the sequence is repeated. Prepared by the author.

Figure 2.3. Femtosecond-laser-induced periodic surface structures formed on silicon under different processing conditions. The images show how the surface morphology changes together with the corresponding structural regime. Reproduced from Ref. [148], under the Creative Commons CC BY licence.

Figure 2.4. Schematic comparison of charge-carrier transfer pathways in (a) a type-II heterojunction and (b) a Z-scheme heterojunction. In the type-II configuration, electrons and holes accumulate in different semiconductors, promoting spatial separation but often reducing redox ability. In the Z-scheme configuration, interfacial recombination of the less energetic carriers preserves the strongly reducing electrons and strongly oxidising holes for photocatalytic or photoelectrochemical reactions. Adapted and redrawn by the author based on Ref. [182]

Figure 2.5. $Ti_3C_2T_x$ MXene as a functional component in semiconductor hybrids. The MXene sheets, bearing terminal groups such as –O, –OH, and –F, are shown as the interfacial phase that can assist electron transfer and influence liquid wetting. Adapted and redrawn by the author based on Refs. [227], [228], [229]

Figure 2.6. Schematic representation of the electrospinning process together with the main parameters that influence fibre formation and membrane morphology, including solution properties, environmental conditions, and electrospinning settings. Reproduced from Ref. [254] with permission from Elsevier.

Figure 2.7. Conceptual overlap between photocatalysis and photoelectrochemistry, showing their shared semiconductor basis and their main format-dependent features. Prepared by the author.

Co-author declarations and full texts of publications

MSc Andrii Lys
NanoBioMedical Centre
Adam Mickiewicz University
Wszechnicy Piastowskiej 3
61-614 Poznań, Poland
E-mail: andrii.lys@amu.edu.pl

A declaration

Hereby I declare my contribution to the following papers included in this dissertation:

---

1. ***Highly regular laser-induced periodic silicon surface modified by MXene and ALD TiO_2 for organic pollutants degradation***

Andrii Lys, Iaroslav Gnilitskyi, Emerson Coy, Mariusz Jancelewicz, Oleksiy Gogotsi, Igor Iatsunskyi
Applied Surface Science 640 (2023) 158336
DOI: 10.1016/j.apsusc.2023.158336

In this publication, I contributed to the investigation, analysis and interpretation of the results, visualisation, and manuscript preparation. My contribution was related to the evaluation of the structured SiNR/MXene/TiO_2 photocatalytic system and to the interpretation of the influence of laser-induced surface architecture, MXene modification, and ALD-grown TiO_2 on photocatalytic dye degradation.

---

2. ***Electrospun Polyimide Nanofibers Modified with Metal Oxide Nanowires and MXene for Photocatalytic Water Purification***

Andrii Lys, Valerii Myndrul, Mykola Pavlenko, Błażej Anastaziak, Pavel Holec, Kateřina Vodseďálková, Emerson Coy, Mikhael Bechelany, Igor Iatsunskyi
Nanomaterials 15 (2025) 1371
DOI: 10.3390/nano15171371

In this publication, I contributed to the synthesis of the hybrid electrospun membranes, investigation, methodology, data curation, interpretation of the results, and preparation of the original draft. My contribution was related to the fabrication and evaluation of PID/TiO_2/WO_3/MXene membranes for photocatalytic water purification.

---

3. ***Core-shell nanofibers of $ZnFe_2O_4$/ZnO for enhanced visible-light photoelectrochemical performance***

Andrii Lys, Viktor Zabolotnii, Mária Čaplovičová, Iryna Tepliakova, Agris Berzins, Martin Sahul, Ľubomír Čaplovič, Alexander Pogrebnjak, Igor Iatsunskyi, Roman Viter
Journal of Alloys and Compounds 984 (2024) 173885
DOI: 10.1016/j.jallcom.2024.173885

In this publication, I contributed to the synthesis and fabrication of $ZnFe_2O_4/ZnO$ core-shell nanofibres, photoelectrochemical characterisation, data analysis, interpretation of the results, and preparation of the draft manuscript. My contribution was related to the development and evaluation of fibrous oxide heterostructures for visible-light photoelectrochemical response.

---

4. *Hierarchically Structured Ti-TiO_2 Membranes Fabricated by Femtosecond Laser Ablation and Atomic Layer Deposition for Enhanced Photoelectrochemical Water Splitting*

Andrii Lys, Iaroslav Gnilitskyi, Emerson Coy, Mariusz Jancelewicz, Mikhael Bechelany, Igor Iatsunskyi
ACS Applied Materials & Interfaces 17 (2025) 43390–43402
DOI: 10.1021/acsami.5c07488

In this publication, I contributed to the investigation, formal analysis, visualisation, interpretation of the results, and preparation of both the original and revised manuscript. My contribution was related to the analysis and interpretation of hierarchical Ti-TiO_2 membrane photoanodes, including the influence of laser-structured titanium geometry, ALD-grown TiO_2 coatings, charge-transfer behaviour, and photoelectrochemical performance.

Andrii Lys

MSc Andrii Lys

Prof. dr hab. Igor Iatsunskyi
NanoBioMedical Centre
Adam Mickiewicz University
Wszechnicy Piastowskiej 3
61-614 Poznań, Poland
E-mail: igoyat@amu.edu.pl

A declaration

Hereby I declare my contribution to the following papers included in this dissertation:

---

1. ***Highly regular laser-induced periodic silicon surface modified by MXene and ALD TiO_2 for organic pollutants degradation***

Andrii Lys, Iaroslav Gnilitskyi, Emerson Coy, Mariusz Jancelewicz, Oleksiy Gogotsi, **Igor Iatsunskyi**
Applied Surface Science 640 (2023) 158336
DOI: 10.1016/j.apsusc.2023.158336

In this publication, I acted as the corresponding author and contributed to the conceptualisation of the study, validation of the results, provision of resources, manuscript review and editing, supervision, and funding acquisition. I was involved in defining the scientific direction of the work, discussing the structured SiNR/MXene/TiO_2 photocatalytic system, interpreting the obtained results, and supervising the preparation of the publication.

---

2. ***Electrospun Polyimide Nanofibers Modified with Metal Oxide Nanowires and MXene for Photocatalytic Water Purification***

Andrii Lys, Valerii Myndrul, Mykola Pavlenko, Błażej Anastaziak, Pavel Holec, Kateřina Vodseďálková, Emerson Coy, Mikhael Bechelany, **Igor Iatsunskyi**
Nanomaterials 15 (2025) 1371
DOI: 10.3390/nano15171371

In this publication, I acted as the corresponding author and contributed to the conceptualisation of the study, supervision, writing, review and editing, funding acquisition, and project administration. I was involved in developing the general scientific concept of the work, coordinating the research, supervising the photocatalytic membrane study, discussing the results, and preparing the final version of the manuscript.

---

3. *Core-shell nanofibers of $ZnFe_2O_4$/ZnO for enhanced visible-light photoelectrochemical performance*

Andrii Lys, Viktor Zabolotnii, Mária Čaplovičová, Iryna Tepliakova, Agris Berzins, Martin Sahul, Ľubomír Čaplovič, Alexander Pogrebnjak, **Igor Iatsunskyi**, Roman Viter
Journal of Alloys and Compounds 984 (2024) 173885
DOI: 10.1016/j.jallcom.2024.173885

In this publication, I acted as the corresponding author and contributed to the conceptualisation of the study, data curation, formal analysis, funding acquisition, project administration, supervision, manuscript review and editing. I was involved in developing the conceptual idea, supervising the work, discussing and interpreting the results, preparing and editing the manuscript, providing resources, and supporting the project administration and funding acquisition.

---

4. *Hierarchically Structured Ti-TiO_2 Membranes Fabricated by Femtosecond Laser Ablation and Atomic Layer Deposition for Enhanced Photoelectrochemical Water Splitting*

Andrii Lys, Iaroslav Gnilitskyi, Emerson Coy, Mariusz Jancelewicz, Mikhael Bechelany, **Igor Iatsunskyi**
ACS Applied Materials & Interfaces 17 (2025) 43390–43402
DOI: 10.1021/acsami.5c07488

In this publication, I acted as the corresponding author and contributed to the supervision and scientific coordination of the work. I was involved in defining the research direction, discussing and interpreting the hierarchical Ti-TiO_2 membrane photoanode system, reviewing and editing the manuscript, supervising the project, and supporting the research within the available funding framework.

.....

Prof. dr hab. Igor Iatsunskyi

dr hab. inż. prof. UAM Emerson Coy
NanoBioMedical Centre
Adam Mickiewicz University
Wszechnicy Piastowskiej 3
61-614 Poznań, Poland

A declaration

Hereby I declare my contribution to the following papers included in this dissertation:

---

1. ***Highly regular laser-induced periodic silicon surface modified by MXene and ALD TiO_2 for organic pollutants degradation***

Andrii Lys, Iaroslav Gnilitskyi, **Emerson Coy**, Mariusz Jancelewicz, Oleksiy Gogotsi, Igor Iatsunskyi
Applied Surface Science 640 (2023) 158336
DOI: 10.1016/j.apsusc.2023.158336

In this publication, I contributed to the investigation of the SiNR/MXene/TiO_2 photocatalytic system. My contribution was related to the experimental characterisation and discussion of the material properties of the structured hybrid surface.

---

2. ***Electrospun Polyimide Nanofibers Modified with Metal Oxide Nanowires and MXene for Photocatalytic Water Purification***

Andrii Lys, Valerii Myndrul, Mykola Pavlenko, Błażej Anastaziak, Pavel Holec, Kateřina Vodseďálková, **Emerson Coy**, Mikhael Bechelany, Igor Iatsunskyi
Nanomaterials 15 (2025) 1371
DOI: 10.3390/nano15171371

In this publication, I contributed to the investigation and validation of the results. My contribution was related to the characterisation and verification of the properties of the PID/TiO_2/WO_3/MXene nanofibre membranes, as well as to the discussion of the obtained data.

---

3. ***Hierarchically Structured Ti-TiO_2 Membranes Fabricated by Femtosecond Laser Ablation and Atomic Layer Deposition for Enhanced Photoelectrochemical Water Splitting***

Andrii Lys, Iaroslav Gnilitskyi, **Emerson Coy**, Mariusz Jancelewicz, Mikhael Bechelany, Igor Iatsunskyi

ACS Applied Materials & Interfaces 17 (2025) 43390–43402
DOI: 10.1021/acsami.5c07488

In this publication, I contributed to the investigation of the Ti-TiO_2 membrane photoanode system. My contribution was related to the characterisation and discussion of the hierarchical Ti-TiO_2 architecture, including the relationship between material properties and photoelectrochemical behaviour.

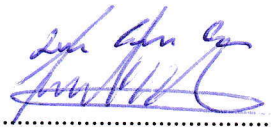

.....

dr hab. inż. prof. UAM Emerson Coy

Dr. Iaroslav Gnilitskyi
"NoviNano" Lab LLC
Lviv, Ukraine
Department of Applied Physics and Nanomaterials Science
Lviv Polytechnic National University
Lviv, Ukraine

A declaration

Hereby I declare my contribution to the following papers included in this dissertation:

---

1. ***Highly regular laser-induced periodic silicon surface modified by MXene and ALD TiO_2 for organic pollutants degradation***

Andrii Lys, **Iaroslav Gnilitskyi**, Emerson Coy, Mariusz Jancelewicz, Oleksiy Gogotsi, Igor Iatsunskyi
Applied Surface Science 640 (2023) 158336
DOI: 10.1016/j.apsusc.2023.158336

In this publication, I contributed to the investigation of the laser-structured silicon surface system. My contribution was related to the preparation and/or analysis of highly regular laser-induced periodic surface structures on silicon, as well as to the discussion of their role in the final SiNR/MXene/TiO_2 photocatalytic architecture.

---

2. ***Hierarchically Structured Ti-TiO_2 Membranes Fabricated by Femtosecond Laser Ablation and Atomic Layer Deposition for Enhanced Photoelectrochemical Water Splitting***

Andrii Lys, **Iaroslav Gnilitskyi**, Emerson Coy, Mariusz Jancelewicz, Mikhael Bechelany, Igor Iatsunskyi
ACS Applied Materials & Interfaces 17 (2025) 43390–43402
DOI: 10.1021/acsami.5c07488

In this publication, I contributed to the investigation and development of the femtosecond-laser-structured titanium membrane system. My contribution was related to laser processing of the titanium substrate, formation of the hierarchical surface architecture, and discussion of the role of laser-induced geometry in light trapping and photoelectrochemical performance.

.....
Dr. Iaroslav Gnilitskyi

Dr. Mariusz Jancelewicz
NanoBioMedical Centre
Adam Mickiewicz University
Wszechnicy Piastowskiej 3
61-614 Poznań, Poland

A declaration

Hereby I declare my contribution to the following papers included in this dissertation:

---

1. ***Highly regular laser-induced periodic silicon surface modified by MXene and ALD TiO_2 for organic pollutants degradation***

Andrii Lys, Iaroslav Gnilitskyi, Emerson Coy, **Mariusz Jancelewicz**, Oleksiy Gogotsi, Igor Iatsunskyi
Applied Surface Science 640 (2023) 158336
DOI: 10.1016/j.apsusc.2023.158336

In this publication, I contributed to the investigation of the SiNR/MXene/TiO_2 photocatalytic system. My contribution was related to atomic layer deposition of TiO_2 on the structured SiNR/MXene surface and to the discussion of the role of the ALD-grown oxide coating in the final photocatalytic architecture.

---

2. ***Hierarchically Structured Ti-TiO_2 Membranes Fabricated by Femtosecond Laser Ablation and Atomic Layer Deposition for Enhanced Photoelectrochemical Water Splitting***

Andrii Lys, Iaroslav Gnilitskyi, Emerson Coy, **Mariusz Jancelewicz**, Mikhael Bechelany, Igor Iatsunskyi
ACS Applied Materials & Interfaces 17 (2025) 43390–43402
DOI: 10.1021/acsami.5c07488

In this publication, I contributed to the investigation of the Ti-TiO_2 membrane photoanode system. My contribution was related to atomic layer deposition of TiO_2 on the laser-structured titanium membranes and to the discussion of how the ALD-grown TiO_2 coating affected the structure, and surface chemistry, of the hierarchical electrode.

Mariusz Jancelewicz

Dr. Mariusz Jancelewicz

Dr. Roman Viter
Institute of Atomic Physics and Spectroscopy
University of Latvia
Jelgavas iela 3
LV-1050 Rīga, Latvia

A declaration

Hereby I declare my contribution to the following papers included in this dissertation:

---

1. ***Core-shell nanofibers of $ZnFe_2O_4$/ZnO for enhanced visible-light photoelectrochemical performance***

Andrii Lys, Viktor Zabolotnii, Mária Čaplovičová, Iryna Tepliakova, Agris Berzins, Martin Sahul, Ľubomír Čaplovič, Alexander Pogrebnjak, Igor Iatsunskyi, **Roman Viter**
Journal of Alloys and Compounds 984 (2024) 173885
DOI: 10.1016/j.jallcom.2024.173885

In this publication, I acted as a corresponding author and contributed to the conceptualisation of the study, formal analysis, funding acquisition, investigation, preparation of the original draft, and manuscript review and editing.

My contribution was related to the development of the scientific concept of the work, supervision of the research, discussion and interpretation of the results, preparation and editing of the manuscript, provision of resources, project administration, and funding acquisition. I was also involved in connecting the structural and optical properties of the $ZnFe_2O_4$/ZnO core-shell nanofibres with their photoelectrochemical behaviour.

.....

Dr. Roman Viter

MSc Viktor Zabolotnii
Institute of Atomic Physics and Spectroscopy
University of Latvia
Jelgavas iela 3
LV-1050 Rīga, Latvia

A declaration

Hereby I declare my contribution to the following papers included in this dissertation:

---

1. ***Core-shell nanofibers of $ZnFe_2O_4$/ZnO for enhanced visible-light photoelectrochemical performance***

Andrii Lys, **Viktor Zabolotnii**, Mária Čaplovičová, Iryna Tepliakova, Agris Berzins, Martin Sahul, Ľubomír Čaplovič, Alexander Pogrebnjak, Igor Iatsunskyi, Roman Viter
Journal of Alloys and Compounds 984 (2024) 173885
DOI: 10.1016/j.jallcom.2024.173885

In this publication, I contributed to the fabrication of the $ZnFe_2O_4$/ZnO core-shell nanostructures, photoelectrochemical characterisation of the nanofibres, analysis of the obtained results, and preparation of the draft manuscript.

My contribution was related to the preparation and evaluation of the core-shell nanofibre system, including its photoelectrochemical response under illumination and the interpretation of the measured PEC behaviour in relation to the structure of the fabricated oxide nanofibres.

.....
MSc Viktor Zabolotnii

MSc Iryna Tepliakova
Institute of Atomic Physics and Spectroscopy
University of Latvia
Jelgavas iela 3[
LV-1050 Rīga, Latvia

A declaration

Hereby I declare my contribution to the following papers included in this dissertation:

---

1. ***Core-shell nanofibers of $ZnFe_2O_4$/ZnO for enhanced visible-light photoelectrochemical performance***

Andrii Lys, Viktor Zabolotnii, Mária Čaplovičová, **Iryna Tepliakova**, Agris Berzins, Martin Sahul, Ľubomír Čaplovič, Alexander Pogrebnjak, Igor Iatsunskyi, Roman Viter
Journal of Alloys and Compounds 984 (2024) 173885
DOI: 10.1016/j.jallcom.2024.173885

In this publication, I contributed to the investigation and structural characterisation of the $ZnFe_2O_4$/ZnO core-shell nanofibres. My contribution was related to the analysis of the nanofibre materials using SEM, XRD, FTIR, and optical spectroscopy, as well as to the description of the experimental part and discussion of the obtained results.

My role supported the identification of the structural and optical features of the core-shell oxide nanofibres and helped connect these properties with their photoelectrochemical behaviour.

.....
MSc Iryna Tepliakova

Dr. Mykola Pavlenko
NanoBioMedical Centre
Adam Mickiewicz University
Wszechnicy Piastowskiej 3
61-614 Poznań, Poland

A declaration

Hereby I declare my contribution to the following papers included in this dissertation:

---

1. ***Electrospun Polyimide Nanofibers Modified with Metal Oxide Nanowires and MXene for Photocatalytic Water Purification***

Andrii Lys, Valerii Myndrul, **Mykola Pavlenko**, Błażej Anastaziak, Pavel Holec, Kateřina Vodseďálková, Emerson Coy, Mikhael Bechelany, Igor Iatsunskyi
Nanomaterials 15 (2025) 1371
DOI: 10.3390/nano15171371

In this publication, I contributed to the synthesis of the hybrid electrospun membrane materials, investigation, and formal analysis of the PID/TiO_2/WO_3/MXene nanofibre membrane system. My contribution was related to the preparation and analysis of the membrane samples, interpretation of the structural and functional properties of the hybrid electrospun materials, and discussion of the obtained results in relation to their photocatalytic behaviour.

Mykola Pavlenko

Dr. Mykola Pavlenko

Dr. Błażej Anastaziak
NanoBioMedical Centre
Adam Mickiewicz University
Wszechnicy Piastowskiej 3
61-614 Poznań, Poland

A declaration

Hereby I declare my contribution to the following papers included in this dissertation:

---

1. ***Electrospun Polyimide Nanofibers Modified with Metal Oxide Nanowires and MXene for Photocatalytic Water Purification***

Andrii Lys, Valerii Myndrul, Mykola Pavlenko, **Błażej Anastaziak**, Pavel Holec, Kateřina Vodseďálková, Emerson Coy, Mikhael Bechelany, Igor Iatsunskyi
Nanomaterials 15 (2025) 1371
DOI: 10.3390/nano15171371

In this publication, I contributed to the investigation of the MXene component used in the PID/TiO_2/WO_3/MXene nanofibre membrane system. My contribution was mainly related to the characterization, and interpretation of $Ti_3C_2T_x$ MXene used for modification of the electrospun membranes.

I was also involved in the discussion of the influence of MXene incorporation on the properties of the hybrid nanofibres, especially in relation to charge-transfer improvement, optical response, and interaction between MXene sheets and the metal oxide components.

Błażej Anastaziak

Dr. Błażej Anastaziak

Applied Surface Science 640 (2023) 158336

Contents lists available at ScienceDirect

Applied Surface Science

journal homepage: www.elsevier.com/locate/apsusc

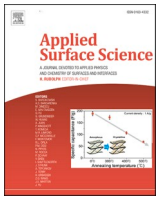

Full Length Article

Highly regular laser-induced periodic silicon surface modified by MXene and ALD TiO_2 for organic pollutants degradation

Andrii Lys [a], Iaroslav Gnilitskyi [a,b,c], Emerson Coy [a], Mariusz Jancelewicz [a], Oleksiy Gogotsi [d], Igor Iatsunskyi [a,*]

[a] NanoBioMedical Centre, Adam Mickiewicz University, 3, Wszechnicy Piastowskiej Str., 61-614 Poznan, Poland
[b] NoviNano Lab" LLC, Pasternaka, 5, 79000 Lviv, Ukraine
[c] Department of Applied Physics and Nanomaterials Science, Lviv Polytechnic National University, 12, Bandery Str., 79013 Lviv, Ukraine
[d] Materials Research Center, Krzhizhanovskogo street, 3, 03680 Kyiv, Ukraine

ARTICLE INFO

Keywords:
Silicon
Laser-induced periodic surface structures
MXene
ALD
TiO_2
Photodegradation

ABSTRACT

The co-catalytic ability of surface groups in MXene renders MXene-based composites efficient photocatalysts for organic dye photodegradation. In this study, we introduce a novel approach combining highly-regular laser-induced periodic surface Si structures (Si nanoripples - SiNR) with MXene and TiO_2, deposited through atomic layer deposition (ALD), to achieve stable, repeatable, and highly efficient photocatalytic materials. The ternary system, SiNR/MXene/TiO_2, exhibits high light absorption across the entire spectrum. Furthermore, the photodegradation efficiency of SiNR/MXene/TiO_2 is approximately 2.6 times higher than that of SiNR/TiO_2 samples. This remarkable enhancement in photocatalytic activity can be attributed to two main factors: increased separation of photogenerated charge carriers and enhanced light absorbance through the light trapping effect. The synergistic combination of SiNRs, MXene, and TiO_2 in the ternary nanocomposite structure enables efficient separation of photogenerated charge carriers, thereby minimizing recombination and enhancing the degradation of organic dyes. Moreover, the introduction of a laser-patterned surface and its ALD modification significantly enhances light absorbance, ensuring effective utilization of a wider range of the solar spectrum for photocatalysis. Therefore, SiNR/MXene/TiO_2 ternary nanocomposites hold great promise for developing high-performance photocatalysts for water purification applications, offering improved stability, repeatability, and enhanced photocatalytic efficiency.

1. Introduction

Nowadays, various synthetic dyes are widely used in diverse production fields such as pharmaceutics, food, textile, papermaking, tannery, and cosmetic industries. However, most synthetic dyes exhibit toxicity, mutagenicity, and carcinogenicity, posing a threat to the environment and water sources. Traditional water treatment approaches have been employed to address this concern, including reverse osmosis, ozonation, UV radiation, membrane filtration, chemical coagulation, and chlorination [1]. Unfortunately, these methods often fall short of completely removing pollutants from water. In contrast, photocatalytic degradation shows strong potential for efficient water treatment [2]. Numerous semiconductor materials such as ZnO, TiO_2, WO_3, CdS, ZnS, etc. have demonstrated a high potential for degrading organic contaminants in wastewater. Among these semiconductors, TiO_2 has been widely used due to its superior chemical stability, nontoxicity, and high photosensitivity in the UV region [3]. However, its main drawback lies in its inability to efficiently utilize visible light, representing 50% of the solar radiation spectrum, thereby limiting the overall photocatalytic efficiency.

Silicon, being one of the most abundant, low-cost, environmentally friendly, and widely used materials in the electronic industry, exhibits high performance as a photoactive material. However, the valence band energy level of silicon (0.6 eV) is lower than the oxidation potential of most environmental pollutants, and the Si surface is prone to surface corrosion and degradation. To overcome these limitations, nanostructuring and incorporating heterojunctions with other materials, such as TiO_2, have been widely explored to enhance the performance of silicon [4]. In our recent work, we demonstrated that Si nanopillars covered by different metal oxides (TiO_2, ZnO) and palladium

* Corresponding author.
E-mail address: igoyat@amu.edu.pl (I. Iatsunskyi).

https://doi.org/10.1016/j.apsusc.2023.158336
Received 29 May 2023; Received in revised form 10 August 2023; Accepted 25 August 2023
Available online 27 August 2023

nanoparticles exhibited superior photoactivity for solar water splitting and photocatalytic degradation of organic pollutants in water [5–7]. We found that by utilizing the Atomic Layer Deposition (ALD) technique, we can precisely control the thickness of the deposited metal oxide layers on the Si nanopillar surface, thereby enhancing the efficiency of the produced photoanodes. However, the complexity of obtaining Si nanopillars necessitates developing and applying new and repeatable methods of Si nanostructuring.

Several techniques enable the production of well-developed functional Si surfaces, including lithography, acid etching, electropolishing, and anodic oxidation. However, some of these methods suffer from limited flexibility, complex equipment, high costs, and poor repeatability of surface morphology (excluding lithography) [8,9].

In recent years, material processing and surface patterning using femtosecond lasers have gained significant attention due to their unique ability to achieve cold ablation, avoiding surface overheating, damage, and recoil pressure [10]. Linearly polarized femtosecond pulses have been utilized to induce periodic surface structures in various materials, including semiconductors, metals, and polymers. In this laser patterning process, the interference between scattered light from random surface defects and the incoming beam creates a regular intensity pattern. This periodicity gives rise to laser-induced periodic surface structures (LIPSS) [11]. Compared to conventional chemical nanostructuring methods, LIPSS is free of chemical contamination, highly durable, and easily controllable in terms of size. However, LIPSS suffers from quality issues due to the absence of a coherency ensuring translational invariance of surface structures. To overcome this limitation, a highly-regular LIPSS (HR-LIPSS) technique has been proposed and demonstrated to produce high-quality surface nanostructures over large areas at an industrially high production rate [12,13]. By employing this method, various Si nanostructured surfaces with regular periodicity can be produced over large areas and have already been successfully exploited in sensor applications [14,15]. Those kinds of morphology pose an advantage in photons absorption over polished silicon wafers through multiple internal reflections effect in nanostructure cavities leading to a lower effective reflectance loss [16].

By combining the ALD and HR-LIPSS methods, we can fabricate highly stable and repeatable Si-TiO_2 nanocomposites with a high surface area and efficient photoactivity.

To further enhance the photocatalytic activity of Si/TiO_2-based nanocomposites, incorporating highly conductive nanomaterials that promote high charge carrier drift and low recombination rates is a promising approach. MXenes, a novel class of 2D materials based on transition metal carbides or carbonitrides, have gained significant attention since the first report of $Ti_3C_2T_x$ by Yury Gogotsi's team in 2011 [17]. The chemical composition and surface functional groups of MXenes provide good metal conductivity, negatively charged surfaces, larger surface areas, superior hydrophilicity, bending stiffness superior to graphene, and other unique properties. These features enable MXenes and MXene-based composites to act as efficient photocatalysts for the photodegradation of organic molecules [18,19]. For instance, Huang et al. modified Bi_2WO_6 with $Ti_3C_2T_x$ through electrostatic adsorption, demonstrating excellent photocatalytic degradation of volatile organic compounds[20]. A ternary system based on AgNPs/TiO_2/$Ti_3C_2T_x$ also showed efficient photocatalytic degradation of organic dyes under UV and solar irradiation [21]. The authors demonstrated that MXenes facilitate charge carrier transfer, reducing the recombination of photogenerated electrons.

In this study, we investigate the effect of MXenes on enhancing the photocatalytic activity (specifically, the photodegradation of rhodamine 6G - R6G) of Si/TiO_2-based nanocomposites. We propose a highly-regular laser-induced periodic surface Si structures (Si nanoripples - SiNR)-$Ti_3C_2T_x$-TiO_2 ternary system. The combination of these materials is expected to further enhance the photocatalytic performance through improved light absorption and reduced recombination rates of photogenerated charge carriers. We present a comprehensive physicochemical characterization of the produced nanocomposites using Raman spectroscopy, Atomic Force Microscopy (AFM), Scanning Electron Microscopy (SEM), Transmission Electron Microscopy (TEM), Energy Dispersive Spectroscopy (EDX), X-Ray Photoelectron Spectroscopy (XPS), Electrochemical Impedance Spectroscopy (EIS), and Ultraviolet–Visible spectroscopy (UV–Vis). Our results demonstrate that the synergistic effect of MXene incorporation and the ordered Si surface significantly improves the photocatalytic performance.

2. Materials and methods

2.1. Materials and synthesis

All chemicals, including hydrochloric acid and lithium fluoride, were purchased from Sigma-Aldrich. Commercially available *n*-type (100) (phosphorus-doped, 0.02 Ω·cm) polished Si wafers were used in this study. Before application, 1x1 cm^2 pieces of Si were cut and cleaned in acetone, isopropanol, and water for 10 min. Si nanoripples (SiNR) were obtained by laser nanostructuring. The experiments are performed in a multiple-pulse laser ablation irradiation regime. The laser exposure was conducted using a Yb: KGW laser system producing pulses with linear polarization, having a pulse width of 266 fs. The experimental arrangement depicted in Fig. 1 also includes a configuration comprising a half-waveplate (HW) and an expander to enlarge the beam before passing through the aperture of the galvoscanner ExcelliScan. Subsequently, the beam was directed towards the galvoscanner ExcelliScan which is equipped with an F-theta lens having a focal length of 80 mm, responsible for focusing the beam onto the sample. The sample was positioned on a motorized stage. The size of the focal spot was measured and computed to be approximately 10.4 μm in diameter at e^{-2} intensity using a CCD camera placed on the focal plane within the Rayleigh range of the lens. The incident energy density of individual laser pulses is estimated to be 0.785 J per square meter for exposure in the atmosphere.

$Ti_3C_2T_x$ MXene was prepared by etching Ti_3AlC_2 (MAX-phase) using the minimally intensive layer delamination (MILD) method in a solution of lithium fluoride (LiF) in hydrochloric (HCl) acid [22]. The etching mixture was prepared from 40 mL of 12 M HCl (37%), 10 mL of DI water, and then 3.2 g of LiF dissolved in this solution. The mixture was placed in a plastic container with a volume of 50 mL. Then 2 g of Ti_3AlC_2 powder with particle sizes of less than 40 μm is gradually added into the etching solution under continuous stirring for 24 h at 25 °C. Then MXene slurry was rinsed with DI-water via repetitive centrifugation. As-prepared MXene slurry is further processed to obtain a colloidal solution of separated MXene flakes using the MILD delamination procedure.

After MXene synthesis, we prepared a water solution with 2 mg/ml of $Ti_3C_2T_x$. MXene flakes were deposited on the SiNR surface by drop casting method – SiNR/MXene sample. Finally, the ALD TiO_2 layer (500 ALD cycles corresponding to approximately 20 nm) was deposited using $TiCl_4$ and water as ALD precursors at 150 °C. The growth rate was typically 0.4 A/cycle on the planar Si surface (this was confirmed by ellipsometry measurements) – SiNR/MXene/TiO_2 sample. The schematic representation of the procedure for sample preparation is presented in Fig. 1.

2.2. Characterization

The structure of produced nanocomposites and separate materials were investigated by scanning electron microscopy (SEM) (JEOL, JSM7001F) with a dispersive energy X-ray (EDX) analyzer and transmission electron microscopy (TEM) (JEOL ARM 200F) high-resolution transmission electron microscope (200 kV) with an EDX analyzer. A Renishaw micro-Raman spectrometer with a confocal microscope measured Raman spectra for produced samples. A KRATOS Axis DLD spectrometer was used for X-ray photoelectron spectroscopy (XPS). The optical properties (absorbance, photoluminescence) have been studied with Ocean Optics spectrophotometer QE65pro. The diffuse reflectance

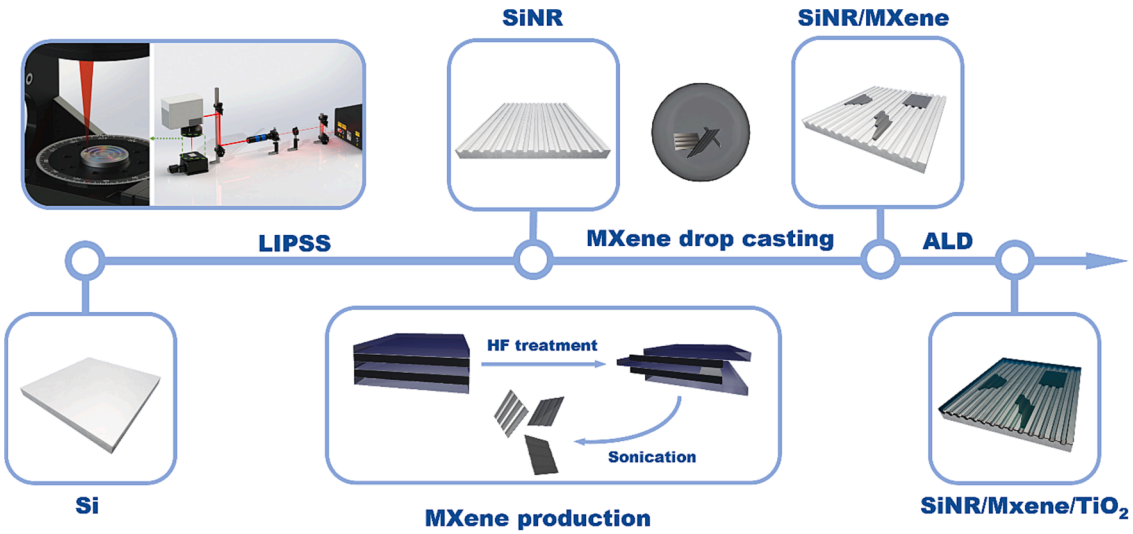

Fig. 1. Schematic representation of the procedure for sample preparation of SiNR, MXene, and ALD coating by TiO_2.

was measured in an Ocean Optics QE PRO spectrometer coupled with an integrating sphere. Electrochemical impedance spectroscopy was performed using potentiostat Gamry Reference 620.

2.3. Photodegradation tests

The photocatalytic degradation tests were conducted using a Xe lamp (300 W) for irradiation, with rhodamine 6G (R6G) selected as the model organic dye. The R6G solution was prepared with a concentration of 10^{-2} mg/mL. UV–Vis light irradiation of the samples was performed in a quartz cuvette positioned at a distance of 10 cm from the light source. The absorption spectrum was continuously recorded using the Ocean Optics USB spectrometer (QE65-PRO). The remaining concentration of R6G in the solution was determined by analyzing the absorbance spectrum at $\lambda = 530$ nm. A calibration curve of absorbance was utilized to estimate the photocatalytic activity of the samples.

3. Results and discussion

3.1. Structural characterization

The morphology and structure of the SiNR, SiNR/MXene, SiNR/TiO_2, and SiNR/MXene/TiO_2 composites were characterized using SEM, AFM, and TEM techniques. In Fig. 2a, the formation of LIPSS on a 1 cm × 1 cm Si sample is shown. The pattern consists of parallel and linear grooves with a distance of approximately 1 μm between them and a depth of around 0.5 μm (Fig. S1). Scatter granules caused by the melting effect can also be observed. Fig. 2b displays delaminated 2D sheets of Ti_3C_2Tx MXene with varying lateral sizes ranging from approximately 4 μm to 20 μm, obtained after ultrasonic shaking. Fig. 2c,d demonstrate the SiNR/MXene/TiO_2 heterostructure, clearly showing the contacts between SiNR, MXene, and TiO_2. The AFM images (Fig. 2e-g) indicate the consistency of the structural pattern throughout the synthesis stages and significant variations in the Root Mean Square (RMS) roughness at

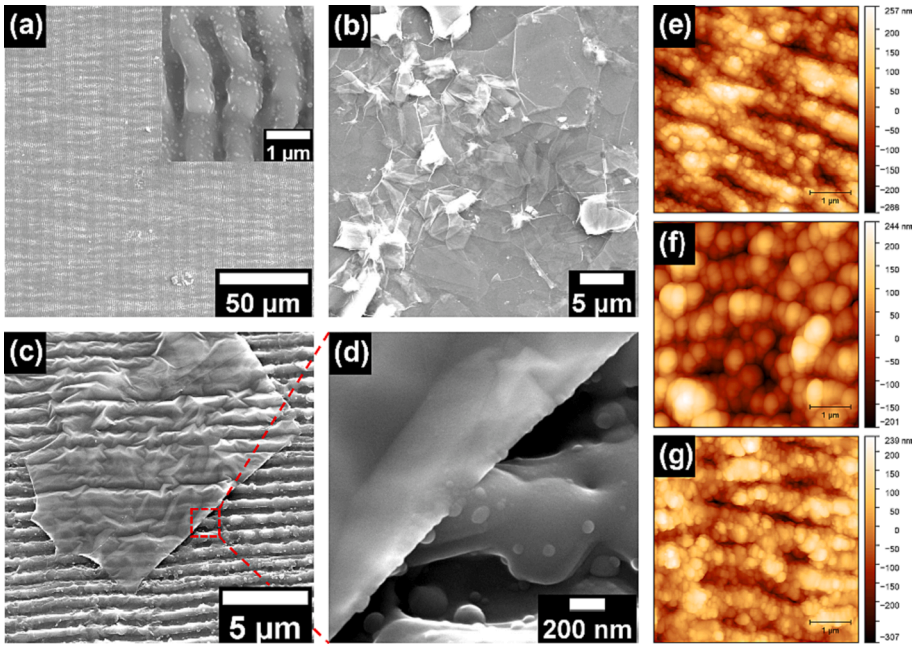

Fig. 2. SEM images of (a) SiNR, (b) $T_3C_2T_x$ MXene on Si surface, (c,d) SiNR/MXene/TiO_2 samples. AFM images of (e) SiNR, (f) SiNR/MXene, and (g) SiNR/MXene/TiO_2.

each step of the sample fabrication. It can be observed that the presence of MXene flakes reduces the *Rq* value of the SiNR surface from 22.10 ± 2.3 nm to 11.60 ± 2.6 nm. However, during the ALD deposition stage, the *Rq* value increases to 17.49 ± 1.8 nm. This suggests that the deposition of MXene flakes makes the rough surface of SiNR, produced by HR-LIPSS, smoother. On the other hand, the ALD process results in the formation of a polycrystalline/amorphous layer of TiO_2 with grain structures, leading to an increase in surface roughness. Similar phenomena of crystalline TiO_2 grain growth and increasing of roughness during ALD cycles was reported by Puurunen et al. [23].

To verify and evaluate the formation of TiO_2-MXene heterostructures, TEM analysis was conducted. MXene solution was dropped onto TEM grids, followed immediately by the ALD process. In Fig. 3a, the TEM image of the MXene flake exhibits an undulation pattern, while Fig. 3c shows a flat surface of the nanocomposite after TiO_2 ALD. This suggests that the ALD process stabilizes the MXene surface and improves its mechanical properties. The high-resolution TEM (HR-TEM) image of a single MXene flake (Fig. 3b) reveals ordered lattice fringes with a lattice spacing of 0.265 nm corresponding to the (10–10) facet of $Ti_3C_2T_x$ [24]. Fig. 3d illustrates the amorphous structure of the deposited TiO_2 layer. However, in the selected area electron diffraction (SAED) analysis (inset of Fig. 3d), the crystal hexagonal structure of $Ti_3C_2T_x$ flakes covered by the amorphous TiO_2 layer can be observed. To examine the elemental composition of the produced heterostructures, EDX mapping was performed. Fig. 3e displays an EDX mapping of the $Ti_3C_2T_x/TiO_2$ nanocomposites, showing a uniform distribution of elements, which confirms the conformal deposition of TiO_2 over the entire surface area of the MXene flakes.

3.2. Chemical and optical characterization

To analyze the chemical composition of developed nanocomposites, Raman spectroscopy and XPS analysis were utilized. Fig. 4a displays the Raman spectra of the SiNR, SiNR/MXene, and SiNR/MXene/TiO_2 samples. The SiNR samples produced by HR-LIPSS exhibit a strong Raman peak at 520 cm^{-1}, corresponding to the crystalline silicon surface [25]. The Raman spectrum of SiNR/MXene shows at least three additional modes centered at 205, 370, and 610 cm^{-1}. Recent studies have indicated that the first two Raman modes correspond to out-plane and in-plane vibrations of carbon and titanium atoms and/or the surface groups of MXene (such as F and –OH) [26–28]. The Raman peak at 610 cm^{-1} may be associated with Ti-C vibrations [29]. After the ALD deposition of TiO_2, the intensity of the peaks corresponding to MXene significantly decreases. Additionally, the Raman mode of anatase (140–150 cm^{-1}) was not observed, indicating the amorphous phase of the deposited TiO_2 (confirmed by TEM analysis).

The electronic properties of pristine MXene and SiNR/MXene/TiO_2 composites were examined using XPS. The survey spectrum of MXene flakes indicates the presence of Ti, C, O, and F elements (SI). The deconvoluted titanium core–shell (Ti 2p) XPS spectrum of MXene reveals two doublets corresponding to Ti–C $2p_{1/2}$, Ti–C $2p_{3/2}$, and Ti–O $2p_{1/2}$, Ti–O $2p_{3/2}$, centered at 454, 460, and 459.3, 465 eV, respectively (Fig. 4b). The spin-orbital splitting between the $2p_{1/2}$ and $2p_{3/2}$ components is 6 and 5.7 eV, corresponding to Ti-C and Ti-O bonds [30–32]. Therefore, XPS confirms the presence of –OH groups on the surface of MXene. After TiO_2 deposition, no peaks related to Ti-C bonds were observed, indicating the presence of only Ti-O bonds. Considering the average thickness of the TiO_2 layer (≈20 nm) and the XPS depth analysis is less than 10 nm, we can conclude that the TiO_2 ALD provides conformal coverage of the entire sample surface. The XPS analysis of carbon and oxygen core-level peaks confirms the aforementioned conclusions (SI, Fig. S2).

The light-harvesting capabilities of SiNR, SiNR/MXene, and SiNR/MXene/TiO_2 composites were evaluated using UV–Vis-NIR diffuse reflectance spectroscopy (DRS), as illustrated in Fig. 5a. The SiNR exhibits a broad absorption that extends from 400 to 950 nm, with absorption peaks at 350 and 950 nm. The deposition of MXene enhances light absorption due to several factors, such as broadband absorption, light harvesting, surface plasmon resonance and multiple reflections and scattering, [33,34], and upon the subsequent deposition of TiO_2, the optical absorption of SiNR/MXene/TiO_2 composites increases threefold across the entire spectrum. This amplified light absorption is expected to increase the concentration of photogenerated charge carriers, consequently enhancing the photocatalytic efficiency of the developed nanocomposites. However, it is unclear how this enhancement in light absorption occurs, considering the low absorption of MXene and TiO_2 in the visible range. One possible explanation for this effect is the occurrence of light multireflection processes within the silicon ripple cavity. To validate this assumption, optical simulations were conducted, which confirmed the presence of a light-trapping effect within the cavity (as discussed in the following section).

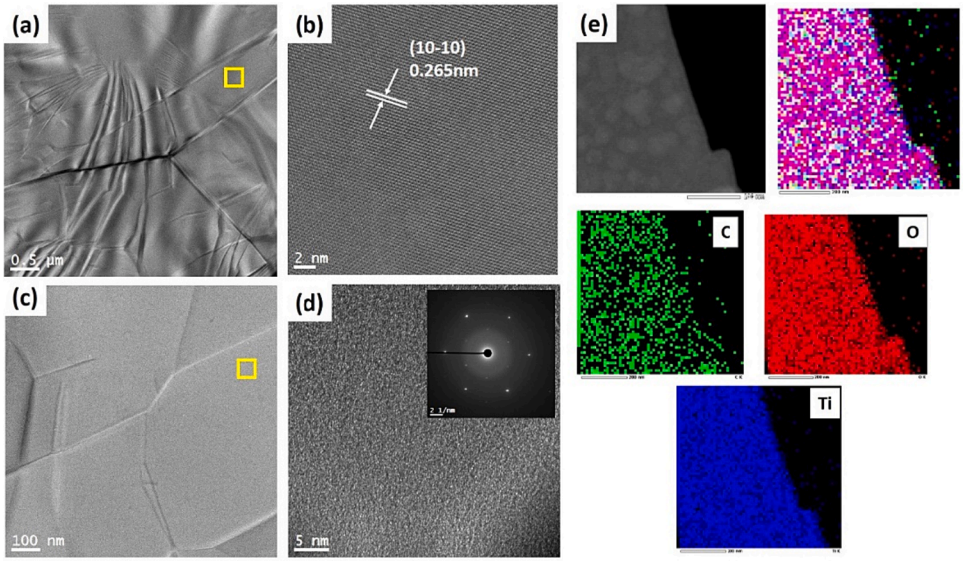

Fig. 3. The TEM and HR-TEM images of $Ti_3C_2T_x$ (a) (b), $Ti_3C_2T_x/TiO_2$ (c), and corresponding SAED in inset (d); the EDX mapping images of C, O, and Ti elements in $Ti_3C_2T_x/TiO_2$ selected area (e).

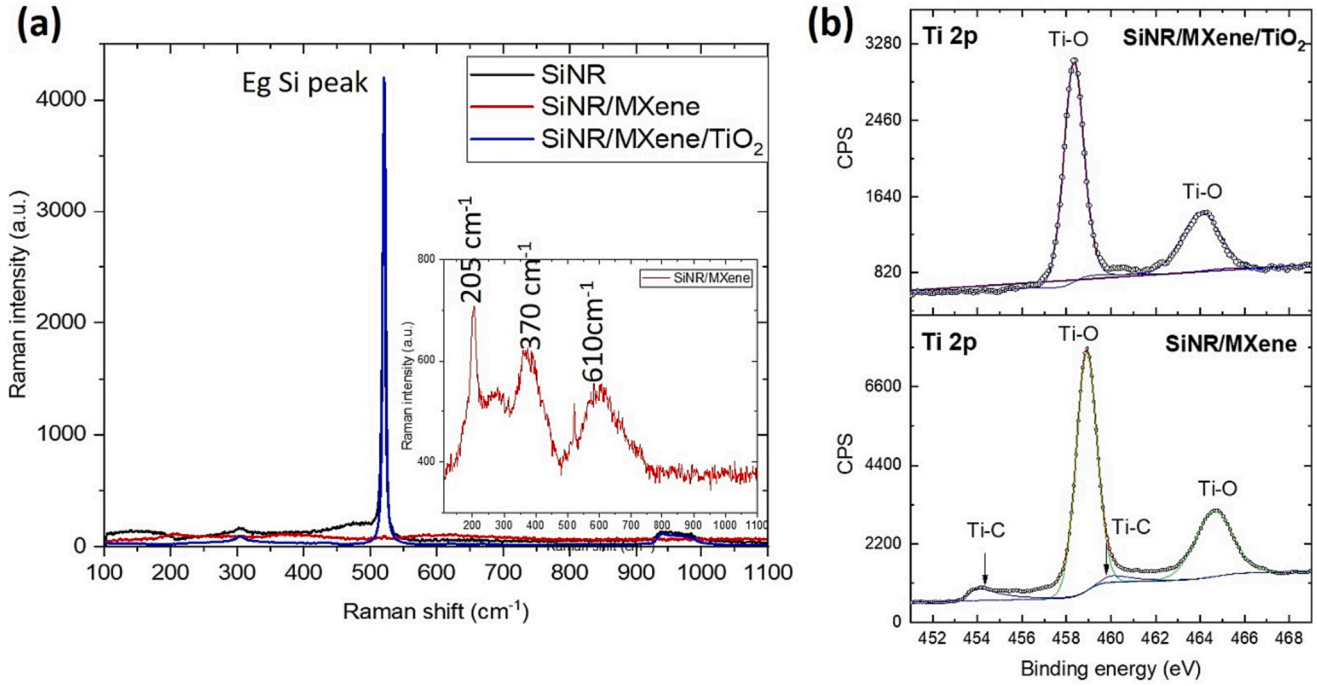

Fig. 4. Raman and XPS spectra for SiNR, SiNR/MXene and SiNR/MXene/TiO_2 samples.

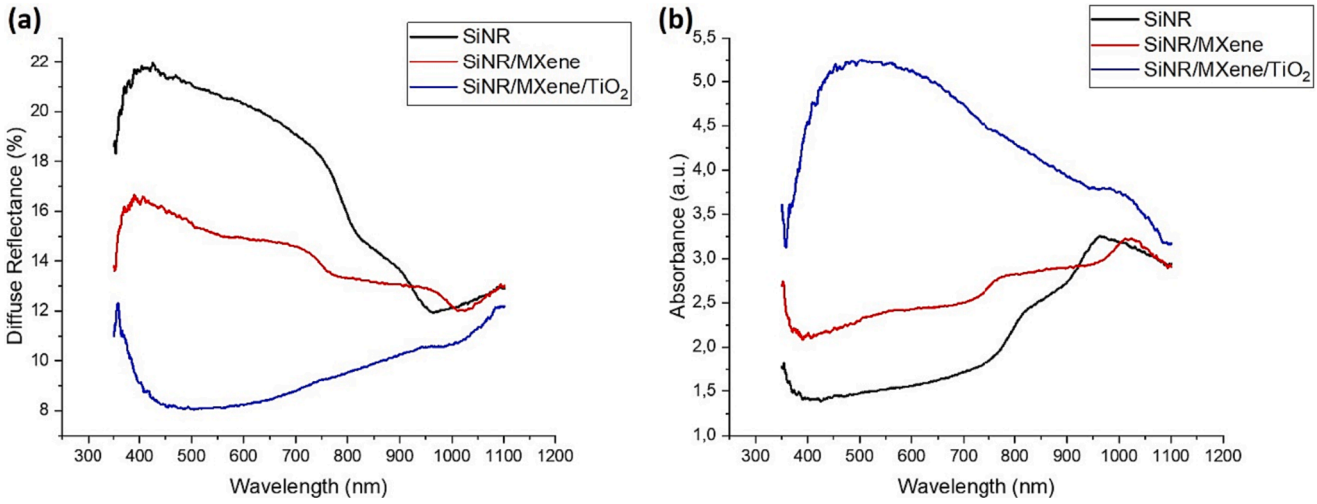

Fig. 5. (a) UV–Vis-NIR diffuse reflectance and (b) the absorption spectra of SiNR, SiNR/MXene, and SiNR/MXene/TiO_2 composites.

3.3. Photodegradation tests

The photocatalytic activity of the synthesized nanocomposites was assessed by performing R6G degradation reactions under Xe light irradiation. In Fig. 6a, the UV–Vis absorption spectra of the R6G solution are presented as a function of irradiation time for the SiNR/MXene/TiO_2 sample. The absorbance peak of R6G, located around 530 nm, gradually diminishes over time, indicating the remarkable photodegradation activity of the SiNR/MXene/TiO_2 composite. Fig. 6b compares the photodegradation performance among the SiNR, SiNR/TiO_2, SiNR/MXene, and SiNR/MXene/TiO_2 samples. After 120 min of light illumination, the R6G photodegradation efficiencies are estimated to be 8%, 30%, 32%, 50%, and 77% for the blank experiment, SiNR, SiNR/TiO_2, SiNR/MXene, and SiNR/MXene/TiO_2 samples, respectively. The photodegradation kinetics of R6G is fitted using a pseudo-first-order model, as depicted in Fig. 6c. The photodegradation process conforms to the pseudo-first-order kinetics model, which can be expressed as follows:

$$ln(C_0/C) = kt \quad (1)$$

where k - the photodegradation rate constant (min^{-1}), t - the photodegradation time (min), C_0 and C are the concentrations of R6G solution before degradation ($t = 0$) and corresponding to time, respectively. The calculated values of k are presented in Fig. 6c. The rate constant of the SiNR/MXene/TiO_2 sample (0.0103 min^{-1}) is 1.8 times that of the SiNR /TiO_2 sample (0.0057 min^{-1}). This sample (SiNR/MXene/TiO_2) demonstrates the best photoactivity compared to others.

Recyclability tests were conducted to evaluate the stability and reusability of the SiNR/MXene/TiO_2 sample, as shown in Fig. 6d. It is evident that the SiNR/MXene/TiO_2 sample exhibits stable behavior even after five consecutive runs of photodegradation tests. In contrast, the parameters and photocatalytic activity of the other samples deteriorated after the first run of experiments. This observation can be attributed to the surface oxidation of Si and degradation of MXene. However, the

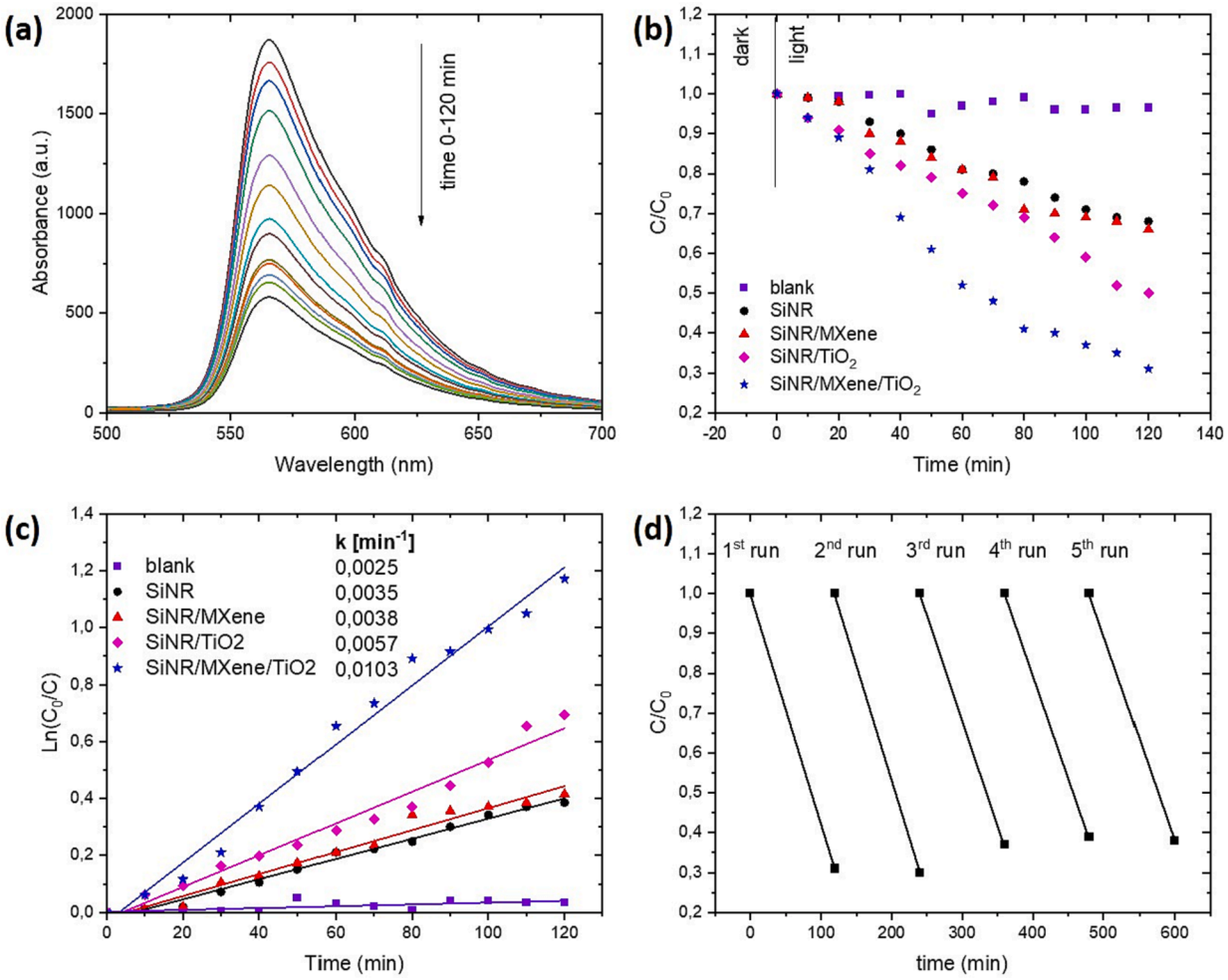

Fig. 6. (a) UV–Vis absorption spectra of R6G vs. irradiation time, (b) Photodegradation efficiencies of produced nanocomposites, (c) the corresponding rate constant k values of nanocomposites under Xe irradiation; (d) Recyclability of the photodegradation for the SiNR/MXene/TiO_2 sample.

presence of the ALD-deposited TiO_2 layer plays a crucial role in protecting the inner Si and MXene, thereby stabilizing the entire heterostructure.

3.4. Mechanism and origin of the photocatalytic enhancement

The high photocatalytic activity of the SiNR/MXene/TiO_2 sample can be attributed to the synergistic effect of increased photogenerated charge carrier separation (I. Hole extraction effect) and enhanced light absorbance (II. Light trapping effect). Fig. 7a illustrates the possible mechanisms behind these effects.

In SiNR/TiO_2 heterostructures, electron-hole pairs are generated under light illumination. The presence of a Si/TiO_2 heterostructure barrier reduces the recombination rate and improves charge carrier mobility. As a result, photogenerated holes migrate to the semiconductor/electrolyte interface, while electrons migrate to the silicon substrate. These separated electrons and holes interact with O_2 and H_2O in water, leading to the generation of superoxide anion radicals ($e^- + O_2 \rightarrow O_2^-$) and hydroxyl radicals ($h^+ + OH^- \rightarrow \cdot OH$), which can decompose R6G molecules ($\cdot OH/\cdot O^{2-} + R6G \rightarrow$ R6G photodegradation) [35]. In order to confirm this assumption, additional photocatalytic tests with scavengers were performed. Isopropyl alcohol (IPA) (10 mM) and disodium ethylenediaminetetraacetate (EDTA) (10 mM) were introduced as scavengers to capture ·OH and h^+ species, respectively, within the photocatalytic reaction. The analysis depicted in Fig. S6 reveals that both ·OH and h^+ play predominant roles in the nanocomposite photocatalytic reaction system, with h^+ demonstrating higher efficiency compared to ·OH.

Introducing MXene in the SiNR/MXene/TiO_2 heterostructure enhances the photogenerated electron-hole pair separation. MXene, due to its high negative potential, facilitates the extraction of photogenerated holes from Si and promotes their migration to TiO_2, improving their overall efficiency. Additionally, MXene exhibits excellent electrical conductivity, resembling metal-like behavior. This implies that the resistivity of the SiNR/MXene/TiO_2 heterostructure should be significantly lower than that of SiNR/TiO_2. Electrochemical Impedance Spectroscopy (EIS) measurements were conducted to validate this assumption. Fig. 7b displays the Nyquist plots for SiNR, SiNR/TiO_2, and SiNR/MXene/TiO_2 samples. The semicircle diameter in a Nyquist plot corresponds to the charge transfer resistance (*Rct*), which characterizes the charge transfer processes [6]. The SiNR/MXene/TiO_2 sample exhibits a lower *Rct* value than SiNR and SiNR/TiO_2, indicating improved conductivity due to the presence of MXene. The MXene flakes between Si and TiO_2 facilitate charge transfer, enhancing photocatalytic performance.

The enhanced photocatalytic activity of SiNR/MXene/TiO_2 samples can also be attributed to increased light absorbance (as shown in Fig. 5) and, consequently, a higher concentration of photogenerated charge carriers in the semiconductors. The complex nanoripple structure of the Si surface might explain this phenomenon. Finite-Difference Time Domain (FDTD) analysis using the Ansys Lumerical FDTD simulation package (Fig. 7c) was conducted to investigate the optical properties of

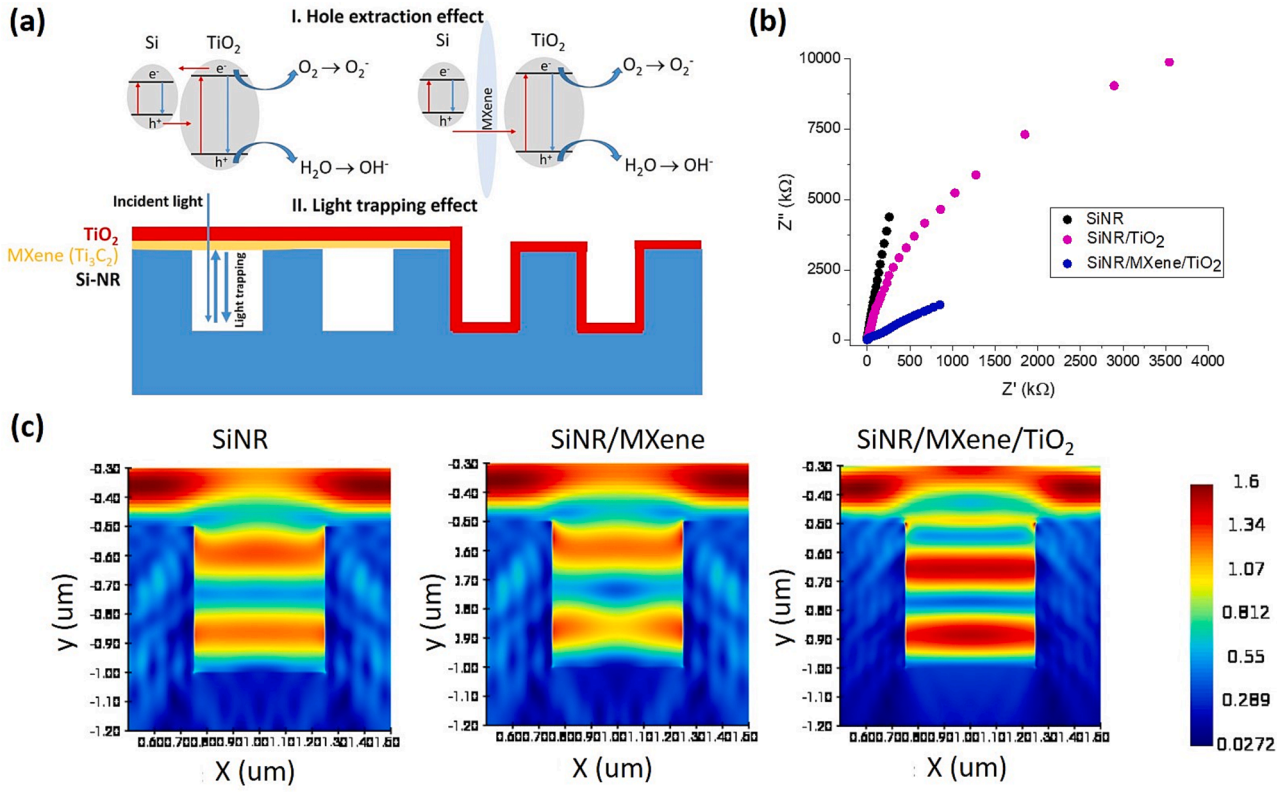

Fig. 7. (a) The mechanisms of photocatalytic activity, (b) the results of EIS experiments, (c) the electric field intensity map in linear scale for SiNR, Si/MXene, and SiNR/MXene/TiO_2 samples.

the Si cavity covered by MXene and MXene/TiO_2. The dimensions of the cavity were obtained from SEM data, and the optical constants of MXene were obtained from Ref. [36]. The analysis focused on the distribution of the electric field (E-field) inside the cavity for SiNR, SiNR/TiO_2, and SiNR/MXene/TiO_2 samples under linear polarized light at $\lambda = 550$ nm. The simulation results clearly show that the electric field intensity for the SiNR/MXene/TiO_2 sample is approximately 1.5 times higher than that of the bare Si cavity. This enhancement is likely due to light multireflection processes occurring within the silicon cavity covered by the MXene/TiO_2 layer.

In Table 1, the performance of the SiNR/MXene/TiO_2 nanocomposites developed in this study is compared with previously reported photocatalysts based on MXene. The SiNR/MXene/TiO_2 photocatalysts exhibit comparable photodegradation performance, surpassing some nanocomposites in terms of their photocatalytic efficiency. The comparison includes various parameters such as the degradation efficiency of a specific pollutant, the concentration, the irradiation source, the photocatalyst composition, and the reaction conditions. It is evident that the SiNR/MXene/TiO_2 nanocomposites are equivalent to the other reported MXene-based photocatalysts in terms of

Table 1
Comparison of photodegradation performance of various photocatalysts.

Photocatalyst	Pollu-tants	Concentration (μg/mL)	Irradiation time (min)	Light source	k (min^{-1})	Removal efficiency (%)	Ref.
SiNR/Ti_3C_2/TiO_2	R6G	10	120	300 W xenon lamp	0.0103	72	this work
Safflower-shaped TiO_2/Ti_3C_2	RhB	9.6	60	300 W xenon lamp	–	95	[37]
Ti_3C_2/g-C_3N_4	MB	10	180	500 W halogen lamp	–	60	[38]
Ti_3C_2 derived oxide	MB	20	180	visible light illumination	0.008	94	[39]
Multilayer -$Ti_3C_2(OH)_2$	MB	10	120	300 W xenon lamp	–	81.2	[40]
	RhB					17.3	
	MO					2.8	
Rare Ag-doped partial etched Ti_3C_2/Ti_3AlC_2	MB	10	20	300 W lamp (UV)	0.048	98	[41]
	RhB		55		0.006	100	
	MO		360		0.0014	100	
AgNPs/TiO_2/Ti_3C_2	MB	10	30	400 W mercury lamp (UV)	0.162	99	[21]
	RhB		40		0.143	99	
Ag/Ag_3PO_4/Ti_3C_2	MO	20	60	300 W xenon lamp	0.014	61	[34,42]
TiO_2/Ti_3C_2	MB	1	30	500 W mercury lamp	0.107	98	[43]
	MO				0.045	80	
TiO_2/Ti_3C_2	BPB	40	40	300 W xenon lamp	–	93.6	[44]
	RhB					95.15	
	MO					99.15	
$CuFe_2O_4$/Ti_3C_2	MB	15	60	visible light illumination	0.0715	94	[45]

their photocatalytic activity. This comparison highlights the considerable performance of the SiNR/MXene/TiO_2 nanocomposites in the degradation of pollutants under Xe light irradiation, underscoring their potential as highly effective photocatalysts for environmental remediation applications.

4. Conclusions

In conclusion, we have successfully developed a novel ternary nanocomposite, SiNR/MXene/TiO_2, for efficient photodegradation of organic dyes (R6G). The combination of highly-regular laser-induced periodic surface Si structures, MXene, and ALD TiO_2 demonstrated remarkable improvements in photocatalytic performance. We demonstrated that the use of SiNRs (silicon nanoripples) in the SiNR/MXene/TiO_2 nanocomposites resulted in enhanced light trapping and absorption properties. The unique morphology of SiNRs, characterized by parallel and linear grooves with specific dimensions, contributed to the efficient trapping of incident light within the cavity. Due to the presence of SiNRs, multiple reflections and light scattering occurred, leading to prolonged interaction between light and the nanocomposite structure. This extended light-matter interaction increased the overall absorption of photons by the SiNR/MXene/TiO_2 nanocomposites, especially in the visible range. Furthermore, the incorporation of MXene in the SiNR/MXene/TiO_2 nanocomposites exhibited unique co-catalytic abilities, which further enhanced the photodegradation efficiency of the nanocomposite system. The presence of MXene between the SiNRs and TiO_2 provided an efficient pathway for the migration of photogenerated holes, reducing their recombination with electrons and improving their availability for surface reactions. This enhanced charge carrier separation and transfer significantly contributed to the overall photocatalytic efficiency of the nanocomposites. The ternary system, SiNR/MXene/TiO_2, exhibited a photodegradation efficiency approximately 2.6 times higher than that of SiNR/TiO_2 samples. This significant enhancement can be attributed to the increased separation of photogenerated charge carriers, which effectively reduced recombination, and the improved light absorbance by the synergistic effect of SiNRs and MXene.

The development of SiNR/MXene/TiO_2 nanocomposites offers promising prospects for the construction of high-performance photocatalysts for water purification applications. These nanocomposites provide stable and repeatable photocatalytic materials with superior efficiency, addressing the need for effective and sustainable solutions in wastewater treatment.

In summary, our study demonstrates the potential of SiNR/MXene/TiO_2 ternary nanocomposites as highly efficient and stable photocatalysts for organic dye photodegradation, paving the way for advanced water purification technologies with enhanced environmental sustainability.

CRediT authorship contribution statement

Andrii Lys: Visualization, Software, Formal analysis, Investigation, Writing – original draft, Writing – review & editing. **Iaroslav Gnilitskyi:** Investigation. **Emerson Coy:** Investigation. **Mariusz Jancelewicz:** Investigation. **Oleksiy Gogotsi:** Investigation. **Igor Iatsunskyi:** Conceptualization, Validation, Resources, Investigation, Writing – original draft, Writing – review & editing, Supervision, Funding acquisition.

Declaration of Competing Interest

The authors declare the following financial interests/personal relationships which may be considered as potential competing interests: Igor Iatsunskyi reports financial support was provided by Adam Mickiewicz University. Igor Iatsunskyi reports a relationship with Adam Mickiewicz University that includes: employment.

Data availability

Data will be made available on request.

Acknowledgments

The authors would like to acknowledge the financial support from the National Science Centre of Poland from the SONATA BIS project 2020/38/E/ST5/00176.

Appendix A. Supplementary material

Supplementary data to this article can be found online at https://doi.org/10.1016/j.apsusc.2023.158336.

References

[1] S. Bolisetty, M. Peydayesh, R. Mezzenga, Sustainable technologies for water purification from heavy metals: review and analysis, Chem. Soc. Rev. 48 (2019) 463–487, https://doi.org/10.1039/c8cs00493e.
[2] K.K. Chenab, B. Sohrabi, A. Jafari, S. Ramakrishna, Water treatment: functional nanomaterials and applications from adsorption to photodegradation, Mater. Today Chem. 16 (2020), 100262, https://doi.org/10.1016/J.MTCHEM.2020.100262.
[3] B. Bakbolat, C. Daulbayev, F. Sultanov, R. Beissenov, A. Umirzakov, A. Mereke, A. Bekbaev, I. Chuprakov, Recent Developments of TiO2-Based Photocatalysis in the Hydrogen Evolution and Photodegradation: A Review, Nanomaterials 10 (2020) 1790, https://doi.org/10.3390/NANO10091790.
[4] M. Pavlenko, E.L. Coy, M. Jancelewicz, K. Załęski, V. Smyntyna, S. Jurga, I. Iatsunskyi, Enhancement of optical and mechanical properties of Si nanopillars by ALD TiO_2 coating, RSC Adv. 6 (2016) 97070–97076, https://doi.org/10.1039/c6ra21742g.
[5] M. Pavlenko, K. Siuzdak, E. Coy, M. Jancelewicz, S. Jurga, I. Iatsunskyi, Silicon/TiO_2 core-shell nanopillar photoanodes for enhanced photoelectrochemical water oxidation, Int. J. Hydrogen Energy 42 (2017) 30076–30085, https://doi.org/10.1016/J.IJHYDENE.2017.10.033.
[6] E. Coy, K. Siuzdak, M. Pavlenko, K. Załęski, O. Graniel, M. Ziółek, S. Balme, P. Miele, M. Weber, M. Bechelany, I. Iatsunskyi, Enhancing photocatalytic performance and solar absorption by schottky nanodiodes heterojunctions in mechanically resilient palladium coated TiO_2/Si nanopillars by atomic layer deposition, Chem. Eng. J. 392 (2020), 123702, https://doi.org/10.1016/J.CEJ.2019.123702.
[7] M. Pavlenko, K. Siuzdak, E. Coy, K. Załęski, M. Jancelewicz, I. Iatsunskyi, Enhanced solar-driven water splitting of 1D core-shell Si/TiO_2/ZnO nanopillars, Int. J. Hydrogen Energy 45 (2020) 26426–26433, https://doi.org/10.1016/J.IJHYDENE.2019.11.231.
[8] F. Priolo, T. Gregorkiewicz, M. Galli, T.F. Krauss, Silicon nanostructures for photonics and photovoltaics, Nat. Nanotechnol. 9 (2014) 19–32, https://doi.org/10.1038/nnano.2013.271.
[9] V.S. Vendamani, S.V.S.N. Rao, A.P. Pathak, V.R. Soma, Silicon Nanostructures for Molecular Sensing: A Review, ACS Appl Nano Mater. 5 (2022) 4550–4582, https://doi.org/10.1021/acsanm.1c04569.
[10] K. Lee, H. Ki, Femtosecond laser patterning based on the control of surface reflectance, Appl. Surf. Sci. 494 (2019) 187–195, https://doi.org/10.1016/J.APSUSC.2019.07.163.
[11] P. Segovia-Olvera, L. Sotelo, Y. Esqueda-Barron, M. Plata, N. Ramos, S. Camacho-Lopez, Femtosecond large-area fabrication of multi-phase titanium oxide LIPSS on thin films, Appl. Surf. Sci. 606 (2022), 154762, https://doi.org/10.1016/J.APSUSC.2022.154762.
[12] I. Gnilitskyi, T.J.Y. Derrien, Y. Levy, N.M. Bulgakova, T. Mocek, L. Orazi, High-speed manufacturing of highly regular femtosecond laser-induced periodic surface structures: physical origin of regularity, Sci. Rep. 7 (2017) 1–11, https://doi.org/10.1038/s41598-017-08788-z.
[13] I. Gnilitskyi, V. Gruzdev, N.M. Bulgakova, T. Mocek, L. Orazi, Mechanisms of high-regularity periodic structuring of silicon surface by sub-MHz repetition rate ultrashort laser pulses, Appl. Phys. Lett. 109 (2016), 143101, https://doi.org/10.1063/1.4963784/32557.
[14] I. Gnilitskyi, S.V. Mamykin, C. Lanara, I. Hevko, M. Dusheyko, S. Bellucci, E. Stratakis, Laser nanostructuring for diffraction grating based surface plasmon-resonance sensors, Nanomaterials 11 (2021) 1–10, https://doi.org/10.3390/nano11030591.
[15] S.V. Mamykin, I.M. Gnilitskyi, M.G. Dusheyko, T.A. DeVol, V.N. Bliznyuk, Femtosecond laser nano-structuring for surface plasmon resonance-based detection of uranium, Appl. Surf. Sci. 576 (2022), 151831, https://doi.org/10.1016/j.apsusc.2021.151831.
[16] S. Ullattil, S. Kakkarath, V. Viswambharanunnithan, S.P. Ramannair, Investigations on the Influence of Surface Textures on Optical Reflectance of Multi-crystalline Silicone (MC-Si) Crystal Surfaces-Simulations and Experiments, Int. J. Renew. Energy Develop. 11 (2022) 375–383, https://doi.org/10.14710/ijred.2022.38538.

[17] M. Naguib, M. Kurtoglu, V. Presser, J. Lu, J. Niu, M. Heon, L. Hultman, Y. Gogotsi, M.W. Barsoum, Two-Dimensional Nanocrystals Produced by Exfoliation of Ti_3AlC_2, Adv. Mater. 23 (2011) 4248–4253, https://doi.org/10.1002/ADMA.201102306.

[18] M. Nagoor Meeran, N. Haridharan, M. Shkir, H. Algarni, V., Reddy Minnam Reddy, Rationally designed 1D CdS/TiO_2@Ti_3C_2 multi-components nanocomposites for enhanced visible light photocatalytic hydrogen production, Chem. Phys. Lett. 809 (2022), 140150, https://doi.org/10.1016/J.CPLETT.2022.140150.

[19] N.H. Solangi, R.R. Karri, S.A. Mazari, N.M. Mubarak, A.S. Jatoi, G. Malafaia, A. K. Azad, MXene as emerging material for photocatalytic degradation of environmental pollutants, Coord. Chem. Rev. 477 (2023), 214965, https://doi.org/10.1016/J.CCR.2022.214965.

[20] G. Huang, S. Li, L. Liu, L. Zhu, Q. Wang, Ti_3C_2 MXene-modified Bi_2WO_6 nanoplates for efficient photodegradation of volatile organic compounds, Appl. Surf. Sci. 503 (2020), 144183, https://doi.org/10.1016/J.APSUSC.2019.144183.

[21] Z. Othman, A. Sinopoli, H.R. MacKey, K.A. Mahmoud, Efficient Photocatalytic Degradation of Organic Dyes by AgNPs/TiO_2/Ti_3C_2Tx MXene Composites under UV and Solar Light, ACS Omega 6 (2021) 33325–33338, https://doi.org/10.1021/acsomega.1c03189.

[22] M. Alhabeb, K. Maleski, B. Anasori, P. Lelyukh, L. Clark, S. Sin, Y. Gogotsi, Guidelines for Synthesis and Processing of Two-Dimensional Titanium Carbide (Ti_3C_2Tx MXene), Chem. Mater. 29 (2017) 7633–7644, https://doi.org/10.1021/acs.chemmater.7b02847.

[23] R.L. Puurunen, T. Sajavaara, E. Santala, V. Miikkulainen, T. Saukkonen, M. Laitinen, M. Leskelä, Controlling the crystallinity and roughness of atomic layer deposited titanium dioxide films, in, J. Nanosci. Nanotechnol. (2011) 8101–8107, https://doi.org/10.1166/jnn.2011.5060.

[24] X. Li, Q. Li, Y. Hou, Q. Yang, Z. Chen, Z. Huang, G. Liang, Y. Zhao, L. Ma, M. Li, Q. Huang, C. Zhi, Toward a Practical Zn Powder Anode: Ti_3C_2T x MXene as a Lattice-Match Electrons/Ions Redistributor, ACS Nano (2021) 14631–14642, https://doi.org/10.1021/acsnano.1c04354.

[25] C. Smit, R.A.C.M.M. Van Swaaij, H. Donker, A.M.H.N. Petit, W.M.M. Kessels, M.C. M. Van de Sanden, Determining the material structure of microcrystalline silicon from Raman spectra, J. Appl. Phys. 94 (2003) 3582–3588, https://doi.org/10.1063/1.1596364.

[26] W. Gao, X. Li, S. Luo, Z. Luo, X. Zhang, R. Huang, M. Luo, In situ modification of cobalt on MXene/TiO_2 as composite photocatalyst for efficient nitrogen fixation, J. Colloid Interface Sci. 585 (2021) 20–29, https://doi.org/10.1016/J.JCIS.2020.11.064.

[27] Q. Li, B. Liu, L. Wang, D. Li, R. Liu, B. Zou, T. Cui, G. Zou, Y. Meng, H. kwang Mao, Z. Liu, J. Liu, J. Li, Pressure-induced amorphization and polyamorphism in one-dimensional single-crystal TiO_2 nanomaterials, J. Phys. Chem. Lett. 1 (2010) 309–314. https://doi.org/10.1021/jz9001828.

[28] A.B. Tambe, S.S. Arbuj, G.G. Umarji, N.S. Jawale, S.B. Rane, S.K. Kulkarni, B. B. Kale, 2D layered MXene/TiO_2 nano-heterostructures for photocatalytic $_H$2 generation, Graphene 2D Mater. 7 (2022) 91–106, https://doi.org/10.1007/s41127-022-00052-0.

[29] Y. Dong, Y. Yin, X. Du, C. Liu, Q. Zhou, Effect of MXene@PANI on the self-healing property of shape memory-assisted coating, Synth. Met. 291 (2022), https://doi.org/10.1016/j.synthmet.2022.117162.

[30] B. Ahmed, D.H. Anjum, M.N. Hedhili, Y. Gogotsi, H.N. Alshareef, H_2O_2 assisted room temperature oxidation of Ti_2C MXene for Li-ion battery anodes, Nanoscale 8 (2016) 7580–7587, https://doi.org/10.1039/C6NR00002A.

[31] M. Cao, F. Wang, L. Wang, W. Wu, W. Lv, J. Zhu, Room Temperature Oxidation of Ti_3C_2 MXene for Supercapacitor Electrodes, J. Electrochem. Soc. 164 (2017) A3933–A3942, https://doi.org/10.1149/2.1541714jes.

[32] V. Natu, M. Benchakar, C. Canaff, A. Habrioux, S. Célérier, M.W. Barsoum, A critical analysis of the X-ray photoelectron spectra of Ti_3C_2Tz MXenes, Matter. 4 (2021) 1224–1251, https://doi.org/10.1016/j.matt.2021.01.015.

[33] H. Li, B. Sun, T. Gao, H. Li, Y. Ren, G. Zhou, Ti_3C_2 MXene co-catalyst assembled with mesoporous TiO_2 for boosting photocatalytic activity of methyl orange degradation and hydrogen production, Chin. J. Catal. 43 (2022) 461–471, https://doi.org/10.1016/S1872-2067(21)63915-3.

[34] B. Sun, F. Tao, Z. Huang, W. Yan, Y. Zhang, X. Dong, Y. Wu, G. Zhou, Ti_3C_2 MXene-bridged Ag/Ag_3PO_4 hybrids toward enhanced visible-light-driven photocatalytic activity, Appl. Surf. Sci. 535 (2021), 147354, https://doi.org/10.1016/j.apsusc.2020.147354.

[35] J. Singh, S. Kumar, A.K. Rishikesh, R.K.S. Manna, Fabrication of ZnO–TiO_2 nanohybrids for rapid sunlight driven photodegradation of textile dyes and antibiotic residue molecules, Opt Mater (Amst) 107 (2020), 110138, https://doi.org/10.1016/J.OPTMAT.2020.110138.

[36] Y. Xu, Y.S. Ang, L. Wu, L.K. Ang, High Sensitivity Surface Plasmon Resonance Sensor Based on Two-Dimensional MXene and Transition Metal Dichalcogenide: A Theoretical Study, Nanomaterials 9 (2019) 165, https://doi.org/10.3390/NANO9020165.

[37] N. My Tran, Q. Thanh Hoai Ta, J.S. Noh, Unusual synthesis of safflower-shaped TiO_2/Ti_3C_2 heterostructures initiated from two-dimensional Ti_3C_2 MXene, Appl Surf Sci. 538 (2021) 148023. https://doi.org/10.1016/j.apsusc.2020.148023.

[38] M.S.I. Nasri, M.F.R. Samsudin, A.A. Tahir, S. Sufian, Effect of MXene Loaded on g-C_3N_4 Photocatalyst for the Photocatalytic Degradation of Methylene Blue, Energies (Basel). 15 (2022) 955, https://doi.org/10.3390/en15030955.

[39] T. Liu, L. Li, X. Geng, C. Yang, X. Zhang, X. Lin, P. Lv, Y. Mu, S. Huang, Heterostructured MXene-derived oxides as superior photocatalysts for MB degradation, J. Alloy. Compd. 919 (2022), 165626, https://doi.org/10.1016/j.jallcom.2022.165629.

[40] J. Qu, D. Teng, X. Zhang, Q. Yang, P. Li, Y. Cao, Preparation and regulation of two-dimensional Ti_3C_2Tx MXene for enhanced adsorption–photocatalytic degradation of organic dyes in wastewater, Ceram. Int. 48 (2022) 14451–14459, https://doi.org/10.1016/j.ceramint.2022.01.338.

[41] Y. Lv, K. Wang, D. Li, P. Li, X. Chen, W. Han, Rare Ag nanoparticles loading induced surface-enhanced pollutant adsorption and photocatalytic degradation on Ti_3C_2Tx MXene-based nanosheets, Chem. Phys. 560 (2022), 111591, https://doi.org/10.1016/j.chemphys.2022.111591.

[42] H.-B. Fan, Q.-F. Ren, S.-L. Wang, Z. Jin, Y.i. Ding, Synthesis of the Ag/Ag3PO4/diatomite composites and their enhanced photocatalytic activity driven by visible light, J. Alloy. Compd. 775 (2019) 845–852, https://doi.org/10.1016/j.jallcom.2018.10.152.

[43] H. Zheng, X. Meng, J. Chen, M. Que, W. Wang, X. Liu, L. Yang, Y. Zhao, In situ phase evolution of TiO_2/Ti_3C_2Tx heterojunction for enhancing adsorption and photocatalytic degradation, Appl. Surf. Sci. 545 (2021), 149031, https://doi.org/10.1016/j.apsusc.2021.149031.

[44] V.Q. Hieu, T.K. Phung, T.Q. Nguyen, A. Khan, V.D. Doan, V.A. Tran, V.T. Le, Photocatalytic degradation of methyl orange dye by Ti_3C_2–TiO_2 heterojunction under solar light, Chemosphere 276 (2021), 130154, https://doi.org/10.1016/j.chemosphere.2021.130154.

[45] I.A. Alsafari, S. Munir, S. Zulfiqar, M.S. Saif, M.F. Warsi, M. Shahid, Synthesis, characterization, photocatalytic and antibacterial properties of copper Ferrite/MXene ($CuFe_2O_4$/Ti_3C_2) nanohybrids, Ceram. Int. 47 (2021) 28874–28883, https://doi.org/10.1016/j.ceramint.2021.07.048.

nanomaterials

MDPI

Article

Electrospun Polyimide Nanofibers Modified with Metal Oxide Nanowires and MXene for Photocatalytic Water Purification

Andrii Lys [1], Valerii Myndrul [2], Mykola Pavlenko [1], Błażej Anastaziak [1], Pavel Holec [3], Kateřina Vodseďálková [4], Emerson Coy [1], Mikhael Bechelany [5] and Igor Iatsunskyi [1,*]

[1] NanoBioMedical Centre, Adam Mickiewicz University, 61-712 Poznan, Poland; andrii.lys@amu.edu.pl (A.L.); mykpav@amu.edu.pl (M.P.); blazej.anastaziak@amu.edu.pl (B.A.); coyeme@amu.edu.pl (E.C.)
[2] Sensor Engineering Department, Faculty of Science and Engineering, Maastricht University, P.O. Box 616, 6200 MD Maastricht, The Netherlands; valerii.myndrul@maastrichtuniversity.nl
[3] Department of Nonwovens and Nanofibrous Materials, Faculty of Textile Engineering, Technical University of Liberec, 461 17 Liberec, Czech Republic; pavel.holec@tul.cz
[4] Nanopharma a.s., 530 09 Pardubice, Czech Republic; vodsedalkova@nanopharma.cz
[5] European Institut of Membranes (IEM)—UMR 5635, University of Montpellier, ENSCM, CNRS, 34090 Montpellier, France; mikhael.bechelany@umontpellier.fr
* Correspondence: igoyat@amu.edu.pl

Abstract

As the demand for clean water continues to rise, the development of reliable and environmentally sustainable purification methods has become increasingly important. In this study, we describe the production and characterization of electrospun polyimide (PID) nanofibers modified with MXene (Ti_3C_2Tx), tungsten trioxide (WO_3), and titanium dioxide (TiO_2) nanomaterials for improved photocatalytic degradation of rhodamine 6G (R6G), a model organic dye. Superior photocatalytic performance was achieved by suppressing electron–hole recombination, promoting efficient charge carrier separation, and the significant increase in light absorption through the addition of metal oxide nanowires and MXene to the PID matrix. Comprehensive characterization confirms a core–shell nanofiber architecture with TiO_2, WO_3, and MXene effectively integrated and electronically coupled, consistent with the observed photocatalytic response. The PID/TiO_2/WO_3/MXene composite exhibited the highest photocatalytic activity among the tested configurations, degrading R6G by 74% in 90 min of light exposure. This enhancement was ascribed to the synergistic interactions between MXene and the metal oxides, which reduced recombination losses and promoted effective charge transfer. The study confirms the suitability of PID-based hybrid nanofibers for wastewater treatment applications. It also points toward future directions focused on scalable production and deployment in the field of environmental remediation.

Keywords: electrospinning; nanofibers; MXene ($Ti_3C_2T_x$); metal oxides; organic dye degradation; advanced functional materials

Academic Editor: Marco Stoller

Received: 23 July 2025
Revised: 28 August 2025
Accepted: 2 September 2025
Published: 5 September 2025

Citation: Lys, A.; Myndrul, V.; Pavlenko, M.; Anastaziak, B.; Holec, P.; Vodseďálková, K.; Coy, E.; Bechelany, M.; Iatsunskyi, I. Electrospun Polyimide Nanofibers Modified with Metal Oxide Nanowires and MXene for Photocatalytic Water Purification. *Nanomaterials* **2025**, *15*, 1371. https://doi.org/10.3390/nano15171371

1. Introduction

Water scarcity is becoming increasingly challenging and difficult to manage in many regions worldwide. This is due in part to rapid population growth, expanding industrial development, and the limited adaptability of conventional purification technologies [1]. Textile manufacturing is a significant source of water pollution, releasing large volumes of wastewater containing synthetic dyes. These compounds tend to be chemically stable, environmentally persistent, and harmful to aquatic ecosystems [2]. The challenges of

operational complexity, high costs, and the production of secondary waste remain significant and critical [3]. These challenges have encouraged researchers to explore new treatment technologies that offer greater reliability, can be scaled up more easily, and have a lower environmental impact. Among them, photocatalysis has gained recognition as a promising approach for breaking down organic pollutants in water through a light-driven, energy-efficient process. Semiconductor photocatalysts such as TiO_2, ZnO, WO_3, CdS, and ZnS are widely studied for dye and pollutant removal, with recent work emphasizing defect engineering and heterostructure design to enhance activity under illumination [4,5]. These materials are favored for their chemical robustness, environmental compatibility, and relatively low production costs [6]. Nevertheless, their practical use remains limited by several intrinsic drawbacks. These include insufficient absorption in the visible range, high rates of electron–hole recombination, and considerable band gap energies, all of which reduce overall photocatalytic efficiency [7,8].

Improving photocatalytic materials often comes down to two main ideas. The initial step in the process is to reduce the particle size, thereby exposing a larger surface area, which helps increase the number of active sites [9,10]. The second approach involves the combination of different semiconductors into heterostructures, which facilitate the movement of charges more freely and maintain their separation for more extended periods. This improves how light is absorbed and utilized, and reduces the likelihood of recombination [11,12]. These changes are most effective when the material structure can be easily adjusted, especially at the nanoscale, where minor differences have significant effects.

Among the various fabrication methods, electrospinning stands out due to its ability to easily produce long, high-porosity fibers with a large surface area. This method is compatible with multiple materials, including polymers and ceramic additives, and allows control over fiber structure, spacing, and surface properties [13]. The fibrous networks created in this manner are beneficial for photocatalysis, as they provide light and reactants with better access to active regions and can be modified to accommodate various reactions.

The incorporation of conductive nanomaterials into photocatalytic systems has recently shown great potential in enhancing charge transport and prolonging the lifetime of photogenerated carriers. MXenes, a family of two-dimensional transition metal carbides and carbonitrides first introduced by Gogotsi and co-workers in 2011 [14], have attracted particular attention. $Ti_3C_2T_x$, the most extensively studied MXene, exhibits excellent electronic conductivity and strong hydrophilicity, along with surface terminations (-OH, -O, -F) that enable tunable interfacial interactions. In hybrid systems, MXenes can function as efficient electron sinks, facilitating charge separation and improving light absorption. For instance, Zheng et al. [15] demonstrated that incorporating $Ti_3C_2T_x$ into a TiO_2 matrix led to enhanced dye degradation performance under light irradiation due to improved charge separation.

In this study, we report a composite nanofiber system based on electrospun polyimide (PID) incorporating TiO_2 and WO_3 nanowires along with $Ti_3C_2T_x$ MXene sheets. This design aims to exploit the synergistic effects of the metal oxides and MXene within a well-structured fibrous network to enhance the photocatalytic degradation of rhodamine 6G (R6G), a model organic dye. AFM, SEM, TEM, XPS, UV-Vis spectroscopy, photoluminescence analysis, and photocatalytic testing under simulated solar irradiation were used to characterize the resulting materials. Our findings indicate that incorporating MXene and metal oxides into the electrospun PID matrix significantly enhances photocatalytic performance, driven by improved light absorption, efficient interfacial charge transfer, and suppressed charge recombination. These results underscore the promise of PID-based composite fibers for next-generation water purification technologies.

2. Materials and Methods

2.1. Reagents and Chemicals

Polyimide pellets (P8TM SG) (PID) were purchased from HP Polymer Inc. (Lenzing, Austria). N,N-Dimethylacetamide (99.8%) (DMA) was obtained from PENTA Chemicals (Prague, Czech Republic). Titanium dioxide (TiO_2) and tungsten trioxide (WO_3) nanowires, along with titanium aluminum carbide (Ti_3AlC_2, MAX phase), were sourced from Sigma-Aldrich (St. Louis, MO, USA). Unless specified, reagents were used as received without further purification; solutions were prepared fresh in deionized water (18.2 megaohm centimeter). Dispersions were sonicated to homogenize and, when required, passed through a 0.22 micrometer syringe filter.

2.2. Synthesis of MXenes

$Ti_3C_2T_x$ MXene was prepared by etching Ti_3AlC_2 (MAX-phase) using the MILD method in a solution of lithium fluoride (LiF) in hydrochloric (HCl) acid. The etching mixture was prepared from 40 mL of 12 M HCl (37%) and 10 mL of DI water, and then 3.2 g of LiF was dissolved in this solution. The mixture was placed in a 50 mL plastic container. Next, 2 g of Ti_3AlC_2 powder with particle sizes less than 40 μm was gradually added to the etching solution under continuous stirring for 24 h at 25 °C. The MXene slurry was then rinsed with DI water via repetitive centrifugation. As-prepared MXene slurry is further processed to obtain a colloidal solution of separated MXene flakes using a mild delamination procedure.

2.3. Solutions Preparation and Electrospinning

The schematic representation of the solution preparation and electrospinning processes is shown in Figure 1a. The polymeric solution for electrospinning was prepared by dissolving 16% *w*/*w* polyimide (PID) pellets in N,N-dimethylacetamide (DMA). The mixture was stirred at 250 rpm for 24 h at room temperature to ensure complete dissolution.

Solutions containing additives were prepared following the same procedure, with an additional 5% *w*/*w* of each planned additive mixed with the 16% *w*/*w* PID pellets. The following composite solutions were prepared: pristine PID, PID/TiO_2, PID/TiO_2/MXene, PID/WO_3, PID/WO_3/MXene, and PID/TiO_2/WO_3/MXene.

A custom-made electrospinning setup was used for fiber fabrication (Figure 1b). The prepared solutions were loaded into 5 mL plastic syringes. Standard sterile injection needles (0.60 mm in diameter, 40 mm length) were modified by cutting the tips to ensure a symmetric electric field and were subsequently used for electrospinning. An antistatic polypropylene spunbond non-woven mat (surface density 18 g/m^2) was attached to the grounded conveyor belt collector, maintaining a 200 mm distance between the needle tip and the collector. An electric field of 10 kV was applied during electrospinning, and the solution was dispensed at a constant flow rate of 5 mL/hour using a syringe pump.

2.4. Characterization

The structural properties of the produced nanofibers were investigated by scanning electron microscopy (SEM) (JEOL JSM-7001F), equipped with an energy-dispersive X-ray (EDX) analyzer with an accelerating voltage of 5–10 kV and working distance of 8–12 mm, and high-resolution transmission electron microscopy (HR-TEM) (JEOL ARM 200F, 200 kV) (JEOL Ltd., Akishima, Tokyo, Japan), also equipped with an EDX analyzer. AFM Bruker ICON was employed to study properties of MXene flakes (Bruker Corporation, Billerica, MA, USA). X-ray photoelectron spectroscopy (XPS) was performed using a KRATOS Axis DLD spectrometer with monochromatic Al Kα (1486.6 eV) (Kratos Analytical Ltd., Manchester, UK); survey and core levels were at 160 eV and 20 eV pass energies (energy

resolution ~0.4 eV); spectra was referenced to C 1s at 284.8 eV and fitted using a Shirley background and mixed Gaussian–Lorentzian profiles. We used Renishaw in-Via micro-Raman system with plane-polarized lasers at λexc = 633 nm with a 50× objective, a laser power of ≤1 mW, and an over measurement range with two to four accumulations and calibrated to the 520.7 cm^{-1} Si line. FTIR spectra by JASCO FT/IR-4700 (with ATR PRO ONE) (JASCO Corporation, Hachioji, Tokyo, Japan) were collected in ATR mode over 4000–400 cm^{-1} at 4 cm^{-1} resolution, and the spectra were baseline-corrected and normalized before analysis. The optical properties, including absorbance and photoluminescence, were examined using an Ocean Optics QE65 Pro spectrophotometer (Ocean Optics, Inc., Dunedin, FL, USA). Diffuse reflectance measurements were performed using an Ocean Optics QE Pro spectrometer, coupled with an integrating sphere, with subsequent conversion via the Kubelka–Munk function F(R), and band gaps were extracted from Tauc plots with n = 2 by linear extrapolation. However, no significant changes or additional insights were observed compared with other characterization methods.

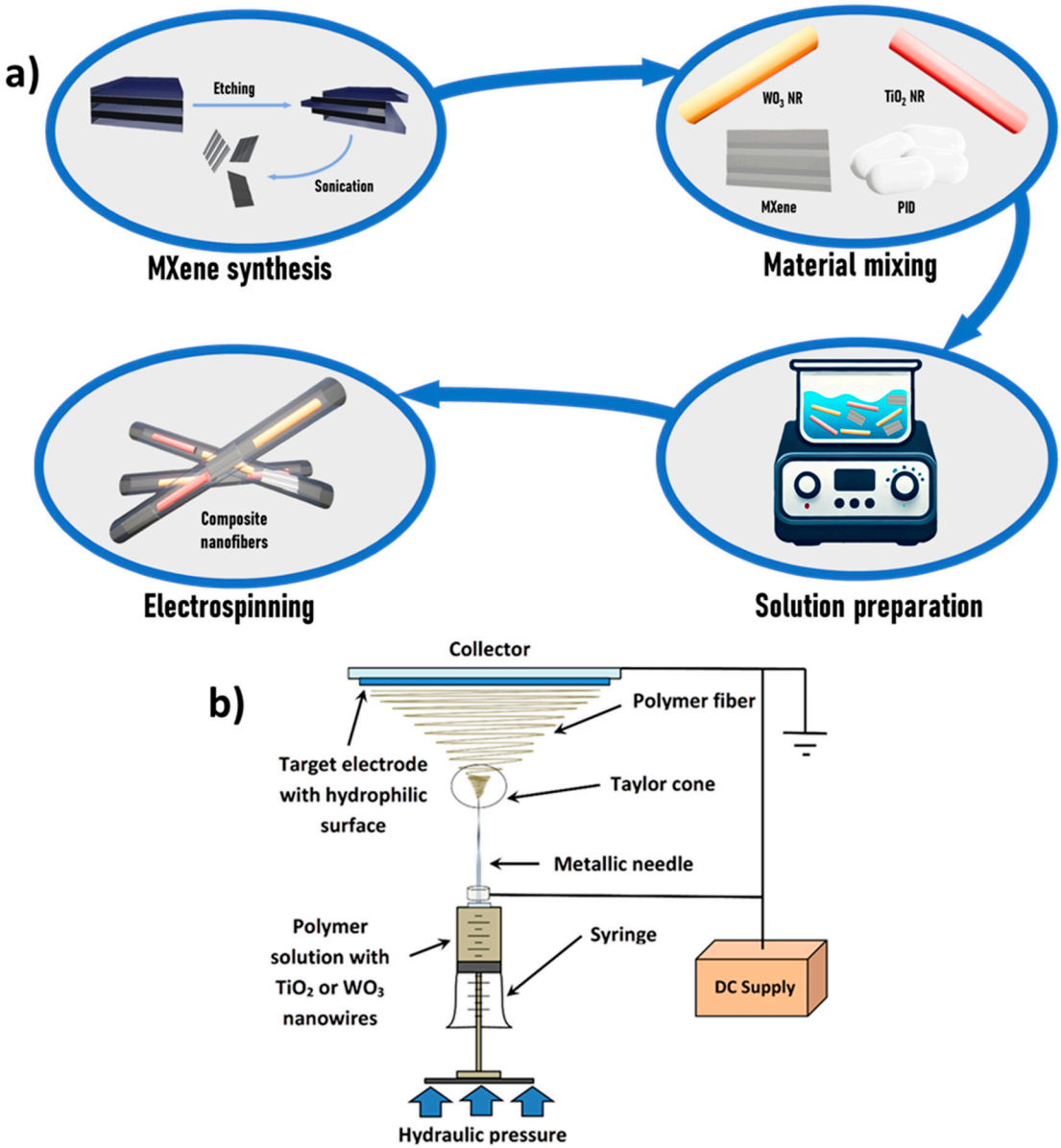

Figure 1. (**a**) Schematic representation of the composite nanofiber synthesis process. (**b**) Experimental setup used for nanofiber fabrication.

2.5. Photodegradation Tests

Photocatalytic degradation tests were performed using a 300 W xenon (Xe) lamp as the irradiation, with Rhodamine 6 G (R6G) selected as the model organic dye. The R6G solution (pH ~7.0) was prepared at a concentration of 10^{-2} mg/mL. Photodegradation used a 1 × 2 cm nanofiber coupon (2.0 cm^2) mounted on a plastic holder; although mats differed between samples, photocatalyst loading was controlled by applying an identical aliquot of the same dispersion per coupon (single-sided) under identical drying/curing conditions, and each test used 2.0 mL of Rhodamine 6G solution. UV-Vis light irradiation of the samples was conducted in a quartz 3.5 mL cuvette positioned 10 cm from the light source. The absorption spectrum was continuously recorded using an Ocean Optics USB spectrometer (QE65-Pro) (Ocean Optics, Inc., Dunedin, FL, USA). The remaining concentration of R6G in the solution was determined by analyzing the absorbance spectrum at λ = 530 nm. A calibration curve of absorbance was used to evaluate the photocatalytic activity of the samples.

3. Results and Discussion

3.1. Structure Characterization

Prior to their incorporation into polymeric nanofibers, the morphological characteristics of the as-prepared MXene flakes were analyzed using AFM. Figure 2a shows MXene flakes deposited on a flat substrate. The flake displays a uniform and planar morphology with sharply defined edges, indicating successful exfoliation of the $Ti_3C_2T_x$ MXene. The average lateral size of the flake is approximately 1.5 μm, consistent with micrometer-scale flakes typically obtained through mild delamination techniques. The inset in Figure 2a shows the height profile along a selected cross-section of the flake, with an average thickness of approximately 1.5 nm. This thickness corresponds to single- to few-layer $Ti_3C_2T_x$ MXene sheets as reported in previous studies [16].

The structural features of the exfoliated $Ti_3C_2T_x$ MXene were first examined by Raman spectroscopy using a 633 nm excitation laser (Figure 2b). The spectrum displays broad and distinct peaks characteristic of few-layer MXene with surface terminations and defect-induced disorder. The prominent peak at 155 cm^{-1} corresponds to the A_{1g} mode of out-of-plane Ti vibrations [17], confirming the preservation of the Ti–C network. A secondary peak at 205 cm^{-1} is attributed to the Eg mode, related to in-plane vibrations. Additionally, bands observed at 405 cm^{-1} and 615 cm^{-1} are associated with Ti–O and Ti–OH surface terminations [16], respectively, and possible lattice distortions caused by delamination or oxidation [18].

XPS analysis (Figure 2c) provided further insight into the surface chemistry of $Ti_3C_2T_x$. The C 1s spectrum revealed peaks at 281.3 eV (C–Ti), 284.7 eV (C–C/C–H), 286.7 eV (C–O/C–OH), and 288.6 eV (C=O/O–C=O) [19], confirming the coexistence of carbide and oxidized carbon species. The Ti 2p spectrum showed three distinct components: Ti–C (451.8 eV), Ti^{3+} (~457.7 eV), and Ti^{4+} (~458.9 eV), indicating partial surface oxidation, likely forming a thin TiO_2 shell while preserving the carbide-rich core. These analyses confirm the successful synthesis of MXene with maintained structural integrity.

The as-synthesized polymeric nanofibers incorporating MXene, TiO_2, TiO_2/MXene, WO_3, WO_3/MXene, and TiO_2/WO_3/MXene were thoroughly examined using SEM coupled with EDX analysis, as well as TEM, to gain a comprehensive understanding of the composites' morphology and internal structure.

In Figure 3a, the morphology of the pristine polymeric nanofibers is displayed, with EDX analysis confirming characteristic polymeric peaks. The morphology of the PID/MXene composite, shown in Figure 3b, maintains a nanofiber structure but exhibits the formation of polymeric beads. The occurrence of these beads is attributed to changes in

net charge density due to the introduction of MXene nanoflakes [20]. The EDX pattern in Figure 3b confirms the presence of Ti_3C_2 MXenes, as indicated by the clear Ti and F peaks. The fluorine peak is associated with surface termination groups remaining on the Ti_3C_2 surface after etching the Ti_3AlC_2 MAX phase [21].

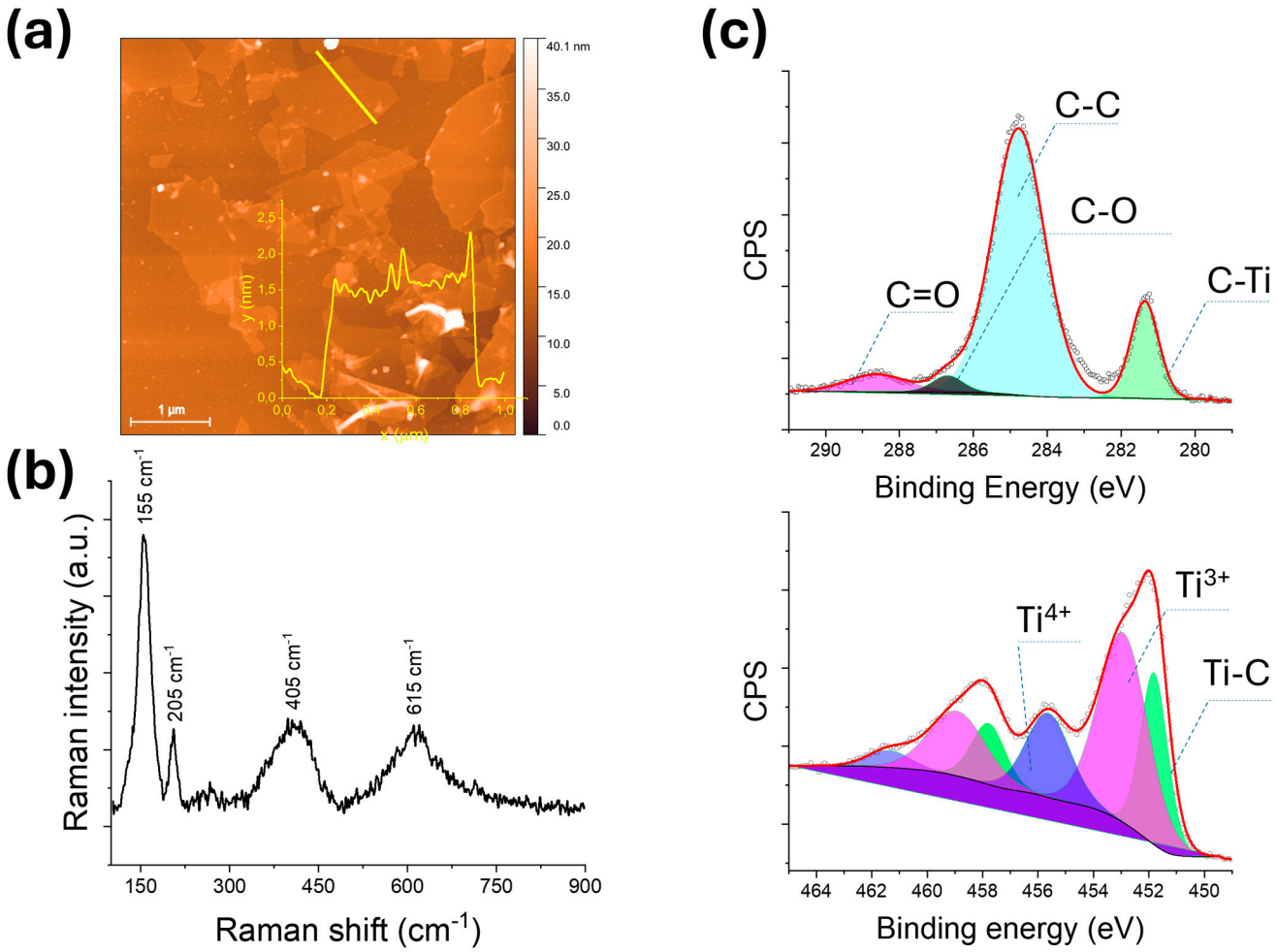

Figure 2. (**a**) AFM image and height profile of an exfoliated $Ti_3C_2T_x$ MXene flake. (**b**) Raman spectrum of $Ti_3C_2T_x$. (**c**) High-resolution XPS spectra of the C 1s and Ti 2p regions.

The most uniform nanofibers, in terms of additive dispersion, are those formed from PID combined with commercial TiO_2 nanowires. As shown in Figure 3c, the TiO_2 nanowires embedded within the PID nanofibers form a coaxial (core–shell) structure, which is analogous to the insulation surrounding traditional wires. This structure enables the fabrication of flexible, conductive, and insulated nanoscale wires suitable for advanced electronic applications.

Figure 3d–f illustrates the morphologies of PID/WO_3, PID/WO_3/MXene, and PID/TiO_2/WO_3/MXene composites. These fiber mats display an uneven distribution of WO_3, TiO_2, and MXene within the fibers. This non-uniformity could result from electrostatic interactions among the components, sedimentation, or blockages in the electrospinning needle [22]. However, the composite containing TiO_2 nanowires (Figure 3f) demonstrates improved uniformity and distribution of solid materials within the nanofiber core.

TEM analysis was conducted to investigate further the structural features of PID nanofibers incorporating TiO_2 and WO_3, as shown in Figure 4. The results reveal the formation of a TiO_2-core/PID-shell structure (Figure 4, upper row), where the TiO_2 nanowire is centrally embedded within the PID nanofiber (the image labeled "Ti" represents elemental

titanium). In contrast, the PID/WO_3 nanofibers exhibit an irregular distribution of WO_3 nanowires or their fragments. The presence of WO_3 is confirmed by the elemental mapping of tungsten (labeled "W") in the lower row of Figure 4.

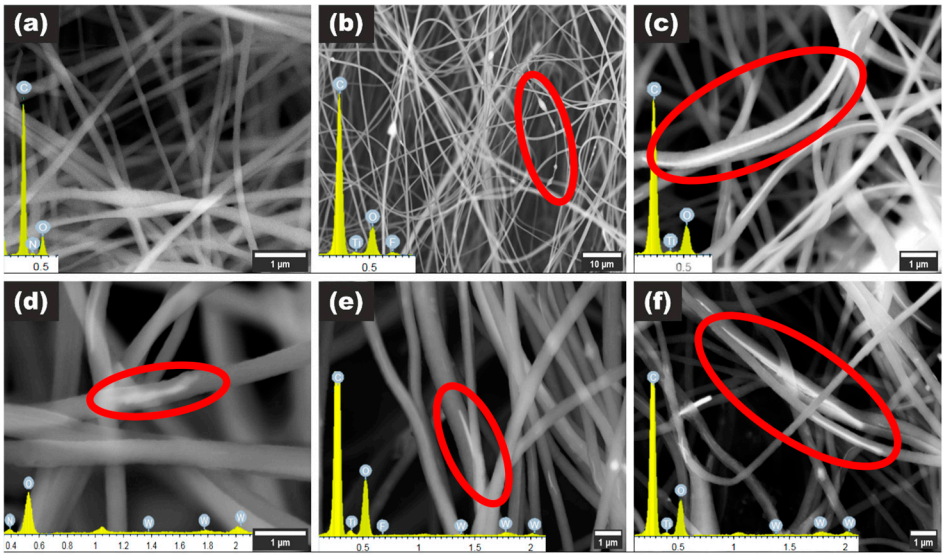

Figure 3. (**a**) SEM images of PID, (**b**) PID/MXene, (**c**) PID/TiO_2, (**d**) PID/WO_3, (**e**) PID/WO_3/MXene, and (**f**) PID/TiO_2/WO_3/MXene nanofibers. Inset graphs represent corresponding EDX measurements. Red circles highlight areas within the nanofiber mats where nanoparticles are incorporated into the fibers.

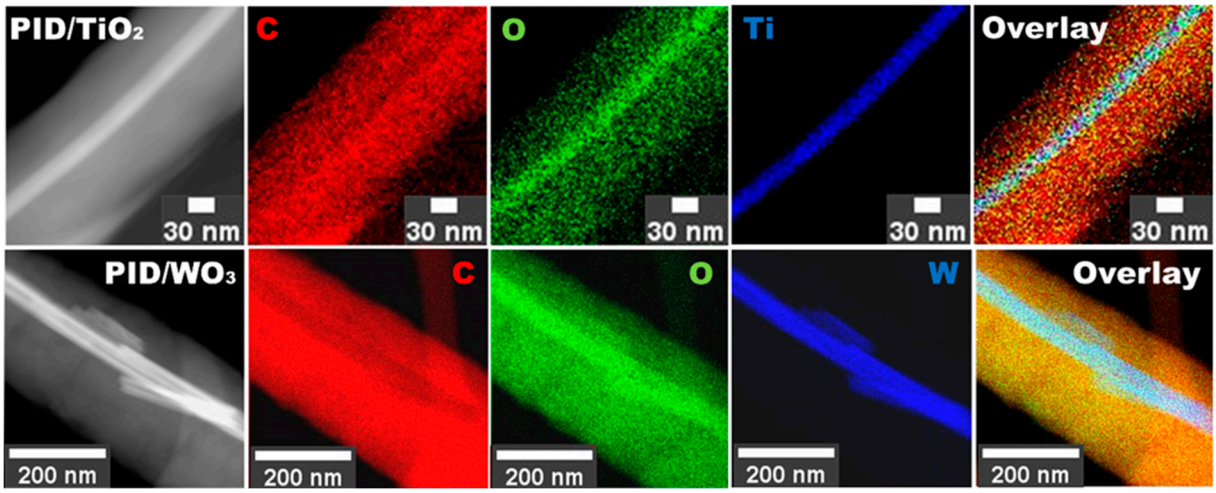

Figure 4. TEM images of PID/TiO_2 (upper line), PID/WO_3 (lower line).

3.2. Chemical and Optical Properties of Produced Nanocaomposites

To investigate the chemical structure and composition of the developed nanocomposite system, a combination of Raman spectroscopy, XPS, FTIR, UV-Vis, and PL analyses was employed.

To evaluate the impact of MXene and metal oxide incorporation into the polyimide (PID) matrix, high-resolution XPS was also conducted on the electrospun nanofibers (Figure 5). In the O 1s region (Figure 5b), the dominant peak at ~530 eV corresponds to O=C bonds, while those at ~531–532 eV are attributed to O–H and O–C functionalities [23]. The appearance of a minor peak near ~533 eV, associated with adsorbed water, suggests slight non-uniformity in the electrospun mats [23]. A noticeable increase in oxygen content and subtle shifts in peak positions were observed upon addition of MX-

ene or TiO_2/WO_3/MXene, suggesting interactions between the polymer and the surface terminations of the nanomaterials [24].

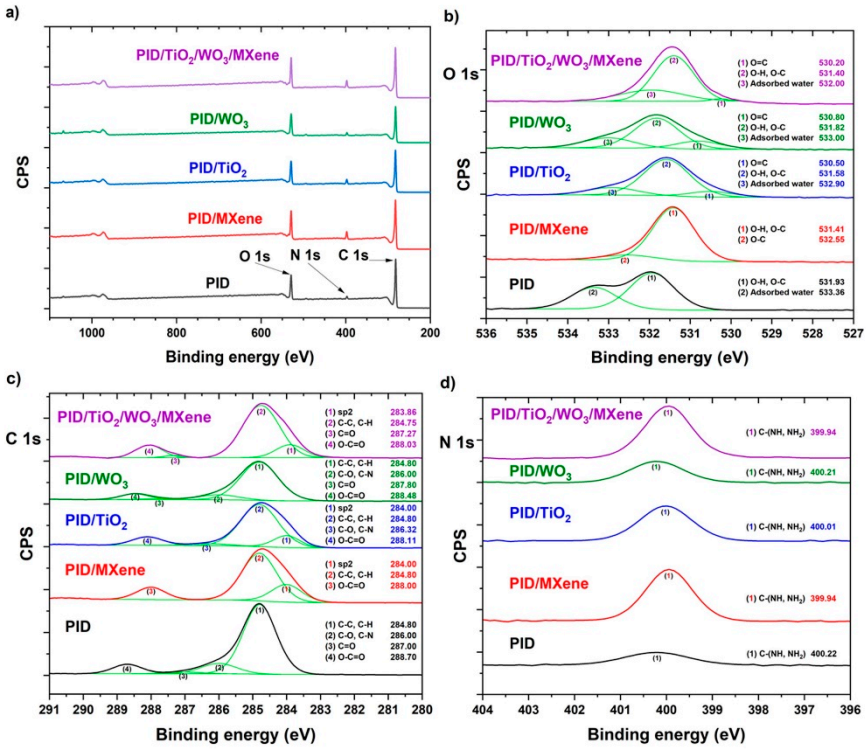

Figure 5. (**a**) Full-range XPS spectra, and (**b**) high-resolution O 1s, (**c**) C 1s, (**d**) N 1s spectra of PID-based nanofibers. Corresponding binding energy values obtained by the deconvolution of the detected peaks are shown in the insets.

The C 1s spectrum (Figure 5c) exhibited consistent peaks at ~283 eV (sp^2 C) [25], ~284.8 eV (C–C/C–H), and ~288 eV (O–C=O), with no significant changes following admixture incorporation [26]. However, the ~286 eV peak (C–O, C–N) showed reduced intensity, indicating possible modification of the polyimide backbone or matrix–additive interactions. The weak and unstable C=O peak at ~287 eV was only occasionally detected, suggesting no significant structural disruption [26].

Nitrogen bonding was assessed via the N 1s spectrum (Figure 5d), where the peak at ~400 eV, assigned to C–(NH, NH_2) groups, increased in intensity upon additive incorporation [26]. This enhancement suggests stronger nitrogen interactions between the polymer and embedded nanomaterials, particularly MXene.

Complementary FTIR analysis (Figure S1) confirmed the preservation of the polyimide molecular structure across all nanocomposite samples. The presence of characteristic absorption bands, including C=O stretching (~1720 cm^{-1}), C–N stretching (~1375 cm^{-1}), and imide ring deformation (~725 cm^{-1}), was consistently observed [27]. The absence of new peaks or significant shifts indicates that TiO_2, WO_3, and MXene were physically embedded, rather than chemically altering the polyimide matrix.

The optical properties of the nanofibers were evaluated by UV-vis spectroscopy (Figure 6a). The pristine PID exhibited strong UV absorption and limited visible activity [28]. The incorporation of TiO_2 and WO_3 enhanced UV absorption [29], while the addition of MXene significantly broadened the absorption into the visible region due to its metallic character and dark coloration [30]. The Tauc plot-derived [31] band gaps (Figure 6b) revealed a slight reduction (~50 meV) in Eg for the composite samples, indicative of enhanced electronic interaction and interfacial charge transfer.

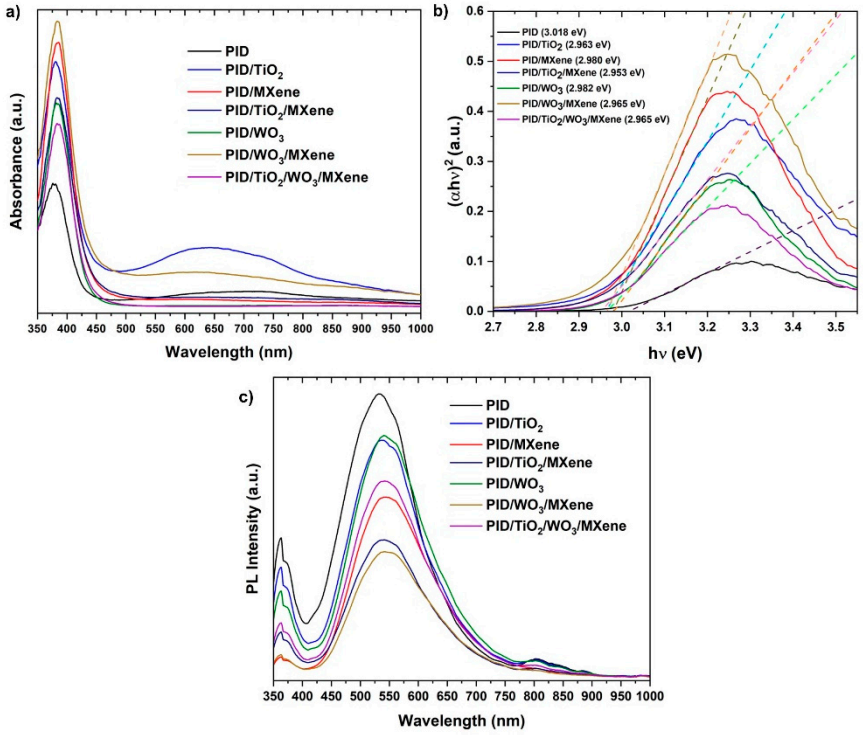

Figure 6. (**a**) UV-Vis absorption spectroscopy, (**b**) Tauc plot, and (**c**) photoluminescence spectra of different samples.

PL spectra (Figure 6c) revealed a broad emission peak centered at approximately 550 nm [32] under 360 nm excitation [33], characteristic of PID. A substantial reduction in PL intensity was observed across all composite samples, with the most pronounced quenching occurring in those containing MXene. This decrease in emissions suggests enhanced charge carrier separation and reduced radiative recombination, likely resulting from improved electrical conductivity and more effective interfacial charge transfer within the hybrid nanofiber network.

These results confirm that the incorporation of MXene and metal oxides into PID nanofibers leads to enhanced surface chemistry, broadened optical absorption, and improved charge carrier dynamics, all of which are beneficial for photocatalytic applications.

Although Figure 6b gives only the optical gaps, the band edges of the oxide phases are well documented. In anatase TiO_2, the conduction-band minimum is placed at about −0.24 V vs. NHE by electronegativity arguments [34], and flat-band measurements in aqueous media cluster near −0.16 V [35]; with a band gap of ~3.2 eV, this sets the valence band at ~+2.96 V vs. NHE. For pristine WO_3, the conduction-band edge is reported close to +0.44 V vs. RHE [36], which, together with its gap, locates the valence band at about +3.0–3.1 V vs. RHE. In such an alignment, photoexcited electrons in TiO_2 have a downhill route into the MXene ($Ti_3C_2T_x$) conductor, while holes reside on the deep WO_3 valence band at potentials sufficient for oxidative steps. Comparable band-alignment analyses reach the same band-alignment scenario [37].

3.3. Dye Photodegradation

The photocatalytic activity of the synthesized PID nanofiber composites was evaluated through the degradation of R6G under Xe lamp irradiation. UV-Vis absorption spectra of the R6G solution were recorded at various time intervals to monitor the degradation process. The characteristic absorption peak of R6G at approximately 530 nm gradually decreased with increasing irradiation time, indicating effective photodegradation facilitated by the nanofiber composites.

Figure 7a presents a comparison of photodegradation efficiencies among the investigated samples: PID, PID/MXene, PID/TiO_2, PID/TiO_2/MXene, PID/WO_3, PID/WO_3/MXene, and PID/TiO_2/WO_3/MXene. After 90 min of light exposure, the degradation efficiencies were calculated to be 53%, 43%, 49%, 51.5%, 51.5%, 65%, and 74%, respectively. The PID/TiO_2/WO_3/MXene composite exhibited the highest degradation efficiency, clearly demonstrating the synergistic enhancement resulting from the integration of TiO_2, WO_3, and MXene.

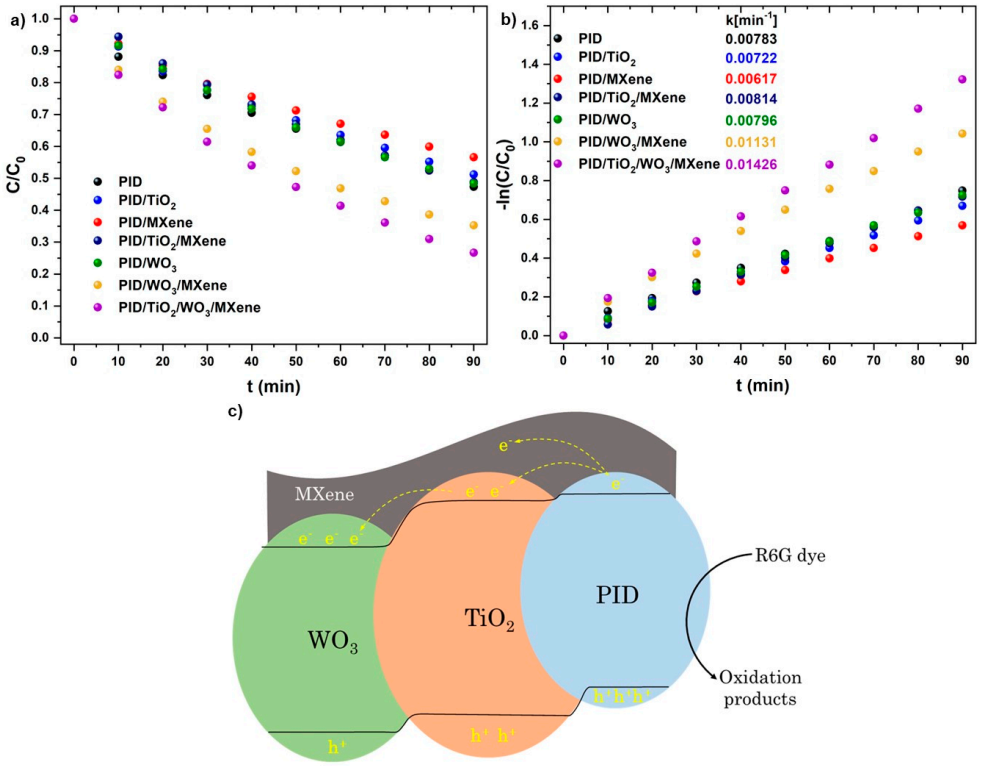

Figure 7. (**a**) R6G decolorization and (**b**) reaction kinetics over pristine and various hybrid PID nanofibers; (**c**) the mechanism of charge transfer in heterojunction during the photodegradation process on PID/TiO_2/WO_3/MXene nanofiber.

To gain deeper insight into the reaction mechanism, the photodegradation kinetics were evaluated using a pseudo-first-order model, expressed as

$$\ln(C_0/C) = k \times t, \quad (1)$$

where k is the apparent rate constant (min^{-1}), t is the irradiation time (min), and C_0 and C are the initial and time-dependent dye concentrations, respectively. The calculated k values are shown in Figure 7b. The highest rate constant, 0.01426 min^{-1}, was observed for the PID/TiO_2/WO_3/MXene composite, which is approximately 1.82 times greater than that of the pristine PID sample (0.00783 min^{-1}), confirming its superior photocatalytic performance. To benchmark the efficiency of the fabricated PID-based nanofibers against other photocatalytic systems reported in the literature, we compared their kinetic parameters and overall degradation efficiencies under different experimental conditions. A summary of representative photocatalysts, pollutants, irradiation sources, and corresponding removal efficiencies is provided in Table 1.

Table 1. Comparison of photodegradation performance of various photocatalysts.

Photocatalyst	Pollutant (C_0, mg/L)	Lamp, Power (W)	Spectrum	Time (min)	k (min^{-1})	Removal (%)	Ref.
PID/TiO_2/WO_3/MXene	R6G (10)	Xenon, 300	UV–Vis	90	0.01426	74	this work
AgNPs/TiO_2/$Ti_3C_2T_x$	MB (10) RhB (10) MB (10) RhB (10)	Mercury, 400 Mercury, 400 Solar simulator Solar simulator	UV UV Sunlight Sunlight	30 40 120 120	0.162 0.143 0.028 0.020	99 99 96 88	[38]
Ag_3PO_4/TiO_2@Ti_3C_2 (Petals)	MB (10)	Xenon, 300	Visible	40	0.289	94–100	[39]
Ti_3C_2@TiO_2/g-C_3N_4 (ternary)	RhB (10)	Xenon, 300	Visible	120	0.01575	-	[40]
g-C_3N_4	RhB (10)	Xenon, 300	Visible	120	0.01575	-	[40]
TiO_2(B)/Ti_3C_2/Ag_3PO_4	RhB (10)	Visible lamp	Visible	60	0.182–0.345	90–100	[41]
TiO_2(B)	RhB (10)	Visible lamp	Visible	60	0.008	-	[41]
TiO_2(B)/20% Ti_3C_2	RhB (10)	Visible lamp	Visible	60	0.011	-	[41]
MXene/g-C_3N_4 (1 wt% Ti_3C_2)	MB (10)	Halogen, 500	Visible	180	~0.0051	~60	[42,43]
TiO_2@Ti_3C_2 (baseline in Petals work)	RhB (9)	Solar simulator	Sunlight	20	0.0093	-	[39]
Supported TiO_2 (Raschig rings)	R6G (5)	White light	Visible	-	0.025	66–77	[44]
Pristine Ti_3C_2	Congo Red (10)	Visible lamp	Visible	120	-	~12	[45]

The remarkable enhancement in photocatalytic activity can be attributed to improved charge separation and interfacial charge transfer between TiO_2, WO_3, MXene, and the polyimide matrix. This finding is consistent with previous reports on polyimide-based hybrid photocatalysts [46]. The degradation of R6G is primarily driven by photogenerated holes (h^+), which directly oxidize dye molecules. Hydroxyl radicals (•OH) act as secondary reactive species, further contributing to the breakdown of R6G into less harmful intermediates. The formation of these species is attributable to the oxidation of water or hydroxide ions by excess photogenerated holes.

Based on the aforementioned conduction and valence band positions of WO_3, superoxide formation is unlikely, and photogenerated holes are expected to be the main reactive species [36]. Studies on WO_3 composites further show that quenching holes causes the largest drop in photocatalytic activity [47].

TiO_2 and WO_3 function as complementary photocatalysts. TiO_2 facilitates efficient electron transfer due to its conduction-band position, while WO_3 stabilizes photogenerated holes through its deeper valence band. MXene, serving as a highly conductive co-catalyst, enhances electron mobility and suppresses charge recombination. The combination of these components yields a multi-component photocatalytic system that harnesses solar energy more effectively, leading to enhanced degradation efficiency. Additionally, in our hybrid, the $Ti_3C_2T_x$ layer acts as an electron sink that draws electrons from the oxides and improves charge separation, leaving the oxidative step to the holes on the oxide domains rather than electrons [48].

We evaluated reusability in five consecutive runs on the same sample (Figure S2). After each run, the coupon was removed, rinsed with deionized water, dried under a gentle argon flow, and then returned to fresh dye solution. In the first run, the removal was about 72%, which corresponds to a concentration ratio of C over C_0 of roughly 0.28. The second and third runs stayed close to 70%. A slight decline appeared thereafter, and by the fifth run, the removal was about 66% with a concentration ratio near 0.34. This modest loss is

consistent with some dye remaining on the surface and partial blocking of active sites, and overall, the results indicate stable performance upon reuse.

4. Conclusions

In this study, electrospun polyimide (PID) nanofibers incorporating TiO_2, WO_3, and MXene ($Ti_3C_2T_x$) nanomaterials were successfully fabricated and systematically evaluated for their photocatalytic efficiency in the degradation of rhodamine 6G (R6G). The integration of metal oxide nanowires and MXene into the PID matrix significantly enhanced photocatalytic activity by improving light absorption, promoting effective charge carrier separation, and suppressing electron–hole recombination. A comprehensive structural and chemical characterization using SEM, TEM, XPS, UV-Vis spectroscopy, and photoluminescence analyses confirmed the successful incorporation of the nanomaterials and the formation of well-organized core and shell fiber architectures. The PID/TiO_2/WO_3/MXene composite exhibited the best photocatalytic performance among the samples, achieving 74% dye degradation within 90 min. This improvement likely results from the combined effects of the three constituents, which improved charge mobility across interfaces and suppressed charge carrier recombination. Core–shell nanofiber platform integrating TiO_2, WO_3, and MXene in a polyimide scaffold outperforms the PID, PID/TiO_2, and PID/WO_3 controls in Rhodamine 6G removal at neutral pH. The TiO_2/WO_3/MXene coupon removes about seventy-four percent in ninety and maintains activity over five reuse cycles, consistent with a hole-driven pathway supported by the band positions and optical data. These results highlight the potential of PID-based hybrid nanofibers as advanced materials for sustainable wastewater treatment. Future work should prioritize scaling up the synthesis process, assessing the long-term stability and recyclability of the composites, and extending their application to a broader range of organic pollutants under varying environmental conditions.

Supplementary Materials: The following supporting information can be downloaded at https://www.mdpi.com/article/10.3390/nano15171371/s1, Figure S1: FTIR spectra of the electrospun nanofibers. Figure S2. Recyclability of the photodegradation for the PID/TiO_2/WO_3/MXene sample over five consecutive runs (90 min each).

Author Contributions: A.L.: investigation, methodology, data curation, writing—original draft preparation; V.M.: investigation, data curation, methodology; M.P.: investigation, formal analysis; B.A.: investigation, visualization; P.H.: investigation; K.V.: resources, investigation; E.C.: investigation, validation; M.B.: investigation, validation; I.I.: conceptualization, supervision, writing—review and editing, funding acquisition, project administration. All authors have read and agreed to the published version of the manuscript.

Funding: This research was funded by the National Center for Research and Development (NCBR), Poland, under the M-ERA.NET 2021 call, project acronym Mem4BoTiReg, grant number M-ERA.NET3/2021/63/Mem4BoTiReg/2023.

Data Availability Statement: The original contributions presented in this study are included in the article/Supplementary Materials. Further inquiries can be directed to the corresponding author.

Acknowledgments: The authors gratefully acknowledge the support of the M-ERA.NET program and the National Centre for Research and Development (NCBR), Poland, for funding the project "Mem4BoTiReg." The authors also thank all consortium partners for their contributions and collaboration throughout the project.

Conflicts of Interest: Author Kateřina Vodseďálková is from company Nanopharma a.s., and declare no conflicts of interests.

Abbreviations

The following abbreviations are used in this manuscript:

PID	Polyimide
R6G	Rhodamine 6G
SEM	Scanning electron microscopy
TEM	Transmission electron microscopy
XPS	X-ray photoelectron spectroscopy
PL	Photoluminescence
EDX	Energy-dispersive X-ray spectroscopy
HR-TEM	High-resolution transmission electron microscopy
FTIR	Fourier-transform infrared spectroscopy
AFM	Atomic force microscopy

References

1. Hafeez, A.; Shamair, Z.; Shezad, N.; Javed, F.; Fazal, T.; Rehman, S.U.; Bazmi, A.A.; Rehman, F. Solar Powered Decentralized Water Systems: A Cleaner Solution of the Industrial Wastewater Treatment and Clean Drinking Water Supply Challenges. *J. Clean. Prod.* **2021**, *289*, 125717. [CrossRef]
2. Al-Tohamy, R.; Ali, S.S.; Li, F.; Okasha, K.M.; Mahmoud, Y.A.-G.; Elsamahy, T.; Jiao, H.; Fu, Y.; Sun, J. A Critical Review on the Treatment of Dye-Containing Wastewater: Ecotoxicological and Health Concerns of Textile Dyes and Possible Remediation Approaches for Environmental Safety. *Ecotoxicol. Environ. Saf.* **2022**, *231*, 113160. [CrossRef] [PubMed]
3. Saeed, M.; Muneer, M.; Haq, A.U.; Akram, N. Photocatalysis: An Effective Tool for Photodegradation of Dyes—A Review. *Environ. Sci. Pollut. Res.* **2022**, *29*, 293–311. [CrossRef]
4. Zhang, J.; Sun, X.; Zhu, W.; Liu, G.; Xian, T.; Yang, H. Design of CdZnS/BiOCl Heterostructure as a Highly-Efficient Piezo-Photocatalyst for Removal of Antibiotic. *J. Environ. Chem. Eng.* **2024**, *12*, 114405. [CrossRef]
5. Mu, W.; Xu, M.; Sun, X.; Liu, G.; Yang, H. Oxygen-Vacancy-Tunable Mesocrystalline ZnO Twin "Cakes" Heterostructured with CdS and Cu Nanoparticles for Efficiently Photodegrading Sulfamethoxazole. *J. Environ. Chem. Eng.* **2024**, *12*, 112367. [CrossRef]
6. Thanh, P.N.; Phung, V.-D.; Nguyen, T.B.H. Recent Advances and Future Trends in Metal Oxide Photocatalysts for Removal of Pharmaceutical Pollutants from Wastewater: A Comprehensive Review. *Environ. Geochem. Health* **2024**, *46*, 364. [CrossRef]
7. Fareza, A.R.; Nugroho, F.A.A.; Abdi, F.F.; Fauzia, V. Nanoscale Metal Oxides–2D Materials Heterostructures for Photoelectrochemical Water Splitting—A Review. *J. Mater. Chem. A* **2022**, *10*, 8656–8686. [CrossRef]
8. Okpara, E.C.; Olatunde, O.C.; Wojuola, O.B.; Onwudiwe, D.C. Applications of Transition Metal Oxides and Chalcogenides and Their Composites in Water Treatment: A Review. *Environ. Adv.* **2023**, *11*, 100341. [CrossRef]
9. Sedghi, R.; Moazzami, H.R.; Hosseiny Davarani, S.S.; Nabid, M.R.; Keshtkar, A.R. A One Step Electrospinning Process for the Preparation of Polyaniline Modified TiO_2/Polyacrylonitile Nanocomposite with Enhanced Photocatalytic Activity. *J. Alloys Compd.* **2017**, *695*, 1073–1079. [CrossRef]
10. Chang, Z.; Sun, X.; Liao, Z.; Liu, Q.; Han, J. Design and Preparation of Polyimide/TiO_2@MoS_2 Nanofibers by Hydrothermal Synthesis and Their Photocatalytic Performance. *Polymers* **2022**, *14*, 3230. [CrossRef] [PubMed]
11. Yue, Y.; Hou, K.; Chen, J.; Cheng, W.; Wu, Q.; Han, J.; Jiang, J. Ag/AgBr/$AgVO_3$ Photocatalyst-Embedded Polyacrylonitrile/Polyamide/Chitosan Nanofiltration Membrane for Integrated Filtration and Degradation of RhB. *ACS Appl. Mater. Interfaces* **2022**, *14*, 24708–24719. [CrossRef]
12. Araújo, E.S.; Da Costa, B.P.; Oliveira, R.A.P.; Libardi, J.; Faia, P.M.; De Oliveira, H.P. TiO_2/ZnO Hierarchical Heteronanostructures: Synthesis, Characterization and Application as Photocatalysts. *J. Environ. Chem. Eng.* **2016**, *4*, 2820–2829. [CrossRef]
13. Keirouz, A.; Wang, Z.; Reddy, V.S.; Nagy, Z.K.; Vass, P.; Buzgo, M.; Ramakrishna, S.; Radacsi, N. The History of Electrospinning: Past, Present, and Future Developments. *Adv. Mater. Technol.* **2023**, *8*, 2201723. [CrossRef]
14. Naguib, M.; Kurtoglu, M.; Presser, V.; Lu, J.; Niu, J.; Heon, M.; Hultman, L.; Gogotsi, Y.; Barsoum, M.W. Two-Dimensional Nanocrystals Produced by Exfoliation of Ti_3AlC_2. *Adv. Mater.* **2011**, *23*, 4248–4253. [CrossRef]
15. Zheng, H.; Meng, X.; Chen, J.; Que, M.; Wang, W.; Liu, X.; Yang, L.; Zhao, Y. In Situ Phase Evolution of TiO_2/Ti_3C_2T Heterojunction for Enhancing Adsorption and Photocatalytic Degradation. *Appl. Surf. Sci.* **2021**, *545*, 149031. [CrossRef]
16. Konieva, A.; Deineka, V.; Diedkova, K.; Aguilar-Ferrer, D.; Lyndin, M.; Wennemuth, G.; Korniienko, V.; Kyrylenko, S.; Lihachev, A.; Zahorodna, V.; et al. MXene-Polydopamine-antiCEACAM1 Antibody Complex as a Strategy for Targeted Ablation of Melanoma. *ACS Appl. Mater. Interfaces* **2024**, *16*, 43302–43316. [CrossRef]
17. Wang, Y.; Yin, L.; Wang, M.; Zhang, B.; Feng, S.; Liu, W.; Liu, Y.; Liu, T.; Bi, Y.; Yang, Q.; et al. Surface Plasmon Effect of Ti_3C_2 Mxene and Degradation of Antibiotics Under Full Spectrum. *SSRN J.* **2022**. [CrossRef]

18. Zhu, Y.; Zhao, X.; Peng, Q.; Zheng, H.; Xue, F.; Li, P.; Xu, Z.; He, X. Flame-Retardant MXene/Polyimide Film with Outstanding Thermal and Mechanical Properties Based on the Secondary Orientation Strategy. *Nanoscale Adv.* **2021**, *3*, 5683–5693. [CrossRef] [PubMed]
19. Kalambate, P.K.; Dhanjai; Sinha, A.; Li, Y.; Shen, Y.; Huang, Y. An Electrochemical Sensor for Ifosfamide, Acetaminophen, Domperidone, and Sumatriptan Based on Self-Assembled MXene/MWCNT/Chitosan Nanocomposite Thin Film. *Microchim. Acta* **2020**, *187*, 402. [CrossRef]
20. Fong, H.; Chun, I.; Reneker, D.H. Beaded Nanofibers Formed during Electrospinning. *Polymer* **1999**, *40*, 4585–4592. [CrossRef]
21. Myndrul, V.; Coy, E.; Babayevska, N.; Zahorodna, V.; Balitskyi, V.; Baginskiy, I.; Gogotsi, O.; Bechelany, M.; Giardi, M.T.; Iatsunskyi, I. MXene Nanoflakes Decorating ZnO Tetrapods for Enhanced Performance of Skin-Attachable Stretchable Enzymatic Electrochemical Glucose Sensor. *Biosens. Bioelectron.* **2022**, *207*, 114141. [CrossRef] [PubMed]
22. Prabu, G.T.V.; Dhurai, B. A Novel Profiled Multi-Pin Electrospinning System for Nanofiber Production and Encapsulation of Nanoparticles into Nanofibers. *Sci. Rep.* **2020**, *10*, 4302. [CrossRef] [PubMed]
23. Lu, Y.; Li, D.; Liu, F. Characterizing the Chemical Structure of Ti_3C_2Tx MXene by Angle-Resolved XPS Combined with Argon Ion Etching. *Materials* **2022**, *15*, 307. [CrossRef] [PubMed]
24. Näslund, L.-Å.; Kokkonen, E.; Magnuson, M. Interaction and Kinetics of H_2, CO_2, and H_2O on Ti_3C_2Tx MXene Probed by X-Ray Photoelectron Spectroscopy. *Appl. Surf. Sci.* **2025**, *684*, 161926. [CrossRef]
25. Ma, H.; Zhang, L.; Yao, N.; Bi, Z.; Zhang, B.; Hu, H. Field-Electron Emission from Polyimide-Ablated Films. *Appl. Phys. A* **2000**, *71*, 281–284. [CrossRef]
26. Natu, V.; Benchakar, M.; Canaff, C.; Habrioux, A.; Célérier, S.; Barsoum, M.W. A Critical Analysis of the X-Ray Photoelectron Spectra of $Ti_3C_2T_z$ MXenes. *Matter* **2021**, *4*, 1224–1251. [CrossRef]
27. Kim, S.-K.; Kim, H.-T.; Park, J.-K. Effects of Thermal Curing on the Structure of Polyimide Film. *Polym. J.* **1998**, *30*, 229–233. [CrossRef]
28. Sheng, W.; Shi, J.-L.; Hao, H.; Li, X.; Lang, X. Polyimide-TiO_2 Hybrid Photocatalysis: Visible Light-Promoted Selective Aerobic Oxidation of Amines. *Chem. Eng. J.* **2020**, *379*, 122399. [CrossRef]
29. Dozzi, M.V.; Marzorati, S.; Longhi, M.; Coduri, M.; Artiglia, L.; Selli, E. Photocatalytic Activity of TiO_2-WO_3 Mixed Oxides in Relation to Electron Transfer Efficiency. *Appl. Catal. B Environ.* **2016**, *186*, 157–165. [CrossRef]
30. Gao, W.; Li, X.; Luo, S.; Luo, Z.; Zhang, X.; Huang, R.; Luo, M. In Situ Modification of Cobalt on MXene/TiO_2 as Composite Photocatalyst for Efficient Nitrogen Fixation. *J. Colloid Interface Sci.* **2021**, *585*, 20–29. [CrossRef]
31. Tauc, J.; Grigorovici, R.; Vancu, A. Optical Properties and Electronic Structure of Amorphous Germanium. *Phys. Status Solidi B* **1966**, *15*, 627–637. [CrossRef]
32. Nirmala, R.; Jeong, J.W.; Navamathavan, R.; Kim, H.Y. Synthesis and Electrical Properties of TiO_2 Nanoparticles Embedded in Polyamide-6 Nanofibers Via Electrospinning. *Nano-Micro Lett.* **2011**, *3*, 56–61. [CrossRef]
33. Li, B.; He, T.; Ding, M. A Comparative Study of Insoluble and Soluble Polyimide Thin Films. *Polymer* **1999**, *40*, 789–794. [CrossRef]
34. Xu, Y.; Schoonen, M.A.A. The Absolute Energy Positions of Conduction and Valence Bands of Selected Semiconducting Minerals. *Am. Mineral.* **2000**, *85*, 543–556. [CrossRef]
35. Patel, M.Y.; Mortelliti, M.J.; Dempsey, J.L. A Compendium and Meta-Analysis of Flatband Potentials for TiO_2, ZnO, and SnO_2 Semiconductors in Aqueous Media. *Chem. Phys. Rev.* **2022**, *3*, 011303. [CrossRef]
36. Kalanur, S.S. Structural, Optical, Band Edge and Enhanced Photoelectrochemical Water Splitting Properties of Tin-Doped WO_3. *Catalysts* **2019**, *9*, 456. [CrossRef]
37. Ye, F.; Qian, J.; Xia, J.; Li, L.; Wang, S.; Zeng, Z.; Mao, J.; Ahamad, M.; Xiao, Z.; Zhang, Q. Efficient Photoelectrocatalytic Degradation of Pollutants over Hydrophobic Carbon Felt Loaded with Fe-Doped Porous Carbon Nitride via Direct Activation of Molecular Oxygen. *Environ. Res.* **2024**, *249*, 118497. [CrossRef]
38. Othman, Z.; Sinopoli, A.; Mackey, H.R.; Mahmoud, K.A. Efficient Photocatalytic Degradation of Organic Dyes by AgNPs/TiO_2/$Ti_3C_2T_x$ MXene Composites under UV and Solar Light. *ACS Omega* **2021**, *6*, 33325–33338. [CrossRef] [PubMed]
39. Nguyen, N.T.A.; Kim, H. Ag_3PO_4-Deposited TiO_2@Ti_3C_2 Petals for Highly Efficient Photodecomposition of Various Organic Dyes under Solar Light. *Nanomaterials* **2022**, *12*, 2464. [CrossRef]
40. Bai, Y.; Xu, S.; Chen, J.; Sun, X.; Zhao, S.; Chang, J.; He, Z. Ti_3C_2@g-C_3N_4/TiO_2 Ternary Heterogeneous Photocatalyst for Promoted Photocatalytic Degradation Activities. *Coatings* **2023**, *13*, 655. [CrossRef]
41. Li, Y.; Zhang, M.; Liu, Y.; Zhao, Q.; Li, X.; Zhou, Q.; Chen, Y.; Wang, S. Construction of Bronze TiO_2/Ti_3C_2 MXene/Ag_3PO_4 Ternary Composite Photocatalyst toward High Photocatalytic Performance. *Catalysts* **2022**, *12*, 599. [CrossRef]
42. Nasri, M.S.I.; Samsudin, M.F.R.; Tahir, A.A.; Sufian, S. Effect of MXene Loaded on G-C3N4 Photocatalyst for the Photocatalytic Degradation of Methylene Blue. *Energies* **2022**, *15*, 955. [CrossRef]
43. Praus, P. 2D/2D Composites Based on Graphitic Carbon Nitride and MXenes for Photocatalytic Reactions: A Critical Review. *Carbon Lett.* **2024**, *34*, 227–245. [CrossRef]

44. Pino, E.; Calderón, C.; Herrera, F.; Cifuentes, G.; Arteaga, G. Photocatalytic Degradation of Aqueous Rhodamine 6G Using Supported TiO_2 Catalysts. A Model for the Removal of Organic Contaminants from Aqueous Samples. *Front. Chem.* **2020**, *8*, 365. [CrossRef]
45. Iqbal, M.A.; Tariq, A.; Zaheer, A.; Gul, S.; Ali, S.I.; Iqbal, M.Z.; Akinwande, D.; Rizwan, S. Ti_3C_2 -MXene/Bismuth Ferrite Nanohybrids for Efficient Degradation of Organic Dyes and Colorless Pollutants. *ACS Omega* **2019**, *4*, 20530–20539. [CrossRef]
46. Li, J.-Y.; Jiang, X.; Lin, L.; Zhou, J.-J.; Xu, G.-S.; Yuan, Y.-P. Improving the Photocatalytic Performance of Polyimide by Constructing an Inorganic-Organic Hybrid ZnO-Polyimide Core–Shell Structure. *J. Mol. Catal. A Chem.* **2015**, *406*, 46–50. [CrossRef]
47. Zhou, M.; Tian, X.; Yu, H.; Wang, Z.; Ren, C.; Zhou, L.; Lin, Y.-W.; Dou, L. WO_3/Ag_2CO_3 Mixed Photocatalyst with Enhanced Photocatalytic Activity for Organic Dye Degradation. *ACS Omega* **2021**, *6*, 26439–26453. [CrossRef] [PubMed]
48. Iravani, S.; Varma, R.S. MXene-Based Photocatalysts in Degradation of Organic and Pharmaceutical Pollutants. *Molecules* **2022**, *27*, 6939. [CrossRef]

Journal of Alloys and Compounds 984 (2024) 173885

Contents lists available at ScienceDirect

Journal of Alloys and Compounds

journal homepage: www.elsevier.com/locate/jalcom

Core-shell nanofibers of $ZnFe_2O_4$/ZnO for enhanced visible-light photoelectrochemical performance

Andrii Lys [a], Viktor Zabolotnii [b], Mária Čaplovičová [c], Iryna Tepliakova [b], Agris Berzins [d], Martin Sahul [c], Ľubomír Čaplovič [c], Alexander Pogrebnjak [c,e], Igor Iatsunskyi [a,*], Roman Viter [b,*]

[a] NanoBioMedical Centre, Adam Mickiewicz University, Wszechnicy Piastowskiej 3, Poznan 61-614, Poland
[b] Institute of Atomic Physics and Spectroscopy, University of Latvia, 19 Raina Blvd, Riga LV 1586, Latvia
[c] Slovak University of Technology in Bratislava, Faculty of Materials Science and Technology in Trnava, J. Bottu 25, Trnava 917 24, Slovakia
[d] Faculty of Chemistry, University of Latvia, 19 Raina Blvd, Riga LV 1586, Latvia
[e] Sumy State University, Department of Nanoelectronics and Surface Modification, Sumy 40007, Ukraine

ARTICLE INFO

Keywords:
Core-shell nanofibers
$ZnFe_2O_4$/ZnO heterostructure
Photoelectrochemical performance
Visible light absorption

ABSTRACT

Recent research places significant importance on the development of innovative nanocomposites for photoelectrochemical applications. This paper presents the fabrication, characterization, and possible photoelectrochemical applications of novel $ZnFe_2O_4$/ZnO core-shell nanofibers. These core-shell nanofibers were fabricated through co-axial electrospinning using PVP solutions containing iron and zinc nitrate precursors for the core and shell. The structural and optical properties of $ZnFe_2O_4$/ZnO core-shell nanofibers were examined through TEM, SEM, XRD, FTIR, Raman spectroscopy, and diffuse reflectance spectroscopy. This comprehensive analysis unveiled that the development of core and shell characteristics was notably influenced by the interdiffusion of [Fe]/[Zn] during the annealing process. The photoelectrochemical properties of $ZnFe_2O_4$/ZnO core-shell nanofibers were assessed through electrochemical impedance spectroscopy (EIS), linear sweep voltammetry (LSV), and the Mott-Schottky method. These core-shell nanofibers demonstrated a robust electrochemical response to visible light. Photocurrent and photoconversion efficiency of the core-shell nanofibers were calculated and compared with the corresponding values for core-shell nanoparticles. The mechanisms underlying the structural, optical, and photoelectrochemical properties of $ZnFe_2O_4$/ZnO core-shell nanofibers were discussed. These advanced nanofibers hold potential applications in photocatalysis, photovoltaics, and energy storage, making this research timely and crucial for advancing sustainable energy technologies and environmental remediation efforts.

1. Introduction

With the growing global demand for renewable energy sources and environmental remediation, the development of nanomaterials with high surface area and tunable absorption in the visible range takes on added importance. Metal oxide nanostructures, including ZnO, TiO_2, WO_3, and others, are essential nanomaterials with applications in sensors, photocatalysis, and water splitting [1–4]. However, due to their high optical band gaps, these materials can only harness UV light for photogenerated charge carriers, limiting their efficiency. The increasing demand for solar light applications necessitates improved optical properties in the visible range [1–3].

Metal oxide heterostructures, composed of two alternating layers of metal oxides, offer a promising solution [5]. The design of electron affinity, work functions, and Fermi levels facilitates the formation of interfaces with significant charge transfer between these alternating layers [6,7]. Recent advancements in techniques such as PVD/CVD, sol-gel, and ALD have demonstrated substantial progress in creating metal oxide heterostructures based on the core-shell geometry [8–11]. Core-shell nanostructures are favored in photoelectrochemical applications because they optimize charge separation, protect core materials from degradation, and enhance light absorption across a broader spectrum, ultimately improving energy conversion efficiency. Their versatile design allows for precise engineering of energy levels and band structures, making them a promising platform for more efficient and sustainable photoelectrochemical systems.

* Corresponding authors.
E-mail addresses: igoyat@amu.edu.pl (I. Iatsunskyi), roman.viter@lu.lv (R. Viter).

https://doi.org/10.1016/j.jallcom.2024.173885
Received 29 October 2023; Received in revised form 12 January 2024; Accepted 14 February 2024
Available online 15 February 2024

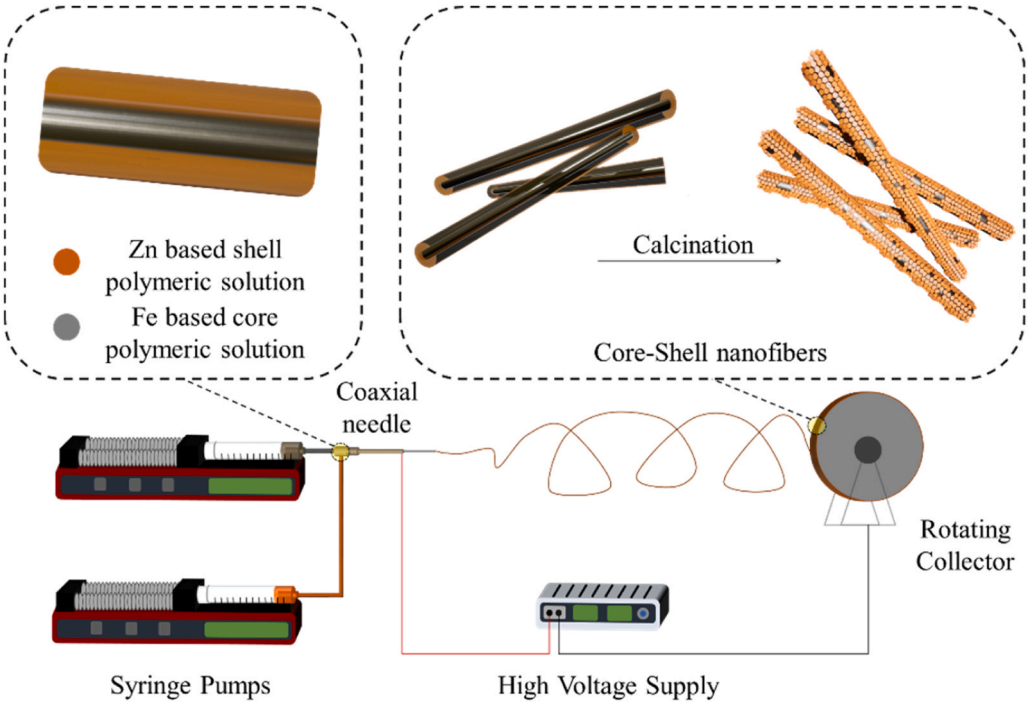

Fig. 1. Experimental setup for fabrication of $ZnFe_2O_4$/ZnO core-shell nanofibers.

Among different fabrication techniques, co-axial electrospinning has emerged as a rapidly developing method [12]. Initially developed for biotechnology applications like wound healing and drug release [13], co-axial electrospinning has proven to be sufficient to fabricate metal oxide heterostructures [14]. Metal oxide precursors introduced into a polymeric matrix undergo transformation into metal oxides during high-temperature post-treatment [14]. This technique has enabled the fabrication of both dense core-shell and hollow single-metal oxide nanofibers.

Various core-shell nanofibers, such as SnO_2/TiO_2 and In_2O_3/SnO_2, have shown promise in UV light photocatalysis and gas sensing applications [15,16]. However, the challenges associated with core-shell metal oxide nanomaterials exhibiting strong absorbance in the visible region include precise synthesis, band alignment, scalability, mechanistic understanding, environmental stability, and integration into practical devices for photoelectrochemical applications.

This paper focuses on the fabrication and examination of optically active in the visible range $ZnFe_2O_4$/ZnO core-shell nanofibers using co-axial electrospinning, providing new insights into their structural, optical, and photoelectrochemical performance. We also delve into the mechanisms underpinning the formation of these core-shell nanofibers and their potential applications in sustainable energy technologies and environmental remediation. The outcomes of this research have the potential to advance the development of materials for visible light photocatalysis and water splitting, making a significant contribution to energy conversion and environmental sustainability.

2. Material and methods

2.1. Materials

Polyvinylpyrrolidone (PVP) (Mw 1300000), N, N-dimethylformamide (DMF), 5% Nafion solution, $Fe(NO)_3{\cdot}9\ H_2O$, $Zn(NO)_2{\cdot}6\ H_2O$ were purchased from Sigma Aldrich.

2.2. Fabrication of solutions

The core solution (Solution A) has been prepared as follows. Ethanol (3 ml) and DMF (2 ml) were mixed, stirred for 30 minutes at room temperature, and warmed to 50 °C. PVP (0.5 g) was added to the hot solution and dissolved under vigorous stirring at 50 °C. 0.3 g of Fe(NO) 3·9H2O were added to the PVP solution. The solution A was cooled down to room temperature and stirred overnight.

Shell solution (Solution B) has been prepared as follows: ethanol (1 ml) and DMF (4 ml) were mixed, stirred for 30 minutes at room temperature, and warmed to 50 °C. PVP (0.7 g) was added to the hot solution and dissolved under vigorous stirring at 50 °C. 0.5 g of Zn(NO) $2{\cdot}6H_2O$ were added to the PVP solution. The solution B was cooled down to room temperature and stirred overnight.

2.3. Electrospinning of core-shell nanofibers

Solutions A and B were each loaded into separate 5 ml plastic syringes. Core-shell electrospinning was conducted using a coaxial needle (Linari Engineering, Piza, Italy) with inner and outer diameters of 0.5 mm and 1 mm, respectively. An aluminum foil was affixed to the rotating collector. The distance between the needle and the collector was maintained at 20 cm. An electric field of 20 kV was applied while the collector rotated at a speed of 200 rpm. The core and shell solutions were delivered using a syringe pump, each with a constant flow rate of 200 and 300 microliters per hour, respectively.

The resultant nanofibers were subjected to vacuum drying at room temperature overnight. Subsequently, the core-shell nanofibers were annealed in air at 500 °C for 2 hours. A schematic representation of this process is provided in Fig. 1.

2.4. Characterization technique

We utilized X-ray Diffraction (XRD) and Fourier-Transform Infrared Spectroscopy (FTIR) techniques to identify the phases present in the core-shell nanofibers we developed. XRD was performed using a Bruker D8 diffractometer equipped with CuKa radiation from Germany. At the

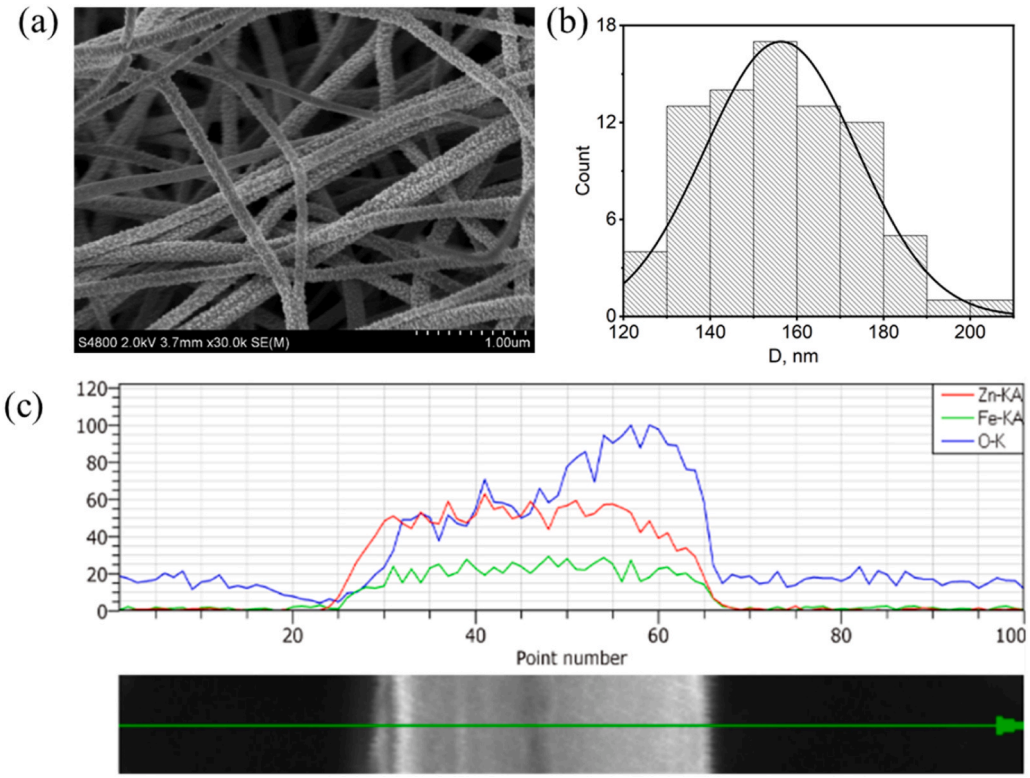

Fig. 2. Structure characterization of core-shell nanofibers by scanning electron microscopy: a) SEM image of the core-shell nanofibers, b) diameter distribution of the core-shell nanofibers, c) EDX line profile across the nanofiber surface.

same time, FTIR analysis was conducted in ATR mode using a Bruker II Alfa instrument from the same source.

Raman spectroscopy measurements were carried out using a Renishaw micro-Raman spectrometer equipped with a confocal microscope (Leica). The excitation wavelength employed was 633 nm.

The structural properties of the deposited nanofibers were investigated through Scanning Electron Microscopy (SEM) using equipment from Hitachi, Japan, and Transmission Electron Microscopy with Energy Dispersive X-ray Spectroscopy (TEM/EDX) utilizing JEOL equipment from Japan.

We employed Diffuse Reflectance Spectroscopy to study the optical properties of the core-shell nanofibers in the UV–visible range. This analysis was conducted using an Ocean Optics fiber optic light source (DH2000, 250–900 nm, USA), an integrating sphere (Ocean Optics, IS-8, USA), and a fiber optic spectrometer (Ocean Optics HR4000, USA).

Furthermore, our investigation included a double-corrected JEM ARM 200cF transmission electron microscope (TEM) from JEOL, Japan, which operated at an accelerating voltage of 200 kV. Energy Dispersive X-ray Spectroscopy (EDX) was performed using a large angle JEOL JED-2300 T CENTURIO SDD (silicon drift) detector, boasting a solid angle of up to 0.98 sr and a detection area of 100 mm^2. To prepare samples for TEM, nanofibers were dispersed in ethanol, sonicated for 10 minutes, and a drop of the suspension was placed on a TEM Cu-grid covered by holey carbon film. After drying in the air, the samples were examined under the microscope.

2.5. Photoelectrochemical characterization

The photoelectrochemical (PEC) properties of the $ZnFe_2O_4$/ZnO core-shell nanofibers were evaluated using a conventional three-electrode cell setup. For the working electrodes, approximately 0.6 cm^2 × 0.7 cm^2 windows were created on photopolymer-masked FTO glass, onto which a slurry consisting of 1 mg of nanofibers, ultrasonicated with 100 μL of DMF solvent and 15 μL of Nafion binder, was drop-cast.

The working electrodes were characterized using the Autolab PGSTAT12 Potentiostat/Galvanostat Electrochemical System in a standard three-electrode configuration at room temperature. The counter electrode was a platinum spiral, while the reference electrode was Ag/AgCl in 3 M KCl.

The 0.5 M KOH electrolyte solution was continuously deaerated with a constant argon (Ar) flow for 30 minutes before and during all measurements. Samples were illuminated with a Halogen lamp at 25 mW/cm^2 power density.

Electrochemical impedance spectroscopy (EIS) measurements were conducted in dark and illuminated conditions, covering a frequency range from 0.1 Hz to 4 kHz with an amplitude of 10 mV. Mott-Schottky analysis was conducted at a frequency of 5 kHz, spanning an amplitude range of −0.8 V to −0.2 V vs. Ag/AgCl in 3 M KCl.

Chronoamperometric measurements were carried out to study photo transient response and stability of prepared electrodes as current versus time at 1.2 V vs Ag/AgCl and chopped light irradiation with 0.8 s period.

The photoconversion efficiency (applied bias photon-to-current conversion efficiency (ABPE,%)) of the fabricated electrodes is calculated as [17]:

$$ABPE(\%) = \frac{\left[I_{ph}\left(\frac{mA}{cm^2}\right) \times \left(1.23 - |V_{app}|\right)(V)\right]}{\left[P_{ls}\left(\frac{mW}{cm^2}\right)\right]} \times 100(\%) \quad (1)$$

where I_{ph} is the measured photocurrent density, P_{ls} - the intensity of the light source, V_{app} is the measured potential of PCE cell recalculated *vs.* reversible hydrogen electrode by the Nernst equation:

$$V_{app} = V_m + V^0_{Ag/AgCl} + 0.059pH, \quad (2)$$

where V_m is the potential measured against the Ag/AgCl reference electrode, $V^0_{Ag/AgCl}$ is the standard electrode potential of the Ag/AgCl

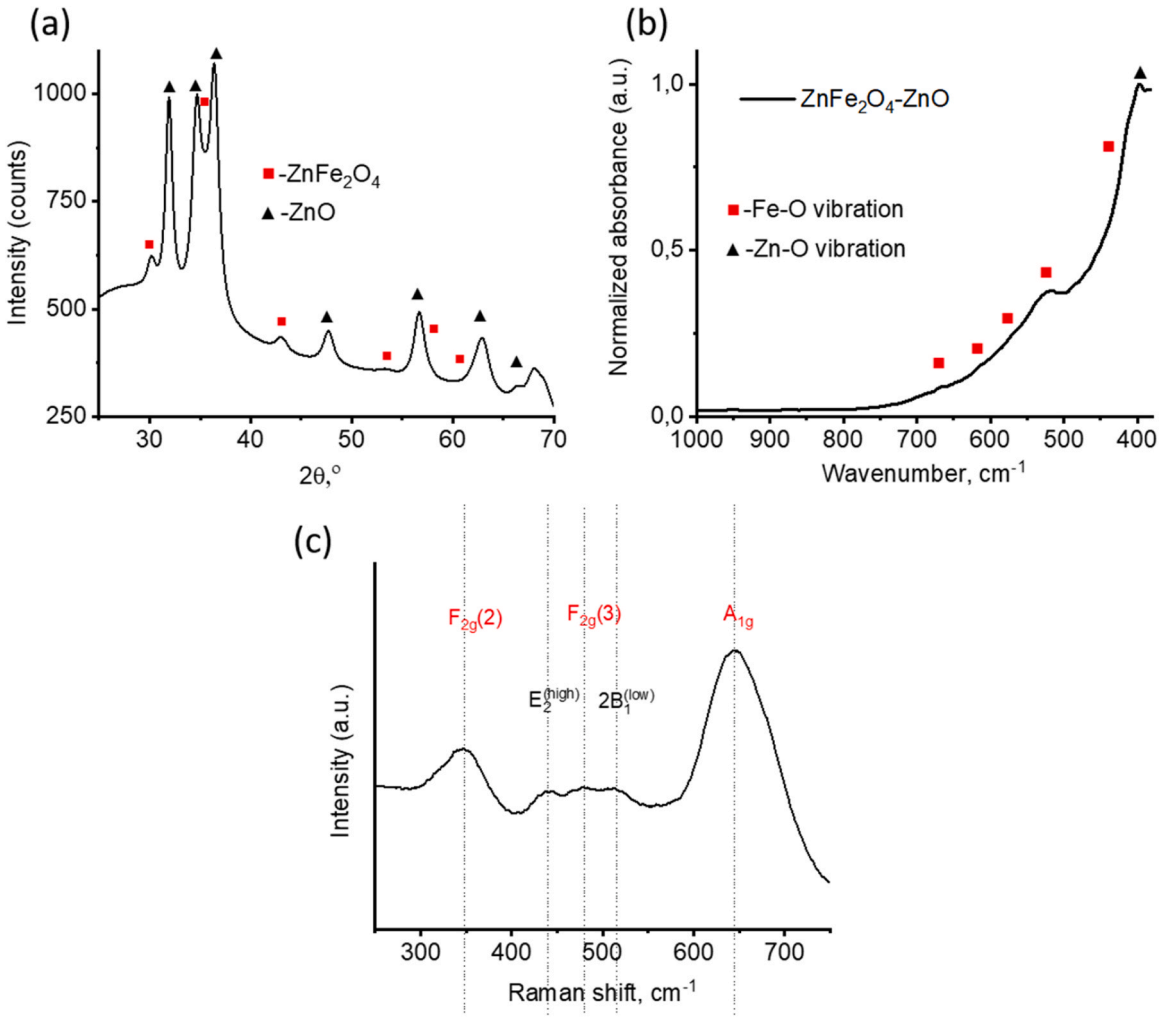

Fig. 3. Structure characterization of the core-shell nanofibers by: a) XRD, b) FTIR and c) Raman spectroscopy.

electrode (0.1976 V).

3. Results and discussion

3.1. Structure properties of the core-shell nanofibers

SEM images illustrating core-shell nanofibers obtained are presented in Fig. 2a. The SEM analysis reveals a network of nanofibers with a random orientation. To assess the distribution of nanofiber diameters, a Gaussian distribution analysis was conducted on a sample of 100 fibers (Fig. 2b). The core-shell nanofibers' average diameter was 156±21 nm. The range of observed diameters spanned from 120 nm to 210 nm. The relatively narrow distribution of fiber diameters can be attributed to the effective alignment of core and shell solution properties, optimized injection rates for the core and shell solutions, and the applied electrical field strength.

An EDX analysis performed on the cross-section of the core-shell nanofibers' surface revealed the presence of Zn, O, and Fe, with atomic percentages of 19.8%, 78.2%, and 2%, respectively (Fig. 2c).

XRD studiesThe have been performed to analyze the atomic structure and crystalline phases of the core-shell nanofibers (Fig. 3a). The XRD spectrum was analyzed by Rietveld refinement using Profex software [18]. Two main phases were identified: ZnO and $ZnFe_2O_4$. The reflections from ZnO have been identified at the following 2θ positions: 31.7 (100), 34.4 (002), 36.2 (101), 47.4(102), 56.1(110), 62.9(103), 66.2 (200) [19]. The reflections from $ZnFe_2O_4$ have been identified at the following 2θ positions: 29.8 (220), 35.3 (331), 42.8 (400), 56.3 (511), 62.1 (440) [20].

Table 1
Structure parameters of $ZnFe_2O_4$/ZnO core-shell nanofibers, obtained from XRD analysis.

	Phase content	a, nm	c, nm	Lattice strain	d, nm
ZnO	0.796 ±0.022	0.32613 ±0.00016	0.52121 ±0.00025	0.007348	14 ±1
$ZnFe_2O_4$	0.204 ±0.022	0.84439 ±0.00055	-	0.017321	23 ±1

The XRD analysis is compiled and summarized in Table 1.

Notably, the XRD data did not indicate the presence of a crystalline phase of iron oxide within the core-shell nanofibers. However, the coexistence of two phases, ZnO and $ZnFe_2O_4$, strongly implies an interdiffusion process between the core and shell precursors during the thermal removal of the polymer.

FTIR spectrum of the core-shell nanofibers is shown in Fig. 3b. Absorption bands have been identified at 410 cm^{-1}, 440 cm^{-1}, 520 cm^{-1}, 610 cm^{-1}, 638 cm^{-1} and 668 cm^{-1}. FTIR studies of $ZnFe_2O_4$ nanostructures revealed Fe-O vibrational peaks at 430, 520, 560, and 575 cm^{-1} [21,22]. On the other hand, FTIR findings in Fe_2O_3 and Fe_3O_4 found Fe-O vibrational peaks at 440, 578, 610, and 668 cm^{-1} [23]. In the present work, the band at 410 cm^{-1} is associated with Zn-O stretching vibration [24]. A shift of Fe-O FTIR peak was observed

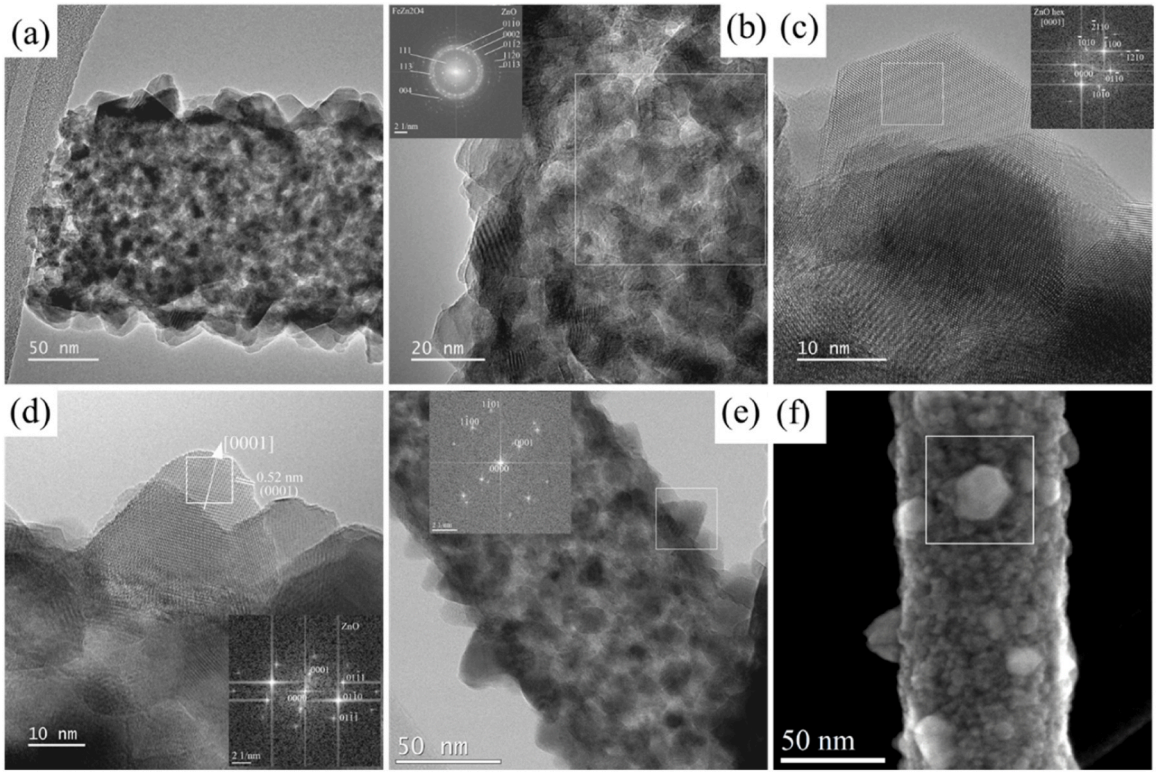

Fig. 4. TEM images of the core-shell nanofibers: a) Low magnification TEM image, b) HRTEM image of nanofiber (FFT pattern in inset), c) HRTEM image of ZnO nanocrystal in the fiber shell (FFT pattern in inset), d) HRTEM of the ZnO nanocrystal shell, e) Low magnification BF STEM image of nanofiber, (f) Nanofibers recorded using SE STEM method.

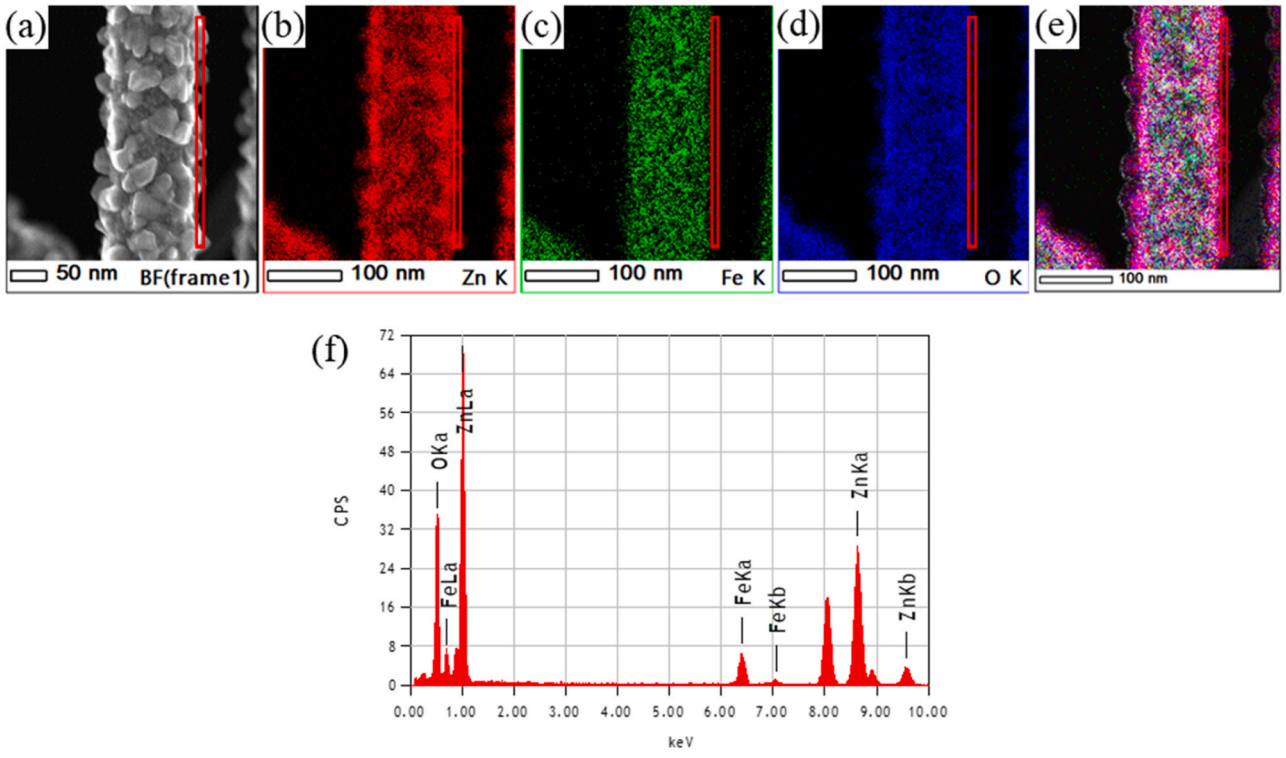

Fig. 5. Elemental mapping of the core-shell nanofiber: a) SE STEM image of core shell nanofiber; EDX mapping of the nanofiber surface b) ZnK map, c) FeK map, d) OK map, (e) overlayed image, (f) EDX spectrum acquired from highlighted area.

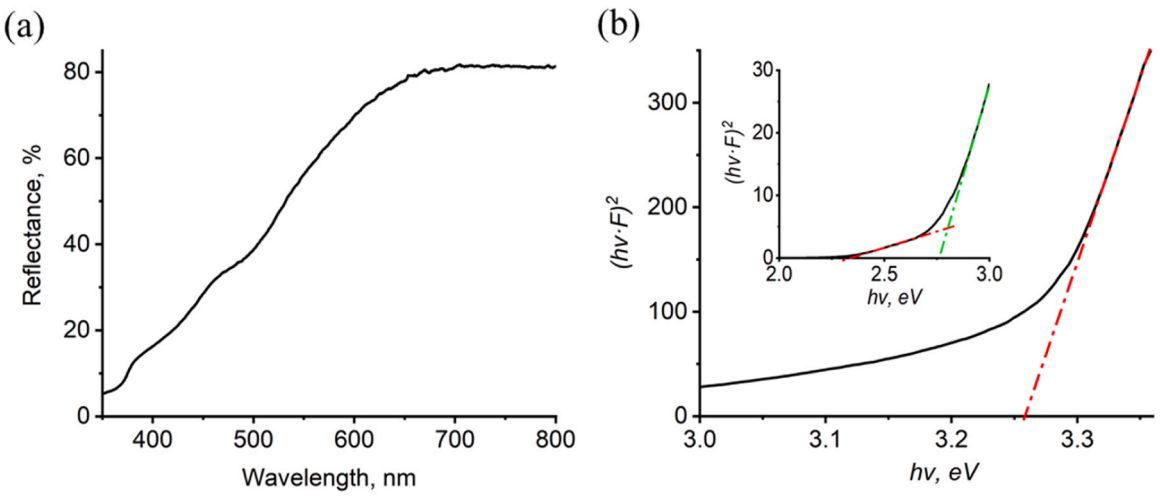

Fig. 6. Optical properties of core shell $ZnFe_2O_4$/ZnO nanofibers: a) diffuse reflectance spectrum, b) band gap calculations.

from 520 cm^{-1} to 528 cm^{-1} when $ZnFe_2O_4$ was deposited on the ZnO surface. The FTIR vibrations of the Zn-Fe-O stretching band and Fe-OH surface bond were associated with peaks at 617 $cm^{-1}$and 630 cm^{-1}, respectively [25,26].

Raman spectrum of the core-shell nanofibers is shown in Fig. 3c. The observed peaks at 438 and 513 cm^{-1} are attributed to wurtzite ZnO $E_2^{(high)}$ and $2B_1^{(low)}$ modes of wurtzite ZnO, respectively [27,28]. The Raman peaks of cubic spinel $ZnFe_2O_4$ were found at 346, 479, and 644 cm^{-1}, referring to $F_{2\,g}$(2) local symmetry vibration of Fe cations in $ZnFe_2O_4$ structure [29], $F_{2\,g}$(3) asymmetric [30] and oxygen breathing vibrations against zinc in tetrahedral ZnO_4 group [31], respectively. The findings from XRD, FTIR, and Raman analyses provide compelling evidence of the presence of $ZnFe_2O_4$/ZnO crystalline phases within the prepared core-shell electrospun nanofibers.

TEM, STEM, and EDX measurements have been performed to characterize the core-shell nanostructure of nanofibers. The TEM images of the core-shell nanofibers are summarized in Fig. 4a-f. The low magnification TEM image in Fig. 4a clearly shows that nanofibers consist of fine-grained core and coarse-grained shell. The average thickness of the surface layer was 23±4 nm, and the core of nanofibers had a thickness of 130±38 nm. More detailed high-resolution TEM (HRTEM) images of nanofiber and relevant FFT patterns gained from the core region are presented in Fig. 4b. Rings in the FFT pattern indicate that crystallites in a core with a size around 10 nm are randomly oriented. Determined interplane distances correlate with data valid for $ZnFe_2O_4$ cubic crystal structure (PDF 98–007–2027).

The shell of the nanofibers consists of well-faceted nanocrystals. Evaluation of the FFT pattern showed a good correlation of the estimated interplane distances with data for the ZnO hexagonal crystal structure (PDF 98–002–9272). Detailed HRTEM image of ZnO nanocrystal in the shell is presented in Fig. 4c, d. Evaluation of the FFT pattern (Fig. 4c) showed that the ZnO crystals are well faceted by [1120] type planes and oriented along [0001] zone axis. The determined [1120] type planes on the surface of the ZnO shell can affect the photocatalytic performance of the developed core-shell nanofibers. In addition, ZnO crystals, oriented along [0001] direction perpendicularly to the growth axis of the nanofiber, have been identified from the relevant FFT patterns (Fig. 4d).

The images of the core-shell nanostructure, recorded using secondary electrons (SE) in STEM mode, are presented in Fig. 4e,f. Faceted ZnO crystals have been observed, grown on the fiber core along [0001] direction. The surface plane at the top of ZnO crystal was {0001} type. Fine-grained core fragments of fibers have also been observed.

EDX mapping, as depicted in Fig. 5, confirmed the core-shell structure of the nanofibers by revealing the distribution of Zn K, Fe K, and O K. The spectrum obtained from the highlighted surface area is presented in Fig. 5, providing further evidence of the structural composition. Quantitative EDX results, recorded from the nanofiber's edge, indicate the atomic percentages of Fe, Zn, and O. Specifically, the analysis revealed the following composition: 7% Fe, 41% Zn, and 53% O, as illustrated in Fig. 5f.

It is noteworthy to mention that, in our current study, we did not observe a distinct demarcation between the core and shell layers, as previously reported in Refs [16,32], particularly when the core and shell are both composed of the same polymer. This absence of differentiation suggests that the polymer degradation properties are consistent between the core and shell components.

However, it is essential to consider the crystalline structure of the core and shell metal oxides, the mass ratio between core and shell precursors, and the extent of interdiffusion between the core and shell materials. The transition from Fe_2O_3 to $ZnFe_2O_4$ phases commences at temperatures exceeding 450–500 °C and is contingent upon the [Fe]/[Zn] precursor mass ratio within the core-shell nanostructures, as indicated in previous work [33]. Notably, Fe_2O_3/ZnO and $ZnFe_2O_4$/ZnO core-shell nanoparticles were successfully formed through annealing at 500 °C, with precursor mass ratios of 1/2 and 2/3, respectively, as detailed in Ref [33]. In our current investigation, the [Fe]/[Zn] mass ratio was 3/5, while the core and shell pumping speeds ratio was maintained at 2/3, consistent with findings in Ref [16].

The ZnO shell in our study was characterized by crystallites oriented perpendicular to the nanofiber's surface. It is important to note that XRD and Raman's measurements did not reveal the presence of iron oxide phases within the deposited core-shell nanofibers. We may speculate that in our study, the formation of $ZnFe_2O_4$/ZnO core-shell nanofibers occurred due to robust interdiffusion between the core and shell materials during high-temperature annealing processes.

3.2. *Optical properties of the core-shell nanofibers*

The optical characteristics of the $ZnFe_2O_4$/ZnO core-shell nanofibers were thoroughly examined through diffuse reflectance spectroscopy, as illustrated in Fig. 6a. These core-shell nanofibers exhibited a broad absorption spectrum spanning from 350 to 640 nm, marked by three distinctive slopes. To further analyze this data, the measured diffuse reflectance (R) was subsequently transformed into the Kubelka-Munk coefficient (F) using the following formula [34]:

$$F = \frac{(1-R)^2}{2 \bullet R} \tag{3}$$

Band gap values E_g of the $ZnFe_2O_4$/ZnO core-shell nanofibers were

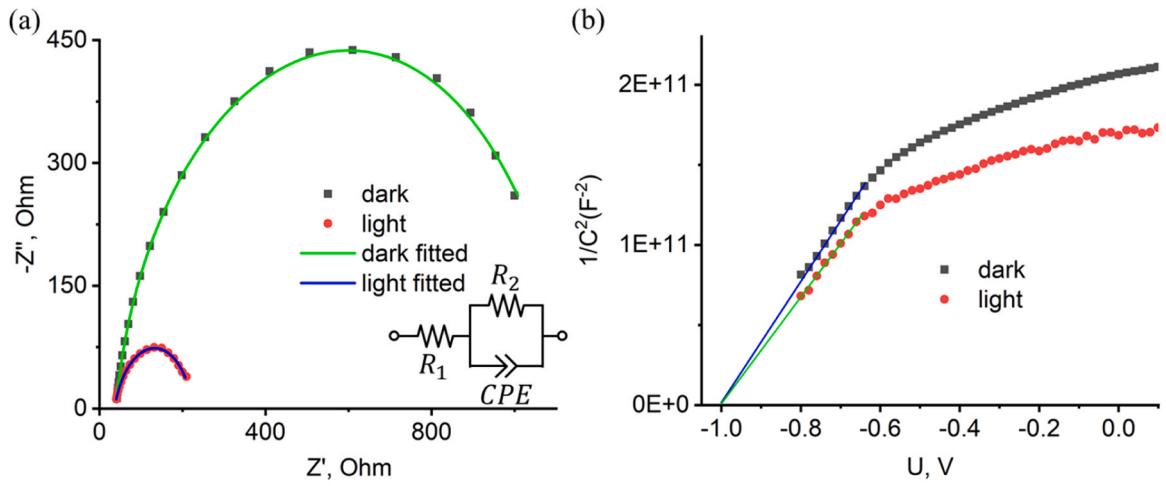

Fig. 7. Electrochemical characterization of $ZnFe_2O_4$ – ZnO core-shell nanofibers: a) EIS spectra, b) Mott-Schottky plot.

Table 2
ESI parameters, calculated for core-shell $ZnFe_2O_4$/ZnO nanofibers.

	Rs	Rct	CPE, F	n	Nd	Vfb, V
Light off	36.6582 ±0.0024	1085.1 ±0.1	$1.1{\cdot}10^{-5}$	0.87	$3.17{\cdot}10^{19}$ cm^{-3}	1.025 ±0.003
Light on	36.55 ±0.01	194 ±0.1	$1.72{\cdot}10^{-5}$	0.83	$3.91{\cdot}10^{19}$ cm^{-3}	1.025 ±0.003

calculated by using the Tauc plot for direct optical transition [27]:

$$(F \bullet h\nu)^2 = A \bullet (h\nu - E_g) \quad (4)$$

where A and $h\nu$ are constant and photon energy, respectively.

In Fig. 6b, we can discern three distinct linear slopes, from which we have computed the following band gap values: 3.26±0.05 eV, 2.76 ±0.06 eV, and 2.3±0.03 eV. Notably, the highest band gap value corresponds to that of ZnO [35], whereas the band gap value of 2.3 eV indicates $ZnFe_2O_4$ [31]. Prior research has reported band gap values for $ZnFe_2O_4$ in the range of 1.9–2.3 eV [35], with a noteworthy observation that a reduction in grain size leads to an increase in the band gap value attributable to the quantum confinement effect [36]. For instance, a decrease in the grain size of $ZnFe_2O_4$ from 60 to 16 nm can result in a blue shift of the absorption edge from 0.15 to 0.65 eV [37]. Furthermore, an elevation in the Zn content within the formation of core-shell $ZnFe_2O_4$/ZnO nanoparticles augments the optical band gap [35].

In several prior studies, an absorption band within the 2.5–2.8 eV range in $ZnFe_2O_4$/ZnO materials has been consistently observed, albeit without a comprehensive explanation [36,38]. To shed light on this phenomenon, the band gap of $ZnFe_2O_4$/ZnO nanoparticles was examined as a function of the [$ZnFe_2O_4$]/[ZnO] mass ratio [38]. Notably, this investigation revealed a noticeable shift in the ZnO band gap from 3.18 eV to 2.9 eV, a change attributed to the integration of $ZnFe_2O_4$ into the ZnO lattice. Based on these findings, we postulate the existence of an additional $ZnFe_2O_4$-doped ZnO layer, possessing a band gap of 2.76 eV, situated between the $ZnFe_2O_4$ core and the ZnO shell. These outcomes regarding the optical properties align well with our structural analysis, providing compelling evidence for the substantial impact of inter-diffusion between the core and shell materials.

3.3. Photoelectrochemical properties of the core-shell nanofibers

EIS, the Mott-Schottky method, and LSV have investigated the (photo)electrochemical properties of the $ZnFe_2O_4$/ZnO core-shell nanofibers.

EIS was employed to probe the charge transport processes occurring on the surface of the core-shell nanofibers. EIS spectra were recorded at a bias potential of 0.6 V (vs. Ag/AgCl) under dark and visible light illumination. The collected EIS spectra for the core-shell nanofibers are presented in Fig. 7a. Notably, the core-shell nanofibers exhibited a significant photoresponse, as evidenced by the changes observed in the EIS spectra upon exposure to light. These EIS spectra were analyzed using Randell's model, a well-suited approach for characterizing porous nanofiber structures [39–41]. The impact of light irradiation was evident in the substantial reduction of the semicircle radius, as depicted in the equivalent circuit diagram shown in Fig. 7a. The values of the fitted resistances (R) and constant phase elements are summarized in Table 2.

The fitted parameters were associated with specific electrochemical properties, including the solution resistance (Rs), charge transfer resistance (Rct), and the double layer capacitance, which can be accurately described using a Constant Phase Element (CPE) model [46]. The notable changes observed in the impedance spectra can primarily be attributed to the light-induced reduction of charge transfer resistance at the interface between ZnO and $ZnFe_2O_4$. Additionally, it is worth mentioning that the double-layer CPE exhibited an increase under light irradiation, suggesting the involvement of defect states in the generation of photocharges [41].

In Fig. 7b, a Mott-Schottky (MS) plot of the samples is presented, with measurements conducted both in the dark and under illumination. Analysis of the Mott-Schottky plots enabled the determination of key parameters, including the flat band potential (V_{fb}) and donor concentration, as outlined in Table 2, using equation [42]:

$$\frac{1}{C^2} = \frac{2}{\varepsilon\varepsilon_0 q N_d A^2}\left(E - E_{fb} - \frac{k_B T}{q}\right) \quad (5)$$

where C is the capacitance of the space charge layer, ε is the dielectric constant of the ZnO layer, ε_0 is the vacuum permittivity, q is the elementary charge, N_d is the donor density, A is the square of the electrode immersed in the electrolyte, E is the applied potential, E_{fb} is the flat-band potential, k_B is the Boltzmann constant, and T is the temperature.

The considerably high flat band potential value indicates the formation of a substantial depletion layer within the ZnO shell layer upon contact with the electrolyte. The donor concentrations estimated for ZnO-based nanomaterials are notably higher, implying a shift of the Fermi level from the conduction band toward the valence band [36,43]. An intriguing observation is that applying visible light irradiation does not significantly alter the flat band potential value. However, a significant discovery from the Mott-Schottky measurements is the increase in donor concentration under visible light irradiation. This suggests that

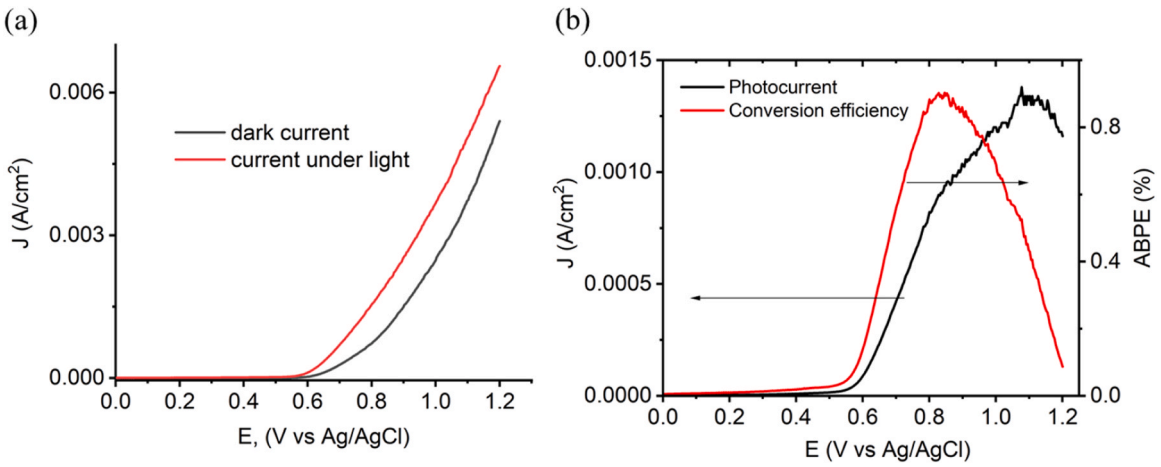

Fig. 8. Photocurrent analysis of $ZnFe_2O_4$/ZnO core-shell nanofibers: a) LVS plot (scanning rate 50 mV/s), b) photocurrent and photoconversion plots.

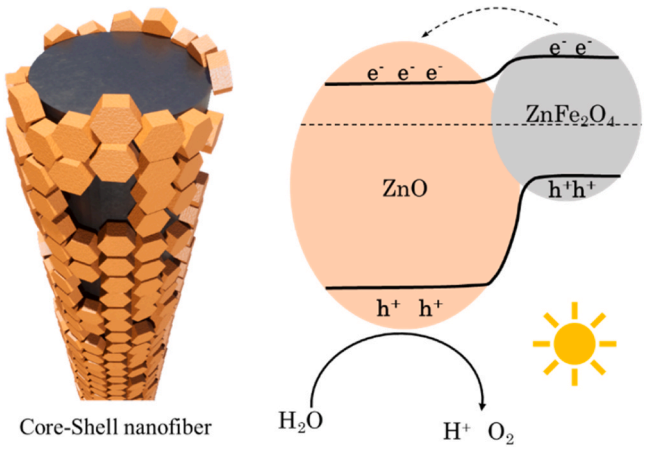

Fig. 9. Schematic structure of photoelectrochemical water splitting measurements by $ZnFe_2O_4$/ZnO core-shell nanofibers.

the transfer of photogenerated charges across the core-shell interface plays a defining role in the photoelectrochemical response of the $ZnFe_2O_4$/ZnO core-shell nanofibers. The findings from the Mott-Schottky measurements align well with those from the EIS spectroscopy, collectively confirming that the absorption of visible light by the $ZnFe_2O_4$ core layer facilitates the transfer of charges toward the ZnO shell layer.

LSV spectra were employed to assess the photoelectrochemical properties of the core-shell nanofibers. These nanostructures exhibited electrocatalytic activity due to their expansive interface and active surface area, even without light (Fig. 8a). The anodic current exhibited an increase within the voltage range of 0.6–1.2 V. When the samples were illuminated with visible light, the current values increased, and the potential at which the current was set shifted to lower values. The photocurrent was calculated as the difference between the currents measured in the dark and under visible light irradiation. The conversion energy, ABPE, was calculated by Eq. (1) [17], and the results for photocurrent and conversion efficiency are presented in Fig. 8b. The photocurrent rapidly increased within the 0.6–0.8 V voltage range and approached saturation at higher voltages. The highest conversion efficiency was observed at 0.85 V.

Comparisons were made between the results of this study and the photoelectrochemical data for $ZnFe_2O_4$/ZnO core-shell nanoparticles [36]. A notable distinction was observed in the dark current between the $ZnFe_2O_4$/ZnO core-shell nanoparticles and core-shell nanofibers. The dark current values in the core-shell nanofibers were two to three orders higher than those in the nanoparticles [43]. Based on the structural characterization, EIS, and Mott-Schottky measurements, the $ZnFe_2O_4$/ZnO core/shell nanofibers exhibited a higher concentration of surface defect states, presumed to be responsible for the enhanced charge transfer.

The photocurrent values and photoconversion efficiency of the $ZnFe_2O_4$/ZnO core-shell nanofibers fell within the same range as those of the core-shell nanoparticles, specifically 0.6–1.5 mA/cm_2 and 0.4–0.8%, respectively. The visible light absorption by the $ZnFe_2O_4$/ZnO core/shell nanofibers led to a 19% increase in charge concentration. This increase can be attributed to the lower power density of

Table 3
Comparison of photoelectrochemical performance of various photocatalysts.

Photoanode	Substrate	Deposition method	Electrolyte	Photo-current density	Light source	Input potential	Ref.
$ZnFe_2O_4$/ZnO film	FTO/glass	Drop casting	0.1 M Na_2SO_4	~0.93 mA/cm^2	1 SUN solar simulated intensity	1.0 V vs. Ag/AgCl	[41]
$ZnFe_2O_4$/ZnO structures	FTO/glass	Electrophoretic deposition	N/A	~5.73 $\mu A/cm^2$	300 W Xenon lamp	N/A	[44]
ZnO/$ZnFe_2O_4$/PbS nanorod arrays	FTO/glass	Solvothermal + dip-coating	0.1 M Na_2SO_4	~0.93 mA/cm^2	300 W Xenon lamp	1.12 V vs. RHE	[45]
$BiVO_4$/$ZnFe_2O_4$ structures	FTO/glass	SILAR	0.5 M Na_2SO_4	~1.60 mA/cm^2	1 SUN solar simulated	1.5 V vs. RCE	[46]
$ZnFe_2O_4$/TiO_2 nanocomposites	N/A	Drop casting	1 M 3KOH	~12.4 $\mu A/cm^2$	1 SUN solar simulated intensity	N/A	[47]
$ZnFe2O_4$ thin film	FTO/glass	Electrodeposition	0.5 M Na_2SO_4	~4.6 $\mu A/cm^2$	35 W Xenon lamp	0.8 V vs. Ag/AgCl	[48]
$ZnFe2O_4$/ZnO nanofibers	FTO/glass	Drop casting	0.5 M KOH	~1.3 mA/cm^2	Halogen lamp 25 mW/cm^2	1.2 V vs. Ag/AgCl	This work

0.025 W/cm^2 compared to the standard solar radiation of 0.1 W/cm^2 [36,43].

Further, photo responsiveness and stability of photoanodes were tested by chronoamperometry measurement using light pulses with 0.8 s period of on/off cycles (Figure S2). The current density is stabilized by time, constantly quickly raised as the light is switched on, and falls when illumination is switched off. Which indicated excellent reproducibility and reasonable stability with time.

The mechanism underlying the photoelectrochemical properties and charge transfer, as illustrated in Fig. 9, is essential for understanding the performance of $ZnFe_2O_4$/ZnO core-shell nanofibers. Upon the formation of these core-shell nanofibers, band alignment phenomena, as reported in previous studies [36,43], come into play. Electrons generated during photoexcitation efficiently migrate from the $ZnFe_2O_4$ core to the ZnO surface due to the favorable band structure. This electron transfer is a crucial step in the photoelectrochemical process and promotes efficient charge separation.

Concurrently, at the surface of the $ZnFe_2O_4$/ZnO core-shell nanofibers, water oxidation reactions occur under the influence of the photoexcited electrons. After moving to the ZnO shell, the electrons participate in the reduction half-reaction of water oxidation, which leads to the liberation of oxygen and the generation of protons. This step is pivotal in the photoelectrochemical water splitting process, as it contributes to the overall production of oxygen gas (O_2) and hydrogen ions (H^+).

The success of $ZnFe_2O_4$/ZnO core-shell nanofibers in this charge transfer and water oxidation mechanism can be attributed to the core-shell architecture's unique structural and compositional features. The core-shell design optimizes the charge transfer processes by facilitating efficient electron movement while providing a high surface area for water oxidation reactions. As a result, these nanofibers exhibit promising photoelectrochemical properties and hold potential for various applications in renewable energy and environmental sustainability. Further investigations and optimizations can harness the full potential of these core-shell nanofibers for enhanced solar-driven water splitting and other photocatalytic processes.

The performance of $ZnFe_2O_4$/ZnO core-shell nanofibers developed in this study was compared (Table 3) with previously reported photoanodes based on $ZnFe_2O_4$. $ZnFe_2O_4$/ZnO photocatalysts` performance is commensurate with other nanocomposites and surpasses some. The comparison includes photoanode composition, deposition method, the electrolyte used for the photoelectrochemical experiments, revealed photocurrent density, light source, and input potential. The results showed that $ZnFe_2O_4$/ZnO nanofibers are apparent on the same level of photocatalytic performance as other reported photoanodes based on $ZnFe_2O_4$. Comparison underscored the potential of developed in this study nanofibers as highly effective photocatalysts for water splitting applications.

4. Conclusion

This study presents our findings on the synthesis, characterization, and photoelectrochemical application of novel $ZnFe_2O_4$/ZnO core-shell nanofibers fabricated using a co-axial electrospinning technique. Characterization techniques, including XRD, FTIR, and Raman measurements, have confirmed the formation of the $ZnFe_2O_4$ phase in the core and the ZnO wurzite phase in the shell. TEM analysis has provided visual evidence of core/shell properties forming through [Fe]/[Zn] interdiffusion. These core-shell nanofibers exhibited light absorption in the range of 330–700 nm, and we have identified three distinct band gaps: one for the ZnFe2O4 core, one for the ZnO shell, and one for the interface layer between the core and shell.

The photoelectrochemical characterization of these $ZnFe_2O_4$/ZnO core-shell nanofibers revealed a significant response to visible light, increasing donor concentration. Notably, the flat band potential value of these nanofibers was higher than that of $ZnFe_2O_4$/ZnO core-shell nanoparticles. However, due to their high surface area and elevated donor concentrations, these nanofibers displayed a considerably higher dark current than core-shell nanoparticles. Encouragingly, the photocurrent response and photoconversion efficiency were compatible with and even exceeded those of core-shell nanoparticles.

These newly developed $ZnFe_2O_4$/ZnO core-shell nanofibers hold promise for various photoelectrochemical and photocatalytic applications. Future efforts to enhance the properties of these nanofibers could include increasing the core/shell thickness ratio to facilitate faster charge transfer, boosting visible light absorption to enhance photoconversion rates, and introducing specific scavengers on the nanofiber surface to augment the photoelectrochemical response.

CRediT authorship contribution statement

Berzins Agris: Investigation. **Sahul Martin:** Investigation. **Čaplovič Ľubomír:** Investigation. **Pogrebnjak Alexander:** Conceptualization, Resources. **Lys Andrii:** Formal analysis, Investigation, Visualization, Writing – original draft, Writing – review & editing. **Zabolotnii Viktor:** Investigation. **Čaplovičová Mária:** Investigation. **Tepliakova Iryna:** Investigation. **Viter Roman:** Conceptualization, Formal analysis, Funding acquisition, Investigation, Writing – original draft, Writing – review & editing. **Iatsunskyi Igor:** Conceptualization, Data curation, Formal analysis, Funding acquisition, Investigation, Project administration, Supervision, Writing – original draft, Writing – review & editing.

Authors contribution

A.L and V.Z. – fabrication of core-shell nanostructures, photoelectrochemical characterization of nanofibers, results analysis, draft preparation; A.B. and I.T.- structure characterization of nanofibers by SEM, XRD, FTIR and optical spectroscopy, description of experimental part and results; M.C., M.S., L.C.,– measurements and analysis of structure properties of nanofibers by TEM/EDX, results analysis and text writing; A.P., I.I and R.V. – supervising, conceptual idea, visualization, results discussion, draft writing/editing, resources, project administration and funding acquisition.

Declaration of Competing Interest

The authors declare the following financial interests/personal relationships which may be considered as potential competing interests: Igor Iatsunskyi reports financial support was provided by National Science Centre Poland. Roman Viter reports financial support was provided by Latvian Council of Sciences. If there are other authors, they declare that they have no known competing financial interests or personal relationships that could have appeared to influence the work reported in this paper.

Data Availability

Data will be made available on request.

Acknowledgments

R.V. acknowledges the Latvian Council of Science's fundamental and applied research projects 'Novel core-shell nanofibers formed by co-axial electrospinning for photocatalytic applications' (lzp-2021/1-0140). I.I. acknowledges the financial support from the National Science Centre of Poland from the SONATA BIS project 2020/38/E/ST5/00176.

Appendix A. Supporting information

Supplementary data associated with this article can be found in the online version at doi:10.1016/j.jallcom.2024.173885.

References

[1] Q. Li, Y. Wu, X. Ye, Y. Zeng, M. Ding, ZnO-based heterostructure constructed using HKUST-1 for enhanced visible-light photocatalytic hydrogen evolution, Appl. Catal. A: Gen. 633 (2022) 118533, https://doi.org/10.1016/j.apcata.2022.118533.

[2] A.R. Fareza, F.A.A. Nugroho, F.F. Abdi, V. Fauzia, Nanoscale metal oxides–2D materials heterostructures for photoelectrochemical water splitting—a review, J. Mater. Chem. A 10 (2022) 8656–8686, https://doi.org/10.1039/D1TA10203F.

[3] E.C. Okpara, O.C. Olatunde, O.B. Wojuola, D.C. Onwudiwe, Applications of transition metal oxides and chalcogenides and their composites in water treatment: a review, Environ. Adv. 11 (2023) 100341, https://doi.org/10.1016/j.envadv.2023.100341.

[4] M. Pavlenko, K. Siuzdak, E. Coy, K. Załęski, M. Jancelewicz, I. Iatsunskyi, Enhanced solar-driven water splitting of 1D core- shell Si/TiO 2 /ZnO nanopillars, Int. J. Hydrog. Energy 45 (2020) 26426–26433, https://doi.org/10.1016/j.ijhydene.2019.11.231.

[5] A.A. Chaaya, R. Viter, I. Baleviciute, M. Bechelany, A. Ramanavicius, I. Europeen, U. Montpellier, P.E. Bataillon, Z. Gertnere, D. Erts, V. Smyntyna, P. Miele, Tuning optical properties of Al 2 O 3 /ZnO nanolaminates synthesized by atomic layer deposition, J. Phys. Chem. C. 118 (2014) 3811–3819, https://doi.org/10.1021/jp411970w.

[6] I. Iatsunskyi, M. Baitimirova, E. Coy, L. Yate, R. Viter, A. Ramanavicius, S. Jurga, M. Bechelany, D. Erts, Influence of ZnO/graphene nanolaminate periodicity on their structural and mechanical properties, J. Mater. Sci. Technol. 34 (2018) 1487–1493, https://doi.org/10.1016/j.jmst.2018.03.022.

[7] M. Pavlenko, K. Siuzdak, E. Coy, M. Jancelewicz, S. Jurga, I. Iatsunskyi, Silicon/TiO2 core-shell nanopillar photoanodes for enhanced photoelectrochemical water oxidation, Int. J. Hydrog. Energy 42 (2017) 30076–30085, https://doi.org/10.1016/j.ijhydene.2017.10.033.

[8] M.H. Raza, R. Di Chio, K. Movlaee, P. Amsalem, N. Koch, N. Barsan, G. Neri, N. Pinna, Role of heterojunctions of core–shell heterostructures in gas sensing, ACS Appl. Mater. Interfaces 14 (2022) 22041–22052, https://doi.org/10.1021/acsami.2c00808.

[9] F. Mukhtar, T. Munawar, M.S. Nadeem, M. Naveed ur Rehman, S.A. Khan, M. Koc, S. Batool, M. Hasan, F. Iqbal, Dual Z-scheme core-shell PANI-CeO2-Fe2O3-NiO heterostructured nanocomposite for dyes remediation under sunlight and bacterial disinfection, Environ. Res. 215 (2022) 114140, https://doi.org/10.1016/j.envres.2022.114140.

[10] M. Nasr, R. Viter, C. Eid, F. Warmont, R. Habchi, P. Miele, M. Bechelany, Synthesis of novel ZnO/ZnAl2O4 multi co-centric nanotubes and their long-term stability in photocatalytic application, RSC Adv. 6 (2016) 103692–103699.

[11] E. Coy, K. Siuzdak, M. Pavlenko, K. Załęski, O. Graniel, M. Ziółek, S. Balme, P. Miele, M. Weber, M. Bechelany, I. Iatsunskyi, Enhancing photocatalytic performance and solar absorption by schottky nanodiodes heterojunctions in mechanically resilient palladium coated TiO2/Si nanopillars by atomic layer deposition, Chem. Eng. J. 392 (2020) 123702, https://doi.org/10.1016/j.cej.2019.123702.

[12] J. Dai, X. Wen, W. Feng, C. Cheng, D. Huang, Correlation of the heat treatment feature and magnetic properties of the SrFe12O19@ZnFe2O4 core-shell nanofibers, Mater. Chem. Phys. 276 (2022) 125393, https://doi.org/10.1016/j.matchemphys.2021.125393.

[13] Q. Wang, S. Liu, W. Lu, P. Zhang, Fabrication of curcumin@Ag loaded core/shell nanofiber membrane and its synergistic antibacterial properties, Front. Chem. 10 (2022), https://doi.org/10.3389/fchem.2022.870666.

[14] X. Zhang, V. Aravindan, P.S. Kumar, H. Liu, J. Sundaramurthy, S. Ramakrishna, S. Madhavi, Synthesis of TiO2 hollow nanofibers by co-axial electrospinning and its superior lithium storage capability in full-cell assembly with olivine phosphate, Nanoscale 5 (2013) 5973–5980, https://doi.org/10.1039/C3NR01128C.

[15] X. Peng, A.C. Santulli, E. Sutter, S.S. Wong, Fabrication and enhanced photocatalytic activity of inorganic core–shell nanofibers produced by coaxial electrospinning, Chem. Sci. 3 (2012) 1262–1272, https://doi.org/10.1039/C2SC00436D.

[16] F. Li, X. Gao, R. Wang, T. Zhang, G. Lu, N. Barsan, Design of core–shell heterostructure nanofibers with different work function and their sensing properties to trimethylamine, ACS Appl. Mater. Interfaces 8 (2016) 19799–19806, https://doi.org/10.1021/acsami.6b04063.

[17] K. Ranganathan, A. Morais, I. Nongwe, C. Longo, A.F. Nogueira, N.J. Coville, Study of photoelectrochemical water splitting using composite films based on TiO2 nanoparticles and nitrogen or boron doped hollow carbon spheres as photoanodes, J. Mol. Catal. A: Chem. 422 (2016) 165–174, https://doi.org/10.1016/j.molcata.2015.10.024.

[18] N. Doebelin, R. Kleeberg, {\it Profex}: a graphical user interface for the Rietveld refinement program {\it BGMN}, J. Appl. Crystallogr. 48 (2015) 1573–1580, https://doi.org/10.1107/S1600576715014685.

[19] R. Viter, V. Khranovskyy, N. Starodub, Y. Ogorodniichuk, S. Gevelyuk, Z. Gertnere, N. Poletaev, R. Yakimova, D. Erts, V. Smyntyna, A. Ubelis, Application of room temperature photoluminescence from ZnO nano-rods for salmonella detection, IEEE Sens. J. 14 (2014) 2028–2034, https://doi.org/10.1109/JSEN.2014.2309277.

[20] M. Fuentes-Pérez, M. Sotelo-Lerma, J.L. Fuentes-Ríos, E.G. Morales-Espinoza, M. Serrano, M.E. Nicho, Synthesis and study of physicochemical properties of Fe3O4@ZnFe2O4 core/shell nanoparticles, J. Mater. Sci.: Mater. Electron. 32 (2021) 16786–16799, https://doi.org/10.1007/s10854-021-06236-3.

[21] B.S. Surendra, T.R. Shashi Shekhar, M. Veerabhadraswamy, H.P. Nagaswarupa, S. C. Prashantha, G.C. Geethanjali, C. Likitha, Probe sonication synthesis of ZnFe2O4 NPs for the photocatalytic degradation of dyes and effect of treated wastewater on growth of plants, Chem. Phys. Lett. 745 (2020) 137286, https://doi.org/10.1016/j.cplett.2020.137286.

[22] Z.D. Rsen, QahtanA. Yousif, Synthesizing nanocomposite TiO2@ZnFe2O4 using a simple one-pot solvothermal technique, J. Phys.: Conf. Ser. 1999 (2021) 12135, https://doi.org/10.1088/1742-6596/1999/1/012135.

[23] J. Zhang, S. Rana, R.S. Srivastava, R.D.K. Misra, On the chemical synthesis and drug delivery response of folate receptor-activated, polyethylene glycol-functionalized magnetite nanoparticles, Acta Biomater. 4 (2008) 40–48, https://doi.org/10.1016/j.actbio.2007.06.006.

[24] R. Viter, I. Iatsunskyi, V. Fedorenko, S. Tumenas, Z. Balevicius, A. Ramanavicius, S. Balme, M. Kempiński, G. Nowaczyk, S. Jurga, M. Bechelany, Enhancement of electronic and optical properties of ZnO/Al 2 O 3 nanolaminate coated electrospun nanofibers, J. Phys. Chem. C. 120 (2016) 5124–5132, https://doi.org/10.1021/acs.jpcc.5b12263.

[25] X. Xing, L. Du, C. Wang, D. Feng, G. Liu, D. Yang, ZIF-8 micro-polyhedron MOF-transformed ZnO/ZnFe2O4 nanosheets for highly selective detection of ppb-level isoprene, Sens. Actuators B: Chem. 372 (2022) 132669, https://doi.org/10.1016/j.snb.2022.132669.

[26] M. Stoia, R. Istratie, C. Păcurariu, Investigation of magnetite nanoparticles stability in air by thermal analysis and FTIR spectroscopy, J. Therm. Anal. Calorim. 125 (2016) 1185–1198, https://doi.org/10.1007/s10973-016-5393-y.

[27] S. Choudhary, D. Hasina, M. Saini, M. Ranjan, S. Mohapatra, Facile synthesis, morphological, structural, photocatalytic and optical properties of ZnFe2O4-ZnO hybrid nanostructures, J. Alloy. Compd. 895 (2022) 162723, https://doi.org/10.1016/j.jallcom.2021.162723.

[28] B. Cao, W. Cai, H. Zeng, G. Duan, Morphology evolution and photoluminescence properties of ZnO films electrochemically deposited on conductive glass substrates, J. Appl. Phys. 99 (2006) 73516, https://doi.org/10.1063/1.2188132.

[29] P. Dolcet, K. Kirchberg, A. Antonello, C. Suchomski, R. Marschall, S. Diodati, R. Muñoz-Espí, K. Landfester, S. Gross, Exploring wet chemistry approaches to ZnFe2O4 spinel ferrite nanoparticles with different inversion degrees: a comparative study, Inorg. Chem. Front. 6 (2019) 1527–1534, https://doi.org/10.1039/C9QI00241C.

[30] Z. Wang, D. Schiferl, Y. Zhao, H.St.C.O. Neill, High pressure Raman spectroscopy of spinel-type ferrite ZnFe2O4, J. Phys. Chem. Solids 64 (2003) 2517–2523, https://doi.org/10.1016/j.jpcs.2003.08.005.

[31] M. Maletin, E.G. Moshopoulou, A.G. Kontos, E. Devlin, A. Delimitis, V.T. Zaspalis, L. Nalbandian, V.V. Srdic, Synthesis and structural characterization of In-doped ZnFe2O4 nanoparticles, J. Eur. Ceram. Soc. 27 (2007) 4391–4394, https://doi.org/10.1016/j.jeurceramsoc.2007.02.165.

[32] X. Gao, F. Li, R. Wang, T. Zhang, A formaldehyde sensor: Significant role of p-n heterojunction in gas-sensitive core-shell nanofibers, Sens. Actuators B: Chem. 258 (2018) 1230–1241, https://doi.org/10.1016/j.snb.2017.11.088.

[33] S.K. Noukelag, F. Cummings, C.J. Arendse, M. Maaza, Physical and magnetic properties of biosynthesized ZnO/Fe2O3, ZnO/ZnFe2O4, and ZnFe2O4 nanoparticles, Results Surf. Interfaces 10 (2023) 100092, https://doi.org/10.1016/j.rsurfi.2022.100092.

[34] S. Kawrani, M. Boulos, M.F. Bekheet, R. Viter, A.A. Nada, W. Riedel, S. Roualdes, D. Cornu, M. Bechelany, Segregation of copper oxide on calcium copper titanate surface induced by Graphene Oxide for Water splitting applications, Appl. Surf. Sci. 516 (2020) 146051, https://doi.org/10.1016/j.apsusc.2020.146051.

[35] M. Kuang, J. Zhang, W. Wang, J. Chen, R. Liu, S. Xie, J. Wang, Z. Ji, Synthesis of octahedral-like ZnO/ZnFe2O4 heterojunction photocatalysts with superior photocatalytic activity, Solid State Sci. 96 (2019) 105901, https://doi.org/10.1016/j.solidstatesciences.2019.05.012.

[36] A.P. Yengantiwar, M.S. Deo, A.D. Sheikh, ZnFe2O4/ ZnO ^{0}D–^{1}Dheterojunction for efficient photoelectrochemical water splitting, Mater. Sci. Eng.: B 284 (2022) 115854, https://doi.org/10.1016/j.mseb.2022.115854.

[37] N. Kislov, S.S. Srinivasan, Yu Emirov, E.K. Stefanakos, Optical absorption red and blue shifts in ZnFe2O4 nanoparticles, Mater. Sci. Eng.: B 153 (2008) 70–77, https://doi.org/10.1016/j.mseb.2008.10.032.

[38] L.T.T. Nguyen, D.-V.N. Vo, L.T.H. Nguyen, A.T.T. Duong, H.Q. Nguyen, N.M. Chu, D.T.C. Nguyen, T.Van Tran, Synthesis, characterization, and application of ZnFe2O4@ZnO nanoparticles for photocatalytic degradation of Rhodamine B under visible-light illumination, Environ. Technol. Innov. 25 (2022) 102130, https://doi.org/10.1016/j.eti.2021.102130.

[39] Z. Masoumi, M. Tayebi, M. Kolaei, B.-K. Lee, Improvement of surface light absorption of ZnO photoanode using a double heterojunction with α–Fe2O3/g–C3N4 composite to enhance photoelectrochemical water splitting, Appl. Surf. Sci. 608 (2023) 154915, https://doi.org/10.1016/j.apsusc.2022.154915.

[40] Y. Li, K. Liu, J. Zhang, J. Yang, Y. Huang, Y. Tong, Engineering the band-edge of Fe2O3/ZnO nanoplates via separate dual cation incorporation for efficient photocatalytic performance, Ind. Eng. Chem. Res 59 (2020) 18865–18872, https://doi.org/10.1021/acs.iecr.0c03388.

[41] A.P. Yengantiwar, M.S. Deo, A.D. Sheikh, ZnFe2O4/ ZnO ^{0}D–^{1}D heterojunction for efficient photoelectrochemical water splitting, Mater. Sci. Eng.: B 284 (2022) 115854, https://doi.org/10.1016/J.MSEB.2022.115854.

[42] K. Sivula, Mott–schottky analysis of photoelectrodes: sanity checks are needed, ACS Energy Lett. 6 (2021) 2549–2551, https://doi.org/10.1021/acsenergylett.1c01245.

[43] M. Chakraborty, D. Roy, A. Sharma, R. Thangavel, Post-treatment with ZnFe2O4 nanoparticles to improve photo-electrochemical performance of ZnO nanorods based photoelectrodes, Sol. Energy Mater. Sol. Cells 200 (2019) 109975, https://doi.org/10.1016/j.solmat.2019.109975.

[44] M. Yang, Y. Zhang, R. Cheng, J. Sun, Y. Peng, J. Yu, Highly efficient solar hydrogen evolution by photoelectro-chemical water splitting over ZnFe2O4-ZnO

heterojunction. in: IOP Conf Ser Mater Sci Eng, Institute of Physics Publishing, 2020, https://doi.org/10.1088/1757-899X/774/1/012018.
[45] H. Jiang, Y. Chen, L. Li, H. Liu, C. Ren, X. Liu, G. Tian, Hierarchical ZnO nanorod/ZnFe2O4 nanosheet core/shell nanoarray decorated with PbS quantum dots for efficient photoelectrochemical water splitting, J. Alloy. Compd. 828 (2020), https://doi.org/10.1016/j.jallcom.2020.154449.
[46] S. Majumder, N.D. Quang, T.T. Hien, N.D. Chinh, N.M. Hung, H. Yang, C. Kim, D. Kim, Effect of SILAR-anchored ZnFe2O4 on the BiVO4 nanostructure: An attempt towards enhancing photoelectrochemical water splitting, Appl. Surf. Sci. 546 (2021), https://doi.org/10.1016/j.apsusc.2021.149033.
[47] M.A. Draz, H.H. El-Maghrabi, F.S. Soliman, H. Selim, A.A. Razik, A.E. sayed Amin, Y.M. Moustafa, A. Hamdy, A.A. Nada, Large scale hybrid magnetic ZnFe2O4/TiO2 nanocomposite with highly photocatalytic activity for water splitting, J. Nanopart. Res. 23 (2021), https://doi.org/10.1007/s11051-020-05122-z.
[48] M. Mohsen Momeni, M. Najafi, Structural, morphological, optical and photoelectrochemical properties of ZnFe2O4 thin films grown via an electrodeposition method, Inorg. Chem. Commun. 132 (2021), https://doi.org/10.1016/j.inoche.2021.108809.

ACS APPLIED MATERIALS & INTERFACES

www.acsami.org

Research Article

Hierarchically Structured Ti-TiO_2 Membranes Fabricated by Femtosecond Laser Ablation and Atomic Layer Deposition for Enhanced Photoelectrochemical Water Splitting

Published as part of ACS Applied Materials & Interfaces special issue "Science in Ukraine: Advances in Applied Materials".

Andrii Lys, Iaroslav Gnilitskyi, Emerson Coy, Mariusz Jancelewicz, Mikhael Bechelany, and Igor Iatsunskyi*

Cite This: *ACS Appl. Mater. Interfaces* 2025, 17, 43390−43402

Read Online

ACCESS | Metrics & More | Article Recommendations | Supporting Information

ABSTRACT: Efficient and scalable photoelectrodes are essential for advancing solar-driven hydrogen production via photoelectrochemical (PEC) water splitting. This work presents a novel binder-free Ti-TiO_2 membrane photoanode engineered by the synergy of femtosecond laser ablation and atomic layer deposition (ALD). Laser processing produced a highly ordered array of micro pyramids on titanium foil, significantly increasing the surface area and light-trapping capability. Subsequent ALD of TiO_2 (10 and 100 nm) yielded conformal coatings with tunable crystallinity. Among the tested configurations, the 100 nm TiO_2 layer showed superior performance, attributed to its enhanced crystallinity, optical absorption, and charge transport properties. The optimized membrane achieved a photocurrent density of ∼27 $\mu A\ cm^{-2}$ at 1.4 V vs NHE, an IPCE (Incident photon to current conversion efficiency) of ∼31% at 275 nm, and a 3-fold increase in ABPE (Applied Bias Photon-to-current Efficiency) compared to the uncoated sample. This strategy presents a scalable and reproducible approach to high-performance, binder-free photoanodes for solar hydrogen production.

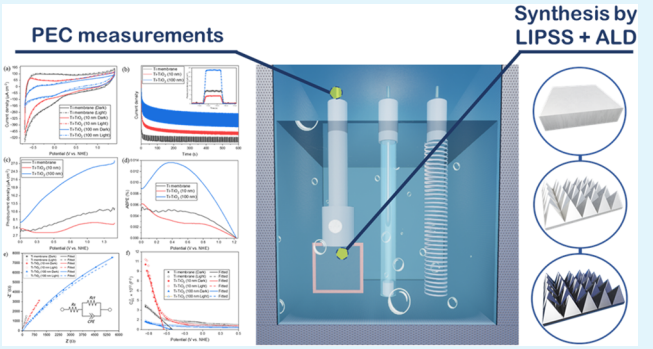

KEYWORDS: *photoelectrochemical water splitting, hierarchical TiO_2, titanium membrane, femtosecond laser ablation, atomic layer deposition, binder-free photoanode, solar hydrogen production*

1. INTRODUCTION

Over the last century, the significant consumption of fossil fuels, technological advancements, and the Industrial Revolution have contributed to a nearly 50% increase in atmospheric CO_2 concentration.[1] This rise, in turn, is the driving force behind climate change, global warming, environmental problems, and deterioration of health conditions.[2] While hydrogen (H_2) is often viewed as a clean, high-energy fuel with strong potential for decarbonization, its current production methods are mainly unsustainable,[3] because over 90% of global hydrogen is still derived from fossil fuel-based technologies, leading to considerable CO_2 emissions.[4] Among all the available alternative technologies, photoelectrochemical (PEC) water splitting is a promising approach for generating clean hydrogen. This method uses semiconductor materials to capture sunlight, producing electron−hole pairs that facilitate the dissociation of water into hydrogen and oxygen.[5]

Titanium dioxide (TiO_2) has attracted significant attention as a photoanode material due to its affordability, chemical stability, and nontoxic nature.[6] Our previous work demonstrated that atomic layer deposition (ALD) allows precise control over the thickness of metal oxide layers, including TiO_2.[7−10] However, its wide band gap (∼3.2 eV) limits its absorption to the UV region, hindering efficient charge separation and negatively impacting the PEC performance. As a result, its overall efficiency remains unsatisfactory.[11] To overcome these challenges, several solutions have been explored, including the incorporation of noble metals,[12,13] dopant engineering,[14,15] heterostructure formation,[13,16] and morphological modifications.[17,18]

In this context, the application of femtosecond laser-based surface engineering has gained growing interest due to its

Received: April 14, 2025
Revised: July 14, 2025
Accepted: July 15, 2025
Published: July 21, 2025

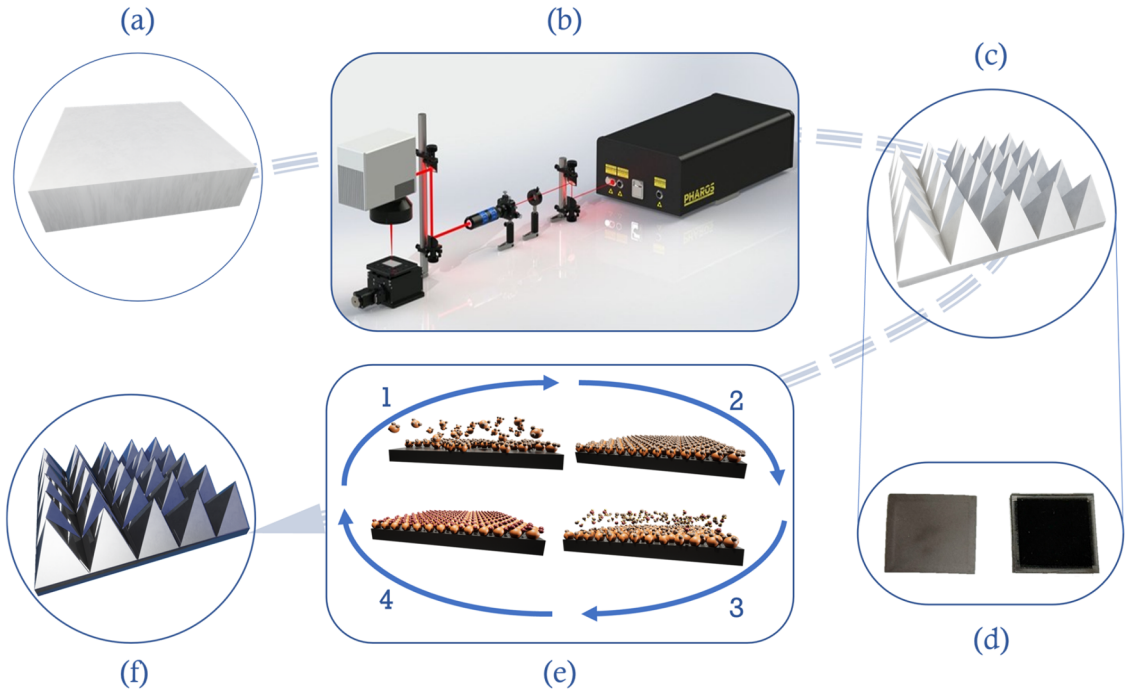

Figure 1. Schematic representation of the production cycle of the Ti-TiO_2 membrane: (a) Ti substrate, (b) laser setup for membrane formation, (c) Ti membrane, (d) photographs of nonprocessed and laser-processed Ti surfaces, (e) ALD TiO_2 deposition process (1. precursor pulse, 2. precursor purge, 3. oxidizer pulse, 4. oxidizer purge), and (f) final Ti-TiO_2 membrane.

precision, speed, high reproducibility, and contactless characteristics. It provides a powerful and versatile tool for tailoring surface properties of materials and significantly enhancing their functionality.[19] Laser-processed functional surface structures (LPFSS) have been extensively explored for diverse applications in surface texturing, wettability control, and functional coatings.[20,21]

Some laser-structured surfaces, referred to as hierarchical structures, have complex shapes and large surface areas that enhance photocatalytic properties.[22] Zhou et al. demonstrated that microstructured arrays alter optical properties and significantly impact impedance, resulting in a considerable reduction in impedance due to morphology-induced changes.[23] When comparing laser treatment with the widely used electrochemical machining (ECM) technique, several key disadvantages of ECM become evident. The factors to consider encompass corrosive characteristics, reliance on the electrical properties of the metal, significant overcut, and scalability constraints for industrial applications.[24] On the other hand, laser-based micromachining has emerged as a highly effective and dependable method for extensive surface treatment and modification. It provides exceptional precision at the microscopic scale, operates without contact, and offers remarkable versatility for working with challenging materials.[25,26]

Several previous studies have explored hierarchical structuring of titanium-based photoelectrodes to enhance light absorption and charge separation. In particular, Liang et al.[27] combined femtosecond laser processing with anodization to fabricate TiO_{2-x} hierarchical nanotube arrays containing oxygen vacancies, which exhibited significantly enhanced photocatalytic activity due to bandgap narrowing and defect-mediated charge transfer. Nonetheless, the introduction of elevated concentrations of oxygen vacancies could potentially undermine long-term stability in photoelectrochemical processes.

In this study, ALD and laser-processed functional surface structures (hierarchical structures) were integrated to fabricate a novel titanium(Ti)-based membrane. The membrane was first structured via femtosecond laser ablation, forming a micrometric array of titanium pyramids, followed by ALD deposition of TiO_2 to introduce a photoactive layer. The resulting highly regular Ti-TiO_2 membrane functions as a photoanode for electrochemical water splitting, aiming to develop a new, binder-free electrode for sustainable hydrogen production. In contrast to conventional Ti/TiO_2 systems, this work introduces a scalable laser-assisted ALD integration strategy that enables precise conformal coating over complex hierarchical structures, providing a versatile platform for future photovoltaic electrochemical (PEC) device optimization. We present a comprehensive physicochemical characterization of the fabricated composites, employing Raman spectroscopy, contact-angle analysis, scanning electron microscopy (SEM), X-ray diffraction (XRD), X-ray photoelectron spectroscopy (XPS), and ultraviolet−visible (UV−vis) spectroscopy. Additionally, we perform a series of photoelectrochemical tests, including cyclic voltammetry (CV), linear sweep voltammetry (LSV), chronoamperometry (CA), electrochemical impedance spectroscopy (EIS), Mott−Schottky analysis, and incident photon-to-current efficiency (IPCE) measurements.

2. EXPERIMENTAL SECTION

2.1. Materials and Synthesis. Titanium tetrachloride ($TiCl_4$, 99.9% trace metals basis, ReagentPlus, Sigma-Aldrich) and sodium sulfate (Na_2SO_4, ≥ 99.0%, ACS reagent grade, anhydrous, Sigma-Aldrich) were used without further purification. Deionized water with a resistivity of 18.2 MΩ·cm was obtained from a Milli-Q system. High-purity argon gas (Ar, 5.0, 99.999%, Linde HiQ, UN 1006) was used to purge the electrolyte solution before PEC measurements. The Ti membrane was fabricated using a Pharos P20 fs laser system from LightConversion (Lithuania). This system delivers a p-polarized (PP) laser beam with excellent beam quality (M^2 < 1.2), a beam diameter of

https://doi.org/10.1021/acsami.5c07488
ACS Appl. Mater. Interfaces 2025, 17, 43390−43402

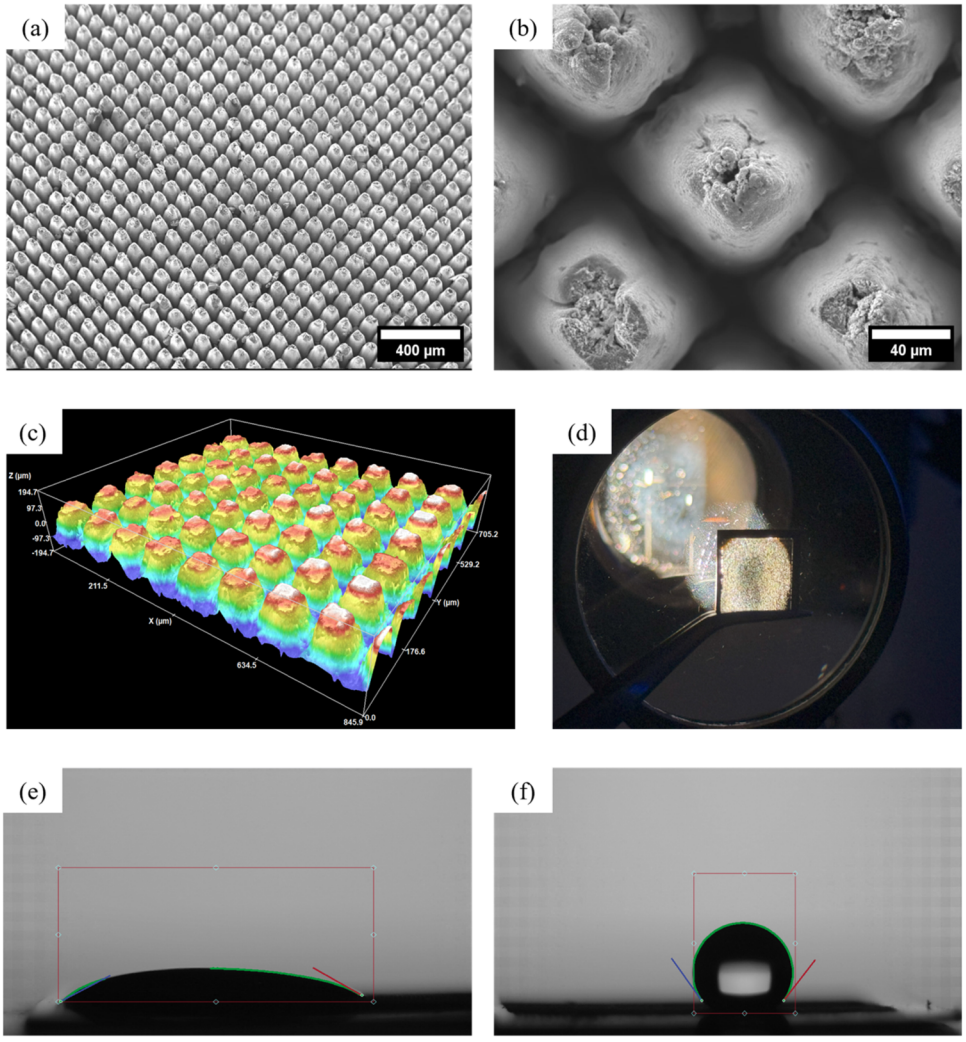

Figure 2. (a) Pyramidal surface structure on the Ti membrane, (b) magnified view of the pyramidal surface, (c) the 3D surface texture scan of the Ti membrane, (d) the light transmission test, (e) the contact angle measurement of the Ti membrane, and (f) the contact angle measurement after ALD deposition of TiO_2.

2.5 mm, a central wavelength of 1030 nm, a pulse duration of 266 fs, a maximum average power of 20 W, and a maximum pulse repetition frequency of 1 MHz. The average laser power and pulse repetition rate were precisely controlled using the Pharos control software. The generated laser beam was enlarged by passing through an expander and then forwarded to a galvanometric scanning head ExcelliScan (Scan Lab, Germany). Quadratic Ti coupons measuring 1 cm × 1 cm were cut from commercially pure titanium (>99% Ti, grade 1). The Ti samples were polished with abrasive papers to increase fineness and remove significant surface imperfections before undergoing laser micromachining. Square pyramid structures were fabricated via raster scanning at an incident angle (θ) of 0°, employing a laser fluence of 1.3 J/cm^2, a repetition rate of 1 MHz, a scanning speed of 3 m/s, a line overlap of 83%, and delivering 300 pulses per spot (PPS), under ambient atmospheric conditions. The chosen fluence, repetition rate, and scanning speed yielded the most uniform and reproducible pyramid arrays. Lower fluence levels (<1.0 J/cm^2) resulted in insufficient ablation and poorly defined surface features, compromising the formation of uniform microstructures, while higher fluences (>1.5 J/cm^2) led to excessive melting and random redeposition. The selected parameters ensured a balance between material removal and morphological definition. The sample-carrying stage moved along the *x*-axis, enabling precise laser spot scanning. Upon completion of each scanline, the stage returned to its initial position and shifted incrementally along the *y*-axis to initiate the subsequent scanline. An electro-optic modulator-based beam shutter was utilized to selectively block the laser beam when traversing designated pyramid locations, thereby ensuring these regions remained unablated. This overscanning procedure was repeated multiple times to attain the desired final pillar height. Additionally, after each overscan cycle, the z-position of the stage was adjusted to maintain the laser focal point on the sample surface. Following the formation of the Ti membrane, two different TiO_2 layers were deposited using ALD at 150 °C with $TiCl_4$ and water as precursors. The protocol for depositing thin TiO_2 layers on nano- and microstructures has been previously optimized and developed.[28,29] The first deposition consisted of 250 ALD cycles, yielding a TiO_2 layer of approximately 10 nm, while the second deposition comprised 2500 ALD cycles, resulting in a TiO_2 thickness of approximately 100 nm. The typical growth rate was 0.4 Å/cycle. Simultaneously, a metal oxide layer was grown on a planar Si surface to confirm the thickness using ellipsometry measurements. A schematic representation of the sample preparation procedure is presented in Figure 1.

2.2. Characterization. The structure of the produced nanocomposites and individual materials was investigated using scanning electron microscopy (SEM) (JEOL JSM7001F). Raman spectra were recorded with a Renishaw micro-Raman spectrometer equipped with a confocal microscope and a 633 nm excitation laser. X-ray photoelectron spectroscopy (XPS) with a monochromatic X-ray source (Al−Kα; hυ = 1486.6 eV) was performed to determine the surface elemental composition. The optical properties, including absorbance and

https://doi.org/10.1021/acsami.5c07488
ACS Appl. Mater. Interfaces 2025, 17, 43390−43402

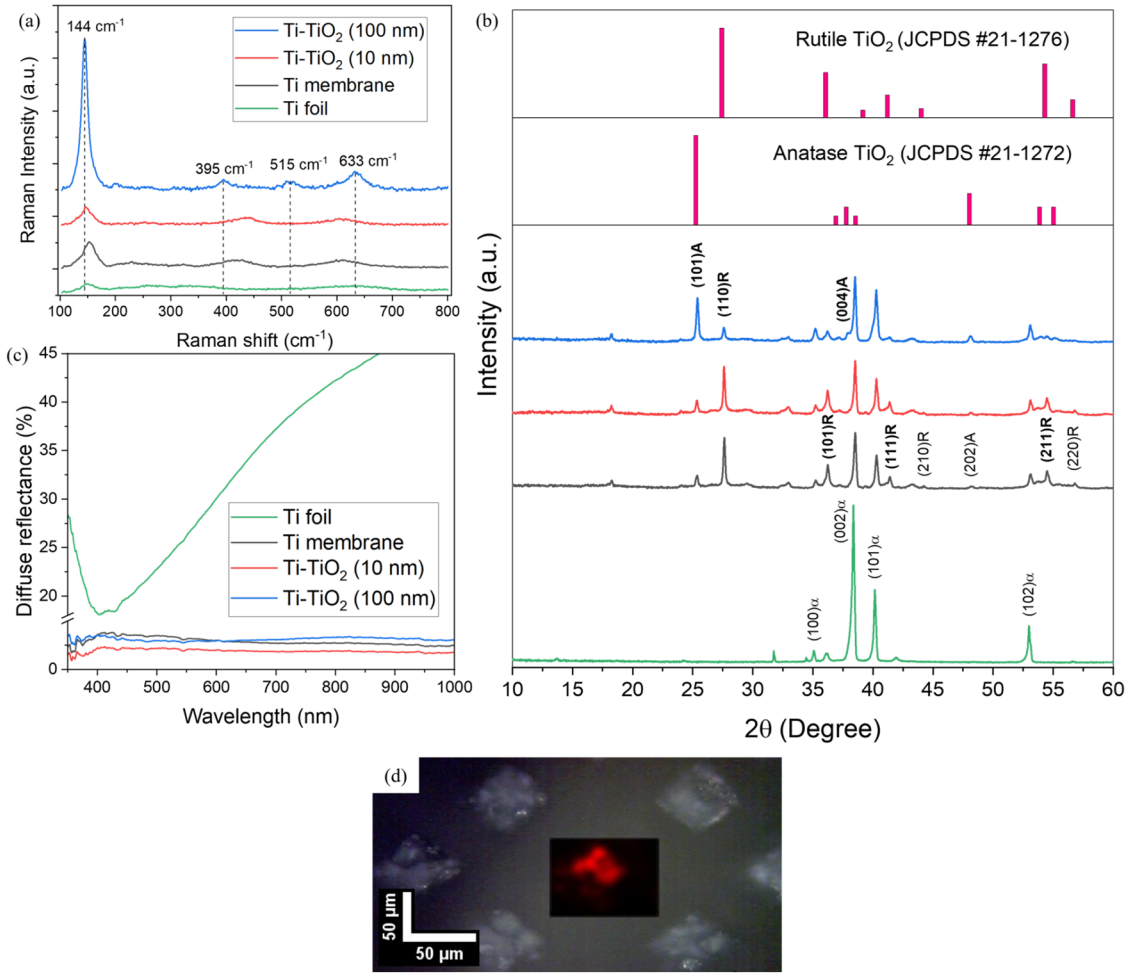

Figure 3. (a) Raman spectra of Ti foil, Ti membrane, Ti-TiO_2 (10 nm), and Ti-TiO_2 (100 nm) samples; (b) XRD patterns of the same samples, with reference diffraction patterns of anatase (JCPDS 21-1272) and rutile (JCPDS 21-1276) inserted for phase identification. Dominant peaks are annotated to highlight crystallinity trends induced by ALD; (c) diffuse reflectance spectra; and (d) Raman mapping of the Ti-TiO_2 (100 nm) sample, highlighting the 144 cm^{-1} peak in red.

photoluminescence, were analyzed using an Ocean Optics QE65Pro spectrophotometer. Diffuse reflectance measurements were conducted using an Ocean Optics QE PRO spectrometer coupled with an integrating sphere. A series of electrochemical tests was performed using a Gamry Reference 620 potentiostat.

2.3. Photoelectrochemical Tests. The PEC properties of the produced Ti-TiO_2 membranes were evaluated using a standard three-electrode system. The membranes served as the working electrodes, a platinum wire was the counter electrode, and an Ag/AgCl (3 M KCl) electrode was used as the reference electrode. All measurements were conducted at room temperature. A 0.5 M Na_2SO_4 electrolyte solution with pH ~7 was diaurated by purging with argon (Ar) gas for 30 min before and during all experiments to remove dissolved oxygen. The samples were irradiated with a 300 W xenon lamp, adjusted to a power density of 100 mW/cm^2. IPCE measurements were performed using a monochromator to control the wavelength of incident light. CA measurements were conducted under continuous illumination at a bias potential of 1.23 V vs the normal hydrogen electrode (NHE) to evaluate the photocurrent stability. Electrochemical impedance spectroscopy (EIS) was conducted both in the dark and under illumination, within a frequency range of 0.1 Hz to 5 MHz, using an amplitude of 10 mV and a bias potential of 1.23 V vs NHE. The Mott−Schottky analysis was performed at a fixed frequency of 1 kHz, over a potential range of −0.8 to 1.23 V vs NHE. The photoconversion efficiency, specifically the applied bias photon-to-current conversion efficiency (ABPE, %) of the fabricated electrodes, was calculated.[30]

$$\mathrm{ABPE}(\%) = \frac{\left[I_{ph}\left(\frac{mA}{cm^2}\right) \times (1.23 - |V_{RHE}|)(V)\right]}{\left[P_{ls}\left(\frac{mW}{cm^2}\right)\right]} \times 100(\%) \quad (1)$$

where I_{ph} is the measured photocurrent density, P_{ls} is the intensity of the light source, and V_{RHE} is the applied potential of the PEC cell, recalculated relative to NHE using the Nernst equation:[30]

$$V_{RHE} = V_{app} + V^0_{Ag/AgCl} + 0.059 \times \mathrm{pH} \quad (2)$$

where V_{app} is the potential measured against the Ag/AgCl reference electrode, $V^0_{Ag/AgCl}$ is the standard electrode potential of Ag/AgCl electrode (0.1976 V).

3. RESULTS AND DISCUSSION

3.1. The Morphology and Structural Characterization. The morphology of the Ti membrane, the Ti membrane with a 10 nm TiO_2 layer deposited by ALD (Ti-TiO_2 10 nm), and the Ti membrane with a 100 nm TiO_2 layer deposited by ALD (Ti-TiO_2 100 nm) were analyzed using SEM and 3D surface texture measurements. Figure 2a illustrates the regular pyramidal surface structure on a large scale, confirming a uniform morphological transformation across the 1 × 1 cm^2 Ti foil. As seen in Figure 2b, the pyramids feature square bases about 85 μm wide and show visible brittleness at the top regions. The

https://doi.org/10.1021/acsami.5c07488
ACS Appl. Mater. Interfaces 2025, 17, 43390−43402

entire pyramidal surface contains rough artifacts resulting from laser ablation. Figure S1 presents a cross-sectional view of the pyramids, showing rough walls and signs of damage at the tops. The 3D surface analysis further confirmed that the structured area maintains a uniform and consistent surface profile. Combined with SEM cross-sectional analysis, these measurements revealed a height range of 300−400 μm from the base of the foil to the apex of the pyramids. A detailed ISO 25178 surface texture analysis is presented in Table S1. The shapes of pyramidal structures are defined by scanning regime applied to the entire surface. The scanning regime is based on a mesh strategy with a tight spot overlap (83%), resulting in significant energy confinement in a subsurface region. The choice of the laser fluence of 1.3 J/cm^2, which is significantly above the typical ablation threshold for titanium, reported to be around 0.2−0.3 J/cm^2, combined with a high repetition rate (1 MHz) and dense spot overlap (83%), ensures highly efficient ablation.[31] Furthermore, the brittle morphology observed at the apex of the pyramids (Figures 2b and S1) might be related to the formation of titanium oxides during laser processing. The associated thermal gradients and rapid solidification may induce residual stresses, making the oxidized regions susceptible to fracture. This hypothesis is supported by XPS analysis, which confirms the presence on surface TiO_2. The inherently brittle nature of the oxide layer compared to metallic Ti likely contributes to the observed structural damage.

Additionally, cross-sectional SEM images confirmed that the laser had drilled entirely through the Ti foil. This was further verified by direct irradiation using a 300 W Xe lamp (Figure 1d), where light transmission through the drilled holes further supports the classification of the material as a Ti membrane after modification. Contact angle measurements demonstrated that after laser modification, the surface became highly hydrophilic, whereas ALD deposition rendered the surface hydrophobic, which is a characteristic behavior of TiO_2 ALD layers.[32] This behavior is attributed to the low density of surface hydroxyl groups and residual chlorine species resulting from the $TiCl_4$/H_2O ALD process, both of which reduce surface polarity and limit water adsorption.[33] Detailed contact angle measurement results are provided in Table S2.

3.2. Chemical and Optical Properties. Raman spectroscopy was conducted to analyze the chemical composition of the developed composites. Figure 3a presents the Raman spectra of the Ti foil, Ti membrane, Ti-TiO_2 (10 nm), and Ti-TiO_2 (100 nm) samples. As a result of laser ablation, not only did the surface morphology change, but the surface also oxidized, as indicated by the formation of TiO_2 phases. This transformation is expected to represent one of the standard methods for TiO_2 formation.[34] The observed peak at 152 cm^{-1} corresponds to the Eg mode of anatase TiO_2, but the shift from the typical position could be due to structural defects or phase mixing effects.[35] The detection of Raman bands at around 440 and 610 cm^{-1}, corresponding to the Eg and Ag modes of rutile, further supports the presence of mixed TiO_2 phases.[36] After the deposition of a 10 nm TiO_2 layer by ALD, shifts were observed in all major peaks. Specifically, the peaks shifted to 146, 440, and 605 cm^{-1}, which can be explained by several factors. The shift to 146 cm^{-1} may be attributed to oxygen deficiency, phonon confinement, or extrinsic doping, reflecting the sensitivity of this peak to structural and compositional changes.[37] The shifts at 440 and 605 cm^{-1} may be due to an amorphous layer formed during the thin ALD coating and its influence on local structural disorder.[38,39] With the deposition of a 100 nm TiO_2 layer, a crystalline phase emerges.[40] This is confirmed by the sharpening of the Raman peaks and their appearance at 144, 395, 515, and 633 cm^{-1}, which correspond to the characteristic modes of crystalline anatase TiO_2, as widely reported in the literature.[41,42] Figure 3d presents a Raman mapping image of the 144 cm^{-1} peak, confirming homogeneous surface coverage of the Ti membrane by the 100 nm ALD layer.

To support the Raman findings, XRD analysis (Figure 3b) was conducted to investigate the long-range crystallographic structure of the synthesized materials. The untreated Ti foil exhibited characteristic reflections of hexagonal α-Ti at 2θ = 35.1° ((100)), 38.4° ((002)), 40.2° ((101)), and 53.0° ((102)), consistent with reference data.[43] Additional weak peaks were attributed to surface oxidation or impurities. The XRD pattern of the laser-processed Ti membrane revealed the formation of mixed-phase TiO_2 corresponding to both anatase and rutile phases. The anatase phase indicates peaks at 2θ = 25.4° ((101)) and 48.3° ((202)), while the rutile phase showed peaks at 27.6° ((110)), 36.2° ((101)), 41.4° ((111)), 44.2° ((210)), 54.5° ((211)), and 56.8° ((220)). These peak positions correspond with values reported in the literature.[44]

The formation of a TiO_2 layer led to a decrease in Ti foil peak intensities without detectable shifts in their positions, which indicates partial surface coverage without significant substrate lattice distortion. Subsequent ALD (10 nm TiO_2 layer) did not result in new diffraction peaks or noticeable intensity changes, confirming the amorphous nature of the thin ALD film. In contrast, the 100 nm ALD layer induced enhanced diffraction features. Specifically, the intensity of anatase reflections at 25.4° ((101)) and 48.3° ((202)) increased markedly, and a new anatase (004) peak appeared at 37.9°, indicating crystallization and preferential orientation of the TiO_2 layer. Simultaneously, a reduction in rutile peak intensities was observed, suggesting a phase shift toward a predominantly anatase structure with increased ALD thickness.

These complementary analyses confirm the formation of mixed-phase TiO_2, with both anatase and rutile phases present. The anatase phase becomes predominant after deposition of the 100 nm ALD TiO_2 layer. The improved crystallinity and phase composition are expected to influence the photoelectrochemical behavior of the fabricated membranes.

The optical properties of the samples were characterized through diffuse reflectance analysis. The Ti foil showed high reflectivity in the visible and near-infrared (NIR) regions, but its diffuse reflectance reached over 40% (>900 nm). In contrast, the laser-processed Ti membrane showed a significant reduction in reflectance, with values dropping below 5% across the entire spectrum. This decrease is attributed to the microstructuring of the Ti surface and the formation of a thin amorphous TiO_2 layer. As depicted in Figure 1c, the laser-processed areas exhibit a significant darkening effect, characterized by a deep black coloration. Since no significant improvement in light absorption was observed after depositing 10 and 100 nm TiO_2 layers via ALD, it can be concluded that the laser-induced surface structure plays the dominant role in boosting broadband absorption. The results clearly indicate that combining microstructured surfaces with TiO_2 coatings enhances light absorption across the solar spectrum, which is crucial for improving PEC water splitting efficiency. Due to the highly structured nature of the Ti-TiO_2 membranes, accurate optical bandgap determination using Tauc plot analysis could not be reliably performed, as scattering and surface morphology effects

https://doi.org/10.1021/acsami.5c07488
ACS Appl. Mater. Interfaces 2025, 17, 43390−43402

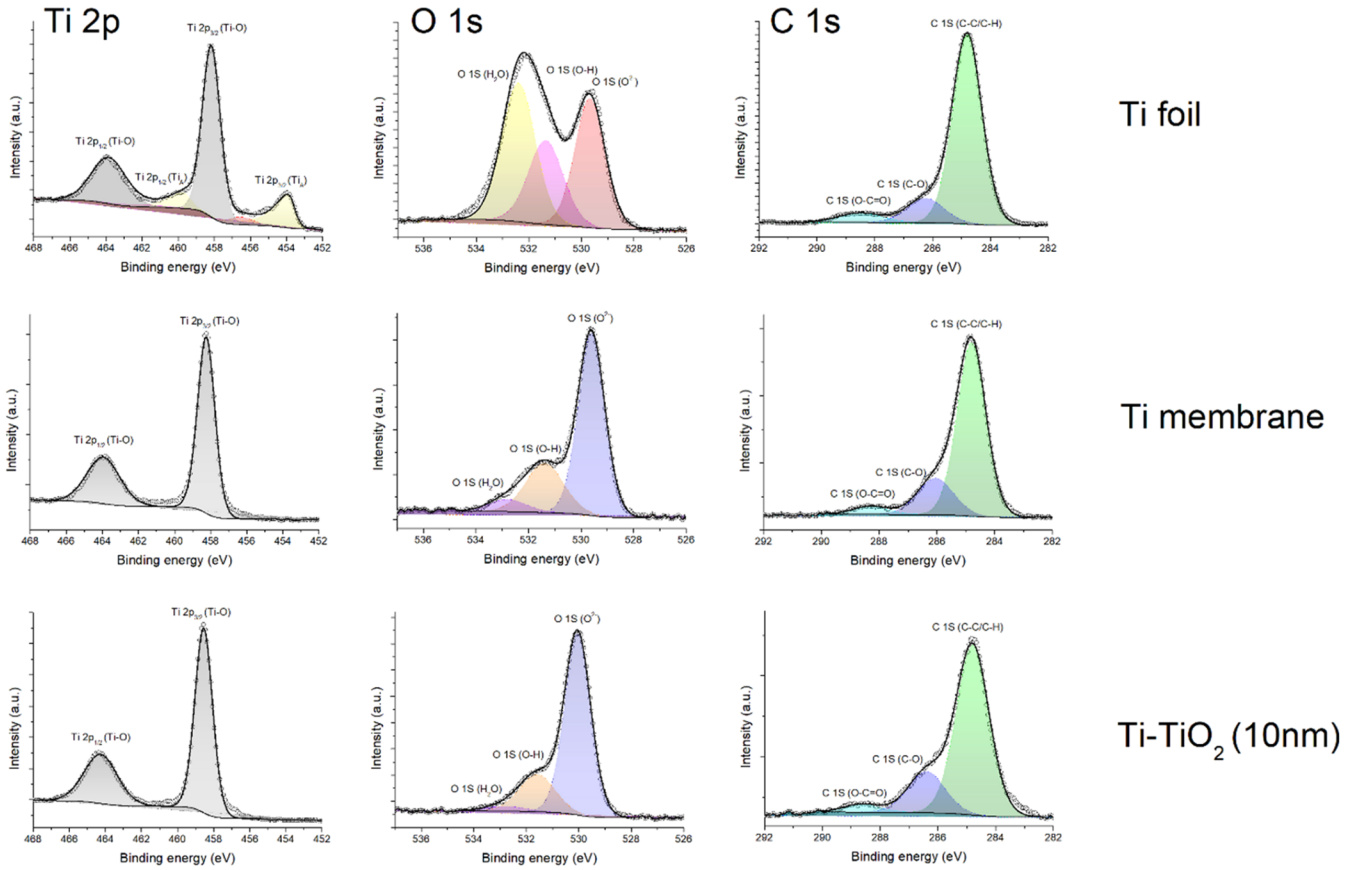

Figure 4. Core-level spectra of pristine Ti foil, laser-nanostructured Ti surface, and ALD-modified samples.

significantly distorted the absorption edge in diffuse reflectance measurements.

3.3. XPS Analysis. XPS analysis was conducted to investigate the chemical state evolution of fabricated samples. The survey spectra reveal mainly titanium (Ti), oxygen (O) and carbon (C) for all samples (Figure S2). In the case of pristine Ti foil, one may observe additional impurities like, calcium (Ca), silicon (Si), sulfur (S) and nitrogen (N).

The core-level spectra for pristine Ti foil, laser-nanostructured Ti surface, and ALD-modified samples reveal distinct transformations in surface composition and oxidation state (Figure 4). In the case of the untreated Ti foil, the Ti $2p_{3/2}$ and Ti $2p_{1/2}$ peaks are observed at binding energies of approximately 454.0 and 460.5 eV, respectively, with a spin−orbit splitting of ∼6.5 eV. The observed peak positions correspond to metallic Ti (Ti^0), suggesting that the surface remains unoxidized mainly. The sharp and symmetric shape of the peaks indicates a clean, well-structured surface. However, a minor shoulder near 458.5 eV may point to the presence of a thin native oxide layer, such as TiO_2 or suboxides like Ti_2O_3, which typically develop upon air exposure.[45] Following laser treatment, the Ti 2p spectrum experiences a notable alteration, characterized by the significant peaks migrating to elevated binding energies: Ti $2p_{3/2}$ around 458.5 eV and Ti $2p_{1/2}$ close to 464.3 eV. This shift suggests the presence of the $Ti4^+$ oxidation state linked to TiO_2. The metallic Ti signal is either absent or significantly suppressed, suggesting extensive surface oxidation induced by the high-power laser pulses. The broadened and asymmetric peaks indicate a mixture of titanium oxidation states, including Ti^{3+} and Ti^{2+}, which likely result from the complex thermal and oxidation processes triggered by femtosecond laser irradiation in air.[45,46] Following the ALD deposition of a 10 nm TiO_2 layer, the Ti 2p core-level spectrum is dominated by sharp and symmetric peaks at 458.8 eV (Ti $2p_{3/2}$) and 464.6 eV (Ti $2p_{1/2}$), corresponding to stoichiometric Ti^{4+} in TiO_2. No detectable signals from metallic Ti or suboxide species are present, confirming the formation of a uniform and fully oxidized TiO_2 overlayer. The reduced peak width and increased intensity reflect the high chemical purity, uniformity, and conformality of the ALD coating.

A comparative analysis of the evaluation of the O 1s spectra was conducted as well. The O 1s spectrum for Ti foil displays a broad asymmetric peak centered around 530.0 eV, which corresponds to lattice oxygen (O^{2-}) in stoichiometric TiO_2. This observation suggests the presence of a thin native oxide layer that forms spontaneously on titanium when exposed to ambient conditions. A minor shoulder near 531.5 eV is also observed, which is attributed to surface hydroxyl groups (−OH) or adsorbed water molecules commonly associated with environmental exposure to the native oxide surface. The O 1s spectral envelope becomes significantly more intense and asymmetric upon high-power femtosecond laser processing. The main peak remains at ∼ 530.0 eV, consistent with TiO_2. A more pronounced shoulder appears in the 532.0−532.5 eV region, indicating a higher concentration of surface hydroxyl groups, adsorbed water molecules, and possibly substoichiometric titanium oxides (TiO_{2-x}).[29] This effect is likely due to more surface area, more defects, and greater oxygen content on the surface. The O 1s spectrum of the ALD modified sample exhibits a distinctly sharper and more intense peak centered at 530.0 eV, accompanied by a notable reduction in asymmetry. The limited presence of the higher-binding energy component indicates a dense, conformal, and stoichiometric TiO_2 coating

https://doi.org/10.1021/acsami.5c07488
ACS Appl. Mater. Interfaces 2025, 17, 43390−43402

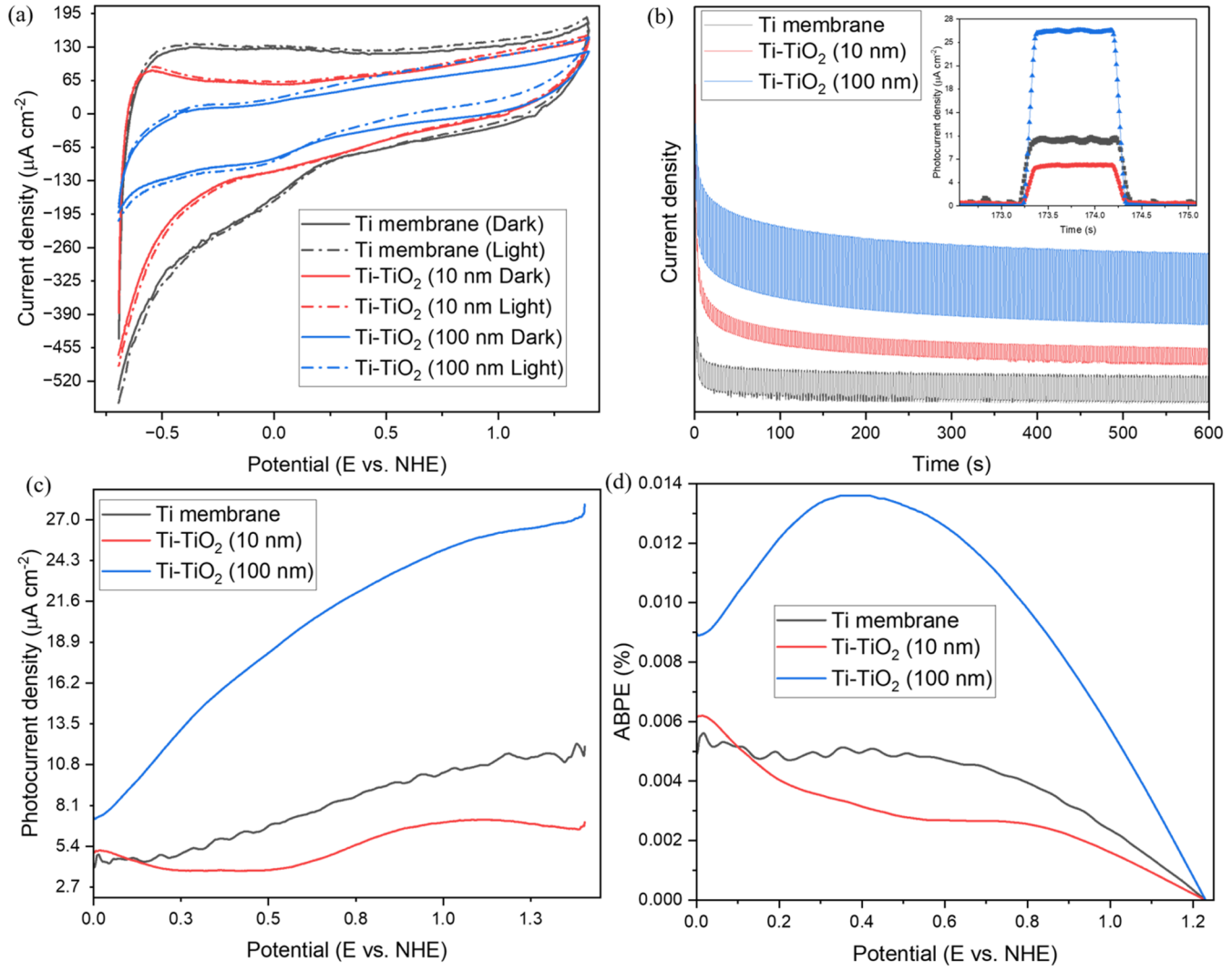

Figure 5. (a) Cyclic voltammetry measurements of all samples at a scan rate of 50 mV/s, (b) chronoamperometry analysis with an inset highlighting one light ON/OFF cycle, (c) photocurrent density from linear sweep voltammetry (LSV) measurements, and (d) calculated applied bias photon-to-current efficiency (ABPE).

characterized by minimal hydroxylation and surface impurities. The narrow fwhm and prominent lattice oxygen peak validate the exceptional chemical purity and uniformity of the ALD-grown TiO_2 film, which efficiently passivates the underlying laser-structured surface.

Finally, the high-resolution C 1s XPS spectra revealed distinct chemical states of carbon across the three samples. For pristine titanium, the C 1s spectrum is mainly centered at ∼284.8 eV, consistent with surface contamination from C−C/C−H species, and includes minor peaks from oxygenated carbon compounds like C−O and O−C═O. After femtosecond laser processing, a noticeable rise in carbon intensity was observed, along with the appearance of a new feature at ∼282.0 eV, indicating the formation of Ti−C bonds likely caused by laser-driven surface modifications. In contrast, the ALD-coated Ti showed a significant reduction in carbon contamination and a sharper Ti−C component, suggesting interfacial carbide stabilization by the ALD process.[47]

We also employed the valence band X-ray photoelectron spectroscopy (VB-XPS) to evaluate the evolution of surface electronic structure (Figure S3). These measurements and their analysis provide insights into the modification of the valence density of states (DOS) resulting from laser surface processing and TiO_2 thin-film deposition.

The untreated Ti foil shows a broad and strong valence band spectrum, with a leading edge starting around ∼2.6−2.7 eV from the Fermi level. The elevated density of states ranging from approximately 3 eV to beyond 10 eV aligns with the metallic characteristics of Ti, primarily influenced by the hybridization of Ti 3d and 3p states. The pronounced valence band maximum (VBM) and elevated intensity are indicative of bulk metallic Ti, reinforcing the notion that there is no substantial oxide layer present at the surface.

The Ti membrane exhibits a notable change in the valence region. The spectrum indicates a shallower VBM around 2.1−2.2 eV, with a noteworthy redistribution of spectral intensity toward midbinding energies. The observed features indicate the development of a surface oxide resembling TiO_2, potentially consisting of both amorphous and crystalline phases, whether formed naturally or through laser induction.[45]

The sample modified by ALD exhibits a VBM around 2.3−2.5 eV, along with a broadened valence band that extends up to approximately 10 eV. The spectrum exhibits features typical of stoichiometric TiO2, highlighting significant contributions from

https://doi.org/10.1021/acsami.5c07488
ACS Appl. Mater. Interfaces 2025, 17, 43390−43402

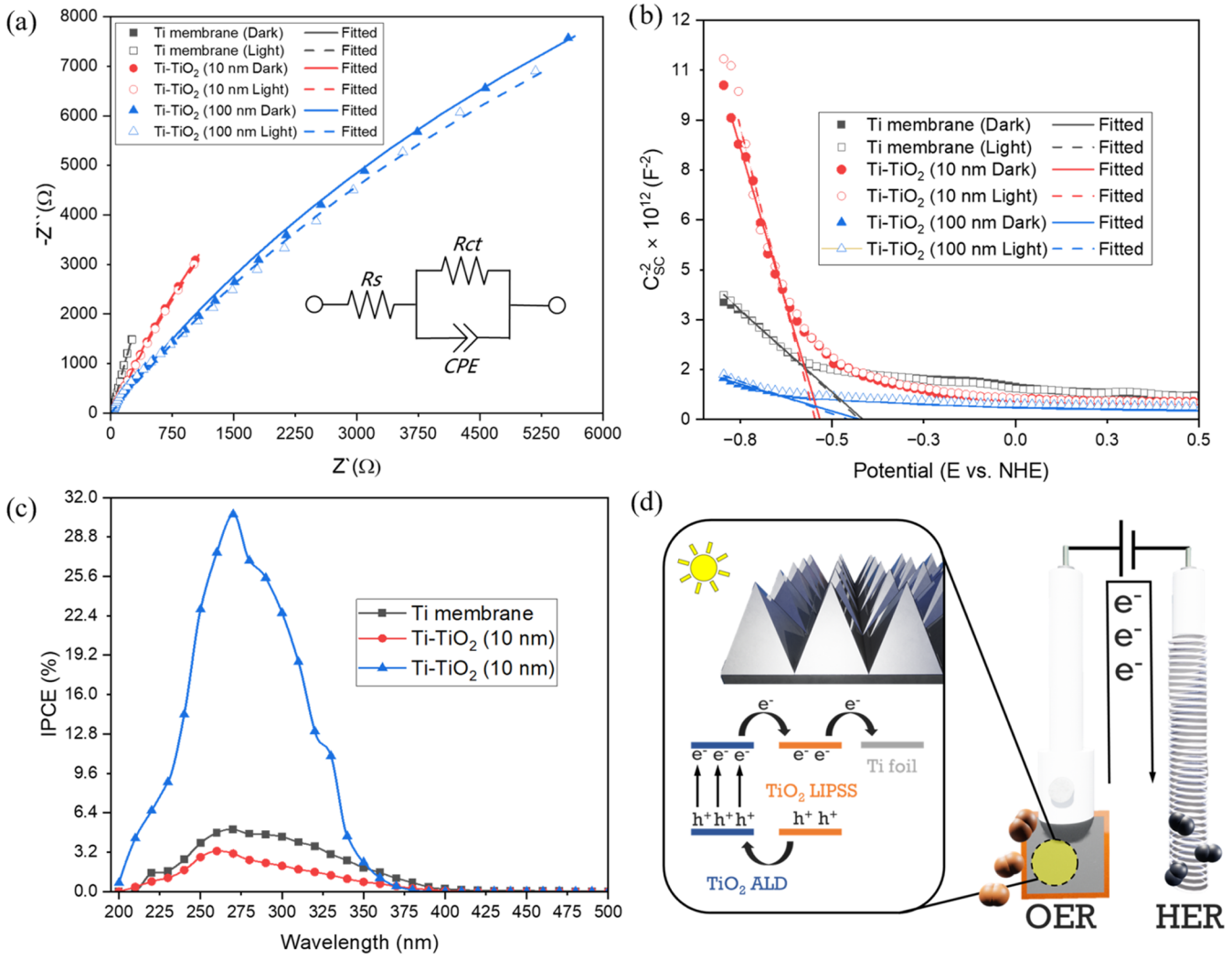

Figure 6. (a) Electrochemical impedance spectroscopy data for all samples, (b) Mott–Schottky plots, (c) incident photon-to-current efficiency measurements, and (d) schematic illustration of the photoelectrochemical behavior and charge transfer mechanism.

O 2p nonbonding states and Ti 3d-O 2p hybridized states, aligning with an anatase-like electronic structure.[45] The lack of notable sub-bandgap characteristics close to the Fermi level implies a minimal presence of Ti^{3+} or oxygen vacancy states, pointing to a well-structured oxide layer. The spectrum shows a more advanced and organized valence band, indicating the successful creation of an ultrathin TiO_2 coating and the reduction of contributions from the metallic Ti surface, which aligns closely with the XPS core-level analysis.

3.4. Photoelectrochemical Performance. The PEC behavior of the Ti-based electrodes was first evaluated using electrochemical methods, including CV, CA, and LSV, performed under both dark and light conditions. CV tests were conducted across a range of scan rates (20–500 mV/s). Representative CV curves at 50 mV/s are shown in Figure 5a, while the complete data set is provided in Figure S4. The Ti membrane exhibited a moderate photocurrent response with clear scan rate dependence, suggesting a predominantly capacitive behavior likely associated with native oxide formation and surface roughness introduced by laser processing. The photocurrent for the Ti-TiO_2 (10 nm) sample was lower, likely because the amorphous ALD coating limited its ability to absorb light efficiently and facilitate charge transfer. Moreover, the hydrophobic surface promotes oxygen bubble entrapment at the electrode–electrolyte interface, reducing the effective contact area and increasing charge-transfer resistance. This interfacial effect becomes particularly critical for ultrathin TiO_2 films, where limited wettability further impairs PEC efficiency.[48] In contrast, the Ti-TiO_2 (100 nm) sample exhibited the highest photocurrent, accompanied by a more significant variation with scan rate. The findings indicate enhanced charge storage at the surface and increased light absorption, likely due to the thicker and more crystalline TiO_2 film. To better understand how charge is stored, peak current was plotted versus scan rate and log (scan rate), as seen in Figure S5a,b. The linear trend in the peak current density versus scan rate plot suggests predominantly capacitive behavior across all samples, with steeper slopes indicating a larger surface-controlled contribution. For a more detailed understanding, b-values were extracted from the log–log plots according to the following relationship:[49]

$$\log\left(\text{peak current density}\left(\frac{\text{mA}}{\text{cm}^2}\right)\right) = b \times \log\left(\text{scan rate}\left(\frac{\text{mV}}{\text{s}}\right)\right) + \log(a) \quad (3)$$

https://doi.org/10.1021/acsami.5c07488
ACS Appl. Mater. Interfaces 2025, 17, 43390–43402

The Ti-TiO_2 (100 nm) sample showed the highest photocurrent along with sharp and stable transitions during the light ON/OFF cycles, as illustrated in the inset of Figure 5b. This points to a fast photoresponse and good photostability for all the samples. In addition, 3-h chronoamperometry ON/OFF photostability measurements were performed to evaluate the operational stability of the Ti-TiO_2 membranes. The corresponding data are provided in the Supporting Information (Figure S6). LSV measurements were carried out to further assess oxidation activity (Figure 5c). The Ti-TiO_2 (100 nm) electrode exhibited a steady increase in photocurrent across the entire potential range, reaching around 27 $\mu A/cm^2$ at 1.4 V vs NHE. A photocurrent of ~11 $\mu A/cm^2$ was recorded for the Ti membrane, with the 10 nm TiO_2-coated sample exhibiting reduced efficiency. This supports the idea that the thin ALD layer may act more as a barrier to charge transport than as an active photoabsorber. The results of LSV measurements under illumination and in the dark are presented in Figure S7. To quantify PEC performance, ABPE was also calculated and is presented in Figure 5d. The 100 nm-coated sample yielded the optimal result, attaining a peak ABPE of 0.014% at 0.39 V vs NHE, about thrice greater than both the untreated and 10 nm-coated electrodes. The diminished ABPE values in the thinner and uncoated samples indicate inferior charge separation and probable recombination losses.

It is worth highlighting that although Liang et al.[27] reported higher photocurrent densities for TiO_{2-x} photoelectrodes, their enhancement primarily originated from oxygen vacancy introduction, which may negatively affect long-term operation due to enhanced recombination and chemical instability under continuous illumination. In contrast, our ALD-based approach provides highly conformal, stoichiometric TiO_2 coatings with controlled crystallinity and superior adhesion to the laser-structured substrate. The combination of hierarchical structuring and defect-free crystalline coatings results in stable photoelectrode operation, ensuring mechanical integrity and sustained PEC performance without deterioration over extended periods.

Electrochemical impedance spectroscopy (EIS) and Mott−Schottky (MS) analyses were conducted under dark and illuminated conditions to investigate the interfacial charge transport characteristics and semiconducting behavior of the fabricated electrodes. The Nyquist plots (Figure 6a) were fitted using a Randles-type equivalent circuit, commonly applied to TiO_2 ALD interfaces.[50,51] This model includes the solution resistance (Rs), charge transfer resistance (Rct), and a constant phase element (CPE) to account for nonideal capacitive behavior at the electrode−electrolyte interface. The extracted fitting parameters are summarized in Table S3. The Ti membrane exhibited high Rct values of 76.17 kΩ (dark) and 73.99 kΩ (light), indicating sluggish charge transfer kinetics. The deposition of a 10 nm TiO_2 layer by ALD significantly reduced the Rct values to 47.69 kΩ (dark) and 52.79 kΩ (light). Notably, the slightly elevated Rct observed under light suggests that the TiO_2 layer could introduce trap states or facilitate surface recombination, which may interfere with efficient charge transport.[52−54] The Ti-TiO_2 (100 nm) electrode exhibited the lowest Rct values, with 40.53 kΩ (dark) and 39.90 kΩ (light), indicating substantially improved charge transfer characteristics due to the increased thickness and crystallinity of the TiO_2 layer. It is also noteworthy that the solution resistance (Rs) for the 10 nm-coated sample was slightly elevated (16.66 Ω dark, 16.09 Ω light) compared to the Ti membrane (~14.7 Ω), likely due to interfacial resistance introduced by the amorphous ALD film. In contrast, Rs decreased significantly in the 100 nm-coated electrode, reaching 3.41 Ω under illumination, reflecting improved electronic contact and lower electrolyte resistance. A drop in the CPE exponent (α) from 0.91 (Ti membrane) to 0.71 (Ti-TiO_2 100 nm, under illumination) points to greater surface irregularity, likely caused by the formation of the nanostructured TiO_2 coating. To further analyze the semiconductor properties, Mott−Schottky (MS) plots were generated (Figure 6b) to determine the flat-band potential (V_{fb}) and acceptor concentration (N_a) of the electrodes, assuming p-type semiconductor behavior. These values were extracted by linear fitting of $1/C_{sc}^2$ versus applied potential, using the following equation:[55]

$$\frac{1}{C^2} = \frac{2}{\varepsilon\varepsilon_0 q N_a A^2}\left(E - E_{fb} - \frac{k_B T}{q}\right) \tag{4}$$

where C is the capacitance of the space-charge layer, ε is the dielectric constant of TiO_2, ε_0 is the vacuum permittivity, q is the elementary charge, N_a is the acceptor density, A is the electrode area, E is the applied potential, E_{fb} is the flat-band potential, k_B is the Boltzmann constant, and T is the absolute temperature.

The extracted data are summarized in Table S4. The Ti membrane exhibited flat-band potentials of −0.44 V (dark) and −0.45 V (light) vs NHE, with acceptor concentrations in the range of (1.39−1.44) × 10^{19} m^{-3}. The 10 nm TiO_2-coated sample displayed more negative flat-band potentials (−0.56 V dark, −0.57 V light) and significantly lower acceptor concentrations (3.28−3.76 × 10^{18} m^{-3}), suggesting reduced carrier availability and a suppressed charge transport capability. These results are consistent with the lower photocurrent and ABPE values observed in PEC tests, likely due to the amorphous nature and higher defect density in the ultrathin film. Compared to other samples, the 100 nm TiO_2-coated electrode showed flat-band potentials between −0.45 and −0.48 V and a much higher acceptor concentration (~4.34 × 10^{19} m^{-3}), pointing to improved p-type conductivity and better overall electronic behavior. The p-type behavior in all electrodes is likely influenced by surface and interfacial defect states,[56] especially in the Ti-TiO_2 (10 nm) sample, where these effects appear to dominate the overall electronic response. While TiO_2 is normally an n-type semiconductor, apparent p-type behavior in Mott−Schottky plots has been reported in thin films exhibiting high concentrations of surface defects or non-stoichiometric phases.[56,57] In our case, the oxygen vacancies and Ti^{3+} defect states evidenced by XPS and VB-XPS, combined with the mixed anatase/rutile phases identified by XRD, likely result in band bending or surface inversion effects that explain the positive slope without indicating true bulk p-type conductivity. The observed trend toward improved conductivity and lower interfacial resistance with increasing TiO_2 thickness confirms that a crystalline, nanostructured TiO_2 layer can overcome charge transfer limitations imposed by defects from laser structuring and thin amorphous films. Together, the EIS and Mott−Schottky results reinforce PEC findings by highlighting that the 100 nm TiO_2 layer provides faster charge transfer, lower solution and interfacial resistance, higher acceptor concentration, and ultimately, enhanced photoelectrochemical performance.

IPCE measurements were conducted to evaluate the wavelength-dependent photoactivity of the fabricated electro-

https://doi.org/10.1021/acsami.5c07488
ACS Appl. Mater. Interfaces 2025, 17, 43390−43402

des, as shown in Figure 6c. The IPCE values were calculated using the equation:[58]

$$\mathrm{IPCE}(\lambda) = 1240 \times \frac{J_{sc}}{P_{in}(\lambda) \times \lambda} \quad (5)$$

where λ is the wavelength in nanometers (nm), J_{sc} is the measured photocurrent density (mA/cm^2), and $P_{in}(\lambda)$ is the incident light power density at the corresponding wavelength (mW/cm^2).

The measurements were performed using a monochromator to isolate specific wavelengths. At each selected wavelength, the incident light intensity was recorded with a calibrated photodetector, and the photocurrent response of the electrodes was measured. All samples showed a clear photoresponse in the UV region (200−370 nm), which aligns with the wide band gap of TiO_2. Among the tested electrodes, the Ti-TiO_2 (100 nm) sample achieved the highest IPCE, reaching around 31% at 275 nm. This suggests better light absorption and more effective charge carrier separation. The Ti membrane showed a moderate IPCE response (∼6.5%), likely due to its laser-induced surface texturing and the formation of mixed-phase TiO_2 during processing. In comparison, the Ti-TiO_2 (10 nm) sample had the lowest IPCE (∼3.5%), confirming the limited performance of the thin, amorphous TiO_2 layer. These results align with photocurrent, ABPE, and EIS data, underscoring the significance of TiO_2 thickness and crystallinity in enhancing the PEC behavior of Ti-based electrodes.

To summarize and better explain the photoelectrochemical behavior and charge transfer processes of the prepared electrodes, a conceptual schematic is shown in Figure 6d. In this diagram, illumination triggers the generation of electron−hole pairs within the TiO_2 regions, both from the laser-induced oxide layer and the ALD-deposited TiO_2 coating. The photogenerated holes move toward the electrode−electrolyte interface, driving the oxygen evolution reaction (OER). At the same time, the electrons are transported through the conductive Ti base and collected at the counter electrode to carry out the hydrogen evolution reaction (HER). This configuration facilitates efficient charge separation, driven by the synergy between the laser-structured surface and the conformal TiO_2 layer, which together enhance light absorption and optimize charge transport pathways. Based on the electrochemical and spectroscopic results, the 100 nm ALD TiO_2 layer enhances carrier generation and transfer. This is supported by the observed increase in photocurrent, lower charge transfer resistance, and higher incident photon-to-current efficiency (IPCE). In addition, the laser-structured Ti membrane significantly contributes to light harvesting, enhancing the PEC performance of both coated and uncoated electrodes by increasing the surface area and promoting effective photon capture. Post-PEC SEM and XRD measurements were performed to evaluate changes in surface morphology and crystal structure after photoelectrochemical tests. No significant changes were observed, confirming that the pyramidal morphology and phase composition remained stable under the applied PEC conditions. The data are presented in the Supporting Information (Figure S8).

To assess our UV PEC performance against recent TiO_2 systems, we note that hierarchical photonic-crystal TiO_2 nanotubes achieved photocurrent densities of approximately 1.4 mA/cm^2 at around 1.23 V versus NHE under UV light,[59] significantly higher than our 27 μA/cm^2. However, this performance relied on complex templated architectures and multilayer photonic structures that involve precise design and fabrication steps. In comparison, Au-decorated TiO_2 nanotubes produced a photocurrent of only approximately 15.8 μA/cm^2 under UV illumination, despite the use of noble metal enhancement.[60] Our binder-free and freestanding Ti-TiO_2 membrane reaches ∼27 μA/cm^2 and ∼31% IPCE at 275 nm, without the need for noble metals, transparent substrates, or templated morphology. This demonstrates a practical and structurally robust UV photoelectrode platform that can serve as a reproducible and scalable baseline for further development.

We can conclude that the enhanced PEC performance observed in our system is attributed to the synergistic effects of hierarchical structuring, controlled composition, which is reached by ALD, and modified optical properties. The femtosecond laser-induced microstructures significantly increase light harvesting by enhancing multiple internal reflections and scattering, as supported by the UV−vis absorption spectra. The conformal ALD-deposited TiO_2 layer provides high crystallinity and uniform coverage of the complex 3D morphology, ensuring efficient charge separation and suppressing bulk recombination. Additionally, laser-induced oxygen vacancies and Ti^{3+} states, identified by XPS and VB-XPS, introduce shallow trap states that may facilitate sub-bandgap absorption and enhance charge carrier dynamics at the semiconductor-electrolyte interface. The coexistence of anatase and rutile phases, as revealed by XRD, may further promote interfacial charge separation due to favorable band alignment. The structural and compositional properties collectively boost photocurrent density, lower onset potential, and improve PEC activity as evidenced by our data.

4. CONCLUSIONS

This study presents an innovative fabrication method for TiO_2-based photoanodes that combines femtosecond laser-induced hierarchical structures with ALD. Laser processing generates microstructured surfaces that improve light trapping and augment the active surface area. Simultaneously, ALD facilitates the deposition of conformal, highly crystalline TiO_2 coatings with precise thickness control and superior interfacial adhesion. This binder-free connection guarantees mechanical durability and enhanced stability during PEC operation. While the absolute photocurrent density achieved in this study is inferior to that of leading TiO_2 photoanodes, our principal aim was to develop a highly controllable and scalable manufacturing platform to produce stable and structurally designed photoelectrodes. The integrated laser-ALD technique has considerable potential for optimization through compositional adjustment, cocatalyst incorporation, and heterostructure development, thereby improving PEC performance. This adaptable platform has the potential to provide a robust foundation for the future advancement of durable and efficient PEC systems for solar water splitting and associated applications.

■ ASSOCIATED CONTENT

Supporting Information

The Supporting Information is available free of charge at https://pubs.acs.org/doi/10.1021/acsami.5c07488.

Cross-sectional view of the pyramidal structures on the Ti membrane; surface roughness of the pyramid walls; damaged and intact pyramid tops of the Ti membrane; SEM image and XRD analysis of the Ti-TiO_2 (100 nm)

https://doi.org/10.1021/acsami.5c07488
ACS Appl. Mater. Interfaces 2025, 17, 43390−43402

sample after PEC tests; 3D surface texture measurement results of the Ti membrane according to the ISO 25178 standard; contact angle measurements of Ti membrane, Ti-TiO_2 (10 nm), and Ti-TiO_2 (100 nm) samples; XPS survey spectra of pristine Ti foil, laser-nanostructured Ti surface, and ALD-modified samples; valence band XPS spectra of pristine Ti foil, laser-nanostructured Ti surface, and ALD-modified samples; cyclic voltammetry measurements at various scan rates for Ti membrane under dark and illuminated conditions, Ti-TiO_2 (10 nm) under dark and illuminated conditions, Ti-TiO_2 (100 nm) under dark and illuminated conditions; Linear sweep voltammetry voltammetry measurements of all samples at a scan rate of 50 mV/s; peak current density versus scan rate and log(peak current density) versus log(scan rate) for all prepared samples; fitted EIS parameters for the measured samples; fitted Mott−Schottky parameters for the measured samples; chronoamperometric measurement conducted over a period of 3 h for the Ti-TiO_2 (100 nm) sample (PDF)

AUTHOR INFORMATION

Corresponding Author

Igor Iatsunskyi − *NanoBioMedical Centre, Adam Mickiewicz University, 61-614 Poznan, Poland;* orcid.org/0000-0001-9420-7376; Email: igoyat@amu.edu.pl

Authors

Andrii Lys − *NanoBioMedical Centre, Adam Mickiewicz University, 61-614 Poznan, Poland*

Iaroslav Gnilitskyi − *"NoviNano" Lab LLC, 79015 Lviv, Ukraine; Department of Applied Physics and Nanomaterials Science, Lviv Polytechnic National University, 79013 Lviv, Ukraine*

Emerson Coy − *NanoBioMedical Centre, Adam Mickiewicz University, 61-614 Poznan, Poland;* orcid.org/0000-0002-4149-9720

Mariusz Jancelewicz − *NanoBioMedical Centre, Adam Mickiewicz University, 61-614 Poznan, Poland*

Mikhael Bechelany − *Institut Européen des Membranes, IEM, UMR 5635, University of Montpellier, ENSCM, CNRS, 34090 Montpellier, France; Functional Materials Group, Gulf University for Science and Technology (GUST), Mubarak Al-Abdullah 32093, Kuwait;* orcid.org/0000-0002-2913-2846

Complete contact information is available at: https://pubs.acs.org/10.1021/acsami.5c07488

Notes

The authors declare no competing financial interest.

ACKNOWLEDGMENTS

The authors would like to acknowledge the financial support from the National Science Centre of Poland from the SONATA BIS project 2020/38/E/ST5/00176.

REFERENCES

(1) Mehtab, A.; Ali, S. A.; Sadiq, I.; Shaheen, S.; Khan, H.; Fazil, M.; Pandit, N. A.; Naaz, F.; Ahmad, T. Hydrogen Energy as Sustainable Energy Resource for Carbon-Neutrality Realization. *ACS Sustainable Resour. Manag.* **2024**, *1* (4), 604−620.

(2) Friedemann, A. J. *Life after Fossil Fuels*; Springer: Cham, 2021, *81*.

(3) Shi, M. M.; Bao, D.; Yan, J. M.; Zhong, H. X.; Zhang, X. B. Coordination and Architecture Regulation of Electrocatalysts for Sustainable Hydrogen Energy Conversion. *Acc. Mater. Res.* **2024**, *5* (2), 160−172.

(4) Song, H.; Luo, S.; Huang, H.; Deng, B.; Ye, J. Solar-Driven Hydrogen Production: Recent Advances, Challenges, and Future Perspectives. *ACS Energy Lett.* **2022**, *7* (3), 1043−1065.

(5) Cheng, W. H.; De La Calle, A.; Atwater, H. A.; Stechel, E. B.; Xiang, C. Hydrogen from Sunlight and Water: A Side-by-Side Comparison between Photoelectrochemical and Solar Thermochemical Water-Splitting. *ACS Energy Lett.* **2021**, *6* (9), 3096−3113.

(6) Eidsvåg, H.; Bentouba, S.; Vajeeston, P.; Yohi, S.; Velauthapillai, D. TiO_2 as a Photocatalyst for Water Splitting—An Experimental and Theoretical Review. *Molecules* **2021**, *26* (6), No. 1687.

(7) Coy, E.; Siuzdak, K.; Pavlenko, M.; Załęski, K.; Graniel, O.; Ziółek, M.; Balme, S.; Miele, P.; Weber, M.; Bechelany, M.; Iatsunskyi, I. Enhancing Photocatalytic Performance and Solar Absorption by Schottky Nanodiodes Heterojunctions in Mechanically Resilient Palladium Coated TiO_2/Si Nanopillars by Atomic Layer Deposition. *Chem. Eng. J.* **2020**, *392*, No. 123702.

(8) Pavlenko, M.; Siuzdak, K.; Coy, E.; Jancelewicz, M.; Jurga, S.; Iatsunskyi, I. Silicon/TiO_2 Core-Shell Nanopillar Photoanodes for Enhanced Photoelectrochemical Water Oxidation. *Int. J. Hydrogen Energy* **2017**, *42* (51), 30076−30085.

(9) Lys, A.; Gnilitskyi, I.; Coy, E.; Jancelewicz, M.; Gogotsi, O.; Iatsunskyi, I. Highly Regular Laser-Induced Periodic Silicon Surface Modified by MXene and ALD TiO_2 for Organic Pollutants Degradation. *Appl. Surf. Sci.* **2023**, *640*, No. 158336.

(10) Pavlenko, M.; Siuzdak, K.; Coy, E.; Załęski, K.; Jancelewicz, M.; Iatsunskyi, I. Enhanced Solar-Driven Water Splitting of 1D Core-Shell Si/TiO_2/ZnO Nanopillars. *Int. J. Hydrogen Energy* **2020**, *45* (50), 26426−26433.

(11) Xing, C.; Liu, Y.; Zhang, Y.; Wang, X.; Guardia, P.; Yao, L.; Han, X.; Zhang, T.; Arbiol, J.; Soler, L.; Chen, Y.; Sivula, K.; Guijarro, N.; Cabot, A.; Llorca, J. A Direct Z-Scheme for the Photocatalytic Hydrogen Production from a Water Ethanol Mixture on $CoTiO_3$/TiO_2 Heterostructures. *ACS Appl. Mater. Interfaces* **2021**, *13* (1), 449−457.

(12) Kunthakudee, N.; Puangpetch, T.; Ramakul, P.; Serivalsatit, K.; Hunsom, M. Light-Assisted Synthesis of Au/TiO_2 Nanoparticles for H_2 Production by Photocatalytic Water Splitting. *Int. J. Hydrogen Energy* **2022**, *47* (56), 23570−23582.

(13) Rafiq, K.; Sabir, M.; Abid, M. Z.; Jalil, M.; Nadeem, M. A.; Iqbal, S.; Rauf, A.; Hussain, E. Tuning of TiO_2/CdS Hybrid Semiconductor with Au Cocatalysts: State-of-the-Art Design for Sunlight-Driven H_2 Generation from Water Splitting. *Energy Fuels* **2024**, *38* (5), 4625−4636.

(14) Saeidi, S.; Rezaei, B.; Ensafi, A. A. Energy Band Engineering by CdTe/Si Codoped TiO_2 Nanoarrays for Enhanced Photoelectrochemical Water Splitting. *ACS Appl. Energy Mater.* **2022**, *5* (3), 2795−2804.

(15) Fazil, M.; Ahmad, T. Pristine TiO_2 and Sr-Doped TiO_2 Nanostructures for Enhanced Photocatalytic and Electrocatalytic Water Splitting Applications. *Catalysts* **2023**, *13* (1), 93.

(16) Saha, S.; Devi, A. A. S.; Kolodziejak, K.; Tymicki, E.; Vadivel, G.; Pawlak, D. A. Unlocking Interfacial Effects in $NiTiO_3$-TiO_2 Eutectic Composite: Enhancing Overall Electrocatalytic and Photoelectrochemical Water Splitting. *Fuel* **2025**, *381*, No. 133273.

(17) Hou, X.; Li, Z.; Fan, L.; Yuan, J.; Lund, P. D.; Li, Y. Effect of Ti Foil Size on the Micro Sizes of Anodic TiO_2 Nanotube Array and Photoelectrochemical Water Splitting Performance. *Chem. Eng. J.* **2021**, *425*, No. 131415.

(18) Asjad, M.; Arshad, M.; Zafar, N. A.; Khan, M. A.; Iqbal, A.; Saleem, A.; Aldawsari, A. An Intriguing Case of Morphology Control and Phase Transitions in TiO_2 Nanostructures with Enhanced Photocatalytic Activity. *Mater. Chem. Phys.* **2021**, *265*, No. 124416.

(19) Cao, J.; Ma, B.; Li, L.; Li, X.; Xu, C.; Wang, X. Research on the Mechanism of Femtosecond Laser Ablation Concave-Convex Microstructure Transformation. *Langmuir* **2024**, *40*, 23218.

(20) Gnilitskyi, I.; Dolgov, L.; Tamm, A.; Ferraria, A. M.; Diedkova, K.; Kopanchuk, S.; Tsekhmister, Y.; Veiksina, S.; Polewczyk, V.;

Pogorielov, M. Enhanced Osteointegration and Osteogenesis of Osteoblast Cells by Laser-Induced Surface Modification of Ti Implants. *Nanomedicine* **2024**, *62*, No. 102785.
(21) Kasálková, N. S.; Juřicová, V.; Rimpelová, S.; Fajstavr, D.; Frýdlová, B.; Kolská, Z.; Švorčík, V.; Slepička, P. LIPSS Pattern Induced by Polymer Surface Instability for Myoblast Cell Guidance. *Polym. Degrad. Stab.* **2024**, *221*, No. 110667.
(22) Wang, H.; Deng, D.; Zhai, Z.; Yao, Y. Laser-Processed Functional Surface Structures for Multi-Functional Applications-a Review. *J. Manuf. Process.* **2024**, *116*, 247−283.
(23) Zhou, W.; Liu, S.; Liu, W.; Zhang, C.; Li, Y.; Xu, W.; Hui, K. S. Novel Dry Metal Electrode with Tilted Microstructure Fabricated with Laser Micromilling Process. *Sens. Actuators, A* **2017**, *264*, 76−83.
(24) Patel, D. S.; Singh, A.; Balani, K.; Ramkumar, J. Topographical Effects of Laser Surface Texturing on Various Time-Dependent Wetting Regimes in Ti6Al4V. *Surf. Coat. Technol.* **2018**, *349*, 816−829.
(25) Kumar, D.; Nadeem Akhtar, S.; Kumar Patel, A.; Ramkumar, J.; Balani, K. Tribological Performance of Laser Peened Ti−6Al−4V. *Wear* **2015**, *322*−*323*, 203−217.
(26) Teleginski, V.; Chagas, D. C.; Costa de Oliveira, A. C.; Santos, J. C. G.; Azevedo, J. F.; Riva, R.; de Vasconcelos, G. Yb:Fiber Laser Surface Texturing of Stainless Steel Substrate, with MCrAlY Deposition and CO_2 Laser Treatment. *Surf. Coat. Technol.* **2014**, *260*, 251−259.
(27) Liang, M.; Li, X.; Jiang, L.; Ran, P.; Wang, H.; Chen, X.; Xu, C.; Tian, M.; Wang, S.; Zhang, J.; Cui, T.; Qu, L. Femtosecond Laser Mediated Fabrication of Micro/Nanostructured TiO_{2-x} Photoelectrodes: Hierarchical Nanotubes Array with Oxygen Vacancies and Their Photocatalysis Properties. *Appl. Catal., B* **2020**, *277*, No. 119231.
(28) Iatsunskyi, I.; Pavlenko, M.; Viter, R.; Jancelewicz, M.; Nowaczyk, G.; Baleviciute, I.; Załęski, K.; Jurga, S.; Ramanavicius, A.; Smyntyna, V. Tailoring the Structural, Optical, and Photoluminescence Properties of Porous Silicon/TiO_2 Nanostructures. *J. Phys. Chem. C* **2015**, *119* (13), 7164−7171.
(29) Iatsunskyi, I.; Jancelewicz, M.; Nowaczyk, G.; Kempiński, M.; Peplińska, B.; Jarek, M.; Załęski, K.; Jurga, S.; Smyntyna, V. Atomic Layer Deposition TiO_2 Coated Porous Silicon Surface: Structural Characterization and Morphological Features. *Thin Solid Films* **2015**, *589*, 303−308.
(30) Ranganathan, K.; Morais, A.; Nongwe, I.; Longo, C.; Nogueira, A. F.; Coville, N. J. Study of Photoelectrochemical Water Splitting Using Composite Films Based on TiO_2 Nanoparticles and Nitrogen or Boron Doped Hollow Carbon Spheres as Photoanodes. *J. Mol. Catal. A Chem.* **2016**, *422*, 165−174.
(31) Trtica, M.; Gakovic, B.; Batani, D.; Desai, T.; Panjan, P.; Radak, B. Surface Modifications of a Titanium Implant by a Picosecond Nd:YAG Laser Operating at 1064 and 532 nm. *Appl. Surf. Sci.* **2006**, *253* (5), 2551−2556.
(32) Xu, Q.; Yang, Y.; Yang, J.; Wang, X.; Wang, Z.; Wang, Y. Plasma Activation of Porous Polytetrafluoroethylene Membranes for Superior Hydrophilicity and Separation Performances via Atomic Layer Deposition of TiO_2. *J. Membr. Sci.* **2013**, *443*, 62−68.
(33) Nazarov, D.; Ezhov, I.; Yudintceva, N.; Mitrofanov, I.; Shevtsov, M.; Rudakova, A.; Maximov, M. MG-63 and FetMSC Cell Response on Atomic Layer Deposited TiO_2 Nanolayers Prepared Using Titanium Tetrachloride and Tetraisopropoxide. *Coatings* **2022**, *12* (5), No. 668.
(34) Białous, A.; Gazda, M.; Grochowska, K.; Atanasov, P.; Dikovska, A.; Nedyalkov, N.; Reszczyńska, J.; Zaleska-Medynska, A.; Śliwiński, G. Nanoporous TiO_2 Electrode Grown by Laser Ablation of Titanium in Air at Atmospheric Pressure and Room Temperature. *Thin Solid Films* **2016**, *601*, 41−44.
(35) Zhang, W. F.; He, Y. L.; Zhang, M. S.; Yin, Z.; Chen, Q. Raman Scattering Study on Anatase TiO_2 Nanocrystals. *J. Phys. D:Appl. Phys.* **2000**, *33* (8), 912.
(36) Mazza, T.; Barborini, E.; Piseri, P.; Milani, P.; Cattaneo, D.; Li Bassi, A.; Bottani, C. E.; Ducati, C. Raman Spectroscopy Characterization of TiO_2 Rutile Nanocrystals. *Phys. Rev. B* **2007**, *75* (4), No. 045416.
(37) Mazzolini, P.; Russo, V.; Casari, C. S.; Hitosugi, T.; Nakao, S.; Hasegawa, T.; Li Bassi, A. Vibrational-Electrical Properties Relationship in Donor-Doped TiO_2 by Raman Spectroscopy. *J.Phys. Chem. C* **2016**, *120* (33), 18878−18886.
(38) Niilisk, A.; Moppel, M.; Pärs, M.; Sildos, I.; Jantson, T.; Avarmaa, T.; Jaaniso, R.; Aarik, J. Structural Study of TiO_2 Thin Films by Micro-Raman Spectroscopy. *Cent. Eur. J. Phys.* **2006**, *4* (1), 105−116.
(39) Ng, S.; Sopha, H.; Zazpe, R.; Spotz, Z.; Bijalwan, V.; Dvorak, F.; Hromadko, L.; Prikryl, J.; Macak, J. M. TiO_2 ALD Coating of Amorphous TiO_2 Nanotube Layers: Inhibition of the Structural and Morphological Changes Due to Water Annealing. *Front. Chem.* **2019**, *7*, No. 38.
(40) Durante, O.; Di Giorgio, C.; Granata, V.; Neilson, J.; Fittipaldi, R.; Vecchione, A.; Carapella, G.; Chiadini, F.; De Salvo, R.; Dinelli, F.; Fiumara, V.; Pierro, V.; Pinto, I. M.; Principe, M.; Bobba, F. Emergence and Evolution of Crystallization in TiO_2 Thin Films: A Structural and Morphological Study. *Nanomaterials* **2021**, *11* (6), No. 1409.
(41) Frank, O.; Zukalova, M.; Laskova, B.; Kürti, J.; Koltai, J.; Kavan, L. Raman Spectra of Titanium Dioxide (Anatase, Rutile) with Identified Oxygen Isotopes (16, 17, 18). *Phys. Chem. Chem. Phys.* **2012**, *14* (42), 14567−14572.
(42) Hyam, R. S.; Choi, D. Effects of Titanium Foil Thickness on TiO_2 Nanostructures Synthesized by Anodization. *RSC Adv.* **2013**, *3* (19), 7057−7063.
(43) Jafari, M.; Vaezzadeh, M.; Noroozizadeh, S. Thermal Stability of α Phase of Titanium by Using X-Ray Diffraction. *Metall. Mater. Trans. A* **2010**, *41* (13), 3287−3290.
(44) El-Desoky, M. M.; Morad, I.; Wasfy, M. H.; Mansour, A. F. Synthesis, Structural and Electrical Properties of PVA/TiO_2 Nanocomposite Films with Different TiO_2 Phases Prepared by Sol−Gel Technique. *J. Mater. Sci.:Mater. Electron.* **2020**, *31* (20), 17574−17584.
(45) Iatsunskyi, I.; Kempiński, M.; Nowaczyk, G.; Jancelewicz, M.; Pavlenko, M.; Załeski, K.; Jurga, S. Structural and XPS Studies of PSi/TiO_2 Nanocomposites Prepared by ALD and Ag-Assisted Chemical Etching. *Appl. Surf. Sci.* **2015**, *347*, 777−783.
(46) Trenczek-Zajac, A.; Synowiec, M.; Zakrzewska, K.; Zazakowny, K.; Kowalski, K.; Dziedzic, A.; Radecka, M. Scavenger-Supported Photocatalytic Evidence of an Extended Type I Electronic Structure of the TiO_2@Fe_2O_3 Interface. *ACS Appl. Mater. Interfaces* **2022**, *14* (33), 38255−38269.
(47) Szewczyk, J.; Iatsunskyi, I.; Michałowski, P. P.; Załęski, K.; Lamboux, C.; Sayegh, S.; Makhoul, E.; Cabot, A.; Chang, X.; Bechelany, M.; Coy, E. TiO_2/PDA Multilayer Nanocomposites with Exceptionally Sharp Large-Scale Interfaces and Nitrogen Doping Gradient. *ACS Appl. Mater. Interfaces* **2024**, *16* (8), 10774−10784.
(48) Xu, R.; Zhu, D.; Du, K.; Cui, D.; Feng, H.; Hao, W.; Tian, D.; Du, Y. Role of Surface Wettability in Photoelectrocatalytic Oxygen Evolution Reactions. *Mater. Today Energy* **2022**, *25*, No. 100961.
(49) Ning, J.; Xia, M.; Wang, D.; Feng, X.; Zhou, H.; Zhang, J.; Hao, Y. Superior Pseudocapacitive Storage of a Novel Ni_3Si_2/NiOOH/Graphene Nanostructure for an All-Solid-State Supercapacitor. *Nano-Micro Lett.* **2021**, *13* (1), No. 2.
(50) Shahmohammadi, M.; Sun, Y.; Yuan, J. C. C.; Mathew, M. T.; Sukotjo, C.; Takoudis, C. G. In Vitro Corrosion Behavior of Coated Ti6Al4V with TiO_2, ZrO_2, and TiO_2/ZrO_2 Mixed Nanofilms Using Atomic Layer Deposition for Dental Implants. *Surf. Coat. Technol.* **2022**, *444*, No. 128686.
(51) Moehl, T.; Suh, J.; Sévery, L.; Wick-Joliat, R.; Tilley, S. D. Investigation of (Leaky) ALD TiO_2 Protection Layers for Water-Splitting Photoelectrodes. *ACS Appl. Mater. Interfaces* **2017**, *9* (50), 43614−43622.
(52) Mortelliti, M. J.; Wang, A. N.; Dempsey, J. L. Interfacial Electron Transfer through Ultrathin ALD TiO_X Layers: A Comparative Study of TiO_2/TiO_X and SnO_2/TiO_X Core/Shell Nanocrystals. *J. Phys. Chem. C* **2021**, *125* (23), 12937−12959.
(53) Motola, M.; Zazpe, R.; Hromadko, L.; Prikryl, J.; Cicmancova, V.; Rodriguez-Pereira, J.; Sopha, H.; Macak, J. M. Anodic TiO_2 Nanotube Walls Reconstructed: Inner Wall Replaced by ALD TiO_2 Coating. *Appl. Surf. Sci.* **2021**, *549*, No. 149306.
(54) Kim, H. J.; Kearney, K. L.; Le, L. H.; Haber, Z. J.; Rockett, A. A.; Rose, M. J. Charge-Transfer through Ultrathin Film TiO_2 on n-Si(111)

Photoelectrodes: Experimental and Theoretical Investigation of Electric Field-Enhanced Transport with a Nonaqueous Redox Couple. *J. Phys. Chem. C* **2016**, *120* (45), 25697−25708.
(55) Sivula, K. Mott-Schottky Analysis of Photoelectrodes: Sanity Checks Are Needed. *ACS Energy Lett.* **2021**, *6* (7), 2549−2551.
(56) Nowotny, M. K.; Bogdanoff, P.; Dittrich, T.; Fiechter, S.; Fujishima, A.; Tributsch, H. Observations of P-Type Semiconductivity in Titanium Dioxide at Room Temperature. *Mater. Lett.* **2010**, *64* (8), 928−930.
(57) Aperador, W.; Yate, L.; Pinzón, M. J.; Caicedo, J. C. Optical and Semiconductive Properties of Binary and Ternary Thin Films from the Nb-Ti-O System. *Results Phys.* **2018**, *9*, 328−336.
(58) Gong, J.; Krishnan, S. Mathematical Modeling of Dye-Sensitized Solar Cells. In *Dye-Sensitized Solar Cells: Mathematical Modelling, and Materials Design and Optimization*; Elsevier, 2019; pp 51−81.
(59) Meng, M.; Zhou, H.; Yang, J.; Wang, L.; Yuan, H.; Hao, Y.; Gan, Z. Exploiting the Bragg Mirror Effect of TiO_2 Nanotube Photonic Crystals for Promoting Photoelectrochemical Water Splitting. *Nanomaterials* **2024**, *14* (21), No. 1695.
(60) Pisarek, M.; Krawczyk, M.; Kosiński, A.; Hołdyński, M.; Andrzejczuk, M.; Krajczewski, J.; Bieńkowski, K.; Solarska, R.; Gurgul, M.; Zaraska, L.; Lisowski, W. Materials Characterization of TiO_2 nanotubes Decorated by Au Nanoparticles for Photoelectrochemical Applications. *RSC Adv.* **2021**, *11* (61), 38727−38738.

https://doi.org/10.1021/acsami.5c07488
ACS Appl. Mater. Interfaces 2025, 17, 43390−43402